Deregulation of E2F-1 and chemosensitivity

Submitted by Constanze Hampel for PhD

at University College London

February 2003

UMI Number: U602560

UMI

®

Dissertation Publishing

ProQuest®

ABSTRACT

The E2F transcription factors are key components of the retinoblastoma tumour suppressor pathway which control the progression from G1 to S phase in the cell cycle and regulate the transcription of proteins required for S-phase entry and DNA synthesis. Deregulation of E2F-1 expression results in the loss of control of normal cell cycle progression. Aberrations of the retinoblastoma pathway have been reported in most human cancers. Alteration in cell cycle regulation may alter the activity of anti-cancer drugs. An increase in E2F-1 activity and transcription of E2F-regulated genes potentially influences the cellular sensitivity to chemotherapeutic agents. This study aimed to investigate the pattern, mechanism and potential inhibition of E2F-1 interactions with chemotherapeutic agents.

Initial experiments performed on an HT1080 cell line stably overexpressing E2F-1 suggested a role in resistance to several DNA interactive agents, in particular the minor groove binding alkylating agent BGIII21. However, further characterisation identified the HT1080 transfectants to be CHO cell lines. Experiments using an inducible E2F-1 cell line showed increased expression of E2F-1 to have a minimal effect on chemosensitivity to BGIII21. A decrease in chemosensitivity was observed in response to BGIIII21 in CHO cells. NER, homologous recombination or mismatch repair deficiency were not found to be the underlying causes for resistance in CHO cells.

Experiments using E2F-1 inhibitory peptides, despite exhibiting marked inter-experimental variations, suggested an inverse correlation between endogenous E2F-1 expression level and peptide activity. Further, cell cycle analysis showed the E2F-1 inhibitory peptides to cause G1 arrest or apoptosis in leukemic cell lines. In conclusion, inhibition of E2F-1 activity through peptides was found to be a valuable but unreliable tool to influence the effect of chemotherapeutic agents on cells expressing increased levels of E2F-1 due to persistent variations in factors affecting peptide activity.

ACKNOWLEDGEMENTS

CONTENTS

5

7

LIST OF FIGURES

LIST OF TABLES

ABBREVIATIONS

AA	acrylamide
APS	ammonium persulphate
ATP	adenosine triphosphate
BER	base excision repair
BSA	bovine serum albumin
CBP	CREB-binding protein
CDK	cyclin-dependent kinase
CF	colony formation
CHO	Chinese hamster ovary
Ci	Curie
CMV	cytomegalo-virus
conc. HCl	concentrated hydrochloric acid
CSA/CSB	Cockayne syndrome protein A and B
ddH_2O	double-distilled water
DHFR	dihydrofolate reductase
DMA	dimethylacetamide
DMF	dimethylformamide
DMSO	dimethylsulphoxide
DNA	deoxyribonucleic acid
Dox	doxocycline
DSB	double strand break
DTT	dithiothreitol
ECACC	European Collection of Cell Cultures
ECL	enhanced chemoilluminescence
EDTA	ethylenediaminesulphate tetraacetic acid
FACS	fluorescent activated cell sorting
FCS	foetal calf serum
FITC	fluorescein iothiocyanate
HLA	human leukocyte antigen
HPRT	hypoxanthine guanine phosphoribosyl transferase

IGEPAL	(octylphenoxy) polyethoxyethanol
IMS	industrial methylated spirit
MDM2	murine double minute chromosome number 2
MEF	mouse embryo fibroblast
MMR	mismatch repair
MNNG	N-methyl-N'-nitro-N-nitrosoguanidine
MNU	N-methyl-N-nitrosourea
MOPS	(3-[N-morpholino] propanesulfonic acid
MTT	[3-(4,5-dimethylthiazol-2-yl)-2,5-diphenyltetrazoliumbromide]
MTX	methotrexate
NER	nucleotide excision repair
NLS	nuclear localisation sequence
OD	optical density
ORF	open reading frame
PBS	phosphate buffered saline
PCNA	proliferating cell nuclear antigen
PCR	polymerase chain reaction
PEG	polyethylene glycol
PI	propidium iodide
PKC	protein kinase C
PS	phosphatidyl serine
PVDF	polyvinylidenedifluoride membrane
PVP	polyvinylpyrrolidone
RF	resistance factor
RFC	reduced folate carrier
RPA	replication protein A
RPM	rounds per minute
RR	ribonuclease reductase
RT	room temperature
s.d.	standard deviations
SDS	sodium dodecylsulphate
SRB	sulphorhodamine B

SSB	single strand break
TBE	tris-borate-EDTA
TBP	TATA box-binding protein
TBS	tris buffered saline
TBS-T	tris buffered saline Tween
TCR	transcription coupled repair
TD-PCR	terminal transferase-dependent PCR
TdT	terminal deoxynuceotidyl transferase
TE	tris-EDTA
TEMED	tetramethylethylenediamine
TFIIH	transcription factor II H
TK	thymidine kinase
TMA	tetramethylammoniumchloride
TS	thymidylate synthase
u	unit
UCL	University College London
UK	United Kingdom
UV	ultra-violet
WBB	washing-binding buffer
XPA-G	Xeroderma pigmentosum protein A to G

DRUG	CHEMICAL NAME
Anthramycin	pyrrolo[1,4]benzodiazepine
BGIII21	not available
CC1065	not available
Cisplatin	Cis-Diammineplatinum (II) dichloride
Distamycin A	Distamycin • HCl
Etoposide	4'-Desmethylepipodophyllotoxin 9-(4,6-O-ethylidene-β-D-g lucopyranoside)
Hoechst 33258	2'-(4-Ethoxyphenyl)-5-(4-methyl-1-piperazinyl)-2,5'-bi-1H-benzimidazole
Melphalan	4-Hydroxy-2-methyl-N-(5-methyl-2-thiazolyl)-2H-1,2-benzothiazine-3-carboxamide 1,1-dioxide
SCIII147	not available

1. INTRODUCTION

Cancer is responsible for a high proportion of mortalities in developed countries and is second only to cardiovascular disease as a cause of mortality. Although understanding of the molecular basis of cancer has increased substantially further research is required for the rational development of potential anti-cancer therapies.

Cancer is defined through uncontrolled cell proliferation with the cell cycle machinery deregulated most frequently upon oncogenesis. Strict developmental controls are exerted upon every cell within the human organism. In normal tissues the number of actively proliferating cells and rate of cell division varies greatly. During a normal cell cycle cells enter an early gap phase (G1) after exiting mitosis (M). Following the G1 restriction point cells enter a phase of DNA synthesis (S) and subsequently a further gap phase (G2) before re-entering mitosis. Some normal as well as cancerous cells exit the cell cycle following mitosis and enter a quiescent phase (G0) or differentiation (Pardee, 1989; Sherr, 1996).

Deregulation of the cell cycle machinery occurs as a result of aberrations in the expression of cell cycle regulatory genes. These include, regulators of G1 to S phase progression and components of the G1 checkpoint mechanism namely the G1 restriction point (Bartek, 1999; Sherr, 1996). The G1 phase checkpoint mechanisms are critical in ensuring fidelity of DNA replication and orderly progression through the cell cycle phases therefore protecting genome integrity. Unlike transit through the S, G2 and M phases, G1 progression relies upon stimulation by extracellular growth regulating signals. Multiple mitogenic signalling pathways as well as growth inhibitory signals converge upon the G1 checkpoint in the form of mitogens, nutrients, cytokines and cell-cell or cell-surface interactions (Helin, 1998; Johnson *et al.*, 1998; Lavia *et al.*, 1999; Sherr, 1996). At the molecular level, several positive and negative regulatory proteins have been identified within the G1 restriction point. These cell regulatory proteins include proto-oncogenes such as cyclin D1, D2, D3, a number of cyclin-dependent kinases including cyclin-dependent kinase 4 and 6 (CDK4/6), tumour-suppressor proteins including CDK4 kinase inhibitor (INK4) and KIP/CIP kinase inhibitors as well as the retinoblastoma tumour suppressor proteins pRb, p130 and p107 commonly known as the pocket proteins due to the presence

of a highly conserved bipartite pocket domain within the protein structure (Helin, 1998; Sherr, 1996).

Another family of cell cycle regulatory proteins includes the E2F transcription factors involved in the regulation of growth inhibition, differentiation, apoptosis and oncogenic transformation. The E2F family of transcriptional activators have been found to be important constituents of the G1 restriction point in determining whether a cell undergoes G1 phase arrest or enters into S-phase by coupling the activities of the cell cycle machinery with the transcriptional regulation of proteins whose expression is required for S-phase entry and DNA synthesis (Johnson et al., 1998; Slansky et al., 1996). The E2F protein family executes these diverse activities through tight regulation of the spatial and temporal expression of distinct E2F factors and through associations with cell cycle-regulatory proteins resulting in various multiprotein complexes containing E2F factors (Johnson et al., 1998). E2F DNA-binding sites are found in the promoters of genes encoding proteins involved in DNA synthesis, DNA replication, DNA repair and cell cycle regulatory activities (Helin, 1998; Johnson et al., 1998; Nevins, 2001). In addition, regulation of some proto-oncogenes involved in cell proliferation, including c-myb, B-myb, c-myc and N-myc is also controlled by E2F activity (Johnson et al., 1998). Deregulation of E2F activity results in the loss of orderly cell cycle progression and division. In abandoning these G1 phase control mechanisms cells are being predisposed to malignant conversion. In conclusion, cancer cells tend to remain in cycle after passing the G1 restriction point and become refractory to extracellular growth regulatory signals (Lavia et al., 1999; Sherr, 1996).

1.1 E2F transcription factor family

The E2F transcription factor was identified as part of the adenovirus E2 promoter transcription complex and a target for transactivation by the adenovirus E1A (Chellapan et al., 1991; Kovesdi et al., 1986). It was first cloned through its association with the pRb pocket protein (Helin et al., 1992; Kaelin et al., 1992). Further, it was found that pRb and E2F interact in vitro and in vivo and it was suggested that E2F preferentially binds to the unphosphorylated form of pRb (Helin et al., 1992; Kaelin et al., 1992). A number of DNA tumour viruses, including adenovirus E1A and simian virus 40 large T antigen, binding to pRb were found to provoke the release of the E2F transcription factor from its complex

with pRb (Bandara *et al.*, 1991; Helin *et al.*, 1992; Kaelin *et al.*, 1992). The E2F transcription factor specifically recognises the E2F recognition sites of E2F-regulated gene promoters and is able to transactivate the adenovirus E2 promoter (Helin *et al.*, 1992; Kaelin *et al.*, 1992).

The E2F transcription factor family consists of at least seven distinct genes divided into two groups. *E2F-1*, *E2F-2*, *E2F-3*, *E2F-4* and *E2F-5* constitute one group while the E2F-associated *DP1* and *DP2* genes constitute a separate group (Girling *et al.*, 1993; Ivey-Hoyle *et al.*, 1993; Lees *et al.*, 1993; Johnson *et al.*, 1998; Sardet *et al.*, 1995). The E2F protein subgroup consists of five members (E2F-1 to E2F-5) that can be further divided based on structure and affinity for members of the pocket protein family (pRb, p130 and p107) (Slansky *et al.*, 1996). E2F-1, E2F-2 and E2F-3 are structurally more closely related to each other than E2F-4 and E2F-5 (**Fig. 1.1**). The DNA-binding domain found in the amino terminus represents the area of greatest homology between the five E2F species (Sardet *et al.*, 1995). Adjacent to the DNA-binding domain is the DP heterodimerisation domain and the carboxy terminus of each of the five E2F polypeptides contains a defined transcriptional activation domain. Embedded within the transactivation domain of each E2F is a region of homology involved in binding to the pocket proteins (Helin *et al.*, 1992). An additional region of homology, termed the Marked box is highly conserved between the different E2Fs and is required for binding to the adenovirus E4(ORF6/7) protein (Cress *et al.*, 1996; Johnson *et al.*, 1998). E2F-1, E2F-2 and E2F-3 contain an additional region of homology not found in E2F-4 or E2F-5. This region was shown to have several functions, including cyclin A protein binding. Finally, the E2F-4 protein contains a stretch of consecutive serine residues between the Marked box and the pocket protein binding domain not found in other E2F family members (Johnson *et al.*, 1998). DP1 and DP2 polypeptides contain DNA-binding and dimerisation domains related to the E2F proteins but do not contain transcriptional activation domains or regions homologous to the pocket protein binding or Marked box domain (Johnson *et al.*, 1998; Slansky *et al.*, 1996).

Recently an additional E2F transcription factor has been isolated called *E2F-6* or *EMA* (E2F-binding site modulating activity). The dimerisation and DNA binding properties of E2F-6 are similar to those of the other E2F family members. E2F-6 shares
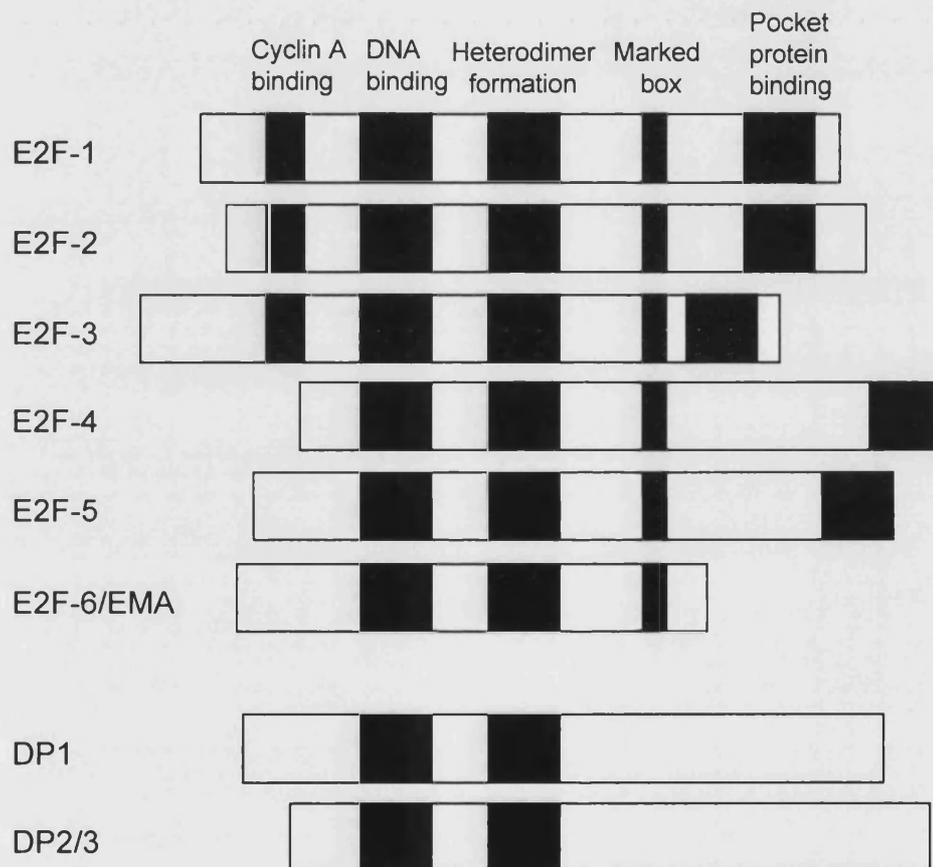
Fig. 1.1: Schematic representation of the E2F protein family
(Johnson *et al.*, 1998)

homology with the other E2F proteins in the DNA-binding domain and the Marked box, but in contrast to all other E2F transcription factors lacks a C-terminal transactivation domain as well as the pocket protein binding domain (Cartwright *et al.*, 1998). Instead it contains a short co-linear motif that mediates binding to the *Rb* family members (Kaelin, 1999).

A functional E2F transcription factor consists of a heterodimer containing an E2F protein subunit and a DP protein subunit (Bandara *et al.*, 1993; Huber *et al.*, 1993). Heterodimerisation of the E2F and DP family members is required for high-affinity binding to E2F consensus sites and to pocket proteins (Bandara *et al.*, 1994; Huber *et al.*, 1993; Slansky *et al.*, 1996). E2F/DP heterodimers binding to consensus E2F sites activate E2F site-dependent transcription in a synergistic fashion (Bandara *et al.*, 1993). To elucidate DNA-binding of the E2F/DP heterodimer, an investigation into the structure of the E2F-4-DP2 heterodimer revealed both protein subunits to make similar contacts to the bases in the major groove of the DNA thereby recognising a CGCGCG binding sequence. In addition, an extension of the original CGCGCG-binding site through the addition of TTT to the 5' end was found to aid in orientating the E2F-DP heterodimer on the promoter. The contact residues for the consensus bases and DNA phosphodiester backbone are highly conserved throughout the E2F protein family suggesting other combinations of E2F/DP heterodimers to bind DNA in a similar way (Zheng *et al.*, 1999).

E2F-6 like all other E2F transcription factors forms heterodimers with DP1 or DP2 and binds E2F DNA-binding sites (Johnson *et al.*, 1998). However, it appears that E2F-6 performs as a repressor of E2F site-dependent transcription independent of pocket protein binding. The mechanism of repression has been proposed to be either through competitive inhibition with other E2F species or through an active transcriptional repression domain located in the amino terminus of E2F-6 (Johnson *et al.*, 1998; Trimarchi *et al*, 1998).

1.2 Temporal and spatial expression of E2F transcription factors

Distinct differences in the pattern of expression, as a result of cell growth, have been reported for the five well-characterised *E2F* family member genes (Helin, 1998; Johnson *et al.*, 1998; Nevins, 1998). However, the transcription control of *E2F-6* has not been elucidated. The *E2F-4* and *E2F-5* genes are constitutively expressed throughout the cell cycle. A small temporary increase in E2F-4 protein expression level in response to growth

stimulation in mid G1 occurs before returning to the base level of expression upon S phase entry (Moberg *et al.*, 1996; Nevins, 1998; Sardet *et al.*, 1995 Slansky *et al.*, 1996). *E2F-4* mRNA is the most abundant and consistent with this finding the E2F-4 protein makes up the majority of E2F complexes as well as DNA-binding activity in cells (Johnson *et al.*, 1998; Verona *et al.*, 1997).

Similarly to E2F-4, E2F-5 expression levels increase in early-to-mid G1 and plateau thereafter as cells enter S-phase (Johnson *et al.*, 1998). Thus, E2F-4 and E2F-5 appear to regulate the transcription of E2F-dependent genes in quiescent cells and early G1 phase prior to synthesis of E2F-1, E2F-2 and E2F-3 (Helin, 1998). The majority of E2F-4 and E2F-5 proteins are located in the cytoplasmic part of the cell but a fraction is found in the nucleus of asynchronously growing cells dependent on tissue specificity (Lindeman *et al.*, 1997; Mueller *et al.*, 1997; Verona *et al.*, 1997). Experiments showed that ectopically expressed E2F-4 and E2F-5 localises predominantly in the cytoplasm and is unable to enter the nucleus (Allen *et al.*, 1997; Lindeman *et al.*, 1997; Verona *et al.*, 1997). Nuclear accumulation of E2F-4 and E2F-5 requires a nuclear localisation signal (NLS) provided by either the DP2 heterodimeric protein subunit or through the association with the pocket proteins, p130 or p107 (Allen *et al.*, 1997; Lindeman *et al.*, 1997; Mueller *et al.*, 1997; Verona *et al.*, 1997).

The mechanisms of nuclear accumulation contribute to the effect E2F-4 and E2F-5 expression has on cell cycle progression. Throughout G0 the pocket protein-mediated nuclear uptake of E2F-4 and E2F -5 prevents cell cycle progression through pocket protein-mediated transcriptional repression of E2F-responsive genes. In contrast, DP-regulated nuclear uptake promotes cell cycle progression through an enhanced transactivation of E2F-regulated genes (Allen *et al.*, 1997). These findings suggest that E2F-4 activity is controlled at the level of sub-cellular localisation in addition to pocket protein binding.

A similar pattern of expression to E2F-4 and E2F-5 is observed with regard to DP1 and DP2 (Johnson *et al.*, 1998; Nevins, 1998). DP1 is expressed constitutively with a peak in mid G1 (Johnson *et al.*, 1998; Sardet *et al.*, 1995). The DP1 protein is predominantly found in the cytoplasm while DP2, containing a NLS, is mainly localised in the nucleus (Allen *et al.*, 1997; Lindeman *et al.*, 1997; Verona *et al.*, 1997). Nevertheless, experiments have shown DP1 to be the prevalent partner in the majority of E2F heterodimeric DNA-binding complexes (Johnson *et al.*, 1998; Sardet *et al.*, 1995).

Expression of *E2F-1*, *E2F-2* and *E2F-3* genes is dependent on stimulation of cell growth and all three proteins are found exclusively in the nucleus as a direct consequence of an innate NLS (Allen *et al.*, 1997; Lindeman *et al.*, 1997; Mueller *et al.*, 1997; Verona *et al.*, 1997). In quiescent cells no *E2F-1*, *-2* or *-3* gene expression is seen, however transcription is rapidly induced in response to mitogenic stimulation (Nevins, 1998). For example, upon stimulation of serum-starved fibroblasts or resting T cells to enter the cell cycle, the level of *E2F-1* mRNA dramatically increases at the G1/S-phase boundary (Johnson *et al.*, 1998). E2F-2 is expressed with similar kinetics although at an overall lower level in fibroblasts (Johnson *et al.*, 1998). Repression of *E2F-1*, *-2* and *-3* transcription in quiescent cells appears to be E2F-dependent as a result of the presence of E2F binding sites within the promoter regions of the *E2F-1*, *-2* and *-3* genes. E2F-4 and E2F-5, in conjunction with p130 are suggested to control the expression of E2F-1, E2F-2 and E2F-3 (Nevins, 1998).

1.3 E2F-regulated genes

E2F regulated genes are involved in DNA synthesis, DNA replication, regulatory control of cell cycle progression and various DNA repair activities (Nevins, 2001). Proteins participating in DNA synthesis include dihydrofolate reductase (DHFR), thymidine kinase (TK) and the DNA polymerase α subunit I and II, proliferating cell nuclear antigen (PCNA) as well as the DNA polymerase δ catalytic subunit (DeGregori *et al.*, 1995; Fry *et al.*, 1997a; Kalma *et al.*, 2001; Sala *et al.*, 1994). Induction of these genes occurs in mid to late G1 phase as a direct result of E2F accumulation.

Experiments using an adenoviral vector containing *E2F-1* cDNA confirmed the E2F-1 dependent activation of S phase genes required for DNA synthesis such as *thymidylate synthase* (TS), *PCNA, ribonucleotide reductase* (RR) and *DNA polymerase* α (DeGregori *et al.*, 1995). Furthermore, regulatory genes active during G1 to S phase progression such as *cyclin E, cyclin A, B-myb* and *cdc2* were activated in the presence of E2F-1 (DeGregori *et al.*, 1995; Furukawa *et al.*, 1994; Ohtani *et al.*, 1995). Several proto-oncogenes were shown to be induced by E2F including *c-myc, N-myc, cyclin-D1, c-myb* and *B-myb* (DeGregori *et al.*, 1995; Ohtani *et al.*, 1995; Sala *et al.*, 1994). In addition, Kalma *et al.* provided evidence for the E2F-1 induced upregulation of novel genes encoding proteins that participate in DNA replication. These include the 32Kd subunit of

the *replication protein A* (RPA2), *topoisomerase IIα* and subunit IV of *DNA polymerase* α (Kalma *et al.*, 2001).

1.4 Pocket protein family (pRb, p130 and p107)

The retinoblastoma gene (*Rb*) was the first tumour suppressor gene to be identified and was isolated by positional cloning from retinoblastoma tumours. The tumour suppressor protein function of pRb was confirmed by its ability to inhibit the malignant phenotype when expressed in retinoblastoma-tumour cells. Tumour suppression by pRb requires the central "pocket" domain, which is disrupted by tumour-promoting mutations and is targeted by viral oncoproteins. The E1A adenovirus protein disrupts pRb-E2F complexes by binding to the pocket region of pRb thereby releasing 'free' E2F which in turn binds DNA (Bagchi *et al.*, 1991). Whereas the *Rb* gene is frequently found mutated in tumours such as retinoblastoma, osteosarcoma, small-cell lung cancer, bladder and mammary cancers, pRb function is found disrupted in the majority of tumours through either deregulation of upstream signalling pathways or mutation or deletion of the *Rb* gene (Harbour *et al.*, 2000; Hatakeyama *et al.*, 1995). Loss of pRb function also creates a selective pressure for the tumour to inactivate the pro-apoptotic tumour suppressor p53, which serves to eliminate cells with mutations in the pRb pathway. As a result many tumours have mutations inactivating both pRb and p53 (Harbour *et al.*, 2000).

The human pocket protein family includes three known members, pRb, p107 and p130, which are highly related in amino acid sequence as well as function (Nevins, 1998). The human pRb protein is a nuclear phosphoprotein spanning 928 amino acids (Herwig *et al.*, 1997; Kaelin, 1999). The defining characteristic of the pocket protein family is a highly conserved bipartite pocket structure. These A and B pocket domains are necessary for interaction with viral oncoproteins such as the adenovirus E1A protein and for association with members of the E2F transcription factor family both containing the binding sequence LXCXE (Bagchi *et al.*, 1991; Classon *et al.*, 2001; Dahiya *et al.*, 2000; Kaelin, 1999). These proto-oncogene-pRb interactions are critical for the transforming activity of the DNA viruses (Hatakeyama *et al.*, 1995).

In addition the pocket proteins contain multiple sites for phosphorylation by CDKs, including a large cluster of sites in the extreme C-terminus of the pocket proteins. However,

p130 and p107 are structurally more closely related to each other than they are to pRb. p107 and p130 each contain insertions within the B domain of the pocket domain that are missing from pRb. In addition the spacer sequences found in p107 and p130 which separate the A and B subdomains of the pocket domain are longer than the analogous region in pRb. The p107 and p130 spacer regions contain homologous sequences and include a high-affinity binding site for cyclin A/CDK2 and cyclin E/CDK2. This motif, not present in pRb, allows p107 and p130 to form stable complexes with these CDKs suggesting that p107 and p130 function as CDK inhibitors (Classon *et al.*, 2001; Herwig *et al.*, 1997).

1.5 Temporal and spatial expression of pRb, p130 and p107

A distinguishing feature of the members of the pocket protein family is the pattern of accumulation of the individual proteins during cell growth. Accumulation of p130 drives cells to enter the quiescent phase of the cell cycle (G0). Within quiescent cells p130 is found complexed to E2F-4, the most abundant member of the E2F family in G0 phase (Mayol *et al.*, 1998; Moberg *et al.*, 1996). The p130-E2F-4 complex has been suggested to actively repress the transcription of E2F-regulated genes such as *E2F-1, –2* and *p107* (Johnson *et al.*, 1994; Mayol *et al.*, 1998; Sears *et al.*, 1997; Zhu *et al.*, 1995). Upon re-entry of quiescent cells into the cell cycle p130 is phosphorylated by cyclin D-CDK4/6 and subsequently degraded by proteasomes (Mayol *et al.*, 1998; Nevins, 1998).

The p107 protein is not found in quiescent cells and starts to accumulate as cells re-enter the cell cycle (Nevins, 1998). The increase in p107 protein level is a result of de-repression of the E2F-responsive *p107* promoter following phosphorylation of the p130-E2F-4 repressor complex. Levels of p107 increase as cells pass through G1 and remain relatively constant in proliferating cells (Nevins, 1998). The synthesis of p107 promotes complex formation with 'free' E2F-4 following the degradation of p130 (Moberg *et al.*, 1996). In contrast to p130, pRb and p107 although phosphorylated by cyclin D-CDK4/6, are not being targeted for degradation. The characteristic that singles p130 out for degradation has been identified as a unique type of phosphorylation, as opposed to the more common types of phosphorylation found in quiescent cells (Mayol *et al.*, 1998). To conclude, whereas p130 is readily detected in quiescent cells, the p107 protein is primarily found in proliferating cells (Nevins, 1998).

In contrast to the cell cycle dependent expression of p130 and p107, pRb expression appears to be independent of the cell growth state. In G1 phase a small increase in pRb accumulation occurs, considered a consequence of E2F accumulation combined with the fact that the *Rb* promoter is responsive to E2F. Generally the level of pRb expression does not vary greatly between quiescent and proliferating cells. A major control of pRb function is the phosphorylation state of the protein. pRb is detected only as a hypophosphorylated form in cells in the G0 and early to mid-G1 phases before phosphorylation occurs in mid-to-late G1 phase disrupting pRb interaction with the E2F proteins. The hyperphosphorylated form of pRb continues to persist until the end of M phase. When cells enter into the next G1 phase attached phosphates are stripped off pRb by phosphatases and the pRb protein is found once again in its hypophosphorylated form. Phosphorylation is shown to be predominantly dependent on the action of D-type cyclins in association with CDK4 and CDK6 (Hatakeyama *et al.*, 1995; Nevins, 1998).

1.6 Control of E2F transcriptional activity

Various levels of control influencing E2F transactivation have been discussed already including spatial and temporal differences in intra-cellular E2F expression, heterodimer formation and associations with pocket proteins. In addition E2F activity is regulated at the level of phosphorylation through cyclin A-CDK2, acetylation, methylation and protein stabilisation. Finally, E2F transactivation activity has also been found dependent on the positioning of the E2F element in relation to the transcriptional start site.

1.6.1 Position of E2F element to transcriptional start site

Transcription of the *E2F-1*, *-2* and *-3* is upregulated during the G1-S phase transition hence the respective DNA-binding activities encoded by these proteins are transient throughout the G1-S phase (Nevins, 1998). All E2F transcription factors except E2F-5 and -6 are able to induce S phase and activate E2F regulated genes. Gene activation is regulated by a differential response to individual E2Fs. Some genes such as *DNA pol α* are activated by all E2F transcription factors except E2F-5 and -6 while others such as *TK* and *DHFR* are preferentially regulated by E2F-2 (DeGregori *et al.*, 1997). Normal progression from G1 to S phase is therefore dependent on the co-ordinated activation of E2F target genes by individual E2F transcription factors.

Transcriptional regulation experiments using the *DHFR* promoter have shown that S phase specific transcriptional activation is dependent on the proximal positioning of the E2F element to the transcriptional start site to ensure high-level activity from the *DHFR* promoter. Thus, E2F-mediated growth regulation is position-dependent specified by the *DHFR* promoter and not by the characteristics of individual E2F elements. In contrast, transcriptional repression is independent of the position of the E2F element (Fry *et al.*, 1997a). Further, investigations into the protein-protein interactions required for *DHFR* promoter activation revealed that only recruitment of cAMP-response element-binding protein (CBP), appeared to play an effective role in promoter activation. Deletion analysis revealed a 38 amino acid long region (399-437) of E2F-1 to be adequate for maximal activation of the *DHFR* promoter and within the core E2F transactivation domain two phenylalanine residues are essential for transcriptional activation of *DHFR* and binding of CBP, TFIIH and the TATA-box-binding-protein (TBP). These have been identified to be up-regulators of E2F activity in contrast to the negative regulatory proteins p53 and pRb (Fry *et al.*, 1997b; Martinez-Balbas *et al.*, 2000).

1.6.2 E2F and acetylation

Binding of the p300/CBP co-activator complex has been shown to increase E2F activity. p300/CBP and the p300/CBP associated factor (P/CAF) both display histone acetylase activity suggesting E2F activity to be regulated through acetylation. P/CAF and p300/CBP have been shown to acetylate E2F-1, -2 and -3 *in vitro* and *in vivo* through an N-terminal acetylation site adjacent to the E2F-1 DNA binding domain (Martinez-Balbas *et al.*, 2000; Marzio *et al.*, 2000). In contrast, acetylation was not detected with respect to E2F-4, -5 and -6 (Marzio *et al.*, 2000). The site-specific acetylation by P/CAF and p300/CBP was found to increase DNA binding ability, transcriptional activation capacity and the protein half-life of E2F-1 (Martinez-Balbas *et al.*, 2000). Finally, E2F acetylation was reversed *in vitro* by incubation with histone deacetylase-1 (HDAC-1) suggesting reversible acetylation as a general mechanism for the regulation of E2F activity (Marzio *et al.*, 2000).

The proposed concept of reversible acetylation as a regulatory mechanism for E2F activity was further validated by an earlier study by Ferreira *et al.* that showed pocket proteins pRb, p130 and p107 were able to bind HDAC-1 through the LXCXE motif located within the A/B pocket in the C-terminus. Through the simultaneous association with

HDAC-1 and E2F-4, p130 and p107 target histone-deacetylase activity to the E2F binding domain of E2F-4 responsive promoters, enforcing an E2F-4-mediated repression of the target promoter. An identical mode of action has been suggested for complexes including pRb, E2F-1 and HDAC-1 (Ferreira *et al.*, 1998).

1.6.3 Methylation of E2F binding sites

Besides acetylation, methylation has been suggested as an additional mechanism involved in the regulation of E2F activity due to the fact that E2F binding sites in many E2F regulated promoters contain one or more CpG motif and, therefore, are candidates for regulation by methylation. A study using the E2F-binding elements of a selection of E2F regulated promoter sequences including *DHFR*, *E2F-1*, *cdc2*, *c-myb* and *c-myc* found hypermethylation of *DHFR*, *E2F-1* and *cdc2* blocked E2F-1 to -5 transcription factor binding. However, hypermethylation of c-myb and c-myc resulted in a selective binding of E2F whereby E2F-2 to –5 were able to bind both E2F elements while E2F-1 failed to bind either, *in vitro* and *in vivo*. All five E2F transcription factors were able to bind to the unmethylated E2F-binding sequences of *DHFR*, *E2F-1*, *cdc2*, *c-myb* and *c-myc* (Campanero *et al.*, 2000).

1.6.4 Regulation of E2F activity through cyclin A/CDK2

Phosphorylation of the DP1 protein associated with E2F-1 by a cyclin A-dependent kinase downregulates E2F activity in S-phase through the loss of DNA-binding and transactivation capacity of the E2F-1/DP1 heterodimer (Dynlacht *et al.*, 1997; Helin, 1998; Krek *et al.*, 1994; Nevins, 1998). This downregulation of E2F-1 activity stands in contrast to the inhibition of E2F-1/DP-1 activity during early-mid G1 phase as a result of binding to pRb and subsequent promoter repression. Hence, the observed transient accumulation of E2F in late G1 phase is the result of both early inhibition by pRb and other pocket proteins and late downregulation of E2F-1 activity by phosphorylation of the E2F protein complex by cyclin A-CDK2. A short region of eight amino acids within the cyclin A binding domain of E2F-1 is required for the binding of E2F-1 to cyclin A and has been shown to be sufficient for the interaction between E2F-1 and cyclin A (Helin, 1998). Furthermore, the E2F-1 sequences recognised by cyclin A-CDK2 are also found in the E2F-2 and E2F-3 associated with p107, p130 and members of the p21-CDKI family suggesting a common basis for control of the

inducible E2F proteins by cyclin A-CDK2 (Dynlacht *et al.*, 1997; Helin, 1998; Nevins, 1998). Neither E2F-4 nor E2F-5 contain the binding motif or binds cyclin A-CDK2. Downregulation of E2F-1 activity in the S-phase of the cell cycle is essential in order to allow cells to enter G2 (Helin, 1998). Disruption of this regulatory mechanism resulting from mutation of the cyclin A binding domain leads to cell cycle arrest, apoptosis and cell death (Nevins, 2001; Nevins, 1998). It appears that certain E2F regulated genes must be downregulated in order for cells to enter G2 and constitutive activity of such genes would be deleterious for the cell (Helin, 1998). Alternatively it has been proposed that prolonged binding of E2F to E2F recognition sites upstream of an origin of replication in certain promoters, like DHFR perturbs DNA replication (Krek *et al.*, 1995).

1.6.5 Ubiquitination of E2F

Recent data have suggested that the activity of the E2Fs is also subject to ubiquitin-mediated degradation via the ubiquitin-26S-proteasome pathway *in vivo* (Campanero *et al.*, 1997; Hateboer *et al.*, 1996; Helin, 1998; Hofmann *et al.*, 1996; Nevins, 1998). By transfecting various cell lines with E2F expression plasmids in combination with *Rb* family members, it was demonstrated that E2F-1 and E2F-4 are stabilised by interaction with pRb or p107/p130, respectively. The half-lives of uncomplexed E2F-1 and E2F-4 are 2-3 hours, and the binding of an Rb family member increases the half-lives to 10-12 hours. Co-transfection of *E2F-1* and *E2F-4* with tagged ubiquitin, and subsequent treatment with proteasome inhibitors, further demonstrated that the E2Fs are able to be ubiquitinated *in vivo* (Campanero *et al.*, 1997; Hateboer *et al.*, 1996; Helin, 1998; Hofmann *et al.*, 1996). The amino acid sequence within the carboxy-terminus of E2F-1 is required for degradation, and binding of pRb protects the E2F-1 protein from degradation. Therefore control of DNA-binding and protein stability regulate the accumulation of E2F-1 and possibly that of the related E2F-2 and E2F-3 proteins as cells progress through the cell cycle (Nevins, 1998).

1.7 Transcriptional repression by pocket protein/E2F complexes

Although there are distinctions in functional properties, each of the pocket proteins binds to E2F and is substrate for phosphorylation by G1 CDKs (Classon *et al.*, 2001; Herwig *et al.*, 1997; Nevins, 1998). pRb, p130 and p107 have been found to block transcriptional

activation by free active E2F and are capable of repressing E2F-regulated promoters (Classon *et al.*, 2001).

The model of pRb binding and masking the E2F transactivation domain led to the assumption that pRb sequesters and inactivates E2F transactivation activity in G0 and G1 and phosphorylation of pRb in late G1 leads to the release of free, transcriptionally active E2F. However, elimination of the E2F sites from many E2F-responsive promoters led to an increase in transcriptional activity in G0/G1 rather than a decrease in S phase. This indicated that the role of E2F sites, at least in certain contexts, was to repress transcription in G0/G1. Furthermore, these findings suggested that pRb rather than simply neutralising E2F transactivation function are able to actively repress transcription when tethered to DNA by means of E2F (Kaelin, 1999) (**Figure 1.2**).
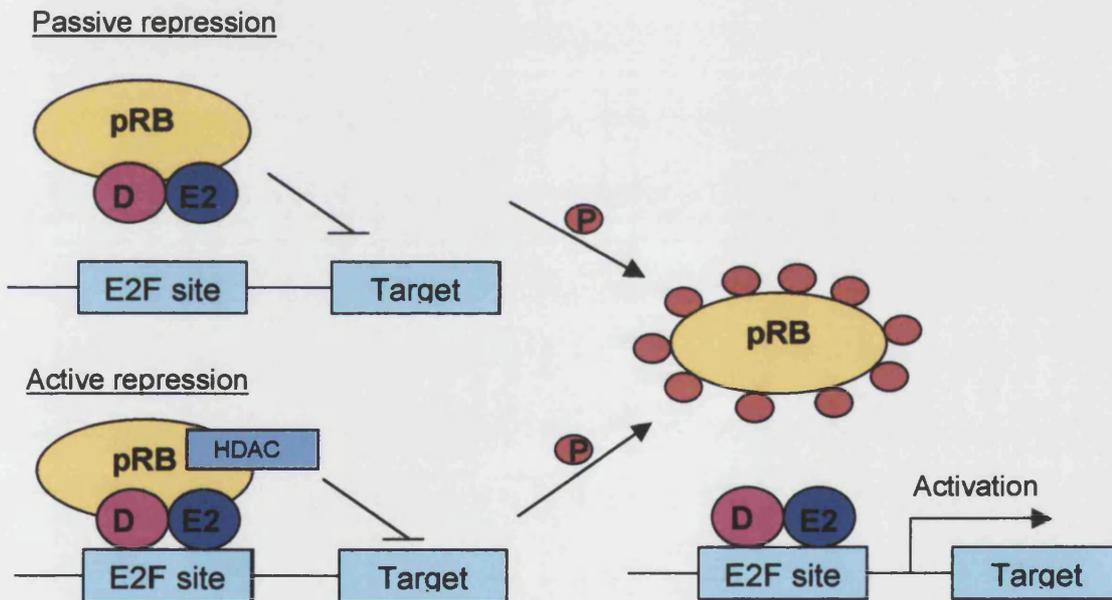
Figure 1.2: Transcription control of E2F-regulated genes by E2F
pRb binds to an E2F-DP complex in cells in the G0/G1 stage of the cell cycle.
This leads to repression of E2F-responsive genes, firstly by inhibiting E2F from activating transcription by binding its transactivation domain, and secondly by active repression whereby it recruits factors such as HDAC, which modifies histone tails and therefore facilitates nucleosome packaging. Cyclin D-CDK4/6 and Cyclin E-CDK2 phosphorylate pRb resulting in the release of E2F, activating E2F responsive genes. Modified from Bell *et al.* 2003.

E2F bound pRb represses transcription of E2F-responsive genes through several mechanisms. For example, pRb prevents direct interaction of E2F with factors such as TATA-binding protein (TBP) thereby inhibiting activation through competitive binding (Connor et al., 2001). Also, pRb tethered to the promoter through E2F binds and inactivates adjacent susceptible transcription factors, blocking their interaction with the basal transcription complex (Connor et al., 2001). The E2F-mediated repressor activity of the pocket proteins results in the inhibition of promoters that include enhancers in addition to E2F sites. The repression of promoters is suggested to require the recruitment of several corepressors such as histonedeacetylases (HDAC) (Di Ciommo et al., 2000).

1.8 E2F and pocket proteins as part of cell cycle regulation

The family of pocket proteins controls gene expression mediated by the E2F family of heterodimeric transcriptional regulators. The pocket proteins interact with any of the 5 well-characterised E2F isomers thereby regulating E2F activity so as to drive the exit from the cell cycle (Nevins, 2001; Nevins, 1998). The various E2F family members differ in their associations with the pocket proteins and E2F activity is either directly inhibited through pocket protein binding or transcription of E2F-responsive promoters repressed through E2F-mediated binding of pocket proteins (Classon et al., 2001; Helin, 1998; Johnson et al., 1998; Kaelin et al., 1998). E2F-1, E2F-2 and E2F-3 bind exclusively pRb and with low affinity p107 or p130 (Helin, 1998). E2F-4 and E2F-5 associate with all three of the pocket proteins in a cell cycle-regulated manner (Johnson et al., 1998; Moberg et al., 1996). The DP heterodimerisation partner appears not to be involved in determining the binding specificity of E2F factors for the pocket proteins. However, DP factors do function in stabilising the interaction between E2F factors and the pocket proteins (Johnson et al., 1998).

The predominant form of E2F in quiescent or differentiated cells is a complex involving either E2F-4 or E2F-5 protein in association with p130 where E2F-mediated gene expression is repressed (Classon et al., 2001; Helin, 1998; Nevins, 1998). This characteristic E2F-4-p130 complex appears following cell cycle exit or differentiation (Nevins, 1998). These complexes play an active role in maintaining the quiescent state by preventing the expression of growth-regulatory genes.

31

Following growth stimulation, the E2F-p130 complex disintegrates following phosphorylation of the p130 protein by G1 CDKs and subsequent degradation of the p130 protein. The result is the de-repression of a number of genes encoding DNA replication and growth-regulatory activities. These include *E2F-1*, *E2F-2* and *E2F-3* (Johnson *et al.*, 1998; Nevins, 1998). In addition elimination of the E2F-4/E2F-5-p130 repressor complex leads to an activation of *p107* expression resulting in the accumulation of p107 protein in late G1 and S phase (Helin, 1998; Nevins, 1998; Sherr, 2000). p107 is found to interact predominantly with E2F-4 and E2F-5 proteins and complexes containing p107 in association with E2F-4 are detected at the G1/S-phase transition, (Johnson *et al.*, 1998; Nevins, 1998). The p107 protein has the capacity to recruit cyclin A-CDK2 kinase into a multimeric complex involving either E2F-4 or E2F-5 and the cyclin A-containing p107 complex represents the predominant state of p107 bound E2F in proliferating cells. It has been suggested that E2F-4 and E2F-5 although lacking the cyclin A binding domain found within E2F-1, E2F-2 and E2F-3 might be regulated by cyclin A-CDK2 with p107 serving as an adaptor to bring the kinase to these proteins (Dynlacht *et al.*, 1997). The fact that E2F-p107 persists and is specifically expressed in proliferating cells suggests a proliferation-related rather than a growth-suppressing role (Nevins, 1998). However, recent studies have demonstrated that E2F-4-p107-cyclin A-CDK2 complexes are found primarily in the cytoplasm where they would be unable to directly regulate transcription (Johnson *et al.*, 1998)

Cyclin-dependent protein kinases (CDKs) control the passage through the G1 restriction point and entry into S phase. CDK activity requires cyclin binding, regulated by cyclins D, E and A, depends on both positive (cyclin activating kinase- CAK) and negative regulatory phosphorylations and can be constrained by two families of CDK inhibitory proteins (INK and CIP/KIP). The expression of D-type cyclins is dependent on extracellular growth factors and both cyclin synthesis and assembly into catalytic units with CDK4 and CDK6 is reliant on mitogenic stimulation. Catalytic activity of the cyclin-CDK enzymes first occurs in mid-G1 and reaches its peak at G1-S transition. The INK and CIP/KIP families of cyclin dependent kinase inhibitor proteins block CDK4 and CDK6 activity and lead to G1 arrest (Sherr, 1996; Sherr 2000) (**Fig. 1.3**).

D-type cyclins modulate the function of pRb by activating the associated cyclin-dependent kinases (CDK4 and CDK6) that in turn phosphorylate pRb (Johnson *et al.*, 1998). pRb phosphorylation occurs during the G1 phase of the cell cycle and is required for G1 exit. Therefore D-type cyclins not only function as regulatory subunits for their associated CDKs but also act to target pRb for phosphorylation through protein-protein binding (Johnson *et al.*, 1998).

As previously discussed in section 1.7. hypophosphorylated pRb binds to a subset of E2F complexes, either resulting in repressor complexes through the recruitment of histone deacetylases and chromosomal remodeling SWI/SNF complexes to E2F-binding sites on E2F regulated gene promoters or inhibits the transactivation activity of E2F through containment of free E2F in pRb complexes (Classon *et al.*, 2001; Sherr, 2000). Mitogen-dependent accumulation of cyclin D-dependent kinases results in the phosphorylation of pRb followed by a rapid increase in free E2F protein causing the de-repression or activation of E2F-responsive genes required for DNA synthesis and replication (**Fig. 1.3**). Sequential phosphorylation of pRb initiated by cyclin D-dependent kinases is completed by the cyclin E-CDK2 complex (Johnson *et al.*, 1998; Sherr, 1996; Sherr, 2000). Cyclin E forms active catalytic complexes with CDK2 and expression is maximal at G1-S transition. A positive feedback mechanism facilitates progressive rounds of pRb phosphorylation and E2F release as cyclin E expression is regulated by E2F (Dynlacht *et al.*, 1994; Sherr, 1996) (**Fig. 1.3**). E2F-1 in turn controls its own transcription by positive feedback. Therefore positive cross-regulation of E2F and cyclin E produces a rapid increase in both activities as cells approach G1-S transition.

As a result pRb inactivation shifts from being mitogen-dependent (cyclin D-driven) to mitogen-independent (cyclin E-driven). This point is referred to as the restriction point defined by the irreversible commitment of the cell to progression through the cell cycle up to the completion of mitosis (Pardee, 1989; Pardee, 1974).
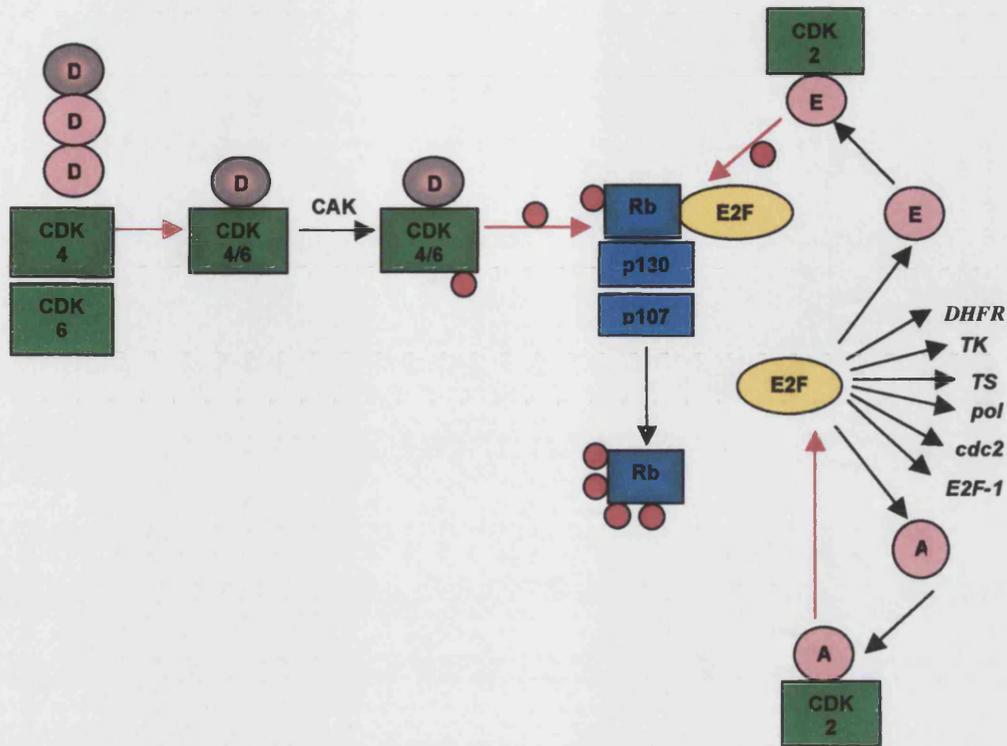
Fig. 1.3: Restriction point control. The proteins most frequently targeted in human cancers are highlighted. Cyclins are shown in pink, CDKs in green. Arrows depicting inhibitory phosphorylation (P) or inactivating steps are shown in red, and those depicting activating steps are shown in black (Sherr *et al.*, 1996). For details refer to text.

Cyclin A- and cyclin B-dependent kinases maintain pRb in its hyperphosphorylated state and dephosphorylation of pRb does not occur until cells complete mitosis and re-enter the G1 phase (Sherr *et al.*, 1999). Entry into S phase also results in the inactivation of cyclin E and E2F. Phosphorylation of cyclin E by CDK2 initiates ubiquitin-dependent proteolysis and the degradation of cyclin E. Cyclin A-CDK2 complexes accumulate throughout S phase, bind to E2F and phosphorylate the DP-1 protein subunit of the active E2F transcription factor thereby abrogating DNA binding of E2F and inhibiting transactivation of E2F regulated genes (Dynlacht *et al.*, 1994; Dynlacht *et al.*, 1997; Sherr, 2000).

Cyclin D-, E- and A-dependent kinases are negatively regulated by a distinct family of CDK inhibitors (p21^{Cip1}, p27 ^{Kip1}, p57^{Kip2}) (**Fig. 1.4**). Levels of p27 ^{Kip1} in quiescent cells are high and decrease upon cell cycle entry. Accumulation of cyclin D-dependent kinases results in the sequestration of p21^{Cip1} and p27 ^{Kip1} kinase inhibitors into complexes with cyclin D-CDK4/6, alleviating repression of cyclin E-CDK2 and cyclin A-CDK2 activity in cycling cells. The p27 ^{Kip1} kinase inhibitor is required for the assembly of the active cyclin D/CDK4/6 holoenzymes and the cyclin D-dependent kinases remain active thereafter (Sherr, 1996; Sherr, 2000) (**Fig. 1.4**). In addition, activation of cyclin E-dependent kinases leads to the phosphorylation of p27^{Kip1} converting it to a form recognized by ubiquitin ligases targeting it for destruction by proteasomes (Sherr *et al.*, 1999; Sherr, 2000). Cyclin D-dependent kinase bound Cip/Kip kinase inhibitors persist throughout subsequent cell cycles until the withdrawal of mitogens releases them resulting in the inhibition of cyclin E-CDK2 and G1 arrest (Sherr *et al.*, 1999).

1.9 E2F and apoptosis

Experiments in which the E2F-1 locus in mice is inactivated by homologous recombination have shown that E2F-1 has functions otherwise than cell proliferation. In addition to promoting cell proliferation E2F-1 suppresses cell proliferation depending on tissue specificity. Results showed that *E2F-1 -/-* mice were viable and fertile. However, with increasing age abnormalities occur including testicular atrophy, exocrine gland dysplasia and the development of tumours such as reproductive tract sarcomas, lung tumours and lymphomas (Tsai *et al.*, 1998; Yamasaki *et al.*, 1996). Defects in thymocyte (T) cell development due to *E2F-1* deficiency resulted in aberrant hyperproliferation of T cells and provided support to the theory that E2F-1 not only functions to positively regulate cell proliferation but is also required for apoptosis and actively suppresses cell proliferation. Therefore E2F-1 alone is not critical for S phase entry but other E2F transcription factors seem to be as important for control of S phase entry (Field *et al.*, 1996).

Studies of adenovirus mutants revealed a role for the viral E1A protein in the induction of p53-dependent cell death, dependent on E1A domains known to be involved in binding to pRb (Debbas *et al.*, 1993; Lowe *et al.*, 1993). Studies by Wu *et al.*, demonstrated that the enforced expression of E2F-1 in quiescent cells led to inappropriate S phase entry and to
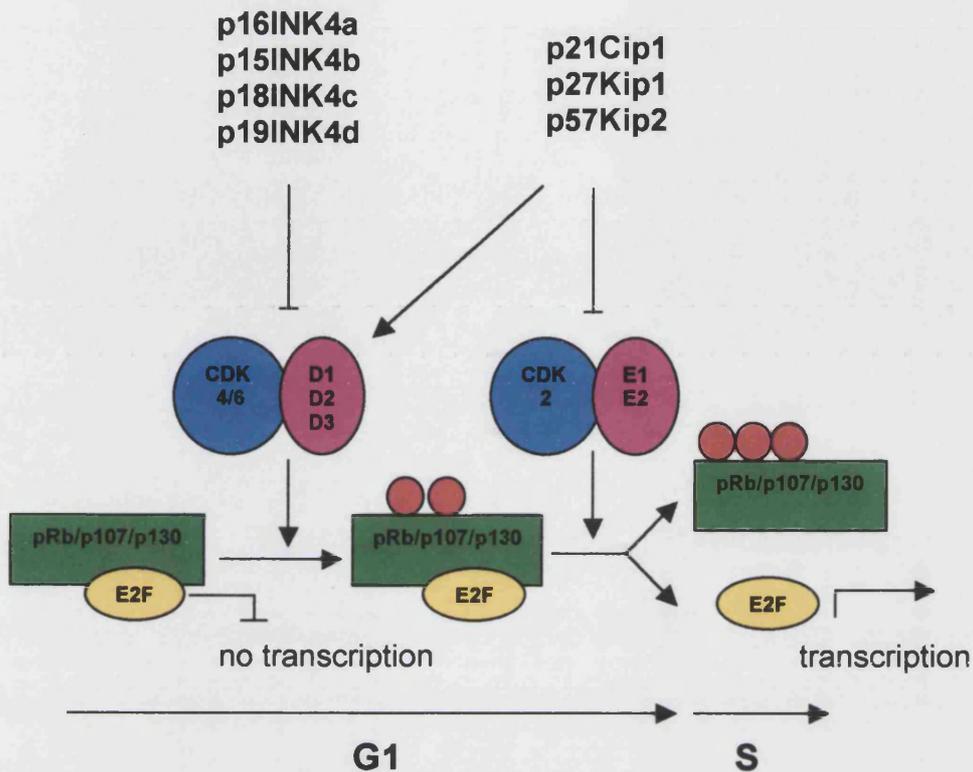
Fig. 1.4: Inhibition of G1/S transition by cyclin-dependent kinase inhibitors.
Progression through G1 phase of the cell cycle is controlled by the functional
state of the *Rb* family of proteins, pRb, p107, p130. Non-phosphorylated pRb
proteins bind to E2F and prevent E2F-dependent transcription. Activation of cyclin-D
dependent kinases 4 and 6 by their mitogen-controlled regulatory subunit results in
phosphorylation of pRb proteins.

     Activity of CDK4/6 is negatively regulated by the *INK4* family of cell cycle
inhibitors by preventing cyclin D binding to CDK4/6. CDK4/6-cyclin D complexes
also activates CDK2 by binding Cip/Kip proteins thus preventing them from
blocking CDK2-cyclin E activity. Hyperphosphorylation of Rb proteins by
CDK2-cyclin E complexes is required for entry into S phase.

induction of p53-dependent apoptosis. Experiments using overexpressed mutant E2F-1 showed that the DNA binding ability of E2F-1 is essential for the initiation of cell death and co-expression of DP-1 augments cell death (Hiebert *et al.*, 1995; Nevins, 2001; Wu *et al.*, 1994). This suggests that E2F-1 regulates genes important for apoptosis.

A role for E2F-1 in apoptosis is supported by analysis of *Rb*-null mice, in which apoptosis associated with loss of pRb function was shown to be efficiently rescued by deletion of *E2F-1* strongly supporting a role of E2F-1 in a protective response to abnormal proliferative signals (Pan *et al.*, 1998; Tsai *et al.*, 1998). Further analysis of *E2F-1* deficient mice exhibited aberrations in T cell development causing the hyperproliferation of T cells by preventing apoptosis (Field *et al.*, 1996). Therefore *E2F-1* functions as part of a tumour-suppressing mechanism whereby uncontrolled or inappropriate *E2F-1* activation results in apoptosis thus protecting the organism against oncogenic transformation (Phillips *et al.*, 1999).

1.9.1 p53-dependent apoptosis

p53 is mutated in more than 50% of human cancers. In response to cellular stress from DNA damage, hypoxia and oncogene activation, the p53 protein stabilises and accumulates. The activated p53 initiates a transcriptional programme thereby triggering either cell cycle arrest or death (Sherr, 2001).

E2F-1 induced apoptosis following induction of S phase is largely dependent on p53. Neither, E2F-2 or E2F-3 induce apoptosis despite the fact that these E2F family members also induce S phase (Kowalik *et al.*, 1998). E2F-4 or E2F-5 both do not have the ability to induce apoptosis either (DeGregori *et al.*, 1997). In addition E2F-1 together with the heterodimeric partner DP1, but not E2F-2 induces the accumulation of p53 (Hiebert *et al.*, 1995; Nevins, 1998). This is consistent with earlier work showing that adenovirus E1A induces p53 accumulation (Kowalik *et al.*, 1998).

Pan *et al.* showed using *Rb-/-* mice that inactivation of E2F-1 resulted in an 80% decrease in apoptosis in the presence of active p53 as a result of a decrease in E2F-1-induced p53 accumulation. Therefore it appears that p53 serves as a checkpoint monitoring *E2F-1* expression during cell proliferation. Further it was proven that E2F-1 lies upstream of p53 in the signalling pathway as expression of p53-dependent *p21^{WAF}*, *murine double minute 2* (MDM2) and *Bax* were reduced following E2F-1 inactivation (**Fig. 1.5**). Although

p53-dependent apoptosis was diminished in the absence of E2F-1 no accelerated tumour growth as seen upon p53 inactivation was observed due to its requirement for efficient cell cycle activity meaning that p53-dependent apoptosis is defective in the absence of E2F-1 but any impact on tumour growth is also counterbalanced by an accompanying reduction in tumour cell proliferation (Pan *et al.*, 1998).

Results by Kowalik *et al.* and Wu *et al.* support findings that p53 and E2F-1 co-operate in the induction of apoptosis, as p53-dependent induction of apoptosis through E2F-1 is regulated by MDM2 and p53 accumulation is inhibited by MDM2 (Kowalik *et al.* 1998). Binding of MDM2 to p53 was found to antagonise the transcriptional activity of p53 as well as induce p53 ubiquitination and enforce the export of p53 from the nucleus to the cytoplasm where p53 is degraded (Sherr, 2001).

The recently discovered p14^{ARF} protein was found to link the deregulated expression of E2F-1 with the subsequent occurrence of p53-dependent apoptosis. The p14^{ARF} protein stems from an alternative reading frame (ARF) within exon 2 of the *INK4a* gene locus that also codes for the *p16^{INK4a}* kinase inhibitor protein. It is suggested that the p53-dependent apoptosis pathway relies on the induction of the tumour suppressor protein *p14^{ARF}*, in response to abnormal proliferation signals, followed by the inhibition of MDM2 resulting in the accumulation and stabilisation of p53 (Bates *et al.*, 1998) (**Fig. 1.5**).

Experiments have shown *p19^{ARF}* deficient mouse embryo fibroblasts (MEFs) from knockout animals grow continuously in culture without undergoing senescence and the MEFs were susceptible to transformation by oncogenic *ras* without any co-requirement for immortalising oncogenes, such as *Myc* or *adenovirus E1A* (Sherr, 2001). Finally, the MEFs were found to proliferate more rapidly in culture than their wild-type counterparts and had properties of permanently established cell lines. *INK4a*-null MEFs have normal cell cycle profiles, arrest upon serum withdrawal and have no colony forming advantage when plated at low density (Sherr, 2001). To conclude, loss of *ARF* or *p53* leads to uncontrolled cell growth and rapid tumour formation.

1.9.2 p53-independent apoptosis

The *p53*-independent apoptosis pathway was shown to involve the *p53* homologue *p73*. E2F-1 induces the transcription of *p73* and disruption of p73 function inhibited E2F-1 induced apoptosis in *p53*-defective tumour cells and *p53$^{-/-}$* mouse embryo fibroblasts.

Hence p73 provides an alternative means for E2F-1 to induce apoptosis in the absence of *p53* (Irwin *et al.*, 2000) (**Fig. 1.5**).

Observations by Lissy *et al.* indicate that *p73* serves to integrate receptor-mediated apoptotic stimuli. Stimulation of the T-cell receptor (TCR) in cycling peripheral T cells causes apoptosis by TCR-activation-induced cell death (TCR-AICD) independent of *p53*. Inactivation of *p73* results in the inhibition of TCR-mediated apoptosis. Therefore, disruption of the *E2F-1* gene significantly increases T cell number and splenomegaly but disruption of *E2F-2*, *E2F-4* or *p53* does not (Lissy *et al.*, 2000).

In addition, E2F-1 is able to induce apoptosis via a death receptor-dependent mechanism and sensitises cells to apoptosis in response to tumour necrosis factor α (TNFα) by downregulating expression of *TNF-receptor associated factor 2* (TRAF2), therefore inhibiting normal activation of anti-apoptotic signals such as *NF-κB*. In addition, loss of *Rb* is sufficient to confer significant sensitivity to TNFα-induced apoptosis in primary cells (Phillips *et al.*, 1999).

1.10 Deregulation of E2F-1

In the majority of tumours deregulation of the retinoblastoma pathway occurs through mechanisms including mutation or deletion of upstream regulators of E2F such as *Rb* and cyclin-dependent kinase inhibitor $p16^{INK4a}$ or cyclin D overexpression as a result of gene amplification, translocation, post-transcriptional or post-translational modifications (Buckley *et al.*, 1993; Kaelin *et al.*, 1999; Schauer *et al.*, 1994; Sharpless *et al.*, 1999). Alterations in the expression of *Rb*, *cyclin D1* and $p16^{INK4a}$ lead to upregulation of the *E2F* transcription factors and a subsequent increase in the expression of genes required for DNA synthesis and progression from G1 to S phase of the cell cycle (Sherr, 1996).

Transfection or microinjection experiments documented the ability of overexpressed E2F-1 protein to activate transcription, to stimulate cell cycle progression and to induce oncogenic transformation (Nevins, 1998). Overexpression of E2F-1 or E2F-1/DP1 co-operates with activated *ras* in fibroblast transformation assays and transformed cells result in tumour growth in nude mice demonstrating that *E2F-1* has oncogenic capacity. The neoplastic transformation potential of E2F-1 is dependent on functional DNA binding and
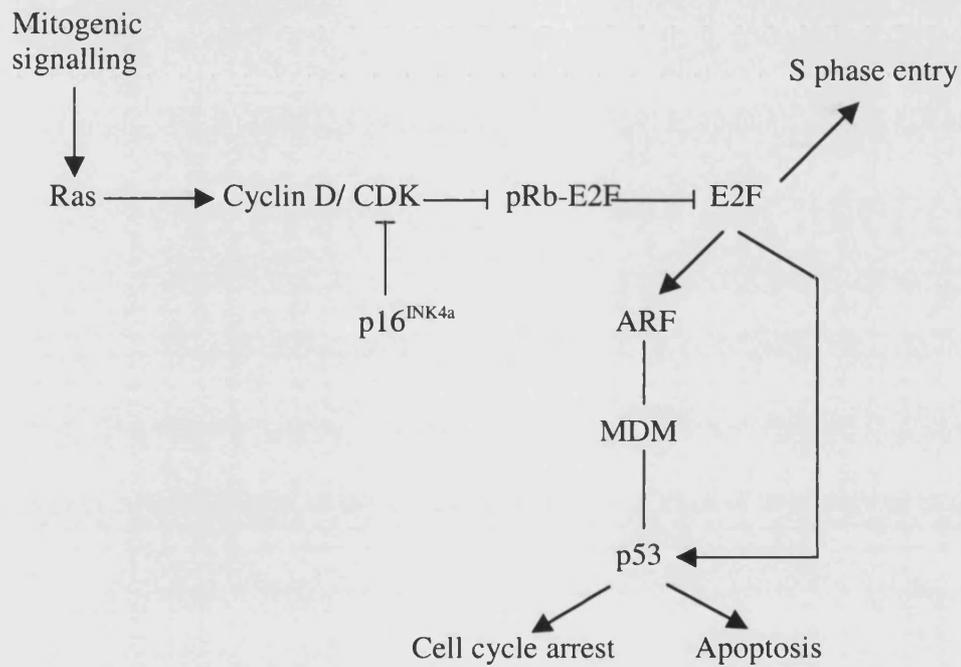
Figure 1.5: E2F involvement in apoptotic pathways
Mitogenic signalling activates E2Fs to advance cells into S phase. Stress signals
that activate the INK4a-ARF locus inhibit the activity of cyclin D-dependent
kinases (p16^{INK4a}) and induce p53 through either ARF-dependent or -independent
pathways, reprogramming the cells to undergo growth arrest or apoptosis.
Modified from Sherr *et al.* 2002.

transactivation domains but does not rely on direct interaction with pRb (Singh *et al.*, 1994; Yamasaki *et al.*, 1996).

Microinjection of a cytomegalo-virus (CMV) promoter controlled *E2F-1* cDNA into quiescent cells induced S phase entry and stimulated expression of DHFR and TK. Apart from promoting S phase entry ectopic E2F-1 expression also induced apoptosis in the presence of wild-type p53 in monkey kidney cells, rat fibroblasts and human osteosarcoma cells (DeGregori *et al*, 1995; Johnson *et al.*, 1993; Qin *et al.*, 1994; Shan *et al.*, 1994). In contrast, ectopic expression of the E2F heterodimeric partner protein DP1 alone failed to promote S phase entry suggesting that the active E2F subunit is required for cell cycle entry. Finally, coexpression of DP1 and E2F-1 resulted in a greater loss of G1 regulation and significantly more apoptosis than E2F-1 alone proposing a synergistic effect as a result of the interaction of E2F-1 and DP1 (Shan *et al.*, 1996).

Experiments using a tetracycline-controlled E2F expression system as well as microinjection experiments showed that the pRb-associated E2F transcription factors (*E2F-1*, *E2F-2* and *E2F-3*) all induced S phase in quiescent rat fibroblasts when expressed alone. In contrast, the p130/p107-associated E2F transcription factors (*E2F-4* and *E2F-5*) both require co-expression of the heterodimeric partner protein *DP1* to promote S phase entry and accelerate G1 progression. Furthermore, the pRb-associated E2Fs were able to overcome a G1 arrest mediated by the p16^{INK4} tumour suppressor protein and E2F-1 was shown to override a G1 block mediated by a neutralising antibody to cyclin D1. In contrast, only simultaneous expression of E2F-4 and DP1 could overcome these cell cycle blocks. It was concluded that E2F activity is rate limiting for G1 progression, is sufficient to induce S phase entry and overcomes a p16-mediated and a cyclin D1 antibody mediated G1 phase block (Lukas *et al.*, 1996).

Previous studies have shown the introduction of an adenovirus vector containing *E2F-1* cDNA into γ-irradiated, S phase inhibited cells to relieve the irradiation block by activating the transcription of *cyclin A*, *cdc2*, *DHFR* and *E2F-1* genes (DeGregori *et al.*, 1995). Increased levels of E2F-1 expression as well as E2F-1 DNA binding activity have also been found in response to UV- or γ-irradiation in human cancer cells implying increased expression of E2F-1 to serve as a mechanism to overcome the γ-irradiation block. This result presents E2F-1 with a role in the DNA damage response pathway involving ATM (Hoefferer *et al.*, 1999).

In vivo knock-out experiments have shown that *Rb(-/-)* mice die during mid-gestation (E13.5-E15.5) with increased apoptosis in a variety of tissues and incomplete haematopoiesis in the foetal liver. An increase in apoptosis in the *Rb(-/-)* central nervous system correlates with an increase in cellular S phase entry, 'free' E2F DNA binding activity and cyclin E expression (Yamasaki *et al.*, 1998). In contrast double mutant mice *Rb(-/-); E2F-1(-/-)* show a prolonged survival extending beyond E16.5 suggesting E2F-1 to determine the timing of lethality of *Rb*-deficient embryos. Therefore, *Rb* deficiency in combination with loss of *E2F-1* results in decreased levels of apoptosis and a reduction in inappropriate S phase entry compared to *Rb* deficiency alone. However, *E2F-1* deficiency could not extend embryonic survival to term (Tsai *et al.*, 1998). Further experiments with *Rb(+/-);E2F-1(+/-)* and *Rb(+/-);E2F-1(-/-)* mice indicated that the majority of control mice *Rb(+/-)* and all of the double heterozygotes developed pituitary tumours while 62% of *Rb(+/-);E2F-1(-/-)* animals developed pituitary tumours. This shows that inactivation of both wild-type E2F-1 alleles reduces the penetrance of pituitary tumourigenesis compared to control mice (Yamasaki *et al.*, 1998). Regarding thyroid tumourigenesis it was found that none of the *Rb(+/-);E2F-1(-/-)* and 6% of the double heterozygotes developed C-cell adenomas or hyperplasias. However, 53% of control mice *(Rb(+/-))* exhibited thyroid lesions. Hence, loss of E2F-1 reduces the occurrence of thyroid tumours significantly and is thought to interfere with thyroid tumourigenesis by reducing proliferation of the C-cell precursor population. Finally, testicular atrophy and exocrine gland dysplasia still developed with 100% penetrance in *E2F-1* deficient animals and lung adeno-carcinoma or lymphoma were detected in E2F-1 deficient animals which developed pituitary tumours. To conclude, loss of *E2F-1* reduced the lethality of the *Rb(+/-)* phenotype regardless of the genetic background (Yamasaki *et al.*, 1998).

Mice deficient in *p130* or *p107* develop normally and exhibit no overt adult phenotypes. This suggests that *p107* and *p130* are either dispensable for development or exhibit redundancy. Mice lacking both *p107* and *p130* are born with shortened limb and rib bones and die after birth. Interbreeding of *Rb-*, *p107-* and *p130*-deficient mouse strains and generation of chimaeric animals lacking one or more *Rb* family members revealed an extensive functional redundancy between the members of this gene family during development (Classon *et al.*, 2001).

1.11 Chemotherapeutic approach in the treatment of cancer

Chemotherapy is the use of cytotoxic drugs to kill cancer cells. Most cytotoxic agents destroy cancer cells by interfering with DNA synthesis, mitosis or other essential function in the cell thereby forcing the cell to arrest or undergo apoptosis. Chemotherapy is most effective against rapidly dividing cells and most cytotoxic agents are only effective against a fraction of cells, traversing a specific cell cycle phase, at any one time. Therefore it is essential to study the specific cell cycle behaviour of cancer cells in order to target the correct cytotoxic agent to the appropriate fraction of cells at the correct time.

At present anti-neoplastic drugs are discovered through empirical testing. Many of these drugs target no more than one cell cycle phase making the combination of drugs acting at different stages of the cell cycle a potentially improved strategy that could yield a synergistic effect therefore making tumour cells more vulnerable compared to individual drug treatment. However, with the discovery of genes that regulate the cell cycle and checkpoint function, new approaches to identify and design anti-neoplastic drugs that will specifically target the biochemical activities of oncoproteins and altered tumour suppressor gene products are being developed.

In the context of uncontrolled cell proliferation as a result of deregulation of E2F, CDK inhibitors (CKI) such as flavopiridols are one example of chemotherapeutic agents implied to counteract the effects of deregulated E2F activity. Flavopiridols were shown to have anti-proliferative effects on the growth of several human tumour cell lines (Meijer *et al.*, 1999; Sausville *et al.*, 1999). Furthermore, the *in vivo* effects of these compounds paralleled the *in vitro* efficiency as confirmed with the use of dominant negatives, the overexpression of natural CKI's and the microinjection of inactivating antibodies and antisense technology (Carnero, 2002; Schwartz *et al.*, 2001; Senderowicz *et al.*, 1998; Stadler *et al.*, 2000; van den Heuvel *et al.*, 1993). Flavopiridol, the first CDK modulator tested in clinical trials, demonstrated clinical features including cell cycle block at G1 and G2, induction of apoptosis, promotion of differentiation, inhibition of angiogenic processes and modulation of transcriptional events. In addition, flavopiridol was found to deplete cyclin D1 and D3 by transcriptional repression (Carlson *et al.*, 1999; Senderowicz, 2001).

A second CDK modulator tested in clinical trials is the staurosporine derivative UCN-01. UCN-01 has also been found to block cell cycle progression and promote

apoptosis. Clinical activity has been shown in the treatment of melanoma, lung cancer and non-Hodgkin's lymphoma (Carnero, 2002).

The knowledge about oncogene function in the cell cycle may serve
- to elucidate the mechanisms of anti-neoplastic drug action
- to improve usefulness of existing drugs by identifying drugs that act synergistically
- to select more specific drugs that target tumour cells more effectively
- to decrease drug dosage

The delineation of pathways that regulate the balance among cellular proliferation, differentiation and apoptosis is currently an area of intense research interest as mutations that upset the balance in favour of proliferation are fundamental to the development of most cancers.

1.12 Combination chemotherapy

Combination chemotherapy describes the combined application of common and novel anti-cancer agents to increase cytotoxic efficacy by attacking different biochemical targets, overcoming established drug resistance to single anti-cancer agents and taking advantage of tumour growth kinetics when considering the administration of the anti-cancer agents (Shah *et al.*, 2001). It is of importance to obtain knowledge of the effects of chemotherapeutic agents on the cell cycle, as well as determine the appropriate administration sequences, time schedules and doses for the combined anti-cancer agents in order to prevent cell cycle-mediated resistance (Shah *et al.*, 2001). The rationale for combination chemotherapy lies in selecting chemotherapeutic agents with different mechanisms of action thereby ensuring maximum effect through the disruption of a variety of cellular pathways essential for the maintenance and replication of genetic information and progression through the cell cycle. An example of the successful combination of two anti-cancer agents with differing mechanisms of action is the administration of paclitaxel followed by flavopiridol. This combination results in an accelerated exit from mitosis associated with an increase in apoptosis (Shah *et al.*, 2001).

A second example of combination treatment improving efficacy of chemotherapy has been reported with respect to the administration of gemcitabine followed by flavopiridol (Jung *et al.*, 2001). Gemcitabine was found to inhibit ribonuclease reductase

(RR), an enzyme involved in DNA synthesis during S phase. The RR-M2 subunit in particular was shown to be involved in RR enzyme activity and protein and activity level were correlated with DNA synthesis.

Flavopiridol was shown to inhibit the activity of CDKs 1,2,4 and 6 and was found to inhibit tumour cell growth *in vitro* through G1 and G2 phase arrest. Cell cycle arrest resulted due transcriptional inhibition of cell cycle specific genes. Hence, administration of gemcitabine and flavopiridol was observed to cause a potentiation of gemcitabine-induced apoptosis in a sequence-dependent manner. Potentiation was correlated with the down-regulation of the RR-M2 subunit that had been found earlier to be regulated by E2F-1. In conclusion, downregulation of RR-M2 transcription as a result of increased proteasome-mediated degradation of E2F-1 and hypophosphorylation of pRb caused an increase in gemcitabine-induced apoptosis (Jung *et al.*, 2001).

1.13 Drug resistance

Drug resistance to chemotherapeutic agents is often considered a major problem in chemotherapy and two types of drug resistance in tumours are recognised in the clinic:

- **intrinsic resistance** is defines as the innate drug resistance of tumour cells prior to treatment

- **acquired resistance** occurs due to newly acquired properties of tumour cells as a result of drug treatment

1.13.1 Mechanisms of drug resistance

Several mechanisms of drug resistance have been described at the cellular level.

- decreased drug uptake - methotrexate and nitrogen mustards enter cells via a carrier system. Alterations in carrier resulting from mutations or decreased protein synthesis may limit entry of drug.

- increased drug efflux through the cell membrane - P-glycoprotein dependent increase in drug efflux leads to multidrug resistance

Colon tumours serve as an example of intrinsic cellular resistance as they are inherently resistant to chemotherapy as a result of P-glycoprotein (P-gp). P-glycoprotein is a trans-membrane protein involved in the ATP-dependent efflux of a number of structurally unrelated anticancer drugs (Fardel *et al.*, 1996). P-gp

overexpression in cancer cells decreases intracellular drug concentrations and confers a multidrug resistant phenotype. Overexpression of P-gp has been shown in a wide variety of cancers including solid tumours and haematological malignancies. A high constitutive expression level of P-gp was found in tumours arising from tissues known to physiologically express P-gp including carcinoma of the colon, kidney, adrenal gland, pancreas and liver. By contrast tumours of the lung, esophagus, stomach, ovary and breast, melanomas, and some leukemias usually display low P-gp expression. P-glycoprotein overexpression maybe detected at the time of diagnosis prior to chemotherapy, or following relapse and has been correlated with treatment failure and poor prognosis in several types of cancer (Fardel *et al.*, 1996). P-gp-mediated multidrug resistance may be reversed by various unrelated compounds called chemosensitisers or reversing agents. These drugs act through inhibition of P-gp function and have entered clinical trials (Fardel *et al.*, 1996).

- increased drug inactivation - occurs via glutathione adduct formation as conjugation of glutathione with free radicals inactivates drugs
- decreased drug activation - e.g. an activating enzyme is required for the activation of 5-fluorouracil
- enhanced repair of drug-induced DNA damage
- decreased formation of drug-target complexes

    - if the mechanism of drug action involves inhibition of enzyme or receptor molecule, resistance can be mediated by an increase in the level of target protein

    - if formation of drug-target complex causes toxicity, resistance can be mediated by a decrease in target protein

Examples of drug resistance involving the above mechanism are found in response to treatment with antimetabolites such as methotrexate and 5-fluorouracil. Antimetabolites are compounds that replace natural substances as building blocks of DNA and other vital components of the cell thereby altering the function of enzymes required for cell metabolism and protein synthesis. This results in the prevention of DNA synthesis and replication subsequently leading to cell death. Antimetabolites are cell cycle specific and are considered to be most effective during the S phase of the cell cycle. Antimetabolites have been used in the treatment of non-Hodgkin's lymphoma and colorectal cancer. The

category of antimetabolites includes folate antagonists (methotrexate) and pyrimidine antagonists (5-fluorouracil) (Souhami and Tobias, 1998).

1.14 Pharmacology of major groove- and minor groove DNA- binding drugs

DNA-binding drugs may be categorised into minor groove-binding or major groove-binding drugs. Representatives of major groove-binding DNA-binding drugs are the nitrogen mustards including Melphalan and the platinum compounds including Cisplatin. The above drugs are classified as major groove alkylating agents and are highly reactive compounds that form covalent bonds with a number of nucleophilic groups on the DNA. In general, DNA-binding alkylating agents form a covalent bond between the reactive group of the drug and the 7-nitrogen group of guanine. Following formation of the initial covalent bond, bifunctional alkylating agents such as Cisplatin proceed to form a second covalent bond with a second nucleophilic group resulting in DNA inter-strand or intra-strand crosslinks .

The class of minor groove -binding anticancer drugs includes cyclopropylpyrrolo-indole (CC-1065) (Hurley et al., 1984; Swenson et al., 1982), the anti-tumour antibiotic distamycin A (Arcamone et al., 1964; Van Dyke et al., 1982) including its derivatives Tallimustine (Herzig et al., 1999), BGIII21 (Wyatt et al., 1995) and SCIII147, the latter two being novel minor groove binding alkylating agents, as well as the fluorochrome Hoechst 33258 (Albert et al., 1999). Molecular pharmacological studies indicate that non-covalent minor groove binding agents such as distamycin A, CC-1065 and Hoechst 33258 interact preferentially with A-T rich sequences that are at least 3-4 base pairs in length. The preference of these drugs for AT sites has been attributed to the minor groove that characterises these sequences and to the complementary crescent shape of the minor groove-binding agent. Strong van der Waals contacts between the sides of the groove and the aromatic rings of the bound drug provide a significant contribution to the stability of the drug-DNA complex. The stability of the bound drugs is further enhanced by interactions between the negative electrostatic potential of the AT sequences and by hydrogen bonding between the drug and DNA. The relative importance of these factors for the stability of the drug-DNA complex remains a matter of discussion (Albert et al., 1999).

In addition, a number of minor groove-binding agents has been found to possess DNA sequence specificity of alkylation. For example, the novel minor groove-binding

alkylating agent BGIII21 has been reported to preferentially alkylate at only two sequences, 5'-TTTTG$\underline{G}$ and 5'-TTTTG$\underline{A}$ (confirmed as guanine-N3 and adenine-N3 lesions at the underlined bases, respectively) in preference to other sites (Brooks *et al.*, 2000).

The effects of minor groove-binding agents on the regulation of gene transcription, the perturbation of the cell cycle, and the mechanism involved in the repair of the DNA lesions induced by these drugs strongly support the view that minor groove binding agents act by a mechanism different from those previously described for other anticancer drugs (D'Incalci *et al.*, 1997).

1.15 Summary and PhD project aims

As previously discussed within this introduction, involvement of the cell cycle mechanism in tumourigenesis is not based on deregulation of individual components but tumourigenic properties of many oncogenes also rely on their ability to deregulate the cell cycle machinery (Hanahan *et al.*, 2000). A number of cell cycle permutations involved in human neoplasia are shown in **table 1.1**

PROTEIN	ALTERATION	TUMOUR
CDK4	Mutation	Melanoma
Cyclin D1	Overexpression	Breast and prostate cancer, parathyroid adenoma, gastric and esophagic carcinoma, multiple myeloma
Cyclin D2	Overexpression	Colorectal carcinoma
Cyclin E	Overexpression	Breast, ovary and gastric carcinoma
Cyclin A	Overexpression	Hepatocellular carcinoma
p27^{KIP1}	Inactivation/ degradation	Colon breast and prostate cancer
p16^{INK4a}	Deletion/ inactivation mutation	Melanoma, lymphomas, non-small cell lung cancer, pancreatic carcinoma
pRb	Inactivation	Retinoblastoma, small cell lung cancer, sarcoma and bladder cancer

Table 1.1: Cell cycle regulatory elements involved in human neoplasia (adapted from Carnero, 2002).

The result of an alteration of one or more cell cycle elements shown in **table 1.1** leads to an increased expression and activity of the E2F transcription factors. A number of approaches using chemotherapy to counteract the occurrence of deregulated E2F activity have been attempted and specific examples of these are given within the relevant sections. However, in general, the studies performed to investigate and exploit mechanisms and downstream effects of E2F-1 deregulation have included:

1) Overexpression of E2F-regulated proteins

Proteins required for DNA synthesis and G1 to S phase transition such as DHFR or TS potentially bind or are a drug target. E2F-1 dependent overexpression of these proteins potentially reduces cellular drug sensitivity due to a decreased formation of drug-target complexes (section 3.1.1).

2) Increase of the proportion of cells in S phase and chemosensitivity

Overexpression of E2F-1 and the resultant increase in E2F-regulated gene expression has been shown to drive cells into S phase (Shan *et al.*, 1994; Shan *et al.*,1996). An E2F-induced increase in the proportion of cells in S phase might lead to an increased cell kill using S phase specific drugs (section 3.1.2).

3) E2F-1 mediated apoptosis and chemosensitivity

As discussed within section 1.9, deregulated E2F-1 activity enhances apoptosis through induction of p14^{ARF} followed by inhibition of MDM2 resulting in the accumulation and stabilisation of p53 (Bates *et al.*, 1998). Alternatively, E2F-1 is able to induce p53-independent apoptosis via p73, a p53 homologue (Irwin *et al.*, 2000). Combination chemotherapy may be considered a useful tool to potentiate drug-specific apoptosis through the sequential administration of a second chemotherapeutic agent (section 3.1.3)

The identified causes and effects of E2F-1 deregulation are useful in targeting the appropriate anti-cancer agent to a characterised tumour. These patterns include the deletion or mutation of cell cycle regulatory genes upstream of the E2F-1 transcription factor leading to an abnormally increased expression of E2F-1.

In addition, the combined loss of the *Rb* and subsequent loss of *p53* thereby preventing activation of the apoptotic pathway in response to deregulated expression of E2F-1. Other genes potentially affected by deletion or mutation include p14^{ARF} or MDM2 and alterations in these genes interfere with the cell's ability to conduct the proapoptotic signal allowing E2F-1 overexpression to stimulate cell proliferation (Dyson, 1998; Muller *et al.*, 2000).

As an example, mutations in *p53*, *p16* and *p14^{ARF}* occur frequently in colon cancer, and coupled with high levels of E2F-1 activity point to a more aggressive phenotype of the

tumour. Along with loss in the apoptotic signalling pathway, overexpression of E2F-1 may also activate transcription of genes implicated in a more invasive phenotype.

To provide a model system portraying the situation of E2F-1 deregulation in cancer cells, an E2F-1 stably transfected HT1080 human fibrosarcoma cell line was used, with an Rb deficient and p53 proficient genetic background. Inspite of the HT1080 transfectants being p53 proficient, no increased level of apoptosis in response to E2F-1 overexpression has been reported. Hence it may be assumed that deletions or mutations of other components, such as the p14^{ARF} or MDM2 gene, of the apoptotic pathway are present.

The aims of this project are:

- to determine the pattern of chemosensitivity secondary to E2F-1 overexpression.

- to determine the mechanisms of E2F-1 interactions with chemotherapeutic agents.

- to examine the effects of a novel E2F-1 inhibitory peptide on cell cycle progression within the HT1080 transfectants as well as other established cancer cell lines. The inhibitory peptide has been shown to inactivate the transactivation potential of E2F-1 by preventing the heterodimerisation of the E2F-1 subunit and DP-1 subunit to form an active transcription factor complex. However, the E2F-1 inhibitory peptide does not prevent E2F-1 from binding to DNA.

- to combine the information from the above investigations in order to set up experiments to investigate possible additive or synergistic effects a combination of anti-cancer agent and E2F-1 inhibitory peptide has.

51

2. MATERIALS AND METHODS

2.1. Materials

2.1.1 Chemical reagents and cytotoxic drug source

All reagents and plastics were obtained from Sigma Chemical Co. Ltd., Poole, UK or VWR International Ltd., Poole UK respectively unless otherwise stated.

Cytotoxic drugs (**table 2.1**) were prepared in advance or fresh before every experiment depending on the individual compounds stability and activity in solution as well as experimental requirements. The concentration ranges used for experiments were adapted from previous personal communications on the cytotoxicity of individual agents if required.

2.1.2 Experimental cell lines

Cell lines were obtained from the departmental cell bank unless otherwise stated. Tissue culture media and supplements including trypsin was supplied by Autogen Bioclear, Calne, UK. Foetal calf serum (FCS) was heat-inactivated for 30 minutes (min.) at 57°C prior to use. The growth medium described for the routine propagation of exponential growing cell lines is referred to as complete growth medium throughout.

2.1.3 Tissue culture procedures

2.1.3.1 Maintenance of cell lines

Cell lines were maintained at 37°C and 5% CO_2 in dry incubators (Forma Scientific, UK) and all procedures were carried out in Class II MDH biological safety cabinet (Intermed MDH, UK) using aseptic techniques. All cell lines were grown in $75cm^2$ (T75) flasks unless otherwise indicated in specific experiments. Exponentially growing cells were maintained at a cell concentration according to the European Collection of Cell Cultures (ECACC), Salisbury, UK.

Cells were routinely passaged when they became confluent (every 2-3 days). The cell monolayer was washed with 10ml of 0.01M phosphate buffered saline (PBS) to remove serum. Then 3ml of 1X Trypsin/EDTA was added to each flask and incubated for 2-5 minutes at 37°C. When cells had detached from the flask, trypsin was inactivated by adding

Drug	Chemical structure	Stock solution (mM)	Solvent	Supplier
Anthramycin		10	100% DMF	departmental drug supply
BGIII21		10 or100	10% conc. HCl + DMSO	Dr. Moses Lee, Furman University, South Carolina, USA
CC1065		10	100% DMA	Upjohn Lab, Kalamazoo, Michigan, USA
Cisplatin		3.3	Solution for injection	DBL, Warwick, UK
Distamycin A		100	ddH$_2$O	Sigma, UK
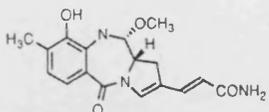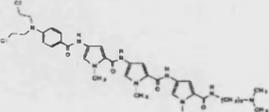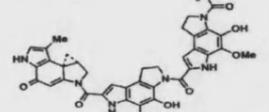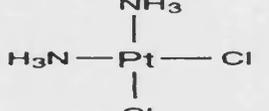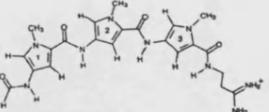
		100	100% DMSO	Sigma, UK
Etoposide		100	100% DMSO	Sigma, UK
Hoechst 33258		100	ddH$_2$O	Sigma, UK
Melphalan		100	200 µl ethanol (100%) per 1ml DMSO (100%)	Sigma, UK
SCIII147	not available	10 or100	100% DMA	Dr. Moses Lee, Furman University, SC, USA
Tallimustine		10	10% conc. HCl + DMSO	Pharmacia, Milan, Italy
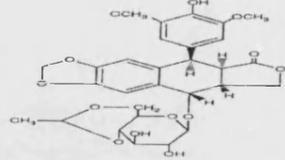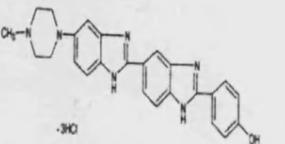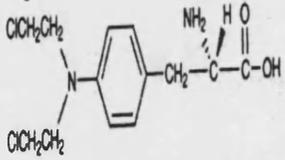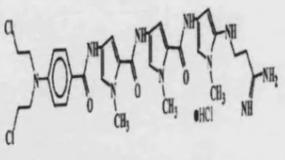
Table 2.1: Cytotoxic drugs used (for chemical name see 'Abbreviations')

10ml of complete growth medium, and the cell suspension was pelleted by centrifugation at 400*g* for 5 minutes at room temperature. The cells were then resuspended in complete growth medium and re-plated at an appropriate passage ratio for the cell line. The passage number was increased by one. Cells were discarded after approximately 20 passages and fresh cells were taken from the initial passage number used.

2.1.3.2 Quantification of attached or suspended cell yield

Cells were trypsinised, resuspended in a known volume of complete growth medium and counted using a haemocytometer. Cell number was determined for each of five separate $1mm^2$ fields, and the average was multiplied by $1x10^4$ to give the number of cells per ml of suspension.

2.1.3.3 Determination of cell doubling time using growth curves

Cells were seeded out at an initial total cell number of $1x10^4$ cells in a total volume of 10ml of complete growth medium for suspension cells, or $1x10^5$ cells per $25cm^2$ (T25) flask containing 10ml of complete growth medium for adherent cell lines. Adherent cell lines required an individual flask for every time-point. For suspension cells, $10\mu l$ samples were taken every 24hrs from the flask and the number of cells counted using a haemocytometer. Adherent cells were trypsinised, centrifuged and resuspended in a known volume of complete growth medium. Again a $10\mu l$ sample was used to count the cell number using the haemocytometer. The cell concentrations (number of (no.) cells $x10^4$/ml) obtained were used in both cases to calculate the total number of cells per flask. Further samples were taken every 24 hours until confluency or plateauing of cell growth was achieved. The doubling time of each cell line was calculated by reading off the exponential portion of the growth curve derived by plotting number of hours against total number of cells counted.

2.1.3.4 *Mycoplasma* testing

Cell cultures were routinely tested for *Mycoplasma* contamination every 6 months. The NIH 3T3 (3T3) mouse fibroblast indicator cell line was grown in DMEM medium supplemented with 10% New born calf serum and 2mM glutamine. The 3T3 cells were maintained at 10% CO_2 at 37°C. A total number of $2x10^4$ 3T3 cells were seeded onto a sterile coverslip which had been placed into a flat bottom Falcon tube. Cells were allowed

to adhere to the coverslips for 24 hours at 37°C and 10% CO_2. Previously, the cell lines to be *Mycoplasma* tested had been set up such that the cells reached confluency concurrently with the set-up of the *Mycoplasma* test. Thus, from a flask containing a confluent cell population to be tested, $500\mu l$ of the supernatant growth medium were removed and transferred to the *Mycoplasma* testing tube. The cell-free supernatant must not contain additives such as hydrocortisone, cholera toxin or antibiotics that might interfere with *Mycoplasma* growth. The 3T3 cells were incubated for 4 days or until confluent. The medium was removed and the cells washed once with 0.01M PBS. Cells were fixed in absolute methanol for 5 minutes. Afterwards the cells were washed twice with 0.01M PBS and stained with $5\mu g/ml$ of Hoechst 33258 dissolved in 0.01M PBS for 10 minutes. Two more washes with 0.01M PBS were carried out, the cover slips were carefully removed from the *Mycoplasma* testing tube, placed cell surface upwards on a glass microscope slide and covered with a coverslip. Analysis was performed under a fluorescent microscope using a x40 objective and ultra-violet (UV) illumination. Control cells showed intense blue-white staining of the nuclei only. *Mycoplasma* infected cells would have been covered in a fine "lawn" of speckles all over.

2.1.3.5 Storage and retrieval of cells in liquid nitrogen

Frozen cell stocks in liquid nitrogen were routinely prepared. Cells were grown in a $175cm^2$ (T175) flask to semi-confluency. They were trypsinised and resuspended in 10ml complete growth medium containing 10% dimethylsulphoxide (DMSO). Aliquots of 1.5ml were frozen slowly in cryotubes in a styrofoam box at −80°C overnight before the cryotubes were transferred into liquid nitrogen tank the next day. Each cryotube contained cells at a 10X higher concentration compared to the concentration at which they were grown.

Cells were recovered from liquid nitrogen by thawing rapidly in a 37°C water bath before being transferred into a T25 flask containing 10ml of complete growth medium. Each cryotube was wiped off with paper towel sprayed with 70% industrial methylated spirit (IMS) to prevent accidental contamination of cell lines through bacteria and other cells stuck to the outer wall of the cryotube. Cells were split after 24 hours to remove any DMSO present in the media.

2.2. Methods

2.2.1 Western Blot Analysis

2.2.1.1 Method 1

This technique was initially employed to analyse the relative E2F-1 content in the HT1080 Neo cell line and the related E2F-1 over-expressing clones (see chapter 3).

Preparation of protein samples

Cells were harvested during exponential growth by aspirating off medium, adding ice-cold 0.01M PBS before continuing with trypsinisation. Cells were lysed in a buffer consisting of 50mM TrisHCl (pH7.5), 150mM NaCl, 1% IGEPAL, 0.2% SDS and 1X Boehringer' complete, EDTA-free protease inhibitor mixture (Roche Diagnostics, UK). Protein concentration was measured and standardised using Bio-Rad protein assay reagent based on the Bradford method at optical density (OD) 595nm. Whole cell protein extracts were made up with ddH_2O to achieve equal protein concentrations per sample and diluted in 2X SDS-sample buffer (4%SDS, 10% β-mercaptoethanol, 20% glycerol, 0.02% bromophenol-blue and 100mM TrisHCl (pH 6.8)) before heating at 95°C for 5 minutes.

Gel preparation and electrophoresis

Two gels were prepared each consisting of a running gel [(30% AA, 42.6% ddH_2O, 25% 4X running buffer (0.4% SDS, 1.5M TrisBase pH8.8), 2.5% APS (10%), 0.08% TEMED)] and a stacking gel [(9.9% AA, 61.6% ddH_2O, 26.1% 4X stacking buffer (0.4% SDS, 0.5M TrisBase pH 6.8), 2.4% APS (10%), 0.04% TEMED)]. Prior to loading of the samples the 10X electrophoresis buffer (1% SDS, 250mM TrisBase pH 8.3, 1.92M glycine) was diluted 1:10 with ddH_2O and the samples and marker (Kaleidoscope pre-stained standards, BioRad, Hemel-Hempstead, UK) were boiled at 90°C for 5 minutes. The samples were separated on the 10% SDS polyacrylamide gels at 70-100V for 2 hours using the Xcell II™ Mini-Cell electrophoresis tank (Novex® Western Transfer Apparatus, Invitrogen, UK).

Protein transfer and immunoblot

Proteins were electrically transferred to polyvinylidenedifluoride membranes (PVDF) (Millipore, UK) at 25V for 1 hour using the XCell II™ Blot Module (Novex® Western Transfer Apparatus) as described in the Novex® provided protocol. Prior to the transfer the 10X protein transfer buffer (3% TrisBase, 14.4% glycine and 20% methanol) was diluted 1:10 with ddH_2O. Membranes were blocked in 1% casein blocking buffer (10mM TrisBase

pH 7.6, 154mM NaCl, 0.5% casein (BDH, UK), 0.02% thimerosal, ddH₂O) and incubated consecutively for one hour each with a E2F-1 specific mouse monoclonal primary antibody (Santa Cruz, UK) (1:1000) in Tris buffered saline (20mM TrisHCl pH7.5, 150mM NaCl) (TBS) followed by 3x 20 minute washing steps with TBS complemented with Tween 20 (TBS-T). A second incubation with an anti-mouse horseradish peroxidase conjugated secondary antibody (Santa Cruz, UK) (1:5000) in TBS was performed followed by 3 separate washing steps with TBS-T lasting 20 minutes each. All incubation and washing steps were carried out at room temperature (RT). Immunocomplexes were visualised using the enhanced chemiluminescence (ECL) system (Amersham Pharmacia, Little Chalfont, UK) by incubating the Western blots in the ECL system solution for 1 minute before wrapping the moist blots in cling film and exposing the blots to Kodak X-OMAT™LS film (Sambrook, *et al.*, 1989).

Modifications to the above method were included in order to perform an increased number of experiments within the same time-span and hence screen clones derived for the E2F-1 inducible system produced during later stages of the project.

2.2.1.2 Method 2

Preparation of protein samples

Cells to be examined were seeded in 6 well plates at a cell density of 4x10⁵ cells/well and incubated overnight to allow them to adhere. The medium was removed and 200μl of 3X sample buffer (60mM TrisHCl pH6.8, 4% SDS, 5% glycerol, 50mM β-mercaptoethanol, 0.01% bromophenol-blue) were added per well. The lysis mixture was transferred to 1.5ml Eppendorf tubes. A further 400μl ddH₂O was added to each well to wash out any remaining lysis mixture and then transferred to the Eppendorf tube. Lysed samples were vortexed, heated at 90°C for 5 minutes and finally frozen down at –20°C.

Gel preparation , electrophoresis, protein transfer and immunoblot

As previously described (section 2.2.1.1) the samples were run on 10% SDS polyacrylamide gels and electrically transferred to PVDF (Millipore) membranes. Membranes were blocked for 1 hour in a dried milk powder based blocking buffer (1X TBS, 5% non-fat dry milk, ddH₂O) at room temperature (RT). Incubation with a specific primary antibody was at 4°C overnight followed by 3 times 20 minute long washing steps

with TBS-T. Subsequent incubation with a horseradish peroxidase conjugated secondary antibody carried out for 1 hour at RT followed by 3 separate washing steps with TBS-T lasting 20 minutes each. For dilution ratios used for individual antibodies refer to previous section (2.2.1.1). As described in method 1 before, immunocomplexes were visualised using enhanced chemiluminescence (ECL). To ensure equal protein loading per well, blots were stained with Coomassie blue (45% methanol, 10% acetic acid, 0.1% Coomassie brilliant blue, ddH$_2$O) for 10 min., washed 4-5 times with destaining solution (45% methanol, 10% acetic acid, ddH$_2$O) and air-dried.

2.2.2 Electrophoretic mobility shift assays (EMSA)

Electrophoretic mobility shift assays were performed following the protocol provided by van der Sman, *et al.*, 1999. This technique was used to examine the binding specificity of E2F-1 and supershift assays were performed to identify proteins present in the E2F-1 protein-DNA complex.

To obtain nuclear proteins, exponentially growing cells were lysed in 450mM NaCl, 25% glycerol, 1mM K-EDTA, 1x Boehringer' complete EDTA-free protease inhibitor mixture, 0.5M DTT (dithiothrietol) and 20mM K-Hepes (pH 7.9) using alternating heat-freeze steps. Pellets were heated at 30°C for 30 seconds followed by transfer to dry ice until pellets were completely frozen. Heat-freeze steps were repeated 3-4 times before centrifugation at 20,000g for 10 minutes. The supernatant (lysate) was transferred to fresh Eppendorf tubes and the protein concentration was measured using a Bio-Rad DC protein assay reagents package based on the Lowry assay at OD 750nm. Samples were stored at -80°C until further use. A double stranded E2F oligonucleotide containing the distal E2F binding site from the adenovirus type 5 E2A promoter (Bandara *et al.*, 1991) was prepared by mixing 2μl Forward primer (200pmol), 2μl Reverse primer (200pmol), 10μl KCl (100mM), 12.5μl Hepes pH7.9 (200mM) and 8.5μl ddH$_2$O. The primers were annealed by PCR (1. 95°C for 5 min.; 2. 70°C for 36 sec. −0.5°C/cycle; 3. 99x go to step 2; 4. 20°C for 60 min.; 5. 20°C for 1 min. 42 sec. −0.5°C/cycle; 6. 32x go to step 5; 7. 4°C). The radioactive probe was prepared by incubating 1.5μl pre-prepared double stranded oligomer, 1μl NaCl$_2$ (5M), Klenow buffer (Promega, Southampton, UK); 7μl α-^{32}P-dGTP (10μCi/μl) (Amersham Bioscience, UK), 13μl ddH$_2$O and 1.5μl Klenow enzyme (5u/μl) (NEB, Hitchin, UK) for 25 minutes at RT. Twenty μg of nuclear extract was incubated in the

presence of binding buffer consisting of 25mM Hepes (pH7.9), 2mM $MgCl_2$, 1mM DTT, 1x Boehringer' complete EDTA-free protease inhibitor mixture, 100ng/ml salmon sperm DNA, 10μg/ml Bovine serum albumin (BSA), 33% glycerol and ddH_2O at 30°C for 3 minutes. Excess unlabelled mutant E2F-1 (contains a mutated E2F-1 site) or excess unlabelled E2F-1 oligonucleotide were added to the binding reaction according to individual experimental requirements. Then 1-2ng of α-^{32}P-labeled consensus oligomer was added to the mixture and incubated at 30°C for 10 minutes. The DNA bound complex was separated on 4% polyacrylamide gel run in 0.5X Tris borate EDTA (89mM TrisBase, 89mM boric acid, 2mM EDTA) (TBE) at 170 Volts for 1.5-2 hours at 4°C. The gel was mounted on Whatman 3MM paper (Maidstone, UK) and Whatman DE81 paper (Maidstone, UK) and dried on gel dryer (BioRad, Hemel-Hempstead, UK) for 2 hours at 80°C. The dried gel was exposed to Kodak X-OMAT™LS film.

In case of supershift, 1μl of concentrated specific antibodies for pRb, p130 and p107 (kindly provided by E. Lam, Ludwig Institute for Cancer Research, Imperial College School of Medicine at St. Mary's, London, UK) were pre-incubated with the nuclear extracts in the presence of binding buffer at 30°C for 5 minutes. Subsequently the radioactive probe was added and the antibody complexes separated as described above.

2.2.3 *In vitro* cytotoxicity assays

2.2.3.1 Sulphorhodamine B growth inhibition assay

The assay is based on the binding of the purple Sulphorhodamine B (SRB) dye to cellular protein.

Cytotoxicity of drugs was determined by the SRB assay in 96-well microtitre plates as described previously (Skehan *et al.*, 1990). The optimal cell concentrations were determined from the previously calculated doubling times in order to achieve a final cell concentration ideal for accurate optical density (OD) measurement. Cells were plated in 96-well flat-bottomed microtitre plates, each well containing 100μl cell solution (2.5x10^3 cells/well or 5x10^3 cells/well depending on cell doubling time). Prior to drug treatment, cells were allowed to adhere at 37°C and 5% CO_2 overnight. Drug incubations performed were either acute (1 hour) or continuous (72 hours). All drugs were diluted in complete growth medium and 100μl of the relevant concentration added to the appropriate wells.

One solvent control lane was included in each experiment. The concentration range for each drug was optimised if necessary following analysis of results from the first experiments. For acute drug exposure cells were incubated for 1 hour with the relevant drug prepared in FCS-free medium. Following this, the drug solution was removed and replaced with 200μl drug free complete growth medium. Plates were incubated at 37°C, 5% CO_2 for 72 hours. Media was carefully removed and the cells subsequently fixed with 100μl 10% trichloroacetic acid solution for 20-30 minutes at 4°C. The fixed cells were washed three times with tap water and any remaining water flicked out of the wells. 100μl SRB stain (0.4% in 1% acetic acid) was then added to each well to allow visualisation of cellular proteins and incubated for 20-30 minutes at 4°C. Any excess SRB was removed by washing 4-5 times with 1% acetic acid. Plates were air-dried overnight. Finally the dye was dissolved in 100μl 10mM Tris/1mM EDTA for 10 minutes on a plate shaker. Plates were read at absorbance of 540nm on a Tecan microplate reader and analysed using computer spreadsheets (Microsoft Excel).

Growth inhibition was calculated using the following equation and the mean of growth inhibition for each drug dose with standard deviations were calculated. At least three independent experiments were carried out for each drug.

$$\frac{OD\ (treated)}{OD\ (control)} \times 100 = \%\ growth\ inhibition$$

Dose-response curves for all cell lines were obtained for each drug tested. The IC_{50} values were calculated from the curves. The IC_{50} is defined as the drug concentration needed to produce a 50% growth inhibition. The relative resistance factor (RF) for the HT1080 E2F 1-1 cell line was determined with the following equation:

$$\frac{IC_{50}\ HT1080\ E2F\ 1\text{-}1}{IC_{50}\ HT1080\ Neo} = RF$$

2.2.3.2 MTT [3-(4,5-dimethylthiazol-2-yl)-2,5-diphenyltetrazoliumbromide] cell proliferation assay

MTT assays were essentially performed as previously described by Carmichael *et al.*, 1987 and Twentyman *et al.*, 1987. Acute (1hr) and continuous (72hrs) drug incubations were performed in 2ml of cell suspension (serum-free medium) at a cell concentration 5×10^4 cells/ml. After 1 hour drug incubation the cells were centrifuged at $400g$ for 5 minutes, the supernatant removed and resuspended in drug free complete growth media. Cells were plated out at $200 \mu l$/well in microtitre plates to give a final cell density of 1×10^4 cells/well and incubated at 37°C, 5% CO_2 for 72 hours. Cell suspensions for continuous drug exposure were plated out immediately and incubated as described above for 72 hours. $20 \mu l$ MTT dye (5mg/ml) was added to each well and plates incubated for 5 hours at 37°C. Plates were centrifuged (5min., $400g$), supernatant was removed, and formazone crystals were dissolved in $200 \mu l$ DMSO. After dye pellet was completely dissolved the absorbance was read at OD 540nm on a Tecan microtitre plate reader. Cell survival was calculated from the following equation and the mean of the cell survival figures for each drug were calculated:

$$\frac{OD\ (treated)}{OD\ (control)} \times 100 = \%\ cell\ survival$$

At least three independent experiments were performed for each drug.

Modifications of the above method were made to account for the frequent insolubility of the E2F antagonising peptide in the presence of FCS. Experiments involving the peptide alone or a pre-incubation with peptide followed by drug exposure included using growth medium supplemented with 2mM glutamine only, for any peptide preparation steps. Invariably, suspension cells were spun down at $400g$ for 5 min., the medium was removed and the cell pellet was resuspended in FCS free medium. Cells were aliquoted out into Eppendorf tubes at a concentration of 5×10^4cells/ml before the appropriate amount of peptide was added. After 10 minutes of incubation at RT, medium supplemented with 10% FCS was added and $200 \mu l$ of cell/peptide solution were plated out in 96-well round bottom plates.

In the case of experiments requiring a peptide pre-incubation step, cells were dosed with the appropriate peptide concentration in T25 flasks for 24 hours, before being aliquoted out and drug dosed as described above. Again the peptide solution was initially made up in FCS free medium before 10% FCS was added and the cells exposed with the peptide solution.

2.2.3.3 Statistical analysis

Multiple regression models were fit using SAS Version 9.0 general linear models. The terms included in the model were linear, quadratic and cubic terms for dose and a linear term for cell line. Where appropriate, each drug was evaluated separately. Bonferroni adjustment to the overall alpha = 0.05 was made as there were about 800 contrasts. Thus, a p-value of 0.0001 was required for evidence of significant difference (Draper and Smith, 1981).

2.2.4 Soft agar clonogenic assay

The clonogenic assay was initially developed as an *in vitro* test for the growth of potential tumour cells in a semi-solid medium without exogenously added cytokines (Hamburger *et al.*, 1978). Inhibition of colony formation is a measure of the effectiveness of a particular drug in inhibiting the expansion of the cell population of the malignant tumour. The assay was essentially carried out as described in the protocol by Plumb *et al.*, 1999.

Clonogenic assays were performed using 5×10^5 exponentially growing cells plated out into a T25 flask. After 50-60% confluency has been reached drug was added at the appropriate concentration and left for the required duration. The cells were harvested using 1.5ml cell dissociation solution, followed by neutralization with 4ml complete growth medium and centrifuged at 400g for 5 minutes at RT. Cells were washed with 0.01M PBS and resuspended in 2ml fresh complete growth medium. Cells were syringed to achieve a single cell suspension before cells were counted as described before (section 2.1.3.2) and a series of dilutions performed to achieve a cell concentration of 200 to 2000 cells/ml in order to plate out the required number of cells per petri dish. The cells were plated out for colony formation in complete growth medium containing 20% FCS and 0.2% low melting point agarose. The sloppy agar medium was prepared earlier and kept at 42°C in the water-bath until required. Cells were plated out in petri dishes at a concentration of 100 cells/

plate. Plates were left for 7-14 days at 37°C and 5% CO_2 for colonies to form depending on the growth rate of the cells. Colonies of approximately 50 cells were visualised by incubating each plate in 5ml 1% methylene blue for 1-2 hours at RT. A Gallenkamp colony counter was used to determine number of colonies formed and percentage colony forming potential was calculated using the formula below (Brown, *et al.*, 1999).

$$\frac{\text{number of colonies counted}}{\text{number colonies plated out}} = \text{plating efficiency}$$

followed by:

$$\frac{\text{plating efficiency (treated)}}{\text{plating efficiency (control)}} \times 100 = \% \text{ colony formation}$$

2.2.5 Flowcytometric (FACS) analysis

A commonly used method for cell cycle analysis is to measure the DNA content of a cell by staining the DNA with a dye that binds to the nucleic acid stoichiometrically and whose fluorescence is enhanced upon binding. The most commonly used dye is Propidium iodide (PI) which is excluded by an intact cell plasma membrane hence cells need to be fixed or permeabilised for analysis (Shenton *et al.*, 1996. The obtained cell cycle histogram is considered an important tool in the study of action of cytotoxic drugs (**Fig. 2.1**). However, the information gained is essentially static and for example does not provide information about whether a cell with S phase DNA content is actually synthesising DNA.
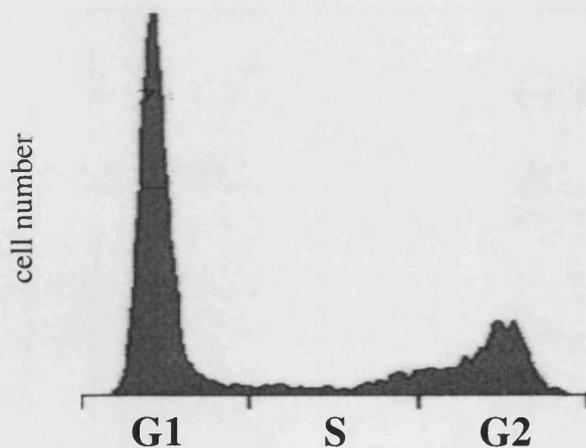
Fig. 2.1: DNA histogram illustrating relative DNA content of cells in G1 phase (G1), S phase (S) and G2 phase (G2) as analysed by FACS analysis

64

Cells were plated out in T25 flasks or 6-well plates as to achieve a total number of $1x10^6$ cells for each FACS sample in order to ensure that at least 10,000 cells could be analysed by the fluorescence-activated cell sorter (FACS). Therefore, depending on the duration of the drug incubation, cells were plated out at densities of $5x10^5$ or $1x10^6$ cells per flask, accounting for loss of cells during subsequent experimental steps.

Exponentially growing cells were incubated with the relevant drug in individual T25 flasks. After drug incubation, cells were washed with 0.01M PBS and lifted from the flask using cell dissociation solution and centrifuged at 400g for 5 min.. Following centrifugation the cells were washed with ice-cold 0.01M PBS and centrifuged for a second time. Cells were resuspended in 200μl ice-cold 0.01M PBS and fixed in 2ml 70% ice-cold ethanol while vortexing. The fixed cells were stored at 4°C for a minimum of 1hr. For the staining procedure cells were centrifuged at 400g for 5 min. and the ethanol fix poured off. The cell pellets were washed in 1ml 0.01M PBS and centrifuged once more. After removal of the PBS, cells were resuspended in 925μl ice-cold 0.01M PBS, treated with 25μl RNAse (10mg/ml) and stained with 50μl PI (1000μg/ml). The FACS samples were stored at 4°C in the dark for a minimum of 30 min. before analysing. Analysis occurred within 1-3 hrs of cell preparation. A minimum of 10,000 cells were analysed on a fluorescence-activated cell sorter (Coulter FACscan) (Ormerod, 1994). PI staining was detected using an Argon-ion laser at 488nm. Acquisition of cell cycle data was performed with WinMDI or CellQuest and further analysis of the acquired data was carried out with FCS Press 3.1 or CellQuest FACS analysis program.

2.2.6 Apoptosis assay (TACS™ Annexin V-FITC Apoptosis Detection kit-R&D Systems)

Apoptosis is an important mode of cell death, both in natural development and in response to cytotoxic insults. Apoptotic cells undergo membrane alterations exposing new entities such as phosphatidyl serine (PS) groups on the membrane surface. The above assay was employed to detect such *in situ* cell surface changes characteristic for early apoptotic processes using Annexin V-fluorescein isothiocyanate (FITC) conjugates that bind PS hence allowing rapid fluorimetric detection of apoptotic cells (Shenton *et al.*, 1996).

Cells were plated out in T25 flasks to achieve a total number of $1x10^6$ cells per sample. Therefore, depending on the duration of the drug incubation cells were plated out at

densities of 5×10^5 or 1×10^6 cells per flask, accounting for loss of cells during subsequent experimental steps. Exponentially growing cells were incubated with the relevant drug in individual T25 flasks. After the drug incubation, cells were washed with PBS, lifted from the flask using cell dissociation solution and centrifuged at $400g$ at 5 min. at RT. Following centrifugation the cells were washed with $500\mu l$ ice-cold 0.01M PBS and centrifuged for a second time. Cells were gently resuspended in $100\mu l$ of the Annexin V-FITC incubation reagent prepared as described in the provided protocol included with the kit and incubated in the dark for 15 minutes at RT. Simultaneously, cells were counter-stained with PI as required by the protocol provided with the kit. Within 1 hour, the cells were analysed by flow cytometry as described for cell cycle analysis (section 2.2.5), including an additional acquisition parameter taking into account the green fluorescent colour emitted by the Annexin V-FITC conjugate. The combination of Annexin V-FITC and propidium iodide allows for the differentiation between early apoptotic cell (Annexin V-FITC positive), late apoptotic and/or necrotic cells (Annexin V-FITC and propidium iodide positive) and viable cells (unstained). Analysis of the data acquired was performed using FCS Press 3.1 as described before.

2.2.7 Genomic DNA isolation

After harvesting by trypsinisation, cells were lysed by resuspending in 5ml lysis buffer (50mM TrisHCl, pH 7.5; 5mM $CaCl_2$) in a 15ml Falcon tube to which $100\mu l$ proteinase K (20mg/ml) and $250\mu l$ SDS (10%) were added. The solution was mixed and incubated at 65°C for 1 hour or until the initially turbid solution had turned clear. To continue, 2.5ml phenol (10mM Tris pH 8.0 saturated) and 2.5ml chloroform (24:1 chloroform:iso-amyl alcohol) were added to the lysed cells. The solution was mixed well by inversion and centrifuged for 15 minutes at $2100g$ at RT. The supernatant was transferred to a clean tube without disturbing the protein interphase. The phenol-chloroform treatment was repeated until the protein interphase had disappeared. An equal volume of chloroform was added to the supernatant collected from the previous step and the centrifugation step repeated. The supernatant was transferred into a clean tube and DNA was precipitated by adding 1/10 volume 3M sodium acetate, pH 5.5 and 2X volume ice-cold 100% ethanol. The precipitated DNA was centrifuged for 15 minutes at $2100g$. The DNA pellet was washed twice with

70% ethanol (RT) and the pellet was dried briefly before finally dissolving in 500μl ddH₂O. The DNA was stored at -20°C for future use.

2.2.8 Polymerase chain reaction (PCR)

For all PCR experiments a PCR mixture was set-up containing 2μg DNA, 2μl primer 1 (100pmol) and 2μl primer 2 (100pmol), 12.5mM dNTPs (Amersham Bioscience, UK), 25mM $MgCl_2$, 1X Taq polymerase buffer (Promega, Southampton, UK), 3u Taq polymerase (Promega, Southampton, UK) in a total volume of 100μl ddH₂O. All custom-made primers were purchased from MWG Biotech, UK (Table 2.2). The PCR mixture was put into PTC-100 Programmable Thermal Cooler (MJ Research Inc., UK) PCR machine and exposed to the following PCR cycle:

1.	94°C	for	5 minutes
2.	94°C	for	1 minute
3.	54°C	for	1 minute
4.	72°C	for	1 minute
5.	35 x go to step 2		
6.	72°C	for	10 minutes
7.	4°C		

Finally 5μl 10X DNA formamide loading buffer [0.5g amberlite added to10ml formamide (stirred for 30 min. and filtered through Whatman 3MM paper), 3mg bromophenol blue, 3mg xylene cyanol, 200μl EDTA (500mM)] was added to PCR product and the PCR product was run on 0.8% - 2% agarose gels (1X TBE, ethidium bromide, agarose). A 1kb DNA ladder (Gibco-BRL, Paisley, UK) was run aside the PCR product to aid in the identification of the correct PCR product. The gel was run at 90-100V for 30-45 minutes depending on how much separation of the PCR products was required.

Name	Sequence
N-*ras* (3.8)	5' - CTT TGG ACA GAT TTA GGA CC- 3'
N-*ras* (5.8)	5' - AAC TTT ATA TCA CGG GAA TG -3'
Topoisomerase IIα FWD	5'-CTC AGC TCT TTG GCT CGA TTG -3'
Topoisomerase IIα REW	5'-TGG CAA AGG TTC TTC TCC ATC-3'

Table 2.2: Custom-made primers used for investigative PCR experiments.

2.2.9 Southern blot analysis

The above method has been previously described by Sambrook *et al.*, 1989 and was used to compare the *Dra*I restriction patterns of the HT1080 Neo cell line and associated E2F-1 overexpressing clones (HT1080 E2F 1-1, HT1080 E2F 1-4 and HT1080 E2F 1-6). The cell lines were grown in individual T175 flask until the cells had reached semi-confluence followed by the isolation of DNA from the four cell lines according to the previously described genomic DNA isolation method (see section 2.2.7).

Preparation of DNA samples

A restriction digest was set up containing 250µl isolated genomic DNA, 5µl *Dra*I (10u/µl) (Promega, Southampton, UK), 50µl 10X reaction buffer and 5µl BSA both supplied with *Dra*I, 5µl Rnase ONE™ (5u/µl) (Promega, Southampton, UK) and 185µl ddH$_2$O at 37°C overnight. The DNA was precipitated using 3M sodium acetate and 100% ethanol and resuspended in 100µl ddH$_2$O as described previously (section 2.2.7) before the DNA concentration was measured fluorimetrically (Kowalski *et al.*, 1979). The measured DNA was stored at -20°C for future use.

Preparation of blot

The DNA samples (20µg) were loaded onto a 0.8 % agarose (0.8% agarose, 1X TBE, ethidium bromide) gel and run in 1X TBE buffer at 28mV for 16-20 hours. A 1kb ladder (Gibco-BRL, Paisley, UK) was run alongside the samples. Under UV illumination a picture was taken with a ruler placed next to the size marker in case size analysis of the DNA bands on the blot was required later. Afterwards any excess gel was trimmed off including the 1kb DNA ladder.

The DNA was denatured by soaking the gel in 1.5M TrisHCl (pH8.0) and 0.5M NaOH for ≥ 30 minutes at room temperature with constant shaking. The gel was neutralised by soaking in 1M TrisCl (pH8.0) and 1.5M NaCl for ≥ 30 minutes, again, at room temperature with constant shaking. Overnight the DNA was transferred onto Hybond N+ membrane as shown in **Figure 2.2**. After 24 hours the blot was exposed (membrane plus DNA) to UV light for 2min. 30sec. If necessary the blot was stored in 2X SSC pH7.0 that had been pre-prepared by diluting 20X SSC (175.3g NaCl, 88.2g sodium citrate, adjust to 1l with ddH$_2$O) at a ratio of1:10 at 4°C for future use.
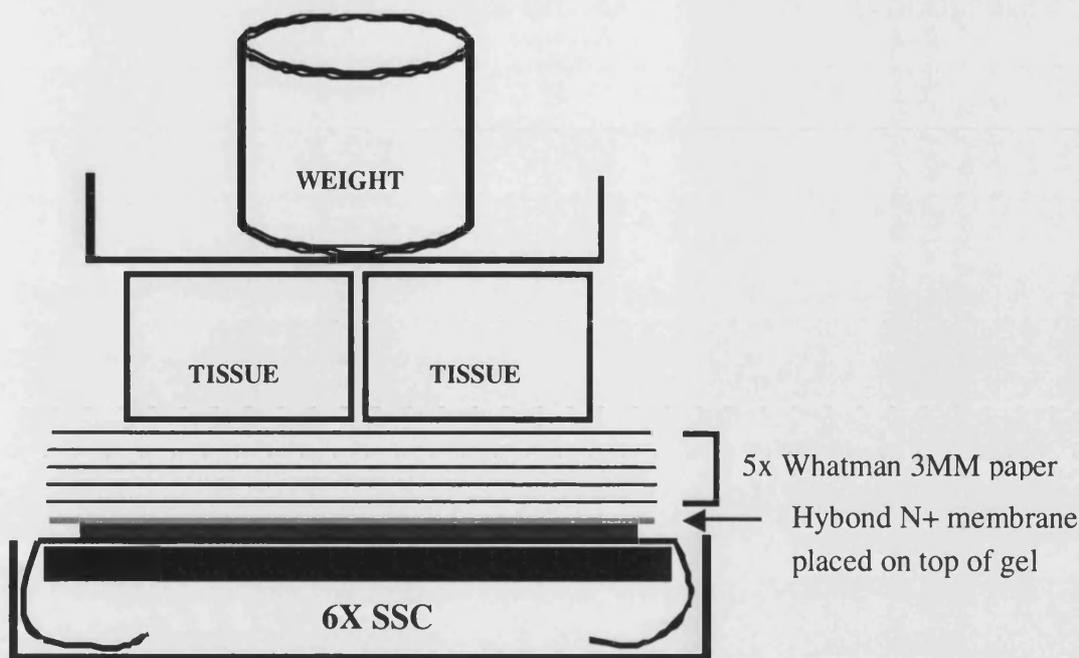
Fig. 2.2: Illustration of set-up to blot DNA onto Hybond N+ membrane (Amersham Pharmacia Biotech, UK) overnight.

Whatman paper was placed on top of a perspex "table" such that the paper may be folded into the tank containing 6X SSC. The gel was placed onto the Whatman paper and the Hybond N+ membrane, as well as 5 sheets of Whatman paper were stacked on top of the gel. Two packs of tissue pressed down by weights complete the set-up that works by drawing up the 6X SSC through the gel onto the Hybond N+ membrane into the tissue hence transferring the DNA onto the membrane in the process. All sheets of Whatman paper as well as the Hybond N+ membrane were presoaked in 2X SSC solution.

Preparation and radio-labelling of probes

The N-*ras* PCR product (see section 2.2.8) and the topoisomerase IIα cDNA insert within the pTRE200 *topoisomerase* IIα vector (gift from B. Tolner) were used as probes. The pTRE200 *topoisomerase IIα* vector was cut with the restriction enzymes *Xho*I and *Not*I to release the *topoisomerase IIα* insert. Following gel separation of insert and cut vector the insert was isolated using the Gene-clean® II kit Bio 101 (Anachem, UK). In addition, the N-*ras* PCR product was extracted from the relevant PCR gel again using the Gene-clean kit. The DNA for both probes was measured fluorimetrically as described by Kowalski *et al.*, 1979.

69

Approximately 20ng of recovered DNA were resuspended in 13.5µl ddH$_2$O and denatured

at 90°C for 10 minutes. On ice, 4µl 5X High Prime (Roche Diagnostics, UK) and 2.5µl

α^{32}P-dCTP (10µCi/µl) were added to the denatured probe and the mixture was incubated at

37°C for 30 minutes. The reaction was stopped through the addition of 60µl 1X TE (10mM

TrisBase, 1mM EDTA pH8.0) before the entire mixture was purified on a Bio-Spin-6 spin

column (Bio-Rad, Hemel-Hempstead, UK). The final product was denatured at 90°C for 10

minutes and left on ice for 3 minutes before being added to the hybridising cylinder.

Hybridisation of blot

The blot was pre-hybridised using pre-hybridising solution made up to 20ml total volume

with ddH$_2$O containing 6X SSC, 0.5% SDS, 5X Denhardt's solution [0.1% BSA, 0.1%

Ficoll™, 0.1% polyvinylpyrrolidone (PVP)] and 100ug/ml denatured (at 90°C for 5

minutes) salmon sperm DNA. The blot together with pre-hybridising solution was placed in

the hybridiser (Techne Hybridiser HB-1D) for 1 hour at 67°C. The relevant labelled probe

was added and the blot was left to hybridise at 67°C for ≥16 hours.

The hybridised blot was washed with the following solutions ensuring that the blot is

covered in solution at all times:

1)   2X SSC, 0.1% SDS for 20 minutes at 65°C

2)   1X SSC, 0.1% SDS for 20 minutes at 65°C

3)   0.1X SSC, 0.1% SDS for 20 minutes at 65°C

The damp blot was wrapped in cling film and placed on a piece of Whatman 3MM paper in

a film cassette. An X-ray film was placed (Kodak X-OMAT™LS) on the blot and exposed

overnight at -80°C.

2.2.10 Single-strand ligation PCR

The method used within this thesis had been described by McGurk *et al.*, 2001. An outline

of the procedure is shown in **Figure 2.3**. The modified method described below was

adapted from already existing TD-PCR and Sslig-PCR procedures. Here, single-strand

ligation PCR is used to identify DNA lesions produced as a result of BGIII21 binding.

Damaged genomic DNA, cut with appropriate restriction enzyme(s)

Linear PCR using biotinylated primer 1.B

Capture on Streptavidin Dynabeads

Ribonucleotide tailing by Terminal Deoxynucleotidyl Transferase

Ligation of double stranded linker by T4 DNA ligase

Exponential PCR with Upper oligo primer and radiolabelled Primer 2

Run DNA on sequencing gel
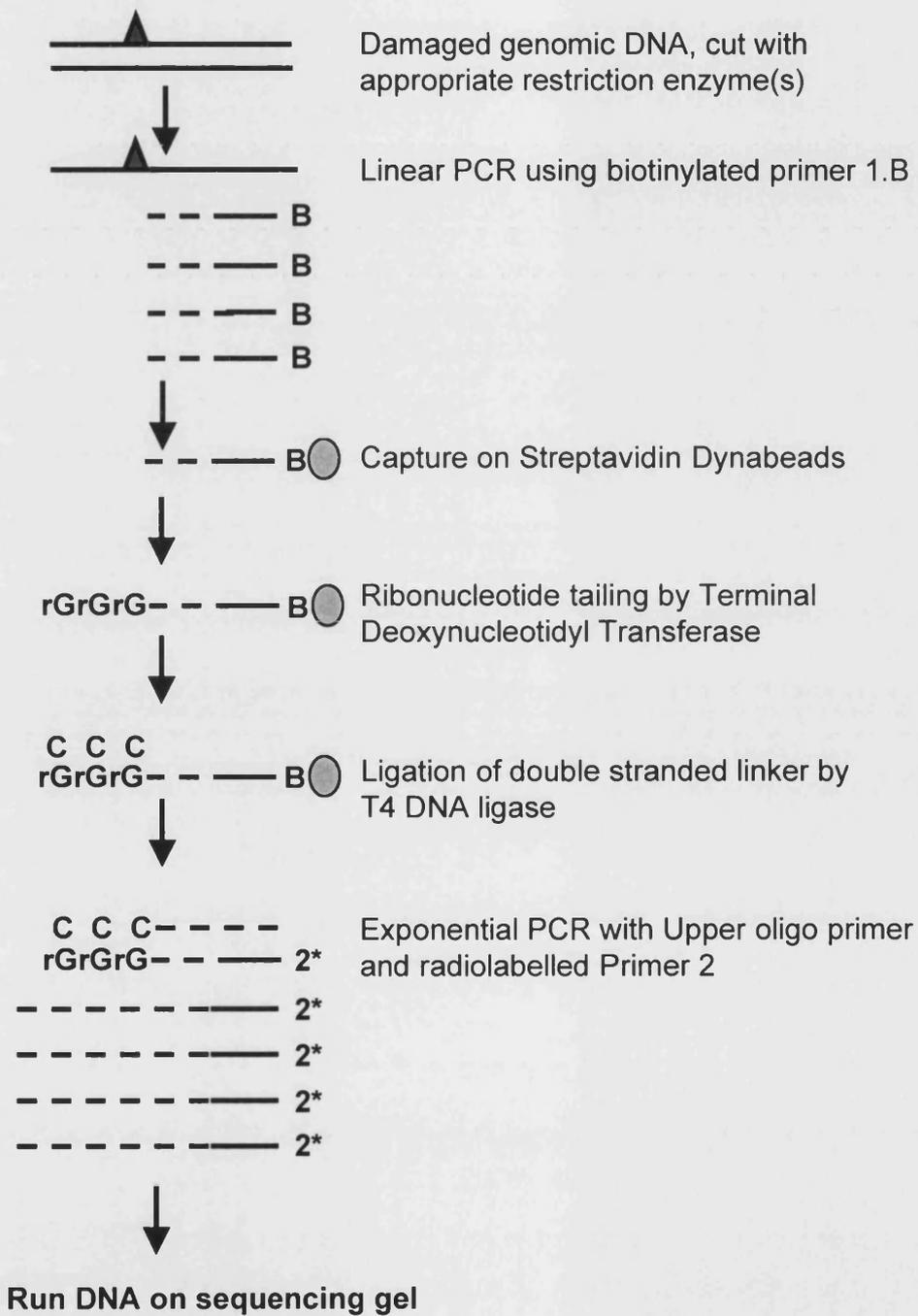
Fig. 2.3: Schematic illustration showing steps involved in the Sslig-PCR (adapted from McGurk, *et al.*, 2000).

<u>Primers</u>

Table 2.3 shows primer sets for N-*ras* promoter and *Hprt* exon 9 region both used in single-strand ligation PCR experiments (section 3.3.10, 4.3.2 and 4.3.3).

Name	Nucleotide sequence
N-*ras* primer 1	5'-GGA CAG ATT TAG GAC CAC AG-3' ; biotinylated at 5' end
N-*ras* primer 2	5'-GAC CAC AGC CGG GAA AAA TGT TGG AGA-3'
Hprt primer 1	5'-GTT TAG AAC AGT GTG AAG CAC TCA-3' ; biotinylated at 5' end
Hprt primer 2	5'- GAA GCA CTC AGT TTT CAT GTC AG-3'

Table 2.3: Primer sets used in single-strand ligation PCR

<u>Preparation of DNA samples</u>

Adherent cells grown to near confluence were treated with relevant BGIII21 doses at 37°C for 5 hours. Cells were harvested by washing gently with 0.01M PBS before trypsinisation. DNA was isolated using the method as described previously (section 2.2.7). It is necessary to include an RNAse step as the DNA is to be measured spectrophotometrically and excess RNA contributes to the total measurement of the DNA in each sample hence leading to an overestimate of the DNA and inconsistency between samples.

To create a natural stop site the DNA was digested with a restriction enzyme chosen to cut between one hundred and a few hundred base pairs downstream of the binding site of the biotinylated primer that is used in the first PCR step. The DNA concentration was measured fluorimetrically as this provides an extremely accurate way of measuring small quantities of DNA (Kowalski *et al.*, 1979).

<u>First-round TD-PCR</u>

For the initial TD-PCR step 3µg of DNA per sample were taken and the volume brought up to 10µl with ddH$_2$O. A PCR mix was prepared containing 1X of reaction buffer [10X: 100mM Tris-HCl (pH9.0 at 25°C), 500mM KCl and 1% Triton® X-100] supplied with the enzyme; 5mM MgCl$_2$ (25mM); 0.25mM dNTP mixture (2.5mM of each dNTP), (Amersham Bioscience, UK); 0.6pmoles oligonucleotide primer '1'; 2% DMSO (50%); 25mM TMA (0.5M) and ddH$_2$O. 25µl of the PCR mix was added to the DNA. The Taq

DNA polymerase (5u/µl; Promega, Southampton, UK) was diluted to 0.2u/µl in a total volume of 5µl per sample using ddH₂O. 5µl (1u) diluted Taq DNA polymerase were added to each sample tube, and tapped gently to mix.

The DNA was denatured at 95°C for 5 min., followed by 10 one-minute cycles at 95°C, 56°C for 3 min. and 74°C for 2 min. For complete extension of all products samples were incubated at 74°C for 5 min., subsequently denatured at 95°C for 2 minutes and then cooled down to 4°C.

Capture of PCR product

Streptavidin-coated magnetic beads (Dynabeads® M-280, Dynal®, UK) were used to capture the biotinylated PCR products. 5µl of beads (10µg/µl) per sample plus an additional 5µl was used. The Dynabeads were sedimented in a magnetic rack (Dynal MPC®-E) to remove the supernatant. The beads were washed twice by resuspending Dynabeads in 1X Washing-binding buffer (WBB) (10mM Tris-Cl, pH7.7; 1mM EDTA; 2M NaCl), followed by sedimentation in magnetic rack to remove supernatant. Dynabeads were resuspended in 40µl/sample 1X WBB. Aliquots of 40µl of Dynabeads were transferred to clean 1.5ml-tubes, sedimented and the supernatant removed.

To each tube containing 40µl products from the first-round PCR 10µl 5X WBB (50mM Tris-HCl, pH7.7; 5mM EDTA; 10M NaCl) were added. The mixture was transferred to tubes containing prepared Dynabeads. Incubation at 37°C for 30 minutes with occasional agitation to resuspend Dynabeads followed. The protocol was continued by washing the Dynabeads three times with 200µl TE (10mM Tris-HCl, pH 7.6, 1mM EDTA) as described before. The Dynabeads were resuspended in 50µl ddH₂O and centrifuged at 20,000g for 10 seconds.

Ribo-tailing of PCR product

During the Terminal Deoxynucleotidyl Transferase (TdT) Ribo-Tailing step riboGs were added to the 3' ends of the single-stranded products from linear PCR. The majority of the ends will possess 3' riboGs (Komura and Riggs, 1998).

All the reagents for ribo-tailing and ligation were stored at –20°C (except polyethyleneglycol (PEG) which was stored at 4°C), defrosted when necessary and kept on ice until needed except for TdT and DNA ligase which were kept at -20°C until needed.

The tubes containing Dynabeads bound to biotinylated PCR products were placed into a magnetic rack and the supernatant was removed. The Dynabeads were resuspended

in 10μl 0.1X TE (1mM Tris-HCl pH7.6, 0.1mM EDTA). A ribo-tail mix was prepared in a 1.5 ml tube containing 4μl of 5X TdT buffer (as provided with enzyme, 0.5M potassium cacodylate, pH7.2, 10mM CoCl2 and 1mM DTT), 4μl of 10mM rGTP (Promega, Southampton, UK), 1.33 μl distilled water; 0.67 μl of TdT (15 u/μl) (GIBCO-BRL, Paisley, UK). All above volumes were multiplied by the number of samples + 1.

Ten microlitre of the ribo-tail mix were placed into the tubes with the Dynabeads and mixed. Incubation at 37°C for 15 min. with occasional agitation followed. Next 180μl TE (10mM Tris-HCl pH7.6, 1mM EDTA) were added, the tubes were placed in a magnetic rack and the supernatant was removed. The Dynabeads were washed again with 2x 200μl TE. The Dynabeads were resuspended in 15μl 0.1X TE (1mM Tris-HCl pH7.6, 0.1mM EDTA).

Preparation of double stranded linker

The double stranded linker was the annealing product of a

'Lower oligo': 5'-AATTCAGATCTCCCGGGTCACCGC-3' and an

'Upper oligo': 5'-GCGGTGACCCGGGAGATCTGAATTCCC-3'.

The 'Lower oligo' was required to be phosphorylated at the 5' end as well as possess a 3'-terminal amine group to block self-ligation. The 'Upper oligo' is complementary to the 'Lower oligo' except for a three C overhang at the 3' terminus. Phosphorylation of the 'Lower oligo' was carried out using a kit containing T4 polynucleotide kinase and Forward reaction buffer (Gibco-BRL, Paisley, UK). Stock solutions of 200pmol/μl of both oligomers were prepared and a reaction mixture set up containing 11.1μl 'Lower oligo' (200pmol/μl), 20μl Forward reaction buffer (5X as provided), 62.9μl ddH$_2$O, 1μl ATP (100mM) and 5μl T4 polynucleotide kinase (10u/μl). The mixture was incubated at 37°C for 2 hours followed by heat inactivation of the kinase at 65°C for 20 min.. To anneal both primers, 11.1μl of 'Upper oligo' (200pmol/μl) were added to the phosphorylated 'Lower oligo'. The mixture was heated to 95°C for 3 min. and gradually cooled to 4°C by placing the sample in a 70°C removable hot block for 1 min. and transferring the hot block into a refrigerator. The linker was stored at -20°C until ready for use in the ligation reaction.

Ligation of double-stranded linker

The families of single-stranded molecules that possess rGTP tails were ligated to the double-stranded linker. The double-stranded limker's 3 C single-stranded overhang is complementary to the 3 riboG tails. The ligation reaction contained PEG that effectively

74

concentrated the reagents and kept the Dynabeads partially suspended important when incubating for long periods of time.

A ligation mix was prepared containing 2.7µl of ligation buffer (622mM Tris-HCl pH7.6, 126mM MgCl$_2$, 126mM DTT and 12.6mM ATP); 3.0µl of 20µM prepared double-stranded linker (see before); 9.1µl of 50% PEG; 0.2µl of T4 DNA ligase (20u/µl, Promega, Southampton, UK). All the above volumes were multiplied by the number samples + 1.

A volume of 15µl of the ligation mix was placed into the tubes with the Dynabeads from the ribo-tailing reaction and mixed. Samples were incubated at 17°C overnight. To continue 170µl TE (10mM Tris-HCl pH7.6, 1mM EDTA) were added, the tubes were placed in the magnetic rack and the supernatant removed. The Dynabeads were washed again twice with 200µl TE. The Dynabeads were resuspended in 40µl distilled water for PCR and transferred to 0.5ml tubes.

Second-round PCR

Ten pmoles of oligonucleotides were required per sample for second-round PCR. Primer '2' was phosphorylated with T4 polynucleotide kinase using kits (GIBCO-BRL, Paisley, UK) with forward reaction buffer. Once labelled the primer was stored at 4°C until ready for use in second-round PCR.

The 5' terminus of the second-round primer '2' was labelled by incubating 1µl of oligonucleotide primer '2' (10 pmoles/µl) per sample + 1, 6µl of 5X forward reaction buffer (as provided with enzyme, 5X is 350mM Tris-HCl pH7.6, 50mM MgCl$_2$, 500mM KCl, 5mM β-mercaptoethanol), 3µl γ-^{32}P-ATP (10µCi/µl), (Amersham Pharmacia Biotech, Little Chalfont, UK), 3µl of T4 polynucleotide kinase (10u/µl). The volume was brought to 30µl with distilled water. Incubation at 37°C for 30 min. followed. Distilled water was added to bring total volume to 10µl per sample + 1. To purify the labelled primer from unincorporated nucleotide the mixture was centrifuged through a Bio-Spin-6 spin column (Bio-Rad, Hemel Hempstead, UK).

The second-round exponential PCR was carried out with template DNA bound to Dynabeads. Ten pmoles of second-round nested region–specific primer '2' and 'upper oligo' primers were required per sample. For each new primer set the number of cycles necessary during the exponential step was determined empirically and fell between 16 and 22 cycles. It is important for the number of cycles to fall in the exponential range especially when quantifying bands.

A PCR cocktail mix was prepared containing 10μl of 10X reaction buffer [as provided with enzyme, 10X is 100M Tris-HCl (pH 9 at 25°C), 500mM KCl and 1% Triton® X-100], 8μl of 25mM $MgCl_2$; 20μl distilled water; 10μl of a mixture containing 2.5mM of each dNTP (Asmersham Pharmacia Biotech, Little Chalfont, UK); 1.0μl pmoles/μl oligonucleotide γ^{32}P-labelled primer '2'; 1μl of 10pmoles/μl 'upper oligo' linker primer. A 50μl volume of the PCR mix was placed into 0.5ml tubes with the Dynabeads from the ligation reaction and mixed well. In a separate 1.5ml tube Taq DNA polymerase (5u/μl; Promega, Southampton, UK) was diluted to 0.2u/μl in a total volume of 10μl per sample using distilled water. Ten microlitre (2u) of diluted Taq DNA polymerase were added to each tube, which were tapped gently to mix.

Next the samples were denatured at 95°C for 5 min., then cycled 16-22 times at 95°C for 1min., 68°C for 2 min. and 74°C for1 min. plus 1 sec.-extension per cycle. For complete extension of all products samples were incubated at 74°C for 5 minutes.

The tubes were centrifuged for 10 sec. at 20,000g and 100μl of supernatant were transferred without Dynabeads to fresh 1.5ml tubes. Distilled water (100μl) were added to the 0.5ml tubes to wash the Dynabeads, respun and 100μl of supernatant were transferred without Dynabeads to the 1.5ml tubes. To precipitate the DNA of each sample, 20μl 3M sodium acetate (pH 5.2) were added as well as 3 volumes of 95% ethanol (-20°C). The samples were vortexed, then all samples were placed in a dry ice bath for 20 min. and centrifuged for 15 min. 20,000g at 4°C. The DNA pellet were washed with 200μl 70% ethanol (RT) by gently inverting the tube, centrifuged for 5 min. at 20,000g at RT and the supernatant was discarded. The wash was repeated and DNA pellet dried under vacuum.

The DNA was resuspended in 5μl sequencing gel-loading buffer [96% (v/v) formamide (deionized), 20mM EDTA, 0.03% xylene cyanol, 0.03% bromophenol blue]. It was important that the samples were completely and uniformly resuspended. To achieve this, each sample was vortexed vigorously for at least 10 sec. and centrifuged at 20,000g for 10 sec. to collect liquid. Samples were stored at –20°C overnight.

The next day radiolabelled amplified fragments were separated in a 50cm x 21cm x 0.4mm, 6% denaturing polyacrylamide sequencing gel (National Diagnostics, Hull, UK; 5.7% acrylamide, 0.3% bisacrylamide, 8.3M urea, 0.1M Tris-borate pH 8.3, 2mM EDTA). The gel was pre-electrophoresed for 30 min. prior to loading. The gels were run in 1X TBE buffer (89mM Tris borate, 2mM EDTA pH 8.3) at 1700-2000 V for 2 hours or until the

bromophenol blue dye reached the bottom of the gel. A γ^{32}P-labelled 10bp marker (Gibco-BRL, Paisley, UK) (see section 2.2.12) was run next to the sample lanes to make it easier to identify potential bands representing BGIII21 drug lesions.

The samples were denatured at 95°C for 2 min. prior to loading, cooled on ice and each sample was loaded into an individual well. After running of the gel is completed, the gel was covered with Saran wrap and placed gel onto Whatman 3MM paper (Maidstone, UK) supported by a layer of Whatman DE 81 paper (Maidstone, UK) which bound the shorter fragments that passed through the 3MM. The gel was dried on a gel dryer (Bio-Rad, Hemel Hempstead, UK) under vacuum at 80°C for at least 1 hour. The gel was exposed to X-ray film (Kodak X-OMAT™LS) or a phosphoimaging screen, for an appropriate time. If an intensifying screen was used, the film is exposed at –80°C. Exposure to X-ray film was usually around 18 hours without the aid of an intensifying screen and exposure to phosphoimager was usually 2 hours to visualise the bands using these conditions.

2.2.11 Labelling of 10bp DNA ladder

TsAP treatment of 10bp DNA ladder (Gibco-BRL, Paisley, UK):

Reaction mixture:	1μl 10bp DNA ladder
	2μl 10X TsAP buffer
	1μl TsAP
	16μl ddH2O
	20μl total

The mix was incubated at 65°C for 30 minutes, followed by the addition of 0.5μl TsAP and a further incubation at 65°C for 15 minutes. A volume of 2.2μl Stop mix (provided with kit) was added to the mixture and the TsAP was inactivated at 65°C for 20 minutes.

Kinase treatment of "TsAP-ed" 10bp DNA ladder:

Reaction mixture:	5μl 'TsAP-ed" 10bp DNA ladder
	1μl 10X kinase buffer
	1μl T4 kinase
	3μl γ-^{32} P-ATP
	10μl total

The mix was incubated at 37°C for 30 minutes. After incubation 90µl TE were added to the mixture and the mixture was applied to a equilibrated column (BioRad, Hemel-Hempstead, UK).

2.2.12 Preparation of competent *E.Coli* cells

The initial stab of *E.coli* cells was Top10F purchased from Invitrogen, UK.

Competent cells were prepared based on the method described by Hanahan, 1983. Cells from a single colony were grown at 37°C in 5ml of Ψ broth (2% bacto tryptone, 0.5% yeast extract, 0.4% magnesium sulphate and 10mM potassium chloride) in 50ml Falcon tubes to an OD^{550} of around 0.3 overnight. Of this culture 2.5ml were used to inoculate 100ml of pre-warmed Luria-Bertani (LB) broth pre-prepared in 2 litre sterile glass flasks. The culture was grown for another 2-3 hours until the OD^{550} was 0.48. This required vigorous aeration provided by the shaker set at 250-350 rpm. The culture was cooled on ice, and transferred to 2 x 50ml Falcon tubes. These were spun in a pre-chilled centrifuge at 400g for 5 min. at 4°C. All subsequent work was carried out on ice. The cells were resuspended in ice-cold filter sterilized TfBI (100mM rubidium chloride, 50mM manganese chloride, 30mM potassium acetate, 10mM calcium chloride, 15% glycerol, pH to 5.8 with 0.2N acetic acid), 30ml per 100ml per culture. Cells were spun down as before and again resuspended in ice-cold filed TfBI. The cultures were left on ice for 30 minutes. The cells were again spun down, and gently re suspended in ice-cold TfBII (10mM MOPS, pH 7.0 [adjust with NaOH], 10mM rubidium chloride, 75mM calcium chloride, 15% glycerol) at a concentration of 4ml per 100ml of starting culture. Aliquots of 0.2ml of the suspension were dispensed into 1.5ml tubes and immediately placed into a dry-ice bath at −80°C. Afterwards all aliquots were moved to the −80°C freezer to be stored for up to 6 months.

2.2.13 Transformation of *E. coli*

An aliquot of pre-prepared competent *E. coli* cells was thawed on ice for approximately 10 minutes. Plasmid DNA was added to the *E. coli* aliquot at a ratio of 5µl plasmid DNA (1-5µg /µl) per 200µl cells. The mixture was incubated on ice for 30 minutes. The cells were heat shocked in a waterbath at 42°C for 90 sec. before being placed on ice for 3 minutes. Meanwhile 1ml of LB broth (20g/l) were pre-warmed at 37°C. The transformed cells were

added to the 1ml pre-warmed LB broth (containing no antibiotics) and incubated at 37°C for 1 hour and 30 minutes.

1) For maxi preps

The complete transformation mixture was transferred into 200ml of media containing 100-150μg/ml ampicillin and left shaking at 320rpm and 37°C overnight. The protocol was continued as described in the instructions provided by the Maxi prep kit (Qiagen, Crawley, UK). The concentration of plasmid retrieved after the maxiprep procedure was measured by adding 15μl of obtained plasmid DNA into 3ml of ddH2O at OD^{260}. An OD^{260} value of 0.1 indicated a concentration of 1μg/μl.

2) For bacterial colonies

After the final incubation step of the transformation protocol the transformed E. coli culture was spun down at 1500rpm for 3 minutes and 1ml of supernatant was discarded. The remaining portion of *E. coli* culture was spread on 5 plates (LB agar, 100μg/ml ampicillin) at a volume of 1 drop per plate. Plates were incubated at 37°C overnight. Colonies were later grown up by transferring single colonies each into 2ml LB broth containing ampicillin in a loosely capped 10ml tube. The colonies were shaken at 320rpm at 37°C overnight. The resulting 2ml of bacterial culture were decanted into a 2ml Eppendorf the next day and the plasmid DNA retrieved by following the protocol provided by the miniprep kit (Qiagen, Crawley, UK).

2.2.14 Transient transfection

This assay was used to determine the transfection efficiency of the HT1080 Tet-Off cell line using the pCH110 plasmid (**Fig. 2.4**) and pTRE-luc plasmid (**Fig. 2.5**). Transfection efficiency was later tested using the β-galactosidase assay kit (Promega, Southampton, UK) and luciferase assay kit (Promega, Southampton, UK) respectively.
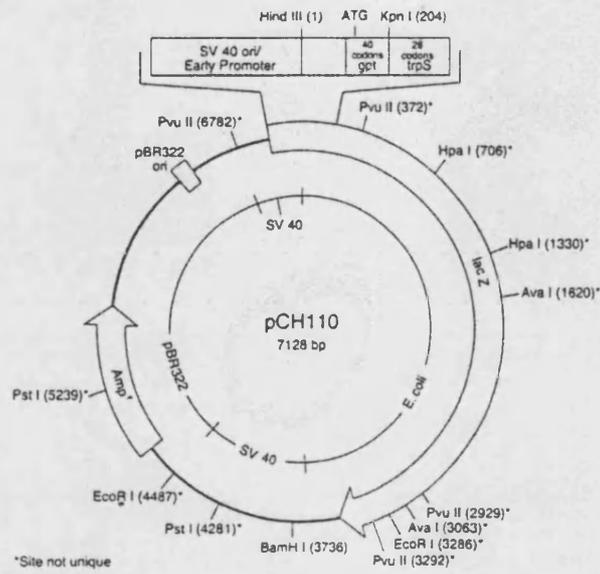
Fig. 2.4: Schematic representation of the pCH110 vector
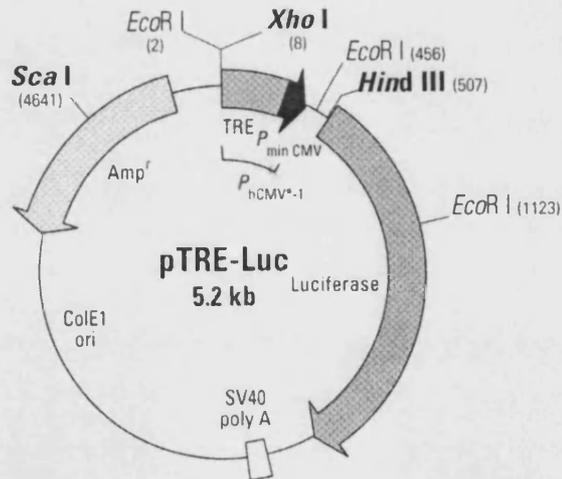
Fig. 2.5: Schematic representation of the pTRE-Luc vector

Initially, 1×10^5 cells per well were plated out in 6 well plates and left for 48hrs to reach 60-70% confluency. On the day of transfection mixtures containing the following ingredients were prepared in order to be able to achieve maximum transfection efficiency.

$$
\left.\begin{array}{l}
2.5\mu g \\
5\mu g \\
7.5\mu g
\end{array}\right\} \text{pTRE-luc} + 1\mu g\ \text{pCH110} + \left.\begin{array}{l}
10\mu l \\
20\mu l
\end{array}\right\} \begin{array}{l} \text{Superfect} \quad + 150\mu l\ \text{free DMEM} \\ \text{(Qiagen, UK)} \quad \text{(no glutamine or FCS)} \end{array}
$$

The transfection mixtures were incubated at RT for 10 minutes. Meanwhile the cells on 6-well plate were washed with FCS-free DMEM medium. Following the incubation period, 1ml of complete DMEM (2mM glutamine, 10% FCS, no antibiotics) medium was added to each of the transfection mixtures and the mixture added to individual wells of the 6-well plate so as to have one well per transfection mixture. Cells were incubated with the transfection mixtures at 37°C for 2 hours. The medium was changed and 4ml of complete growth medium was added to the cells. The medium was changed again after a further 18hours. Finally the cells were left to grow for 48 to 72 hours before being harvested for analysis using the β-galactosidase kit and luciferase kit.

2.2.15 Stable transfection

The protocol for stable transfection was the same as for transient transfection described previously. After transient transfections carried out to determine the amount of DNA and Superfect required for meaximum transfection efficiency, stable transfections were performed using 5μg plasmid DNA and 20μl Superfect. Therefore, the transfection mixture contained:

5μg plasmid DNA + 1μg pTK-Hyg (**Fig. 2.6**) + 20μl Superfect + 150μl free DMEM

The pTK-Hyg vector is required for selection of transfected cells using hygromycin containing medium. The plasmid DNA was either pTRE-E2F-1, pTRE-E2F-1 AS or pTRE300 (section 2.2.17) depending on whether E2F-1 inducible, E2F-1 inducible anti-sense or control clones were produced. All clones were further propagated in DMEM

81

medium containing 10% FCS, 4mM glutamine, 100 units/ml penicillin, 100ug/ml streptomycin, 100µg/ml of G418, 25µg/ml hygromycin and 500ng/ml doxocycline as recommended by Clontech,UK and verified by repeat experiments. Induction of E2F-1 expression in clones was initiated by the removal of doxocycline from the medium.
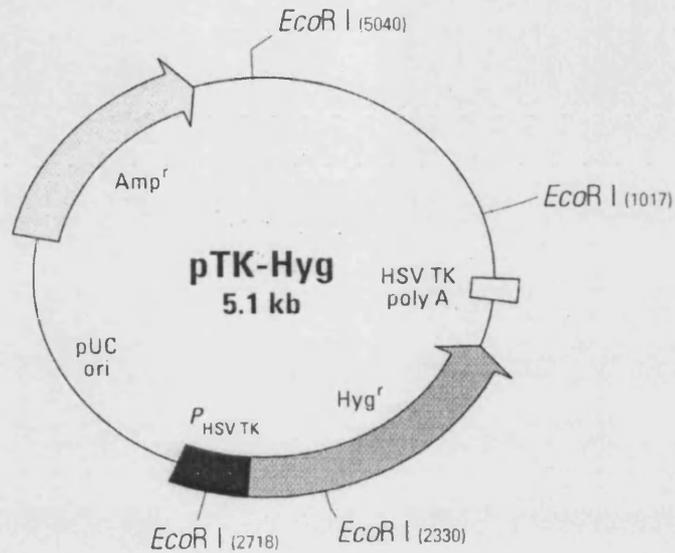
Fig. 2.6: Schematic representation of the pTK-Hyg vector

3. DEREGULATION OF E2F-1 AND CHEMOSENSITIVITY

3.1 Introduction

Aberrations in the expression levels of genes associated with the regulation of cell proliferation and apoptosis are found in all cancers. Alterations in gene expression are observed in particular with respect to the retinoblastoma pathway, regulating the transition from G1 to S phase, and the p53 pathway, responsible for induction of cell cycle arrest and apoptosis in response to DNA damage and inappropriate proliferative signalling. Deregulation of the retinoblastoma pathway occurs through several mechanisms including mutation or deletion of Rb, cyclin D overexpression and mutation and/or deletion of the cyclin-dependent kinase inhibitor $p16^{INK4a}$. Mutations or deletions of Rb have been reported in hereditary and sporadic retinoblastoma, small cell lung cancer, breast cancer and osteosarcoma (Kaelin, 1999; Schauer et al., 1994; Weinberg, 1995).

Overexpression of cyclin D1 has been observed as a consequence of gene amplification, translocation, post-transcriptional or post-translational modifications in a variety of cancers including breast cancer, head and neck cancer and non-small cell lung cancer (Bartkova et al., 1995; Buckley et al., 1993; Schauer et al., 1994; Scully et al., 2000).

Mutation and/or deletion of $p16^{INK4a}$, the cyclin-dependent kinase inhibitor regulating the activity of cyclin D-dependent kinases has been reported for many human cancers including pancreatic adenocarcinomas, and melanomas (Sharpless et al., 1999). Mutation and deletion of $p16^{INK4a}$ was found in non-small-cell lung cancer, but hypermethylation of the $p16^{INK4a}$ gene promoter was an additional mechanism found to be involved in gene silencing (Chen et al., 2002; Zöchbauer-Müller et al., 2001).

Alterations in the expression of Rb, cyclin $D1$ and $p16^{INK4a}$ lead to upregulation of the E2F transcription factors and a subsequent increase in the expression of genes required for DNA synthesis and progression from G1 to S phase of the cell cycle. An increase in E2F activity and transcription of E2F-regulated genes such as $DHFR$ and TS potentially influences the cellular sensitivity to chemotherapeutic agents leading to altered drug responses through one or more of the following mechanisms (Hochhauser, 1997; Kohn, 1996).

3.1.1 Overexpression of E2F-1 regulated proteins and chemosensitivity

Proteins required for DNA synthesis and G1 to S phase transition such as DHFR or TS potentially bind or are a drug target. Hence, E2F-1 dependent overexpression of these proteins potentially reduces cellular drug sensitivity. Hochhauser *et al.*, investigating the effects of cyclin D1 overexpression on chemosensitivity, observed a decrease in sensitivity to methotrexate as a result of an increase in *DHFR* expression levels (Hochhauser *et al.*, 1996).

An investigation into the effects of human *E2F-1* cDNA overexpression on growth, tumourigenicity and sensitivity to chemotherapeutic agents was conducted using an E2F-1 overexpressing HT1080 human fibrosarcoma cell line (Banerjee *et al.*, 1998). HT1080 cells were co-transfected with an E2F-1 expression vector and neomycin resistance vector to yield stable clones overexpressing E2F-1. Following selection, protein expression was determined by Western blot. Immunohistochemical analysis revealed a differential pattern of subcellular E2F-1 expression within chosen clones. E2F-1 expression pattern ranged from predominantly nuclear, to nuclear and cytoplasmic expression, to exclusively cytoplasmic expression of E2F-1. In addition, doubling times of E2F-1 overexpressing clones and tumour growth in nude mice were faster compared to the control. Cells from clones with predominantly nuclear E2F-1 expression were found to show the fastest rates of growth *in vitro* and *in vivo* (Banerjee *et al.*, 1998).

Further, E2F-1 overexpressing cells were able to overcome a G1 cell cycle block induced by methotrexate in comparison to control cells that exhibited a persistent G1 block following methotrexate treatment. Growth inhibition studies showed HT1080 E2F-1 overexpressing cells to be less sensitive to 5-day exposure to 5-fluorouracil (5-FU). This decrease in chemosensitivity observed after treatment with 5-FU appeared as a direct consequence of an E2F-1 dependent increase in *TS* expression, a 5-FU target gene (Banerjee *et al.*, 1998). No increase in resistance to methotrexate, a DHFR specific drug, was observed. E2F-1 overexpressing HT1080 cells were more sensitive to etoposide and doxorubicin, both topoisomerase II inhibitors, and SN38, a topoisomerase I inhibitor. Western blot analysis showed topoisomerase II expression levels to be higher in the E2F-1 transfectants compared to the control cells (Banerjee *et al.*, 1998).

3.1.2 Increase of the proportion of cells in S phase and chemosensitivity

Overexpression of E2F-1 and the resultant increase in E2F-regulated gene expression has been shown previously to drive cells into S phase (Shan *et al.*, 1994; Shan *et al.*, 1996). Hence, an E2F-induced increase in the proportion of cells in S phase might lead to an increased cell kill using S phase specific drugs. A recent study by Hofland *et al.* reported an increase in chemosensitivity in response to etoposide. Etoposide, a topoisomerase II inhibitor forms stable drug-protein-DNA complexes resulting in a double-strand break (DSB) upon collision with the replication machinery. The increase in chemosensitivity to etoposide was correlated with an observed increase in the percentage of cells in S phase as a result of E2F-1 induction. Further, an S phase-mediated increase in topoisomerase IIα expression was observed as *topoisomerase IIα* promoter activity is regulated independently of direct E2F-1 protein interaction (Hofland *et al.*, 2000). An investigation using an E2F-1 overexpressing myeloid progenitor cell line also found that E2F-1 overexpression resulted in an increase in chemosensitivity to etoposide through increasing the fraction of cells in S phase thereby causing an increase in topoisomerase IIα expression levels. Furthermore, the observed increase in the rate of apoptosis in response to etoposide treatment was found to be independent of p53 accumulation, hence was initiated via a p53-independent pathway (Nip *et al.*, 1997). Finally, a study using an E2F-1 overexpressing HT1080 human fibrosarcoma cell line observed an increase in chemosensitivity in response to etoposide and found the same observation to hold true for doxorubicin (Banerjee *et al.*, 1998)

3.1.3 E2F-1 mediated apoptosis and chemosensitivity

As discussed previously in the introduction (section 1.9) deregulated E2F-1 activity enhances apoptosis through induction of $p14^{ARF}$ followed by inhibition of MDM2 resulting in the accumulation and stabilisation of p53 (Bates *et al.*, 1998). Alternatively, E2F-1 is able to induce p53-independent apoptosis via p73, a p53 homologue (Irwin *et al.*, 2000). In a study to evaluate the *in vitro* and *in vivo* effects of adenovirus-mediated E2F-1 gene transfer alone or combined with topoisomerase II inhibitors, both etoposide and adriamycin were found to inhibit cell growth alone through arresting cells in G2 phase. Neither drug was able to induce cell death effectively. However, etoposide and adriamycin in combination with an increased exogenous expression of adenovirus-mediated E2F-1 led to an synergistic loss of viability in human osteosarcoma cells compared to treatment with

either E2F-1 or chemotherapeutic agents alone. The increased loss of cell viability was found to be independent of p53. Instead the activation of the caspase cascade appeared to be involved in triggering the apoptotic processes. *In vivo* experiments supported the above findings, as adenoviral-E2F-1 gene transfer or a single topoisomerase II inhibitor alone had a minimal anti-tumour effect while the combination of adenovirus-mediated E2F-1 and topoisomerase II inhibitor treatment produced an enhanced response and a significant reduction in tumour size (Yang *et al.*, 2001).

3.1.4 Chapter aims

Understanding the interactions between drug mechanisms of action and genetic alterations within cancer cells provides a basis for exploitation of the potential vulnerability of tumours harbouring genetic alterations. For example, attempts have been made to counteract cyclin D1 overexpression with flavopiridol, a flavonoid derivative of the plant alkaloid rohitukinea. Flavopiridol has been shown to be a potent inhibitor of CDKs 1,2,4 and 7 by decreasing the expression of cyclins D1 and D3 through affecting the transcription of cyclin D mRNA (Owa *et al.*, 2001).

The aims of this chapter are

- to evaluate the possibility of enforced expression of E2F-1 to selectively sensitise cancer cells to chemotherapeutic agents.

- to establish the underlying mechanism that causes the differential chemosensitivity to a variety of anti-cancer drugs.

- to translate the understanding of mechanisms of chemosensitivity into a potential therapeutic approach.

To achieve the above, a validated E2F-1 overexpressing cell system previously described by Banerjee *et al.* was taken for studies, using a wide range of common and novel chemotherapeutic agents (Banerjee *et al.*, 1998).

- [Cis-diamminedichloroplatinum (II)] (cisplatin), a cross-linking agent prevents cell division by binding to DNA and preventing the unwinding of the DNA double helix for replication thereby inhibiting mRNA synthesis. DNA damage is predominantly caused through the generation of intra-strand cross-links although inter-strand and DNA-protein cross-links have also been identified (Murray, 2000). Cisplatin is cell cycle non-specific and has been shown to be effective in the treatment of adenocarcinomas of ovary, breast and stomach, bone and soft tissue sarcomas, liver and bladder cancer (Souhami and Tobias, 1998).

- Melphalan, a nitrogen mustard compound is an alkylating agent that exerts its effect by forming monofunctional adducts at the N7-guanine and the N3-adenine as well as by producing inter- and intra-cross-links of DNA strands, abnormal base pairing, or DNA strand breaks thereby preventing uncoiling of the DNA and preventing DNA replication and cell division. Melphalan is considered to be cell cycle non-specific (Murray, 2000; Souhami and Tobias, 1998).

- Etoposide, a topoisomerase $II\alpha$ inhibitor produces cleavable complexes involving etoposide, topoisomerase $II\alpha$ and DNA, resulting in DNA strand breaks.

- BGIII21, a novel minor groove-binding agent was selected (**Fig. 3.1**). BGIII21 is a distamycin A derivative first described by Wyatt *et al.*, 1995. It is a tri-pyrrole compound that specifically binds to the minor groove of DNA in a sequence specific manner. The preferred binding site of BGIII21 is TTTTGPu. BGIII21 is a monofunctional alkylating agent, alkylating the N3-guanine or N3-adenine of the binding sequence, represented by Pu (Wyatt *et al.*, 1995).

3.2 Materials and Methods

3.2.1 Experimental cell lines

Unless otherwise stated adherent cell lines were maintained in Dulbecco's Modification of Eagles Medium (DMEM) containing 10% FCS and 2mM glutamine.

3.2.1.1 HT1080 and derivatives HT1080 Neo/ HT1080 E2F1-1, E2F1-4 and E2F1-6

HT1080 is a human fibrosarcoma cell line. Confluent cultures were passaged and seeded at a concentration of $1\text{-}4\times10^4$ cells/cm^2 as recommended by the European Collection of Cell
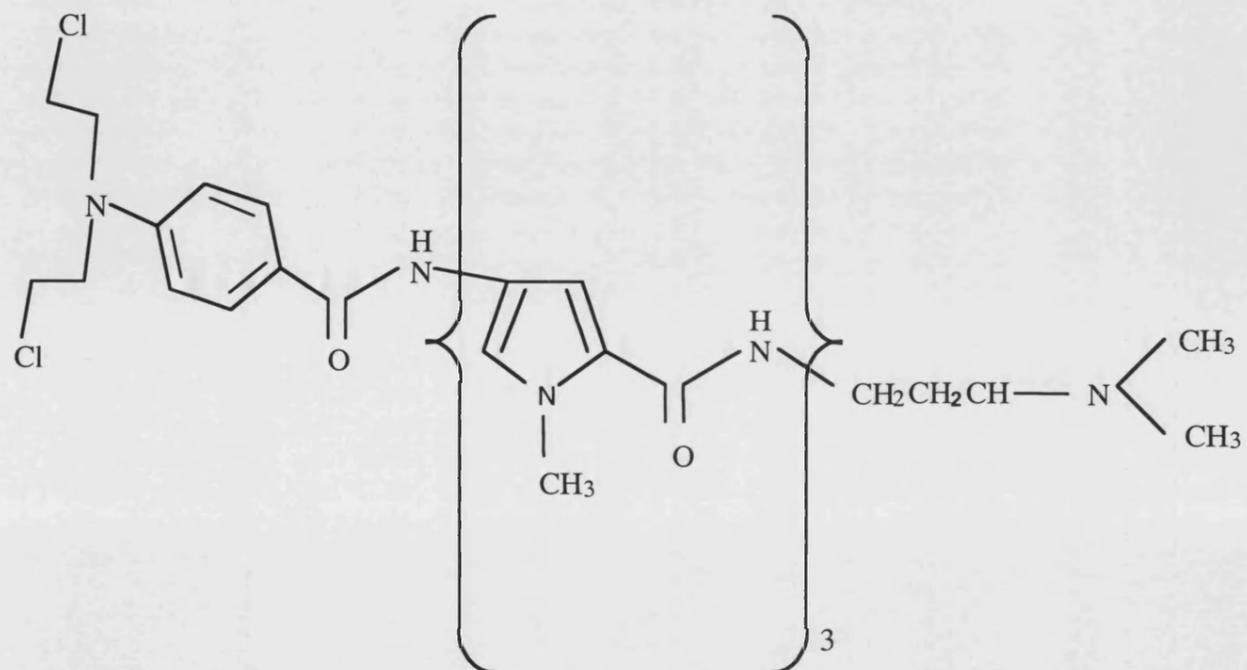
Fig. 3.1: Chemical structure of the novel minor groove binding alkylating agent BGIII21

Cultures (ECACC, Porton Down, UK). A variety of E2F-1 stably transfected HT180 human fibrosarcoma cell lines were provided by the Sloan-Kettering Institute, New York, USA (Banerjee *et al.*, 1998).

3.2.1.2 Chinese hamster ovary (CHO)

The Chinese hamster ovary cell line (CHO-AA8) purchased from Clontech, Basingstoke, UK was maintained in F-12 HAM medium supplemented with 10% FCS and 2mM glutamine. Confluent cultures were seeded at a concentration of $1-3x10^4$ cells/cm^2 unless otherwise stated (ECACC).

3.2.1.3 HT1080 Tet-Off E2F-1 inducible clones

The human fibrosarcoma Tet-Off cell line was purchased from Clontech, Basingstoke, UK and maintained in DMEM containing 10% Tet-Off FCS (Clontech, UK), 4mM glutamine, 100units/ml penicillin, 100µg/ml streptomycin and 100µg/ml of neomycin (G418) as recommended by the supplier. The cells were split as described for HT1080 cell lines (section 3.2.1.1).

3.3 Results

3.3.1 Growth curves and cell morphology

Of initially eight E2F-1 overexpressing HT1080 clones obtained, four representative clones were selected at random for the experimental investigation. All four clones are listed in **Table 3.1** and include the control and three E2F-1 overexpressing cell lines.

Name	Characteristic	Doubling time
HT1080 Neo	control neo transfectant	21 hours
HT1080 E2F 1-4	E2F-1 transfectants	21 hours
HT1080 E2F1-1	E2F-1 transfectants	10 hours
HT1080 E2F 1-6	E2F-1 transfectants	12 hours

Table 3.1: E2F-1 stably transfected HT1080 human fibrosarcoma cell lines selected for experimental investigation showing characteristics and cell doubling time of cell lines.

The doubling time for each of the cell lines was established using the method previously described in section 2.1.3.3. Two of the E2F-1 transfected cell lines, HT1080 E2F 1-1 and HT1080 E2F 1-6, exhibited a doubling time of 10 and 12 hours respectively. In comparison the HT1080 Neo and HT1080 E2F 1-4 cell lines both had a doubling time of 21 hours.

A comparison of cell morphology revealed a marked difference in morphology between the HT1080 E2F 1-1 and HT1080 E2F 1-6 cells on one hand and the HT1080 Neo and HT1080 E2F 1-4 cells on the other hand, as shown in **Figure 3.2**. The HT1080 Neo and HT1080 E2F 1-4 cells are larger and irregular in shape and are of a more granular appearance. In comparison both HT1080 E2F 1-1 and HT1080 E2F 1-6 are much smaller and exhibit a regular and round to spindle-like shape as well as a smooth appearance.

3.3.2 Increased E2F-1 expression in E2F-1 transfectants

Initial Western blot analysis confirmed the increased E2F-1 expression levels in the E2F-1 overexpressing transfectant cell lines (**Fig. 3.3A**). The E2F-1 protein appeared as the characteristic doublet of 60kd as determined by a Pre-stained Standard size marker (BioRad, Hemel-Hempstead, UK). The upper protein band depicts the phosphorylated E2F-1 protein while the lower protein band depicts the unphosphorylated E2F-1 protein. **Figure 3.3A** shows E2F-1 expression in all HT1080 E2F-1 transfectants. However, HT1080 E2F 1-1 and HT1080 E2F 1-6 exhibit a higher level of E2F-1 expression compared to HT1080 Neo. HT1080 E2F 1-4 shows an increase in E2F-1 expression compared to HT1080 Neo. Further analysis of HT1080 E2F 1-1 indicated that expression of E2F-1 in total cellular protein extracts was increased to a lower extent compared to nuclear extracts (**Fig. 3.3B**).

Following the observed increase of E2F-1 expression in the HT1080 E2F 1-1 and E2F 1-6, the HT1080 E2F 1-1 cell line was selected as a representative E2F-1 overexpressing cell line for further experiments. As Western blot analysis does not demonstrate functionality of the overexpressed E2F-1 protein, EMSA and supershift analyses were used to examine DNA binding as well as protein complex formation ability of the overexpressed E2F-1 protein.

HT1080 Neo
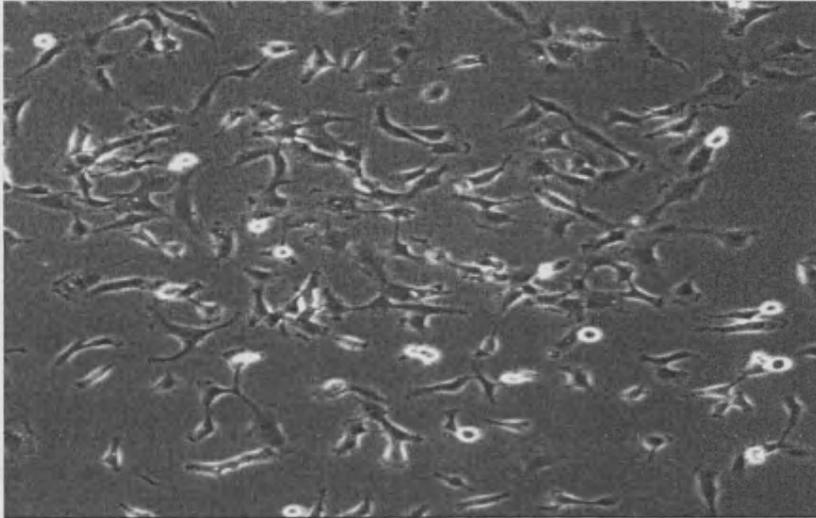
HT1080 E2F 1-1
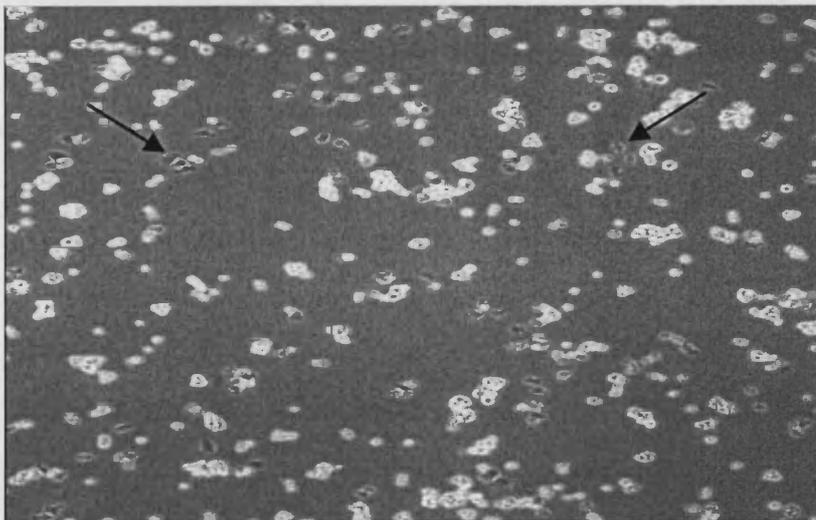
Fig. 3.2: Images of HT1080 Neo and HT1080 E2F 1-1 cells taken at x40 magnification to highlight differences in size and morphology.

91
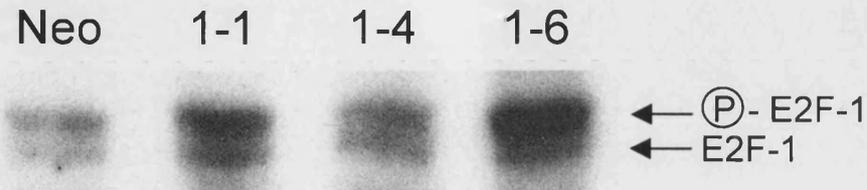
Fig. 3.3A: Increased expression of E2F-1 in E2F-1 transfected cells.
E2F-1 appears as the characteristic doublet of ~60kd as determined by
Pre-stained Standard size marker. 10μg cellular extract was separated on
10% SDS-PAGE gel as described by Western blot protocol.
Neo (HT1080 Neo); 1-1 (HT1080 E2F 1-1); 1-4 (HT1080 E2F 1-4);
1-6 (HT1080 E2F 1-6)
Coomassie staining of the blot to verify equal protein loading was not
included as the blot did not photograph well.
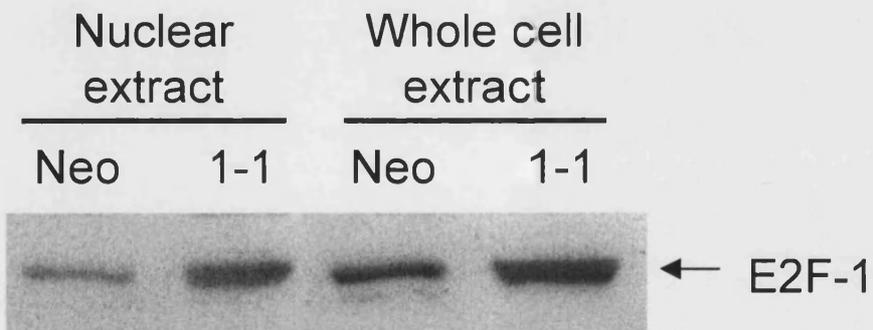
**Fig. 3.3B: Increased nuclear and cellular expression of E2F-1
in E2F-1 transfected cells** (1-1) compared to control cells (Neo)
as determined by Western blot analysis. 10μg of nuclear or
cellular protein extract were separated on 10% SDS-PAGE gel.
Coomassie staining of the blot to verify equal protein loading was not
included as the blot did not photograph well.

92

3.3.3 Overexpressed E2F-1 exhibits DNA binding and complex formation

In a representative mobility shift experiment (**Fig. 3.4**) an increased level of E2F-1 expression within HT1080 E2F 1-1 compared to HT1080 Neo was demonstrated. In addition, the mobility shift analysis identified one species of DNA binding complex containing E2F-1 (complex B, lane 'C') therefore verifying the DNA binding ability of the overexpressed E2F-1. In order to identify additional proteins present in the observed DNA binding complex containing E2F-1, supershift analysis using an E2F-1 antibody and antibodies against the pocket proteins pRb, p130 and p107 were performed. The resulting complex A confirmed the identity of the overexpressed protein to be E2F-1 (lane 'E2F-1') but did not indicate complex formation between E2F-1 and pRb (lane 'pRb'), p130 (lane 'p130') or p107 (lane 'p107'). However, persistence of complex B in lane 'pRb' and 'p130' suggested the presence of 'free' E2F-1. 'Free' E2F-1 is defined as the heterodimer consisting of E2F-1 and DP1 not found in higher complexes with pocket proteins (Bandara *et al.*, 1993; Huber *et al.*, 1993). In conclusion, the identity of the overexpressed E2F-1 protein was confirmed and the E2F-1 protein was shown to be functional as it binds DNA.

3.3.4 Deregulated expression of E2F-1 induces S phase entry

As stated in the introduction (section 1.10), a number of previous investigations revealed E2F-1 overexpression to result in an increase in the percentage of cells in S phase of the cell cycle as a consequence of inappropriate S phase entry (Johnson *et al.*, 1993; Shan *et al.*, 1994). To confirm that the E2F-1 overexpressing cell line (HT1080 E2F 1-1) contains functional E2F-1, FACS analysis was carried out as previously described (section 2.2.5). HT1080 Neo and HT1080 E2F 1-1 cells were fixed and stained with propidium iodide and subsequently sorted according to DNA content (**Fig. 3.5**). It was found that in a representative experiment 31% of HT1080 E2F 1-1 cells were present in S phase of the cell cycle compared to 13% HT1080 Neo cells. A concomitant decrease of HT1080 E2F 1-1 cells in G1 and G2 phase was observed.

3.3.5 Resistance to BGIII21 in E2F-1 overexpressing cells

To examine the effect of E2F-1 overexpression on chemosensitivity, a range of chemotherapeutic agents was selected for growth inhibition studies (section 3.1.4).

93
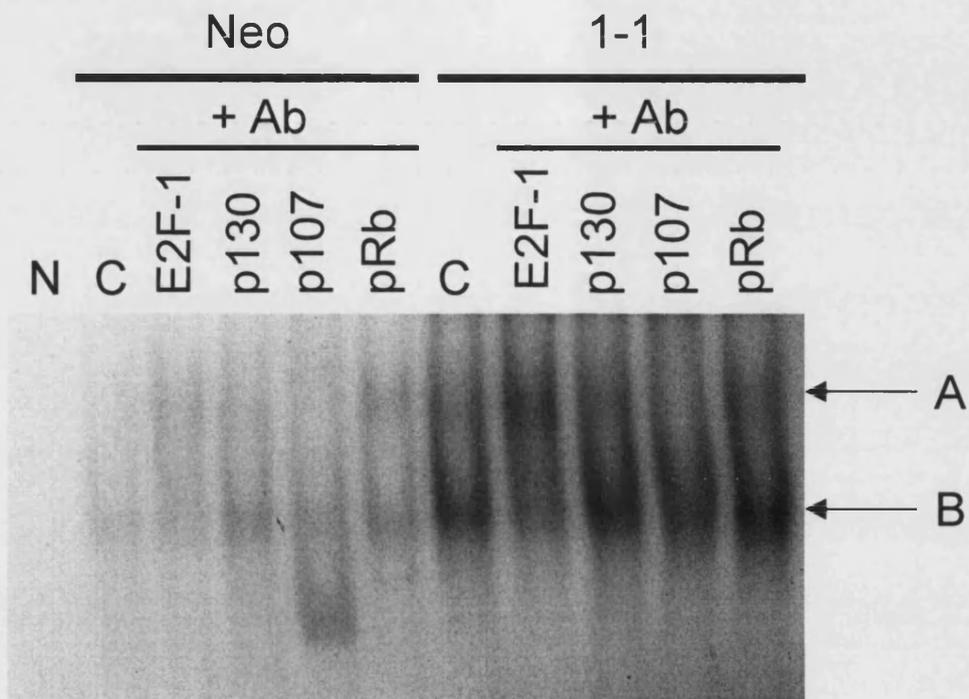
Fig. 3.4: DNA binding and complex formation of overexpressed E2F-1
as shown by EMSA and supershift analysis. E2F-1 protein of HT1080 Neo
(Neo) and HT1080 E2F 1-1 (1-1) bound radio-labelled E1A probe (lanes 'C')
(B). E2F-1 protein fraction was identified by E2F -1 antibody (+Ab)
(lane 'E2F-1') in supershift analysis (A). Additional protein components of
E2F-1 DNA-binding complex were not verified by supershift analysis (A)
(lane 'p130'), (lane 'pRb') and (lane 'p107').
20μg of nuclear extract was separated on 4% polyacrylamide gel.
Cold E2A probe was used as a negative control (lane 'N').

HT1080 Neo   **G1: 58%**
                         S : 13%
                         G2: 29%

HT1080 E2F 1-1   **G1: 46%**
                         S : 31%
                         G2: 23%
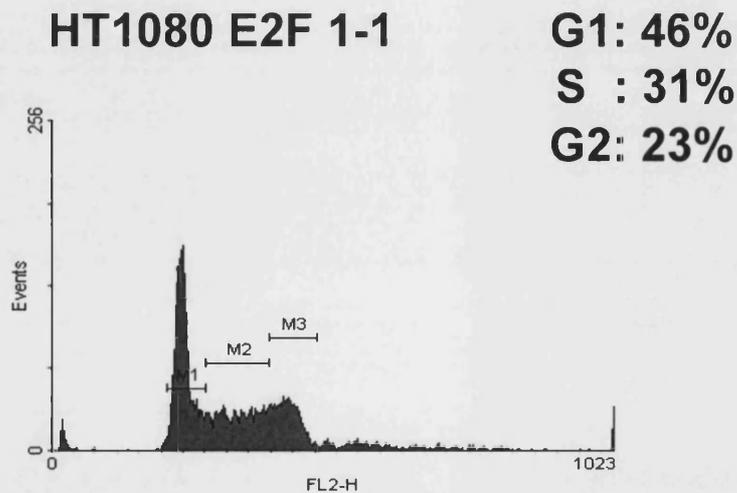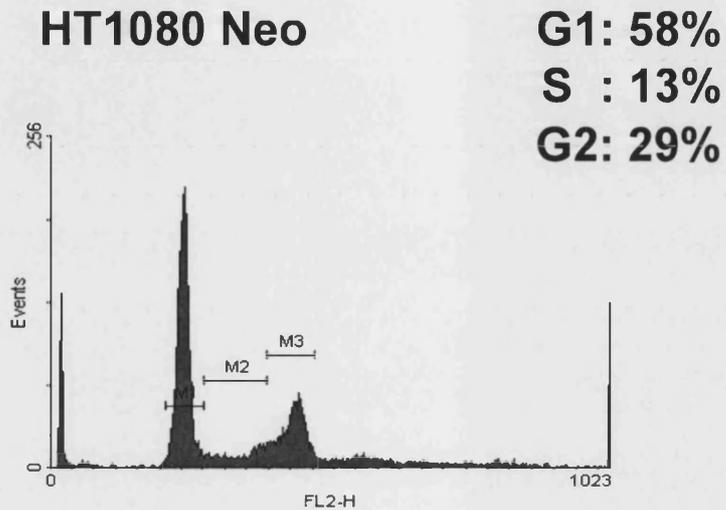
Fig. 3.5: Increased percentage of cell accumulation in S phase of cell cycle in E2F-1 overexpressing cell line (HT1080 E2F 1-1). Exponentially growing cells were stained with propidium iodide and sorted according to DNA content (FL2-H) using FACS analysis. The resulting histogram was analysed by gating the individual cell cycle phase populations to obtain the % cells in each cell cycle phase.
M1 (G1 phase-2n); M2 (S phase-2n/4n); M3 (G2 phase-4n)

95

Sulphorhodamine B (SRB) growth inhibition assays were used to investigate the growth inhibitory effect of selected chemotherapeutic agents on E2F-1 overexpressing cell lines as this method provides a rapid and sensitive way of screening by way of measuring the total cellular protein content (Skehan *et al.*, 1990). Growth inhibition analysis based on 3 or more repeat experiments from which the mean IC_{50} (± s.d.) was derived, revealed the continual survival of HT1080 E2F 1-1 (>50μM ± N/A) compared to HT1080 Neo (0.72μM ± 0.26) in response to BGIII21, following continuous drug exposure (**Fig. 3.6**). Additional, statistical analysis found the difference in chemosensitivity of HT1080 Neo and HT1080 E2F 1-1to BGIII21 to be significant (p-value < 0.0001) (section 2.2.3.3). After 72hours drug treatment with etoposide a decrease in chemosensitivity was observed in the HT1080 E2F 1-1 cells (0.89μM ± 0.08) compared to HT1080 Neo (0.36μM ± 0.1) cells. However, further analysis showed the difference in chemosensitivity between the two cell lines to be non-significant (p = 0.1642). Results for cisplatin indicated an increase in chemosensitivity in HT1080 E2F 1-1 (1.7μM ± 0.26) compared to HT1080 Neo (3.95μM ± 0.84) but statistics revealed the difference in chemosensitivity to cisplatin to be non-significant (p = 0.2824). The same result applied to melphalan as although HT1080 E2F 1-1 cells were found to be more sensitive (6.8μM ± 1.65) than HT1080 Neo cells (8.86μM ± 1.53) using IC_{50}s, the difference in chemosensitivity was not found to be statistically non-significant (p = 0.0333).

Additional SRB analysis including the HT1080 E2F 1-4 and E2F 1-6 cell line were performed and representative results for HT1080 E2F 1-6 showed an equally increased resistance to BGIII21 treatment as was shown for the HT1080 E2F 1-1 (**Fig. 3.7**). Results for the HT1080 E2F 1-4 cell line were similar to the HT1080 Neo cell line indicating the E2F-1 expression level to influence chemosensitivity to BGIII21. To conclude, the IC_{50} for HT1080 E2F 1-1 and HT1080 E2F 1-6 were both >50μM and the HT1080 Neo and HT1080 E2F 1-4 cell lines had IC_{50} of 0.72μM and 0.43μM respectively following 72 hours of BGIII21 treatment. Further statistical analysis of the data using a global multivariate model showed significant differences in chemosensitivity between HT1080 Neo and HT1080 E2F 1-4 on one side and HT1080 E2F 1-1 and HT1080 E2F 1-6 on the other side (p < 0.0001). Therefore, overexpression of E2F-1 appears to modulate the cellular sensitivity in response to minor groove binding alkylating agents such as BGIII21.
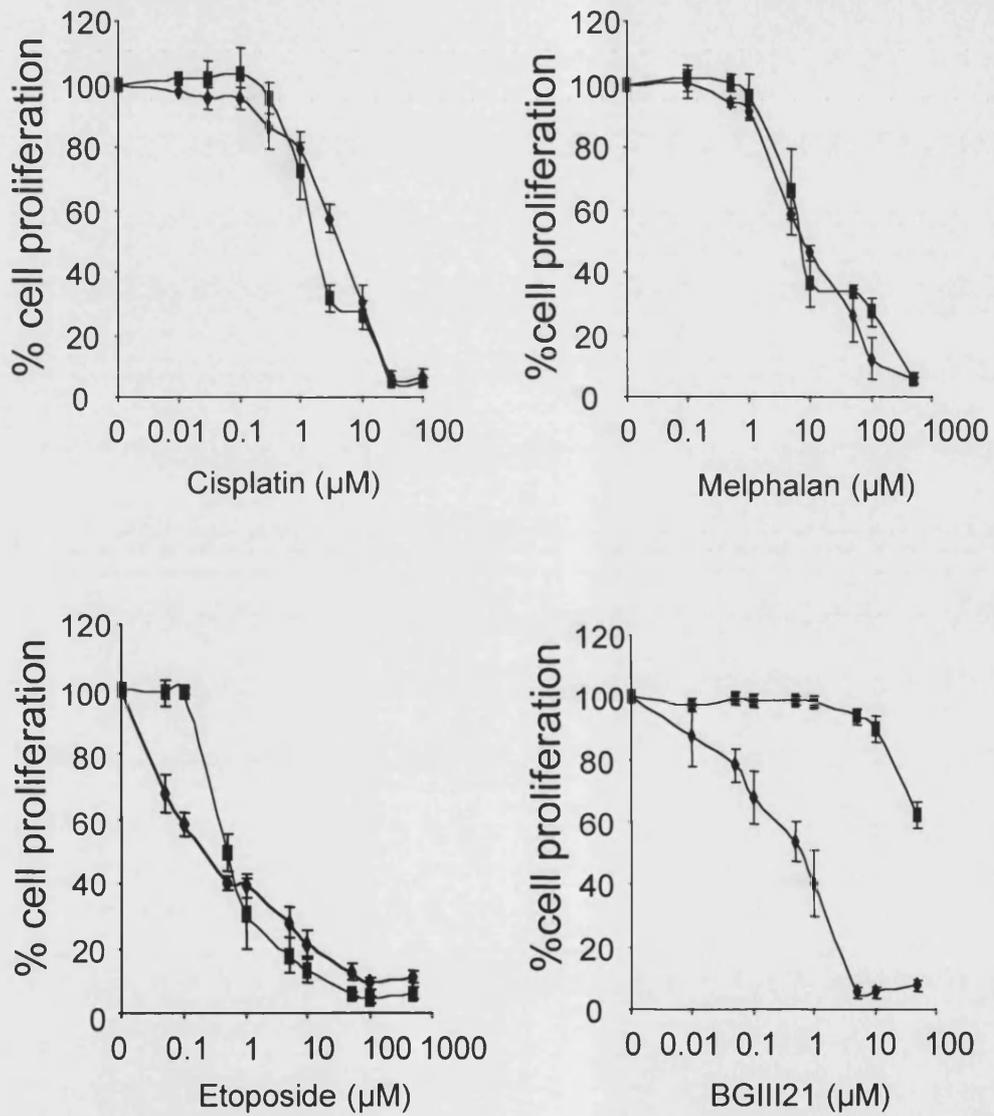
Fig. 3.6: Growth inhibitory effect of common chemotherapeutic agents and a novel minor groove binding alkylating agent (BGIII21) as measured by Sulphorhodamine B assay. All drug exposures were continuous (72hrs) and graphs represent 3 or more individual experiments.

◆ Neo (HT1080 Neo); ■ 1-1 (HT1080 E2F 1-1)
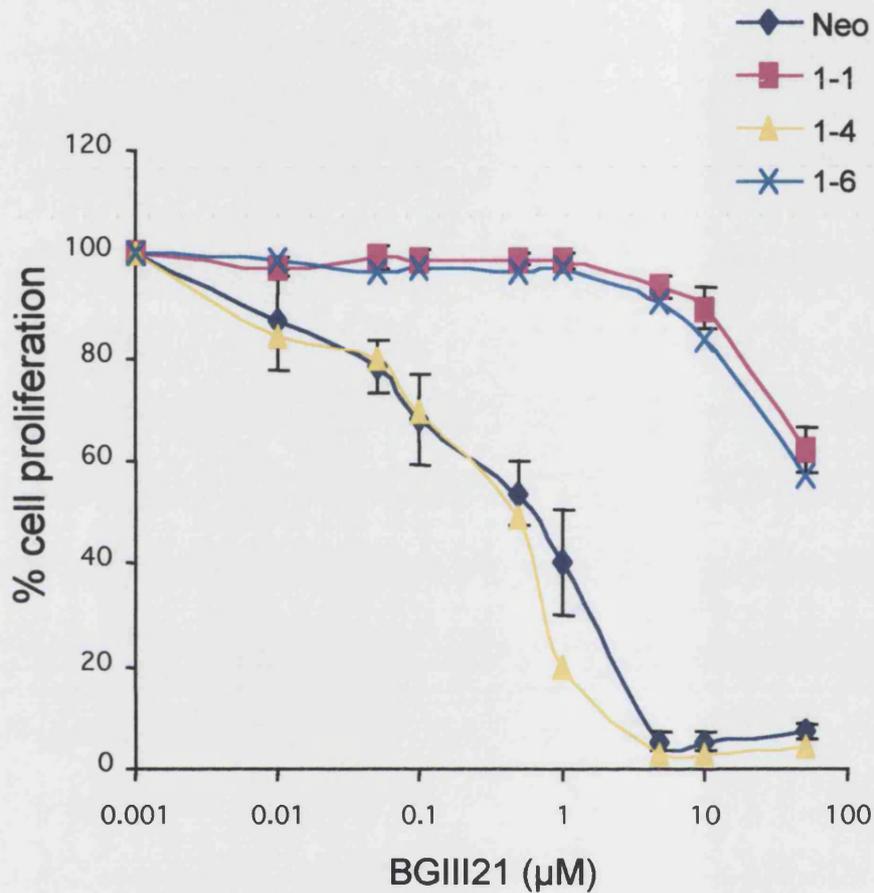
Fig. 3.7: Growth inhibitory effect of a novel minor groove binding alkylating agent (BGIII21) as measured by Sulphorhodamine B assay. All drug exposures were continuous (72hrs) and graphs for Neo (HT1080 Neo) and 1-1 (HT1080 E2F1-1) represent 3 or more individual experiments while graphs for 1-4 (HT1080 E2F 1-4) and 1-6 (HT1080 E2F 1-6) depict representative experiments.

3.3.6 E2F-1 overexpression results in resistance to minor groove binding agents

To expand the investigation with respect to the novel minor groove binding agent BGIII21, further SRB growth inhibition experiments were performed. These included a range of minor groove binding agents such as Distamycin A, Hoechst 33258 and anthramycin and minor groove binding alkylating agents such as Tallimustine, CC-1065 and SCIII147 (Murray, 2000). The range of drugs selected was used to investigate the mechanism of action responsible for the resistance effect observed in E2F-1 overexpressing HT1080 cells. Results obtained are based on 3 or more repeats performed for each individual experimental set-up i.e. cell line, drug and exposure time. The mean IC_{50} for each set of results was calculated and the relative resistance (RF) was normalised according to the formula shown in section 2.2.3.1 (**Table 3.2**).

Calculated values for relative resistance were either above or below 1. Any value above 1 signified a decrease in sensitivity of the cell line of interest i.e. HT1080 E2F 1-1 compared to the control cell line (HT1080 Neo) in response to a specific drug tested. Values below 1 represented an increase in sensitivity of the cell line of interest (HT1080 E2F 1-1) compared to the control cell line (HT1080 Neo) for a specific drug tested. The exact value of 1 represented no observed difference in chemosensitivity to a particular agent in the HT1080 E2F 1-1 compared to the control cell line (HT1080 Neo) (Colella *et al.*, 1999). Previously obtained results for cisplatin, melphalan and etoposide were included in **Figure 3.8** for comparative purposes.

Figure 3.8 shows an increase in relative resistance with respect to all minor groove binding agents in the HT1080 E2F 1-1 cell line compared to HT1080 Neo following acute or continuous drug exposure. However three exceptions to the above statement were observed. Anthramycin and CC-1065 both resulted in an increase in sensitivity of HT1080 E2F 1-1 after 1 hour (RF = 0.77) and 72 hours (RF= 0.53) drug incubation respectively. In addition only a negligible increase in relative resistance of HT1080 E2F 1-1 cells to Distamycin A (RF = 1.05) was observed after 1 hour drug incubation.
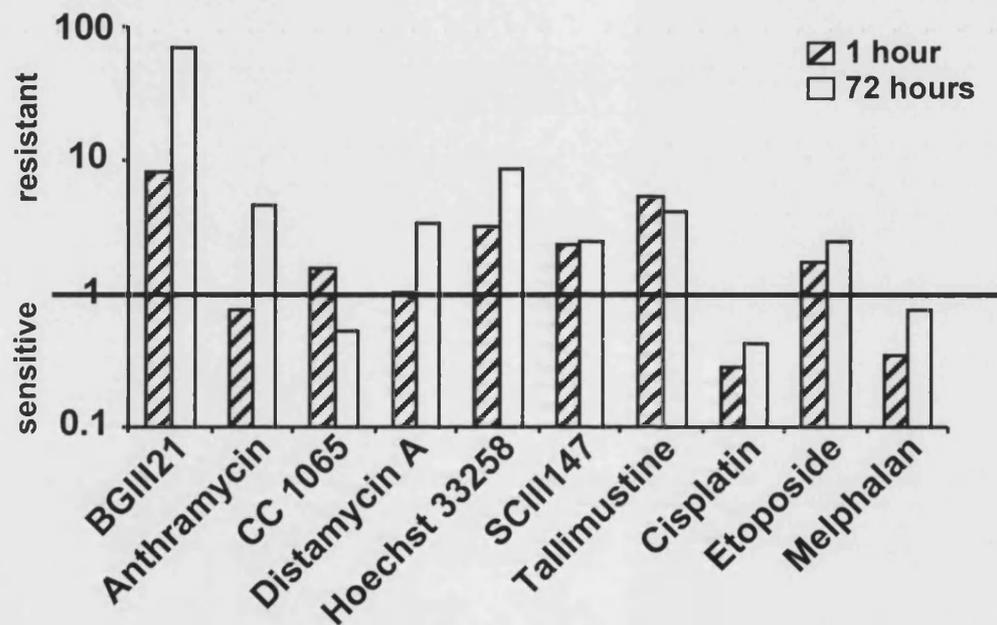
Fig. 3.8: Relative resistance of HT1080 E2F 1-1 to a range of minor groove binding and alkylating agents. Drug exposures were either acute or continuous for SRB assays performed. The resistance factor (RF)was calculated, using the average IC_{50} of 3 or more repeats for each experimental set-up, as described in section 2.2.4.1. RF values below 1 indicate an increased sensitivity, values above 1 indicate an increased resistance of HT1080 E2F 1-1 to a specific drug in comparison to HT1080 Neo.

Drug	RF (1 hr drug exposure)	RF (72 hrs drug exposure)
BGIII21	>8.06	>69.4
Anthramycin	0.77	4.68
CC 1065	1.6	0.53
Distamycin A	1.05	3.49
Hoechst 33258	3.2	8.54
SCIII147	2.41	2.54
Tallimustine	5.48	4.13
Cisplatin	0.29	0.43
Etoposide	1.71	2.47
Melphalan	0.34	0.77

Table 3.2: Resistance factor values for minor groove binding, alkylating agents and chemotherapeutic agents cisplatin, etoposide and melphalan. RF was calculated, using the mean IC_{50} of 3 or more repeats for each experimental set-up, as described in section 2.2.3.1.

Relative resistance factors calculated for acute and continuous drug exposures to cisplatin, etoposide and melphalan confirmed results obtained in section 3.3.5. These showed an increase in chemosensitivity of HT1080 E2F 1-1 cells to cisplatin and melphalan while a decrease in chemosensitivity is observed with respect to etoposide.

Tallimustine, structurally most closely related to BGIII21 (**Fig. 3.9**) resulted in a 5fold increase in resistance of HT1080 E2F 1-1 following acute or continuous drug exposure. This stood in contrast to the RF values obtained for BGIII21 which indicated a 8 fold and 70 fold increase in resistance of E2F-1 overexpressing cells after acute and continuous drug exposure respectively.
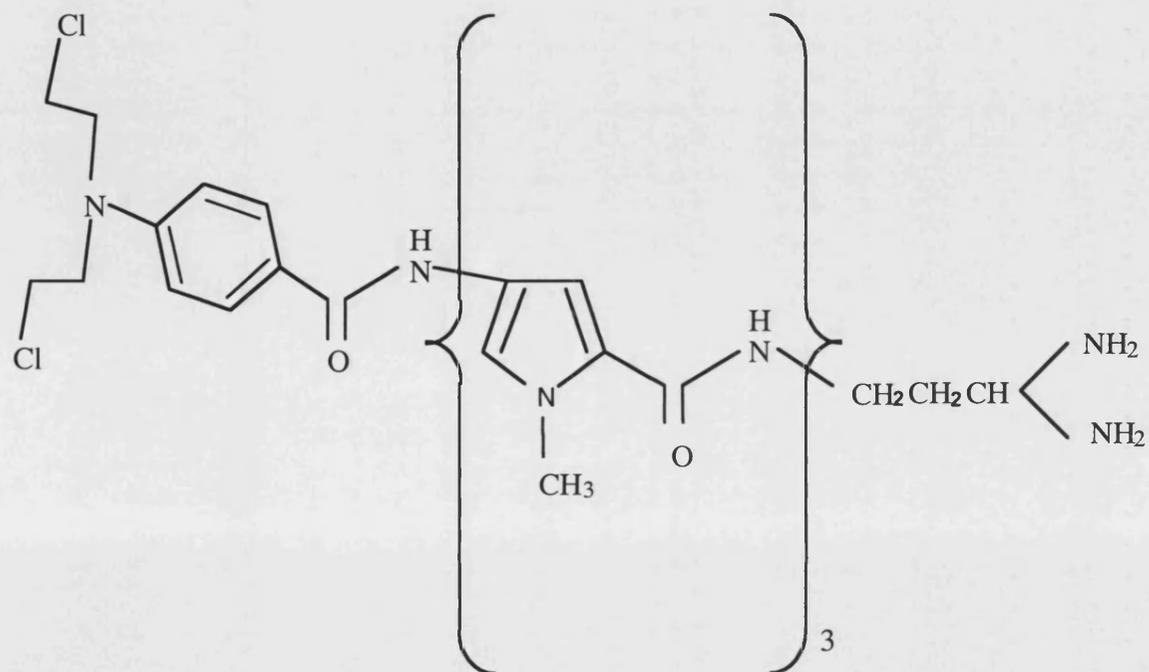
Fig. 3.9: Chemical structure of the minor groove binding agent alkylating tallimustine

3.3.7 No effect on colony forming potential of E2F-1 overexpressing cells in response to BGIII21 treatment

Previous studies were performed using the Sulphorhodamine B (SRB) method, which gives a measure of growth inhibition only. To answer the question whether cells treated with a particular drug underwent cell cycle arrest or cell death further studies, looking at colony formation were performed to investigate cell survival (Brown *et al.*, 1999).

To determine the response of HT1080 E2F 1-1 cells to BGIII21 treatment, cell survival assays were carried out to measure the effects of drug exposure on cells resulting in either cell death or recovery. A survival assay thus required a measure of the ability of cells to proliferate and this is usually an estimate of the ability of the individual cells to form colonies. In a representative clonogenic assay HT1080 E2F 1-1 cells demonstrated continued proliferation throughout the range of BGIII21 concentrations applied, while HT1080 Neo cells were cell cycle arrested or dead after 10μM and 50μM BGIII21 treatment (**Fig. 3.10**). Continued cell proliferation is represented as the percentage of colony formation. Percentage colony formation was calculated by determining the cloning efficiency i.e. the number of colonies formed divided by the initial fixed number of control cells plated out. The value representing the cloning efficiency was then multiplied by the fraction obtained when dividing the number colonies attained for the drug treated cells by the number treated cells initially plated out (see section 2.2.4). The above illustrated the proliferative potential of HT1080 E2F 1-1 after treatment with BGIII21 compared to HT1080 Neo.

3.3.8 BGIII21 treatment results in S phase block in HT1080 E2F 1-1 cells

Further investigation was required into the way in which BGIII21 influences the cell cycle of E2F-1 overexpressing cells. FACS cell cycle analysis was performed on cells treated with increasing concentrations of BGIII21 for 1 hour followed by the cells being fixed and stained with propidium iodide (see section 2.2.5) (**Fig. 3.11**). In a representative experiment the results for HT1080 Neo cells showed that an increased accumulation of cells in G2 phase occurred from 30% at 0μM to 52% at 1μM BGIII21, before complete cell death is observed at 5μM BGIII21. The percentage of cells in S phase doubled from 12% at 0μM to 24% at 5μM BGIII21 while the percentage of cells in G1 phase decreased concomitantly. In contrast, HT1080 E2F 1-1 cells exhibited an initial gain in percentage of
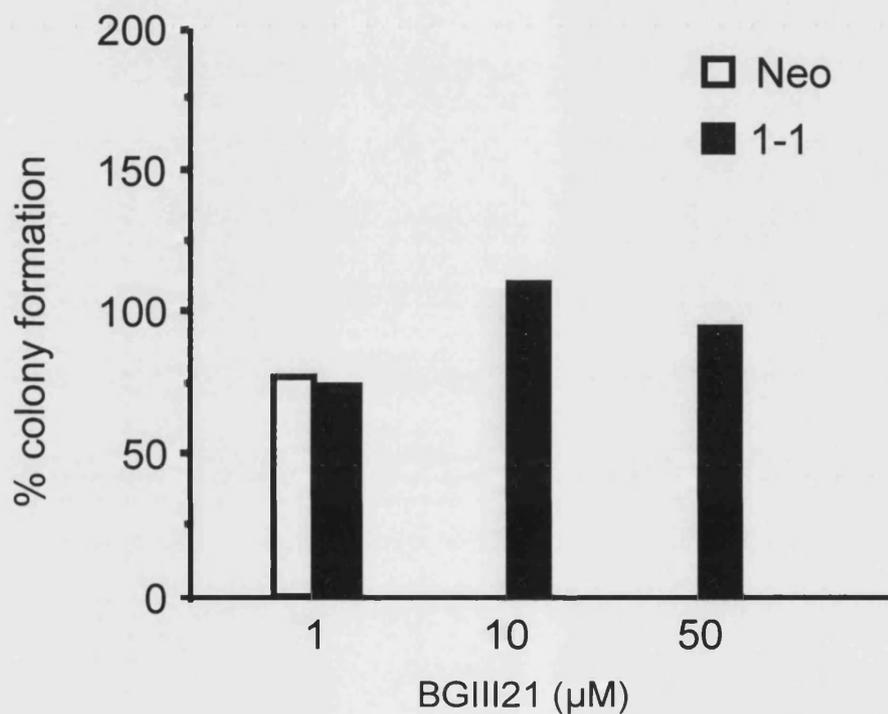
Fig. 3.10: Effect of BGIII21 treatment on colony forming potential of HT1080 Neo and HT1080 E2F 1-1 cells. 50-60% confluent cells were treated with BGIII21 for 1 hour beforebeing plated out on petri dishes and left to proliferate and form colonies for 7-14 days. The cloning efficiency for HT1080 Neo and HT1080 E2F 1-1 was deduced to be ~50% and ~100% respectively. % colony formation was calculated as described previously in section 2.2.5.

HT1080 Neo   **HT1080 E2F 1-1**

0µM

G1: 58%
S: 12%
G2: 30%

G1:45%
S:32%
G2:23%

1 µM

G1: 24%
S: 24%
G2: 52%

G1:59%
S:23%
G2:18%

5 µM

G1:51%
S:19%
G2:30%

50 µM

G1:24%
S:62%
G2:14%
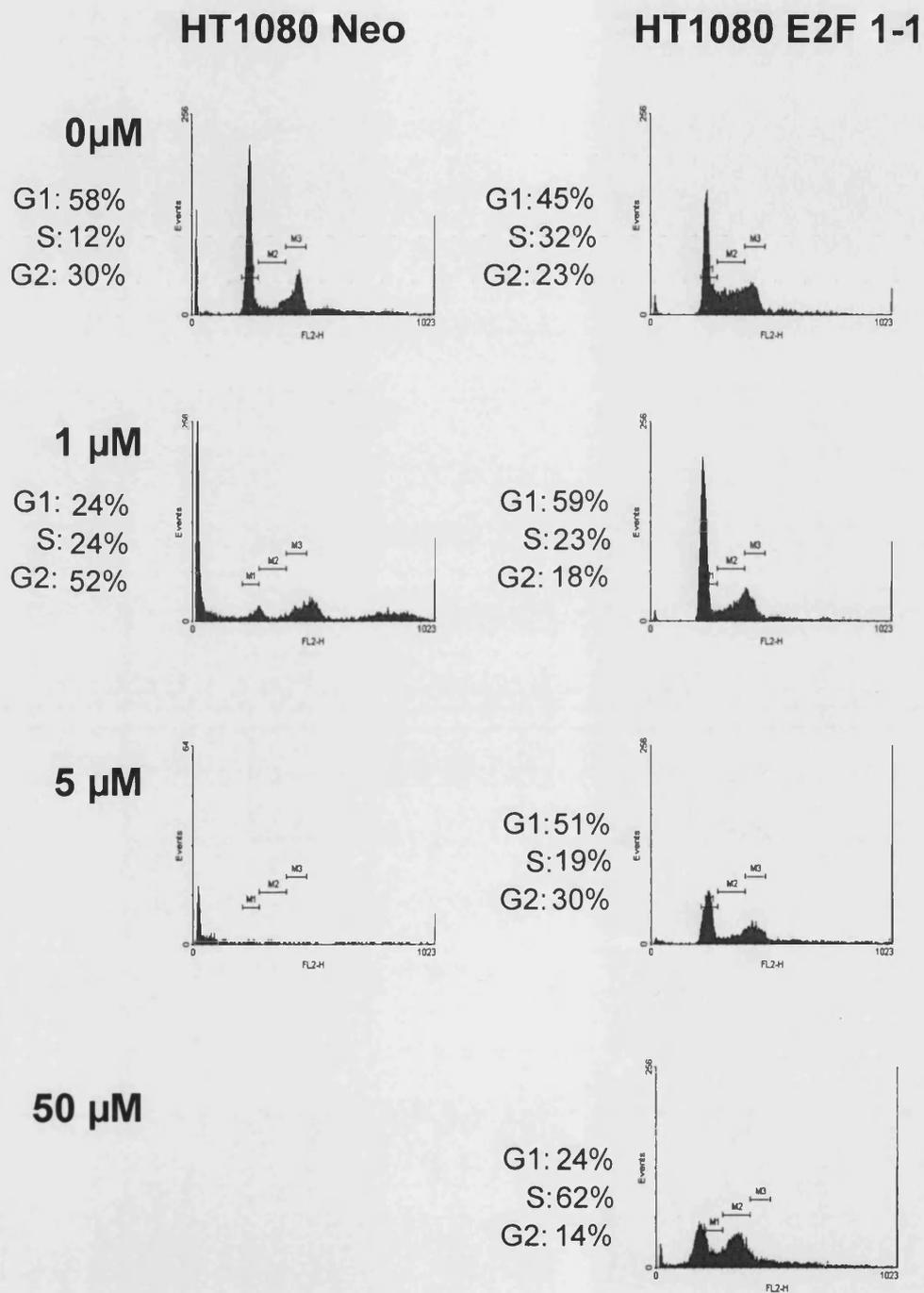
**Fig. 3.11: Effect of BGIII21 on the cell cycle distribution of HT1080 Neo
and HT1080 E2F 1-1 cells.** Cells were exposed to increasing doses of BGIII21
for 1 hour before being fixed, stained with PI and sorted according DNA content
using FACS. The resulting histogram was analysed by gating the individual cell
Cycle phase populations to obtain the percentage of cells in each cell cycle phase.
M1 (G1 phase-2n); M2 (S phase-2n/4n); M3 (G2 phase-4n)

105

cells in G1 phase at 1μM BGIII21 (59%) that progressively declined with increasing drug concentrations of 5μM (51%) and 50μM BGIII21 (24%). The fraction of cells in S phase showed an increase at 50μM BGIII21 (62%) resulting in an S phase block. The number of cells in G2 phase exhibited variations with increasing concentrations of BGIII21 concomitant with changes seen in the distribution of cells in G1 and S phases of the cell cycle. Further, the appearance of a sub-G1 peak at 50μM BGIII21 was noticed indicating that a fraction of E2F-1 overexpressing cells did undergo apoptosis and die. In conclusion, following treatment with 50μM BGIII21 E2F-1 overexpressing cells continued to proliferate albeit with an altered cell cycle distribution and the appearance of a sub-G1 peak implying apoptotic cell death.

3.3.9 E2F-1 overexpressing cells do not undergo apoptosis in response to 10μM BGIII21

To complement the studies into the effect of BGIII21 on cell proliferation and cell cycle distribution, apoptosis assays using the TACS™ Annexin V-FITC detection method were carried out as described in section 2.2.6. HT1080 Neo and HT1080 E2F 1-1 cells were treated with 10μM BGIII21 for 1 hour and samples taken immediately after drug treatment (0 hr) as well as at 24 hours, 48 hours and 72 hours time intervals post drug treatment (**Fig. 3.13A** and **3.13B**). The results are presented in the form of a quadrate containing four sectors each representing a distinct population of cells (**Fig. 3.12**).
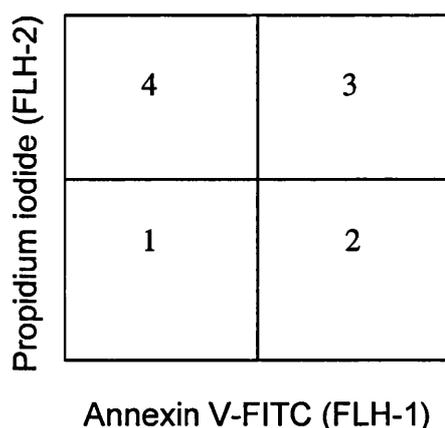
Fig. 3.12: Example of the quadrate used for analysis of apoptosis assay results.

Sector 1: viable cells (PI –ve / Annexin V-FITC -ve)

Sector 2: apoptotic cells (PI –ve / Annexin V-FITC +ve)

Sector 3: necrotic cells (PI +ve / Annexin V-FITC +ve)

Sector 4: damaged and fractionated cells (PI +ve)

Within 24 hours post BGIII21 drug treatment a distinct shift of viable HT1080 Neo cells into apoptosis or necrosis was observed (**Fig. 3.13A**). At 48 hours post drug treatment the majority of cells (51.2%) was necrotic as illustrated by the Annexin V/PI double-staining of the cells. At 72 hours post drug treatment the majority of HT1080 Neo cells were evenly divided between apoptotic (39.6%) and necrotic (34.4%) cells. The observed reduction in the percentage of necrotic cells at 72 hours post drug treatment may occur as a result of the analysis having been performed on an ungated (total) population of cells. Analysis of an ungated (total) population includes cells that would be otherwise excluded if analysing a gated (selected) population of cells. In the control experiment, 80-90% untreated HT1080 Neo cells remained viable throughout the timecourse as illustrated by cells not being stained by either propidium iodide or Annexin V-FITC. A fraction of cells damaged by experimental processes invariably occurred and was disregarded for analysis.

When the same experiment was performed on E2F-1 overexpressing cells the result was different in that BGIII21 treated cells even at 72 hours post drug treatment did not exhibit any apoptosis or necrosis (**Fig. 3.13B**). Instead the cells were as viable as the untreated control cells. This supported results obtained from the clonogenic assay that altered cell cycle distribution as established by cell cycle analysis.

3.3.10 BGIII21 specific DNA lesions produced in HT1080 Neo and E2F 1-4

The investigations into the effects of BGIII21 treatment on E2F-1 overexpressing cells required detailed analysis of DNA damage produced and potential repair pathways involved.

To answer the above questions Single strand-ligation (Sslig) PCR as described in section 2.2.10 was carried out. Sslig PCR is a useful method to analyse DNA damage qualitatively and quantitavely at a single nucleotide level (McGurk *et al.*, 2001). For the Sslig PCRs performed in this investigation the previously well-characterised N-*ras* promoter exon 1 region was selected (Thorn *et al.*, 1991).

Untreated

Treated

0 hr

17.07%   0.14%
82.74%   0.05%

15.98%   0.08%
83.93%   0.01%

24 hrs

9.43%   0.39%
89.98%   0.20%

42.27%   0.07%
0.00%
57.66%

48 hrs

6.91%   0.27%
92.76%   0.06%

16.07%   51.18%
16.42%   16.33%

72 hrs

16.22%   0.08%
83.97%   0.03%

4.25%   34.44%
12.37%   39.58%
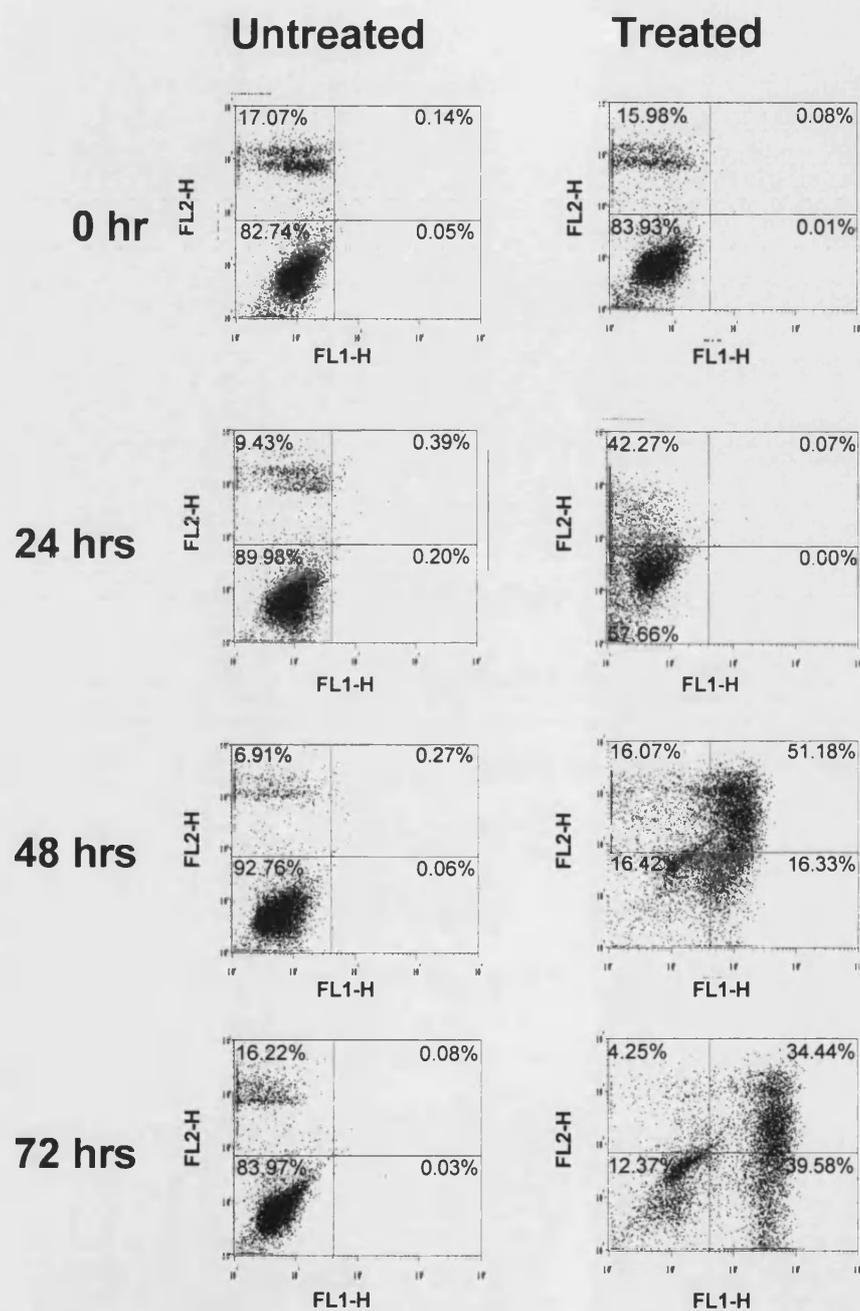
Fig. 3.13A: HT1080 Neo cells undergo apoptotic cell death after 1hr exposure to BGIII21. In a representative experiment an ungated cell population was analysed according to the Annexin V-FITC apoptosis detection protocol. Annexin V-FITC (FLH1) and PI (FLH-2) are plotted against each other resulting in a quadrate with 4 sectors each representing a distinct cell population (section 3.3.9).

108

Untreated **Treated**

0 hr

Untreated: 46.21% | 0.06% / 53.71% | 0.02%
Treated: 35.56% | 0.10% / 64.18% | 0.16%

24 hrs

Untreated: 15.01% | 0.00% / 84.96% | 0.03%
Treated: 33.52% | 0.01% / 66.47% | 0.00%

48 hrs

Untreated: 25.43% | 0.00% / 74.56% | 0.01%
Treated: 25.87% | 0.02% / 74.09% | 0.02%

72 hrs

Untreated: 52.39% | 0.08% / 47.50% | 0.03%
Treated: 58.70% | 0.13% / 41.07% | 0.10%
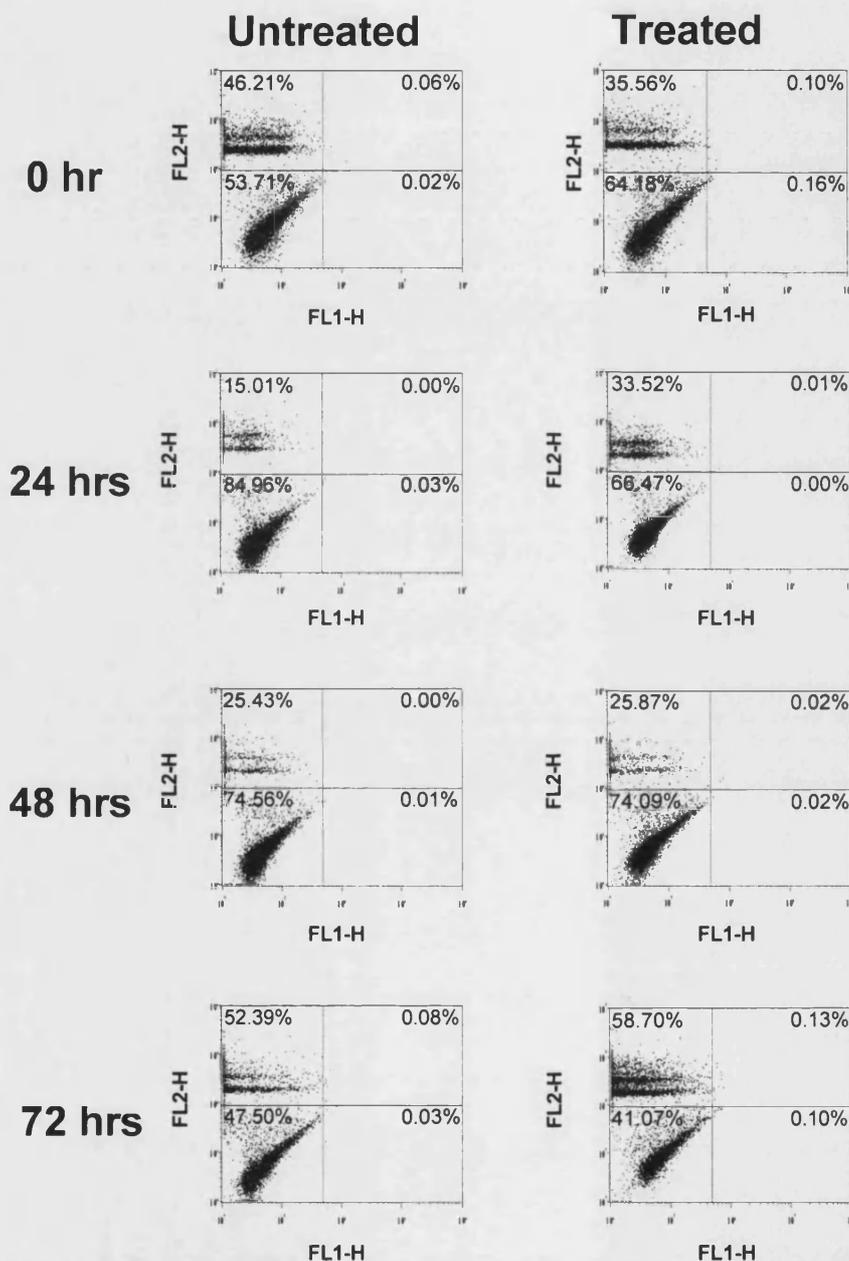
Fig. 3.13B: HT1080 E2F 1-1 cells do not undergo apoptotic cell death after1hr exposure to BGIII21. In a representative experiment an ungated cell population was analysed according to the Annexin V-FITC apoptosis detection protocol. Annexin V-FITC (FLH1) and PI (FLH-2) are plotted against each other resulting In a quadrate with 4 sectors each representing a distinct cell population (section 3.3.9).

109

The N-*ras* promoter region produced a fragment of DNA of 274bp length when digested with *Mse*I restriction enzyme and contained a single BGIII21 specific binding site (TTTTGA).

All four previously characterised cell lines were included in the first set of Sslig-PCR experiments. Cells were exposed to increasing doses of BGIII21 for 5 hours. In a study, Brooks *et al.*, have previously shown that an exposure time of 5 hours was sufficient to produce DNA lesions in yeast cells (Brooks *et al.*, 2000). As no published data was available on exposure times required to produce BGIII21 specific DNA lesions in mammalian cells a 5 hours exposure time was selected for initial experiments in HT1080 cells. The representative result in **Figure 3.14**, showed that BGIII21 specific DNA lesions are produced at 5μM and 50μM BGIII21 in HT1080 Neo and HT1080 E2F 1-4 cells as determined by a 10bp ladder run alongside the samples. No results were obtained for either HT1080 E2F 1-1 or E2F 1-6. This lack of results could not be explained by failure of the method or experimental error as results were obtained for both HT1080 Neo and E2F 1-4 cell line. A number of repeats including adjustments of experimental variables such as MgCl$_2$ concentration in PCR reactions and PCR cycle number consistently produced an identical result to the one above. The possibility of an impaired drug uptake BGIII21 by HT1080 E2F 1-1 and E2F 1-6 cells was rejected as even failure of BGIII21 to enter cells would have resulted in a full length (FL) PCR product band being detectable on the gel.

3.3.11 DNA amplification experiments reflect Sslig result

As experiments in section 3.3.10 gave no results for either HT1080 E2F 1-1 or E2F 1-6 cells the investigation was extended to elucidate the possibility of any differences in DNA sequence and accessibility between the two sets of clones. Restriction digest experiments using a number of restriction enzymes covering the range of primarily purine to solely pyrimidine based restriction sites were set up. In addition, the DNA extraction method was modified by including an increased number of phenol-chloroform purification steps to ensure that extracted DNA was free of any DNA associated proteins, hence eliminating the possibility of DNA bound proteins blocking access of restriction enzymes or primers to the DNA sequence. All restriction enzyme experiments resulted in the DNA of all four cell lines being completely digested as observed in the characteristic DNA smear produced
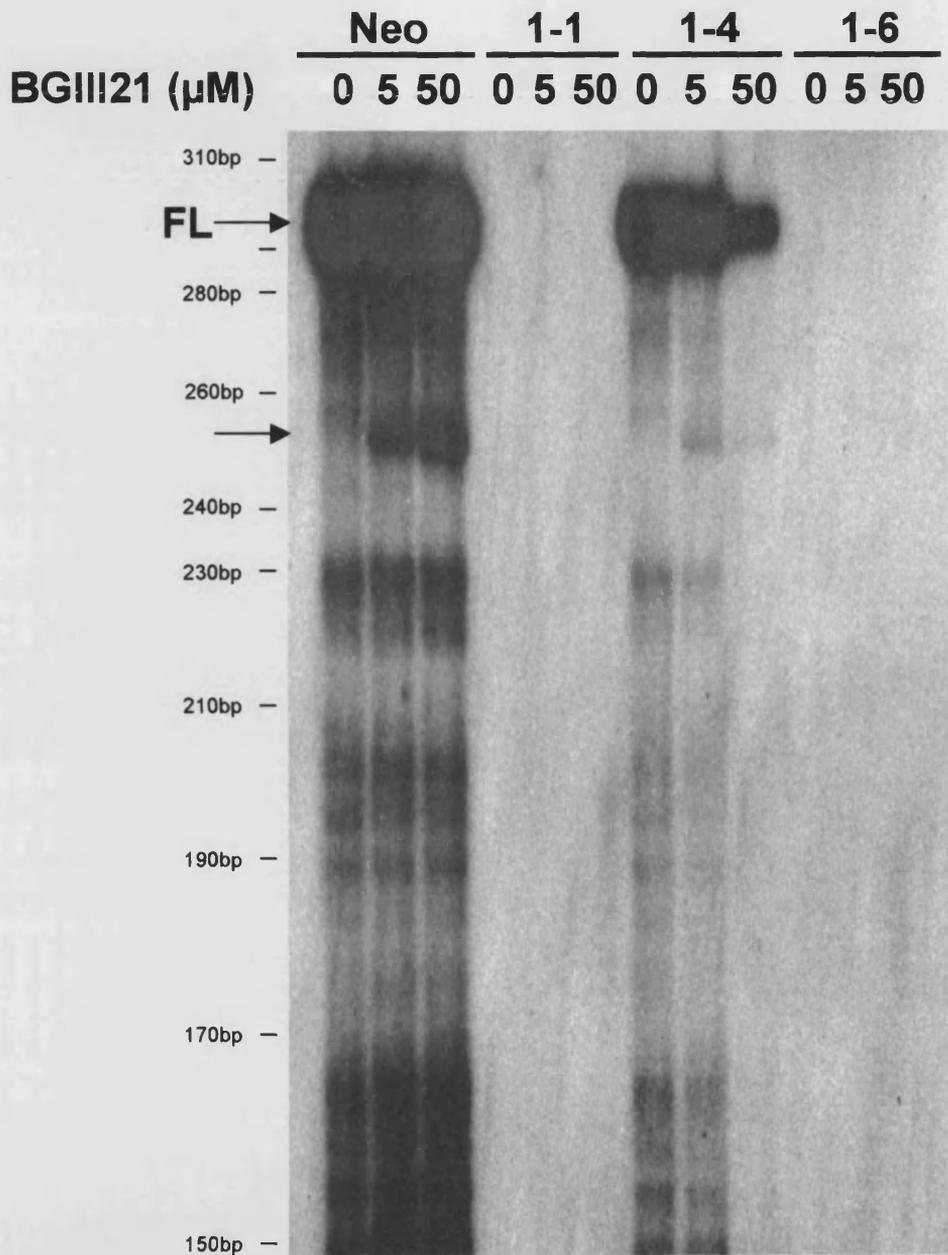
**Fig. 3.14: BGIII21 specific DNA lesions (⟶) produced within
HT1080 Neo (Neo) and HT1080 E2F 1-4 (1-4)** as measured by Sslig-PCR.
No result was obtained for HT1080 E2F 1-1 (1-1) or HT1080 E2F 1-6 (1-6).
Cells were incubated with BGIII21 for 5hours with BGIII21.
Correct size of BGIII21 lesions was verified with radio-labelled 10bp DNA
ladder run alongside samples. FL (full length PCR product)

111

when run on a 0.8% agarose mini-gel. Hence it was assumed that the DNA was accessible to restriction enzymes and henceforth should allow primer binding.

To investigate further why no Sslig result was obtained for two of the four clones, a number of PCR reactions were set up to examine primer binding in all four cell lines. A range of available primer sets was used to cover a variety of unrelated primer and DNA sequences. As shown in **Figure 3.15** the PCR experiments using primer sets for the N-*ras* promoter region (Thorn *et al.*, 1991) and topoisomerase IIα gene sequence (Accession no. J04088) produced a similar result. The sequence of the N-*ras* primers used for PCR reactions were different from the nested N-*ras* primer set used for Sslig-PCR experiments previously (**Table 2.3**). PCR products were obtained for HT1080 Neo and HT1080 E2F 1-4 but neither for HT1080 E2F 1-1 and E2F 1-6. Results for an additional set of MDR1 primers gave the same result as observed for the N-*ras* and topoisomerase IIα gene sequence.

3.3.12 Restriction patterns produced by Southern blot analysis reveal two sets of cells

Based on the above experimental outcome Southern blot analysis was performed to compare the restriction patterns of all four cell lines when the DNA was digested with the *Dra*I restriction enzyme (Promega, Southanpton, UK) overnight (**Fig. 3.16**). The *Dra*I restriction enzyme was chosen as it digested DNA at a relatively high frequency at the 5'-TTT-AAA-3' recognition site and produced complete restriction digests in all four cell lines. The Southern blots were probed with N-*ras* and *topoisomerase IIα* sequences that had been derived from the previous PCR experiments (section 2.2.9). The findings revealed a distinct difference in the restriction patterns between HT1080 Neo and E2F 1-4 on one hand and HT1080 E2F 1-1 and E2F 1-6 on the other hand. Nevertheless, within those two subsets of cell lines the restriction patterns were shown to be identical (**Fig. 3.16**). The differences in restriction patterns imply DNA sequence alterations as restriction patterns should be identical or similar in the case of DNA sequence alterations due to mutations occurring.

N-ras

3kb —
2kb —

1kb —

0.5kb — ← 601bp

Topoisomerase IIα

3kb —
2kb —

1kb —

← 234bp
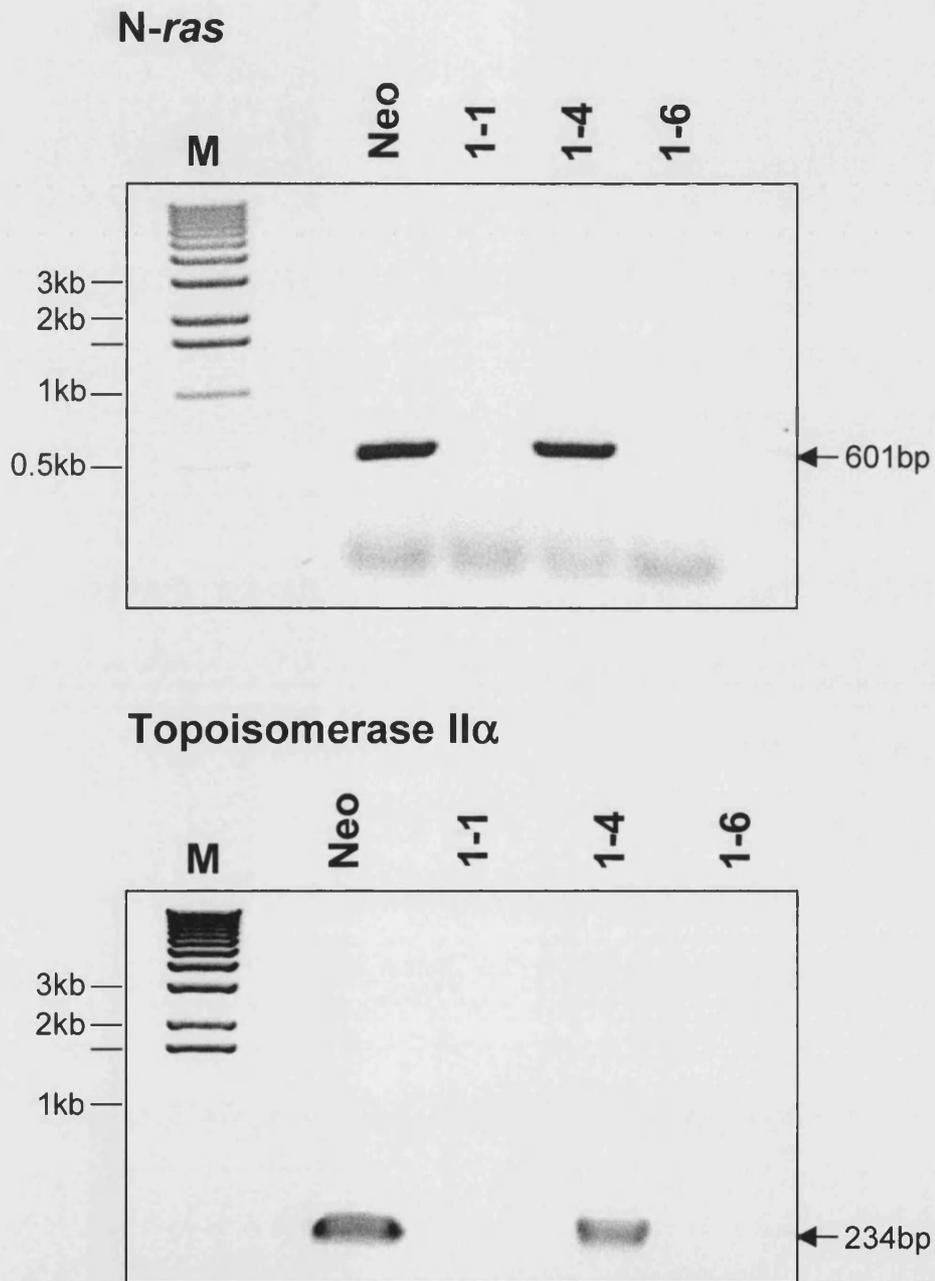
Fig. 3.15: Investigation into the binding of the N-*ras* promoter
and topoisomerase IIα primer sets to DNA of E2F-1 transfectants.
PCR products were separated on 0.8% agarose mini-gels.
M (1kb DNA ladder); Neo (HT1080 Neo); 1-1 (HT1080 E2F 1-1);
1-4 (HT1080 E2F 1-4); 1-6 (HT1080 E2F 1-6)

N-*ras*

Neo   1-1   1-4   1-6

Topoisomerase IIα

Neo   1-1   1-4   1-6
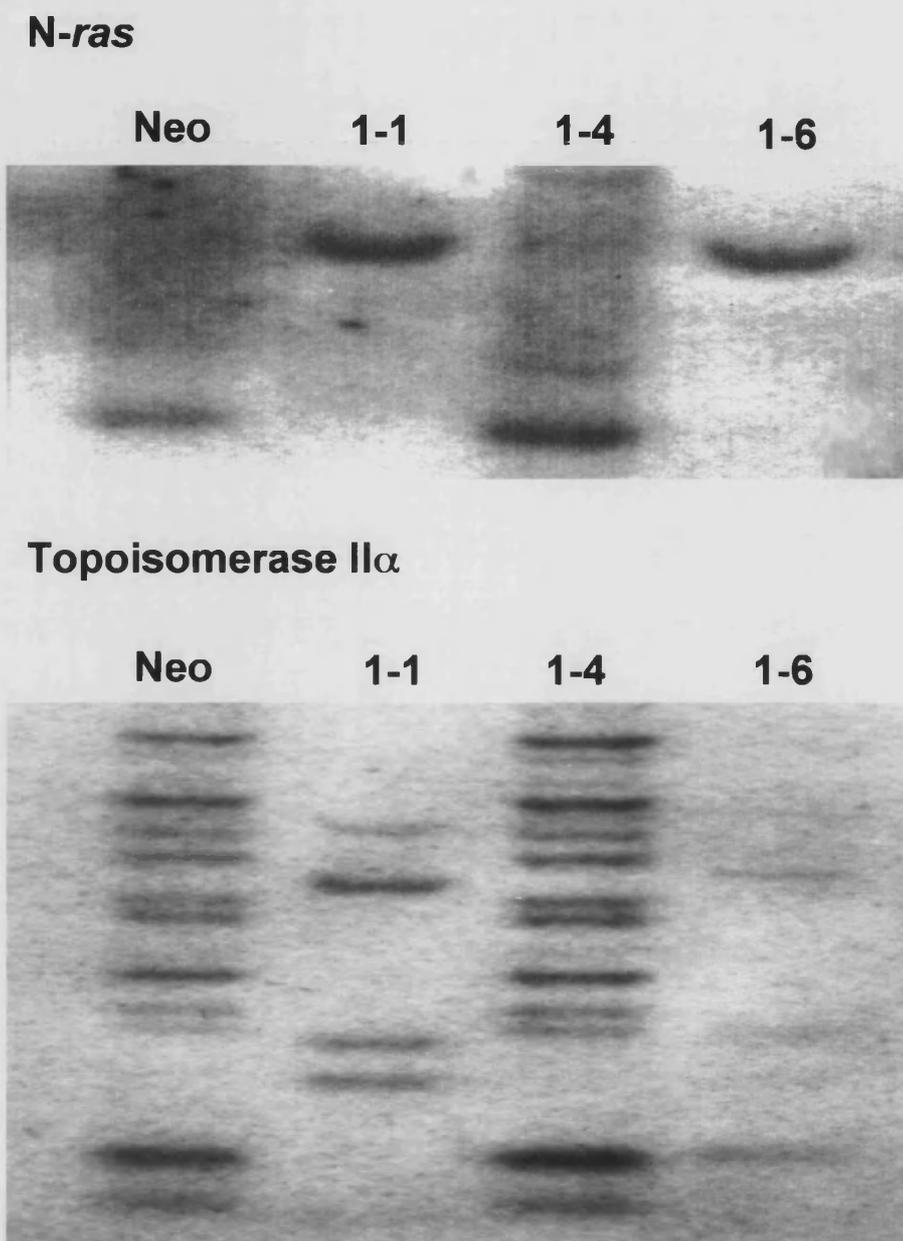
Fig. 3.16: Restriction digest pattern of E2F-1 transfectants as
determined by Southern blot analysis. Genomic DNA was cut with
*Dra*I restriction enzyme overnight, resulting restriction fragments
were separated on a 4% polyacrylamide gel and probed with N-*ras*
promoter and topoisomerase IIα radioactively labelled probes. Neo
(HT1080 Neo); 1-1 (HT1080 E2F 1-1); 1-4 (HT1080 E2F 1-4);1-6
(HT1080 E2F 1-6)

114

3.3.13 Karyotypic analysis of E2F-1 overexpressing cell lines

The finding of DNA sequence alterations suggested that the four cell lines which had been proposed to be derived from the same HT1080 parent cell line were in fact two unrelated sets of cell lines. To confirm this, the cell lines were sent for karyotypic analysis (Royal Free Hospital, London, UK). Metaphase chromosome analysis verified the hypothesis that the two subsets of cell lines were unrelated. Initial investigations revealed unique differences between the HT1080 Neo/HT1080 E2F 1-4 and HT1080 E2F 1-1/HT1080E2F 1-6 cell lines In **Figure 3.17** HT1080 Neo and HT1080 E2F 1-1 are shown as representative cell lines for each sub-set. Both cell lines exhibited aneuploidy as well as chromosome amplification and deletion. For example, chromosome pair 13 is deleted in the HT1080 Neo cells while the pair is present in the HT1080 E2F 1-1. In contrast the chromosome pair 22 is present in the HT1080 Neo cells while being deleted in the HT1080 E2F 1-1 cells. Of significance is the absence of the Y chromosome in the HT1080 E2F 1-1 cells while it is present in the HT1080 Neo. The suggestion that HT1080 Neo and HT1080 E2F 1-4 were of the same origin and completely different compared to the HT1080 E2F 1-1 and HT1080 E2F 1-6 cell lines was proven. Further karyotypic analysis including a purchased CHO-AA8 cell line (Clontech, UK) verified the suggestion that the HT1080 E2F 1-1 and HT1080 E2F 1-6 cell lines were in fact Chinese hamster ovary cell lines. Further discussion with the laboratory that had sent the cell lines confirmed that work had also been in progress with CHO cell lines. Therefore the source for this contamination was mixing of strains.

HT1080 Neo
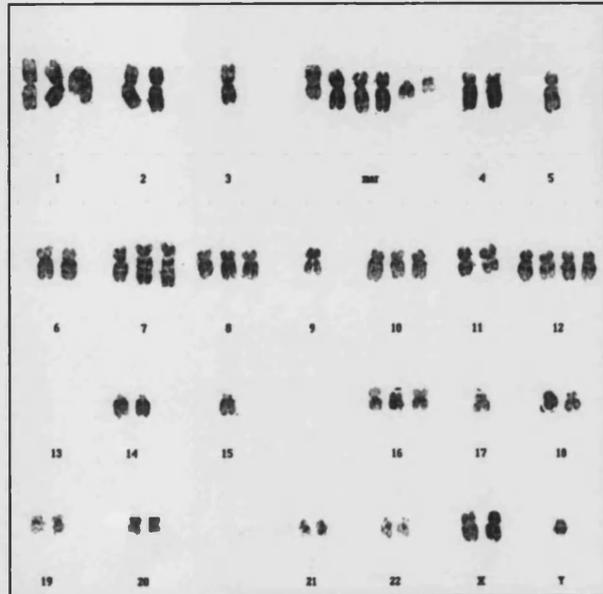
HT1080 E2F 1-1
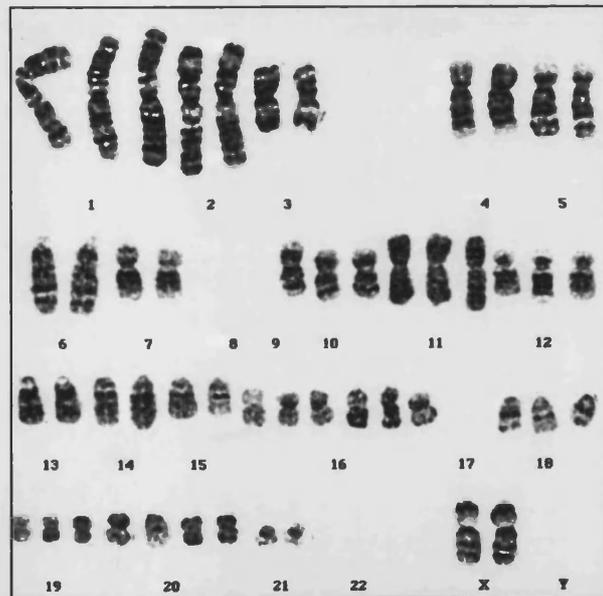
Fig. 3.17: Karyotypes of HT1080 Neo and HT1080 E2F 1-1 examining differences in chromosome arrangement. Analysis revealed differences in chromosome pair deletion (chromosome 13 in HT1080 Neo and chromosome 22 in HT1080 E2F 1-1) and highlighted absence of Y chromosome in HT1080 E2F 1-1.

116

3.3.14 *E2F-1* inducible expression system

Following the discovery that two of the four HT1080 E2F-1 overexpressing clones were CHO rather than human fibrosarcoma cell lines, an E2F-1 inducible expression system was chosen to continue the investigation into the mechanism underlying the resistance to BGIII21 and to determine a possible correlation between overexpression of E2F-1 in HT1080 cells and resistance to BGIII21. To this end an E2F-1 inducible expression system in HT1080 Tet-Off cells was produced.

The E2F-1 cDNA insert in a pcDNA3-*E2F-1* plasmid (gift from E. Lam) was excised and subsequently ligated into the modified multiple cloning site of the pTRE plasmid. HT1080 Tet-Off cells were stably transfected with the new pTRE-*E2F-1* plasmid construct (**Fig. 3.18**). The exogenous E2F-1 expression levels in the resultant clones were determined using Western blot analysis. Functionality of the overexpressed E2F-1 protein was examined by performing FACS analysis on serum starved and cell cycle arrested cells using nocodazole to determine the relative percentage of cells in S phase in non-induced and induced HT1080 Tet-Off cells. Finally, growth inhibition studies were carried out to analyse the effect of E2F-1 overexpression on BGIII21 chemosensitivity.

3.3.15 Construction of *E2F-1* inducible expression system in HT1080 Tet-Off cells

The Tet-Off gene expression system (Clontech, Basingstoke, UK) and the pre-made HT1080 Tet-Off cell lines (Clontech, Basingstoke, UK) provide ready access to the regulated, high-level gene expression systems previously described by Gossen *et al.* (Gossen *et al.*, 1992). In the Tet-Off system gene expression is turned on upon removal of doxocycline (Dox) from the culture medium. Gene expression is tightly regulated in response to varying concentrations of Dox. Expression levels in Tet systems are high and gene regulation is highly specific eliminating pleiotropic effects and non-specific induction (Clontech, Basingstoke, UK).

3.3.15.1 Release of *E2F-1* cDNA insert from pcDNA3-E2F-1 plasmid

A large-scale preparation of pcDNA3-E2F-1 vector (**Fig. 3.19**) was prepared according to the *E. coli* transformation protocol (section 2.2.13) followed by the maxiprep procedure outlined within the protocol supplied with the Maxi-prep kit (Qiagen, UK) (section 2.2.13). The *E2F-1* cDNA insert located in the multiple cloning site of the original pcDNA3 vector was released by restriction digest with *Bam*HI and *Eco*RI as shown in **Figure 3.20**. The
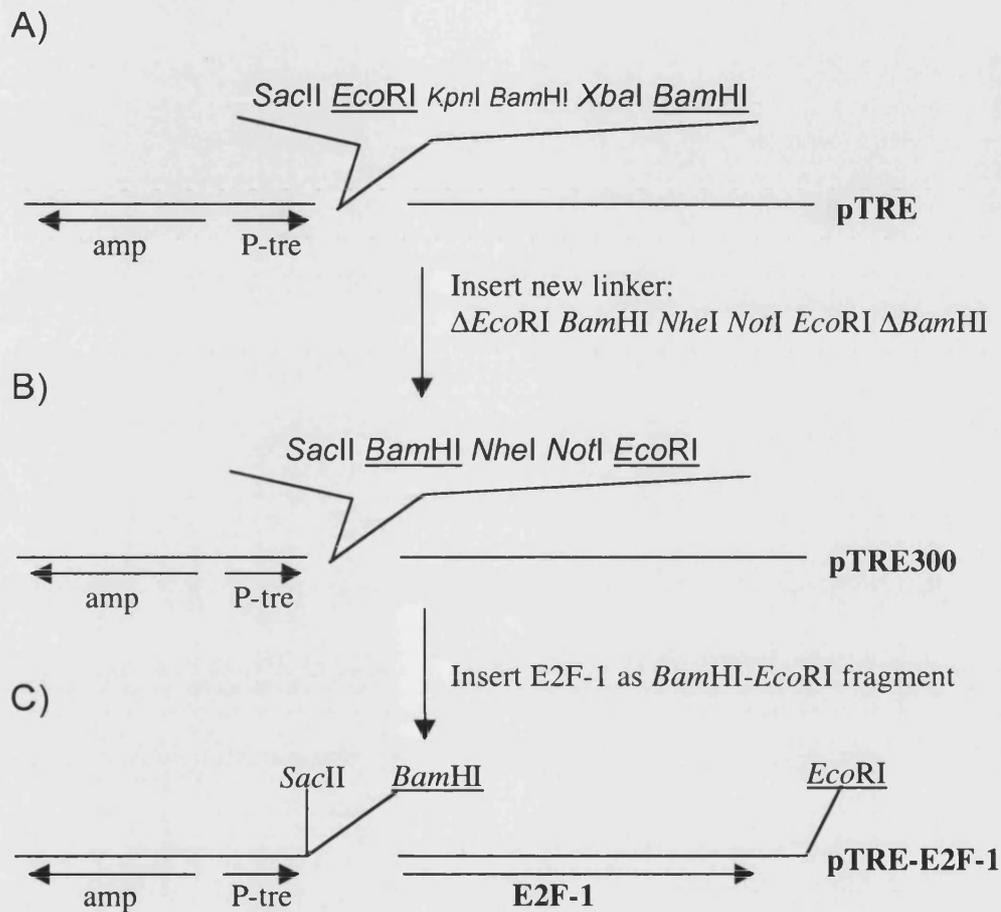
Fig. 3.18: Diagrammatic illustration of steps in the development of the pTRE-E2F-1 inducible expression plasmid.
A) pTRE plasmid with the multiple cloning site downstream of P-tre promoter element. amp (ampicillin resistance gene)
B) Modified pTRE300 plasmid after insertion of linker. Former *Eco*RI and *Bam*HI restriction sites in pTRE were deleted and new *Bam*HI and *Eco*RI were created.
C) Insertion of E2F-1 cDNA as *Bam*HI-*Eco*RI fragment into pTRE300. E2F-1 cDNA located downstream of P-tre promoter element.
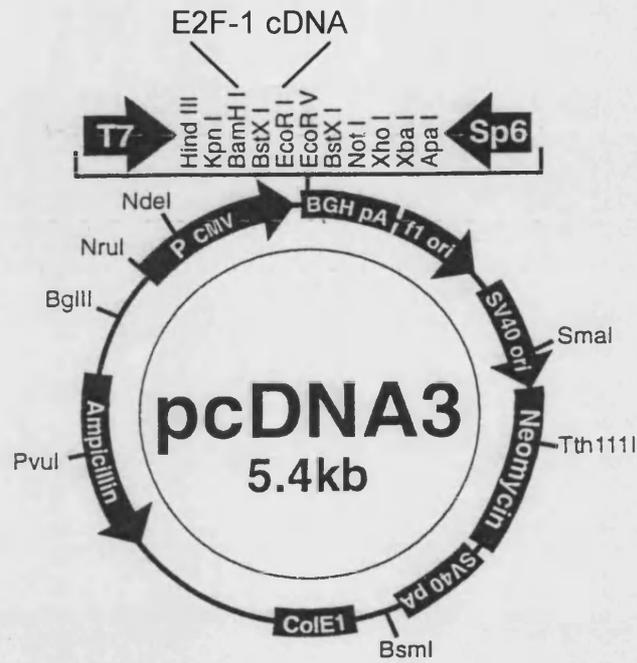
Fig. 3.19: Map of pcDNA3-E2F-1 plasmid highlighting location of
E2F-1 cDNA insert between *Bam*HI and *Eco*RI restriction sites
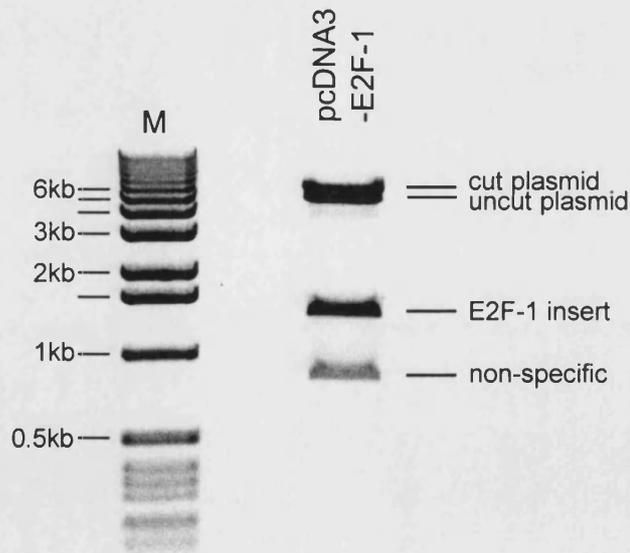
**Fig. 3.20: Restriction digest with *Bam*HI / *Eco*RI to release E2F-1
cDNA insert** from pcDNA3-E2F-1 plasmid. 1kb DNA ladder (M).

digested pcDNA3 plasmid DNA and *E2F-1* insert were separated on a 0.8% agarose mini-gel containing ethidium bromide (**Fig. 3.20**). The released *E2F-1* cDNA was 1.3kb in size as predicted from prior sequence analysis of the E2F-1 open-reading frame (ORF) (Accession number M96577).

3.3.15.2 Construction of linker required for restriction site modification

Part of the construction of the E2F-1 inducible expression system was the insertion of the released E2F-1 cDNA (1.3kb) into the pTRE plasmid (3.1kb). However, in order for the E2F-1 cDNA to be correctly transcribed, the *Eco*RI and *Bam*HI restriction sites within the multiple cloning site of the pTRE plasmid required modification. To achieve this, two 37bp oligomers were annealed and the linker inserted into the *Eco*RI/*Bam*HI digested pTRE plasmid thereby abolishing the existing *Eco*RI and *Bam*HI restriction sites and creating a new *Bam*HI and *Eco*RI in the correct orientation (**Fig. 3.18**). The two oligomers pTRE-BE-FW and pTRE-BE-AS were annealed in such a way as to produce a 4 bp overhang on either side in order to abolish the *Eco*RI (Δ*Eco*RI) and *Bam*HI (Δ*Bam*HI) restriction sites and create the new 5' *Bam*HI and 3' *Eco*RI restriction sites (**Fig. 3.21**).

Δ*Eco*RI   *Bam*HI   *Nhe*I   *Not*I

5'-AATT GGATCCTATAGCTAGCAAAGCGGCCGCGAATTC-3'

3'-CCTAGGATATCGATCGTTTCGCCGGCGC TTAAG CTAG-5'

                                                                 *Eco*RI   Δ*Bam*HI
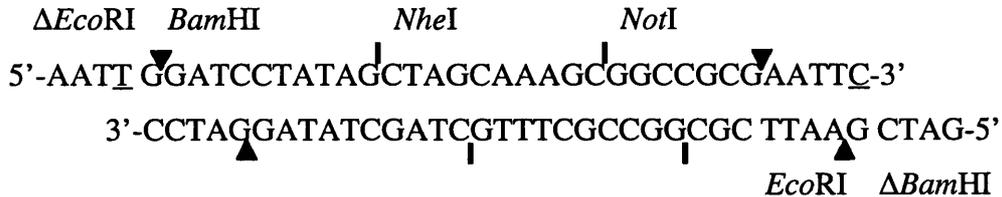
Fig. 3.21: Annealing product of pTRE-BE-FW (5'-3') and pTRE-BE-AS (3'-5'). The introduced base-pair mutations necessary to abolish existing *Eco*RI and *Bam*HI restriction sites are underlined. New *Bam*HI and *Eco*RI restriction sites are marked ▼ and ▲.

New previously non-existing *Nhe*I and *Not*I restriction sites introduced for verification purposes are marked with **I**.

3.3.15.3 Insertion of linker into pTRE

Next pTRE plasmid (**Fig. 3.22**) was digested with *Eco*RI and 20u *Bam*HI. The digested plasmid was separated on a 0.8% agarose gel containing ethidium bromide and was subsequently extracted from the gel using the Gene-clean® II kit Bio 101 (Anachem, UK).

The isolated DNA fragment was resuspended and a ligation reaction was set up containing digested pTRE plasmid.
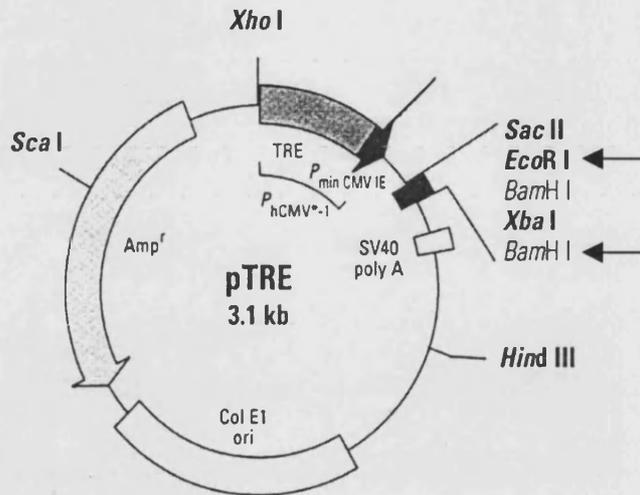
Fig. 3.22: Map of pTRE plasmid including multiple cloning site high-lighting *Eco*RI and *Bam*HI restriction site selected for deletion to allow insertion of *E2F-1* cDNA fragment.

Furthermore, the ligation reaction was digested with *Xba*I in order to linearise any remaining parental pTRE vector void of linker insert as the pTRE vector specific *Xba*I restriction site was eliminated upon insertion of the linker into the linearised pTRE plasmid.

To increase the amount of ligation product, *E.coli* were transfected with pTRE300 as described previously (section 2.2.13) and plated out on ampicillin (100μg/ml) containing agar plates. The plates were left for 24 hours or until distinct visible colonies had grown. Twenty randomly selected single colonies were further processed and the plasmid DNA extracted from the bacterial cells according to instructions supplied with the Mini-prep kit (Qiagen, UK).

3.3.15.4 Verification of correct restriction sites in modified pTRE plasmid (pTRE300)

Restriction digests with *Xba*I, *Eco*RI, *Bam*HI, *Nhe*I, *Not*I and *Sac*II were set up. These consisted of the pTRE300 plasmid DNA retrieved in the previous section. The restriction

121

products were subsequently separated on 0.8% agarose gels containing ethidium bromide. Non-digested pTRE300 plasmid DNA was run next to the digested samples as a control (**Fig. 3.23**).

3.3.15.5 Ligation of *E2F-1* cDNA insert into pTRE300

Before ligation both the pcDNA3-*E2F-1* and pTRE300 were digested with the restriction enzymes *Bam*HI and *Eco*RI in order to isolate the *E2F-1* cDNA insert and open the recipient plasmid, respectively. Each sample was taken and separated on a 0.8% agarose mini-gel containing ethidium bromide to confirm completion of the enzyme reaction and separate the individual components needed for further processing (**Fig. 3.24**).

The *E2F-1* cDNA insert and the digested pTRE300 plasmid were extracted from the gel using the Gene-clean® II Bio 101 kit (Anachem, UK). Following the instructions of the protocol provided with the kit only the last washing step was modified this time, as both samples were pooled together beforehand. The retrieved and pooled plasmid and insert DNA was resuspended and subsequently ligated.

To purify the ligation reaction of any undigested pTRE300, a restriction digest with *Nhe*I (NEB, UK) was performed. As before *E.coli* were transformed with the newly constructed pTRE-E2F-1 plasmid and plated out on agar plates containing ampicillin. Bacterial colonies were harvested and the plasmid DNA was retrieved with a Mini-prep kit (Qiagen, UK).

3.3.15.6 Verification of pTRE-*E2F-1* and transfection of HT1080 Tet-Off

All DNA minipreps were digested with *Bam*HI and *Eco*RI to confirm the presence of the *E2F-1* cDNA insert. **Figure 3.25** shows 3 randomly selected restriction digested DNA mini-preps. All three DNA minipreps feature E2F cDNA of the correct size (1.3kb). A further verification step was carried out as both the original pcDNA3-E2F-1 and newly made pTRE-E2F-1 was digested with *Bam*HI and *Eco*RI. A comparison of both digested plasmids is shown in **Figure 3.26**. Sizes of both E2F-1 inserts were equal hence providing proof of the correct insertion of *E2F-1* cDNA into pTRE300 to obtain pTRE-E2F-1.

In addition to the above pTRE-*E2F-1* plasmid, an E2F-1 anti-sense plasmid had been developed simultaneously. For this design the *E2F-1* cDNA insert was ligated directly into the pTRE plasmid therefore switching the *E2F-1* ORF around resulting in transcription
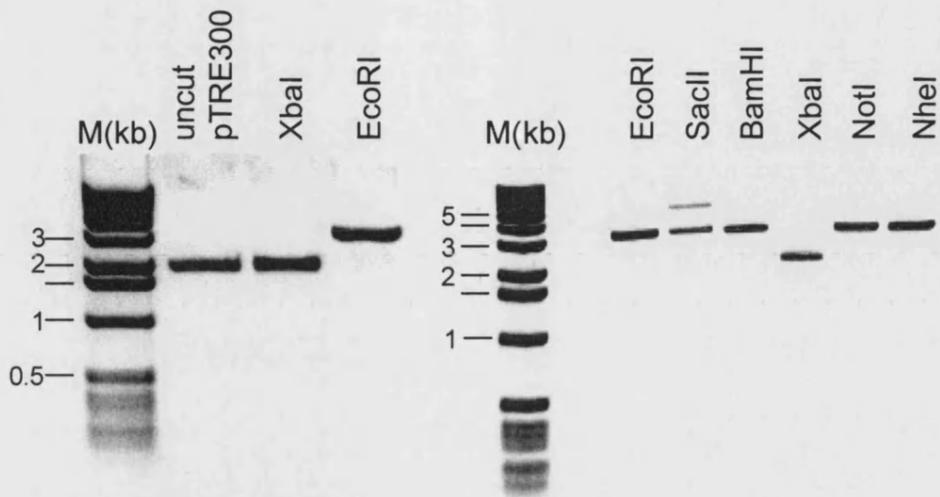
Fig. 3.23 Verification of pTRE300 plasmid with several restriction digests. Complete restriction digest of pTRE300 with EcoRI, *Bam*HI, *Not*I and *Nhe*I and *Sac*II. No restriction cut of pTRE300 with *Xba*I.1kb DNA ladder (M)
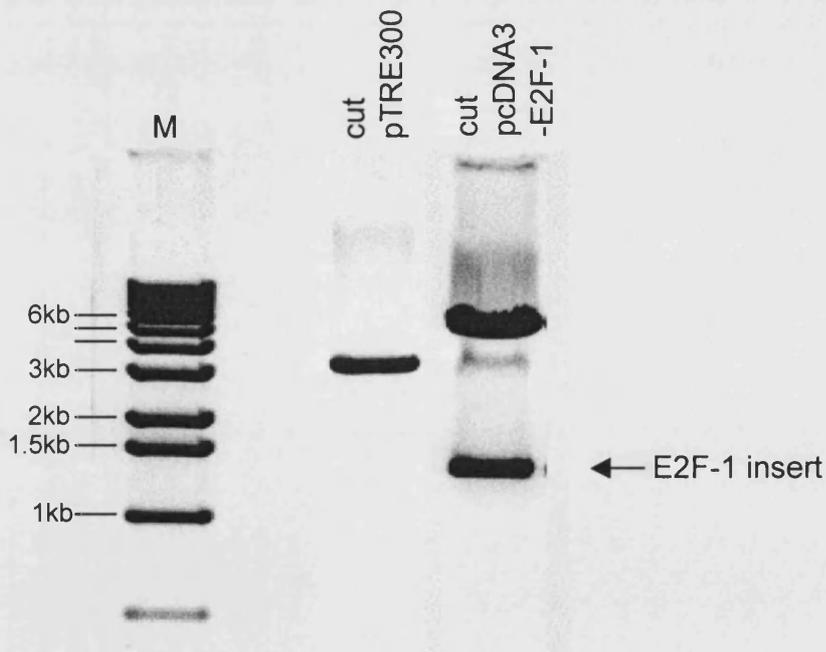
Fig. 3.24: Restriction digest with *Bam*HI / *Eco*RI of modified pTRE300 and pcDNA3-E2F-1 plasmids to release E2F-1 cDNA insert prior to ligation of E2F-1 cDNA insert into opened pTRE300 plasmid. 1kb DNA ladder (M)
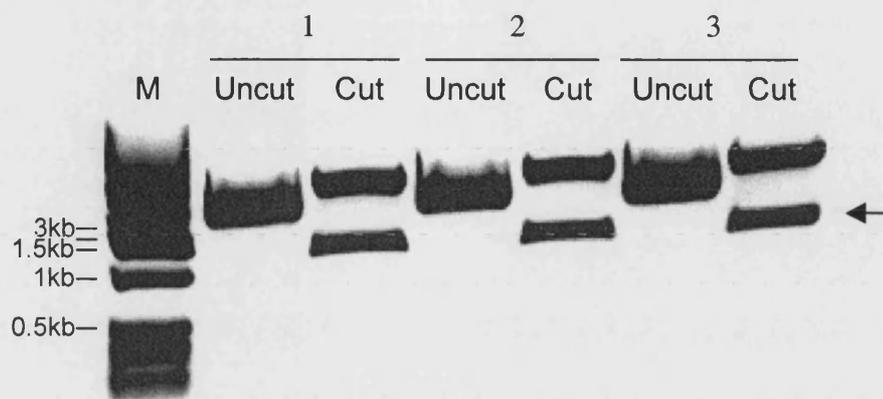
Fig. 3.25: Analysis of pTRE-E2F-1 plasmid minipreps by restriction digest with *Bam*HI and *Eco*RI to release inserted E2F-1 cDNA (◄—). Overall 9 correct plasmid minipreps were obtained and analysed for the presence of E2F-1 insert . 1kb DNA ladder (M).
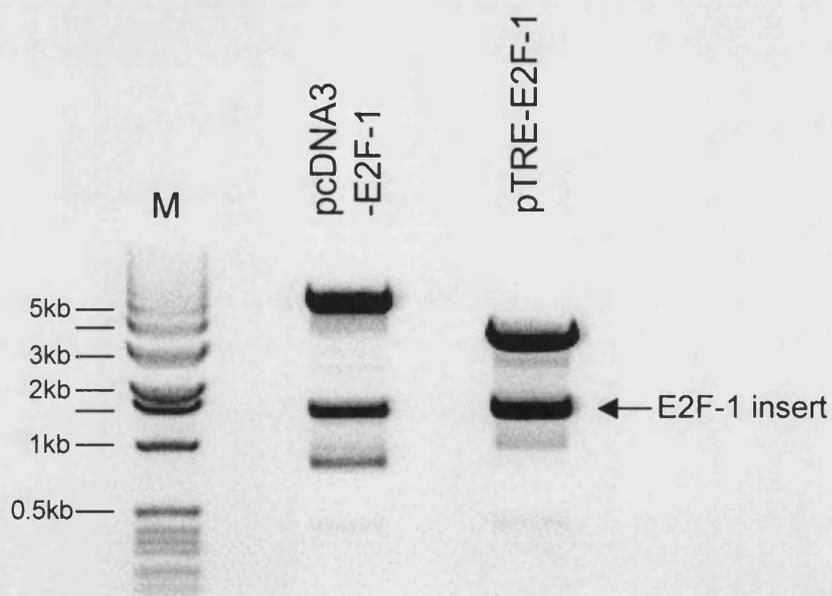
Fig. 3.26 Restriction digest with *Bam*HI/ *Eco*RI to confirm correct size of E2F-1 cDNA insert in pTRE-E2F-1 plasmid by comparison to original pcDNA3-E2F-1 plasmid. 1kb DNA ladder (M).

of anti-sense *E2F-1* mRNA. The pTRE300 plasmid was used as an empty control plasmid for transfection into HT1080 Tet-Off cells. All plasmids were sent off to MWG, Ebersberg, Germany for sequencing to ensure correct sense and anti-sense orientation of *E2F-1* cDNA insert.

Transfection of HT1080 Tet-Off cells was performed as described in section 2.2.15. The transfection efficiency had been determined prior to stable transfection using the pTRE-luc and pCH110 plasmids (section 2.2.14)

3.3.16 Increased expression of E2F-1 in HT1080 E2F-1 2 and E2F-1 13 clones

Of all transfected *E2F-1* sense, *E2F-1* anti-sense and pTRE300 clones, four were selected for further experiments. These included two *E2F-1* sense clones HT1080 E2F-1 2 and E2F-1 13, one *E2F-1* anti-sense clone HT1080 E2F-1 AS 44 and one pTRE300 11 clone. The selection was based on Western lot analysis performed to determine E2F-1 expression levels within each non-induced and induced clone. A time-course experiment was set up with protein samples taken every 24 hours for 12 days to determine the time-point of peak E2F-1 expression following doxocycline removal. The E2F-1 peak expression level within induced cells was established at 240 hours with expression levelling off at any further time-points. Upon 240 hours induction of the pTRE promoter following the removal of doxocycline, E2F-1 expression was increased in HT1080 E2F-1 2 and E2F-1 13 (**Fig. 3.27**). In contrast, E2F-1 expression decreased in HT1080 E2F-1 AS 44 cells due to the transcribed anti-sense *E2F-1* mRNA binding sense *E2F-1* mRNAs (**Fig. 3.27**). No significant change in E2F-1 expression levels was observed in the pTRE300 control clone after induction (**Fig. 3.27**).

3.3.17 *E2F-1* inducible system promotes S phase entry following serum-starvation

Previous studies by Shan *et al.* using a tetracycline controlled expression system to overexpress exogenous E2F-1 found induced expression of E2F-1 to promote premature S phase entry in Rat-2 fibroblasts (Shan *et al.*, 1994). In a similar investigation Johnson *et al.* had shown that microinjection of *E2F-1* cDNA was able to activate transcription in serum-starved REF-52 cells and induce S-phase entry in quiescent cells (Johnson *et al.*, 1993).

To analyse the potential of exogenous E2F-1 expression within the doxocycline repressible system to induce S phase in quiescent cells, HT1080 E2F-1 2, E2F-1 13, pTRE300 11 and E2F-1 AS 44 cells were grown in the absence of doxocycline for 240 hours. Following induction cells were grown in 0% FCS medium for 96 hours to arrest cells in G0/G1 phase. FACS samples of induced and non-induced cells of each clone were prepared following cell cycle arrest and DNA content of the cells measured to determine the percentage of cells in S phase. In **Figure 3.28** a representative experiment shows induced and non-induced cells continued cell cycle progression suggesting serum starvation to have no marked effect on the E2F-1 inducible system under these conditions. However, a 5% increase of cells in S phase in induced compared to non-induced E2F-1 2 and E2F-1 13 clones suggested exogenously expressed E2F-1 to be functional and able to promote S phase entry in the absence of serum. In contrast the percentage of cells in S phase in non-induced and induced pTRE300 11 cells remained at 17%, while a decrease in the percentage of cells in S phase was observed comparing non-induced (14%) and induced (13%) AS 44 cells.

3.3.18 Increased percentage of E2F-1 overexpressing cells in S phase after G2 block

In a further attempt to analyse the potential of exogenous E2F-1 expression within the doxocycline repressible system to induce S phase entry in quiescent cells the above experiment was repeated using nocodazole rather than serum starvation to induce a cell cycle arrest. Nocodazole has been shown to arrest cells in G2 phase through inhibition of mitosis (Bowdon *et al.*, 1987). In **Figure 3.29** representative data for non-induced (A) and induced clones (B) E2F-1 2 clones is shown. A 5% increase in the percentage of cells in S phase was observed in induced compared to non-induced E2F-1 2 clones as a result of induction of E2F-1 expression for 240 hours (0hrs). Following 18 hours of treatment with 0.5μg/ml nocodazole a distinct G2 block was observed in both non-induced and induced cells. Upon release of cells from the G2 block through the removal of nocodazole, induced clones showed a higher percentage of cells in S phase compared to non–induced E2F-1 2 clones. At 4 hours post arrest 14% of induced compared to 8% non-induced E2F-1 2 cells were in S phase. The percentage of induced E2F-1 2 cells in S phase was observed for 19% for 8, 21% for 12 and 17% for 24 hours post G2 arrest. In comparison, the percentages for non-induced cells in S phase were 17% for 8, 21% for 12 and 13% for 24 hours following G2 arrest (**Fig. 3.29**).
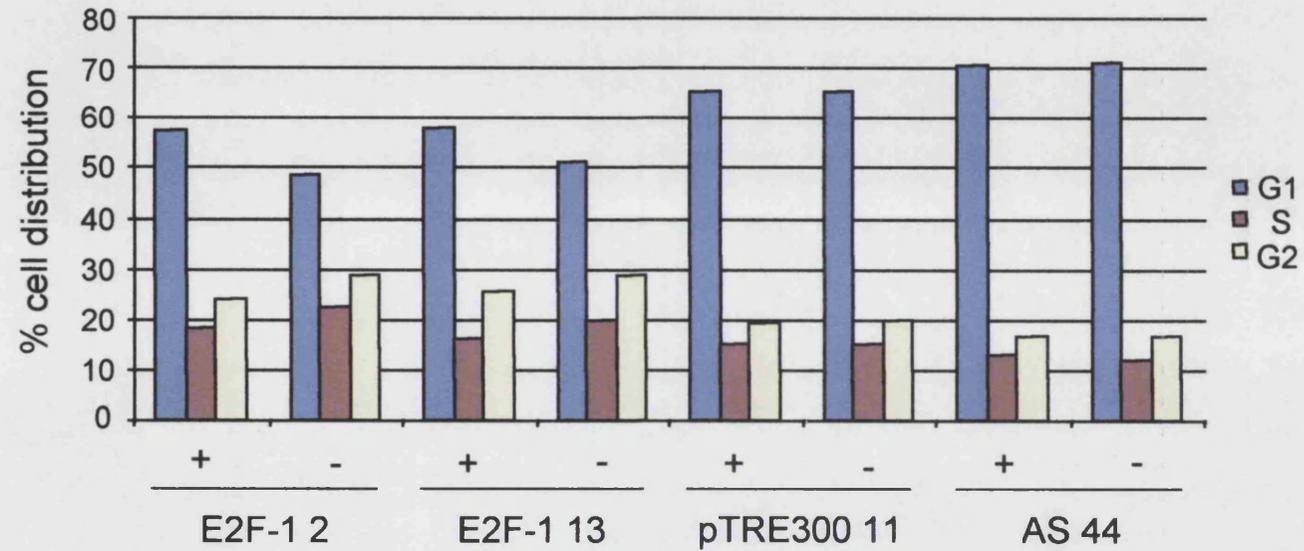
Fig. 3.28: Cell cycle analysis showing the percentage increase in S phase of E2F-1 overexpressing E2F-1 2 and E2F-1 13 clones after 240hrs induction followed by 96 hours growth in 0% FCS. + (+Dox); - (-Dox)

Non-induced

Induced with doxocycline
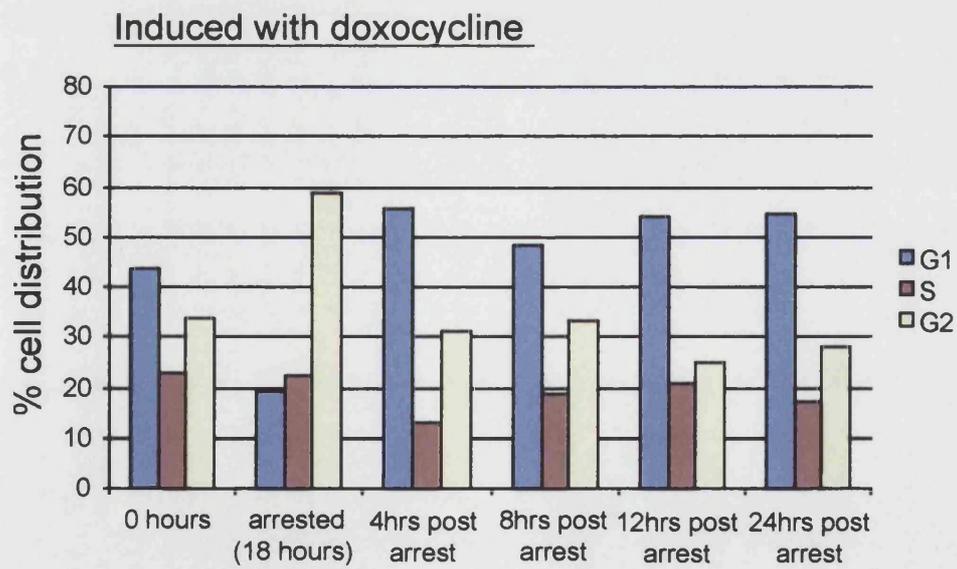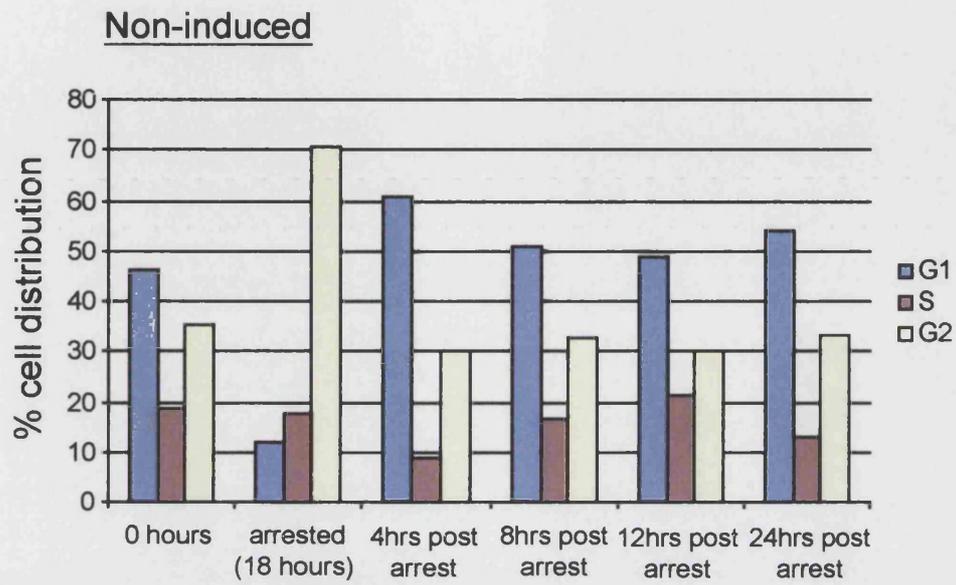
Fig. 3.29: Percentage of non-induced and induced (240hrs) E2F-1 2 cells after G2 arrest following 18hours treatment with nocodazole.

3.3.19 No increased resistance to BGIII21 in E2F-1 overexpressing HT1080 cells

After the construction of an inducible *E2F-1* system and an analysis of inappropriate S phase entry after serum starvation and release from nocodazole induced G2 arrest, SRB growth inhibition assays were performed to investigate the effect of E2F-1 overexpression on BGIII21 chemosensitivity. Non-induced and induced (240hrs) E2F-1 2 cells were exposed to increasing concentrations of BGIII21 for 72 hours (**Fig. 3.30**). In a further assay E2F-1 2 cells were exposed to cisplatin as a means of control. No significant difference in chemosensitivity to BGIII21 or cisplatin was observed in non-induced and induced E2F-1 2 cells ($p < 0.0001$). Increased expression of E2F-1 following induction did not lead to an increase in resistance to BGIII21. IC_{50} values for non-induced and induced E2F-1 2 cells following exposure to BGIII21 were identical ($IC_{50} = 1\mu M \pm 0.001$). Equally, IC_{50} values were identical in both non-induced and induced E2F-1 2 cells after treatment with cisplatin ($IC_{50} = 10.3\mu M \pm 0.003$).

In conclusion E2F-1 overexpression in HT1080 human fibrosarcoma cells has no effect on chemosensitivity to BGIII21 and cisplatin. Resistance to BGIII21 does not occur as a result of E2F-1 overexpression.

3.4 Discussion

The results of the above investigation into the effects of E2F-1 overexpression on chemosensitivity in the HT1080 human fibrosarcoma cell line were overshadowed by the discovery of inter-species cross-contamination. Nevertheless a number of valid results were obtained. The connection between the elevated level of E2F-1 expression in the CHO cells as established by Western blot analysis and the decreased sensitivity to BGIII21 observed in the CHO cells requires further investigation. Further, the lack of significant differences in chemosensitivity in response to etoposide in CHO cells ('HT1080 E2F 1-1') and HT1080 Neo contradicted data by Nip *et al.* and Banerjee *et al.* showing an increased level of E2F-1 expression resulting in an increase in chemosensitivity to etoposide. This result suggests that not only the expression level of a protein *per se* is important in determining the effects on chemosensitivity, but cell lineage appears to be also critical.

In addition, the production of BGIII21 specific DNA lesions in CHO cells and the type of repair pathways involved in their removal needs to be examined. As the N-*ras*
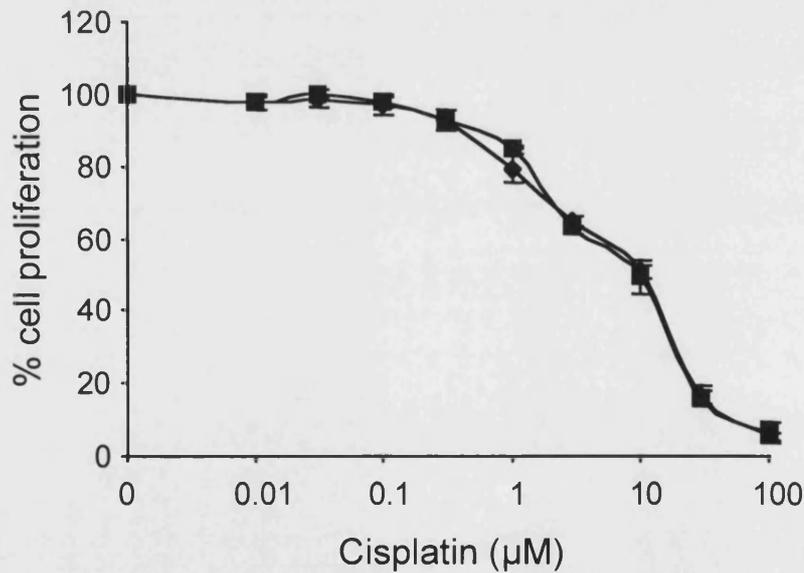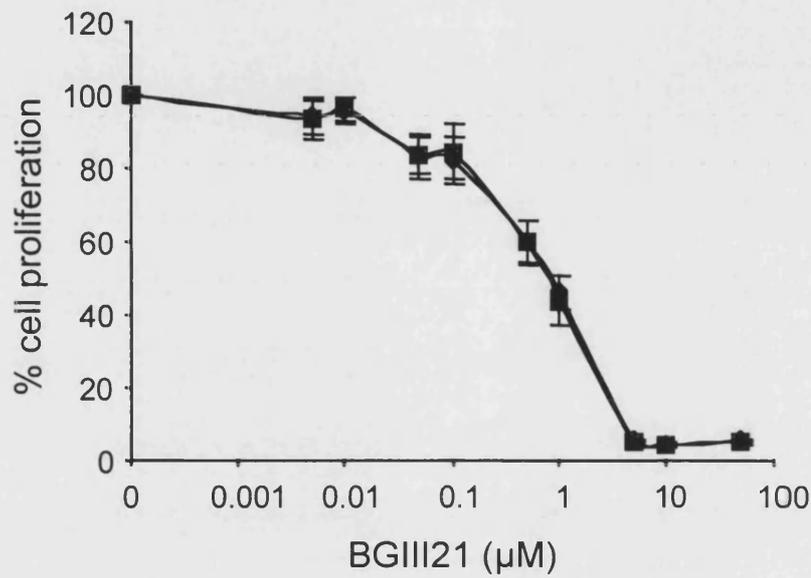
Fig. 3.30: Inhibition of cell proliferation following continuous exposure (72hours) to BGIII21 and cisplatin in non-induced and induced E2F-1 2 cells as measured by SRB growth inhibition assay.
━◆━ E2F-1 2 (+ Dox); ━■━ E2F-1 2 (- Dox)

promoter sequence has been shown, using Southern blot analysis, to contain sequence alterations preventing the nested N-*ras* primers from binding, a different DNA region in the CHO genome needs to be selected to detect BGIII21 lesions and analyse DNA repair.

To examine the possibility of E2F-1 overexpression directly influencing the chemosensitivity of HT080 to BGIII21, an E2F-1 inducible system was developed. *E2F-1* cDNA was inserted into the modified multiple cloning site of the pTRE plasmid and two E2F-1 overexpressing HT1080 clones were selected. Induction of *E2F-1* expression was dependent on doxocycline removal from the growth medium. In addition, an *E2F-1* anti-sense and pTRE300 control plasmid were constructed.

An inducible *E2F-1* expression system reduces the appearance of changes in protein expression levels related to a constitutive overexpression of E2F-1. Temporary induction of E2F-1 expression above normal level reveals more accurately the effect E2F-1 overexpression has on E2F-1-regulated protein levels and the subsequent effects with respect to cell cycle progression. However, the use of an *E2F-1* inducible system to examine the effect of E2F-1 overexpression on chemosensitivity provides several limitations. No natural amplification of the E2F-1 gene has been reported as yet, therefore artificially increasing the expression level of E2F-1 is prone to produce artefactual results. As an alternative it has been suggested to construct a cyclin D overexpressing system or selectively silence the cyclin-dependent kinase inhibitor $p16^{INK4a}$ to create a genetic environment more similar to situations observed in normal human tumours. These alternative approaches would also allow to investigate the effects of cyclin D overexpression or $p16^{INK4a}$ silencing on other members of the *E2F* transcription factor family thereby providing a more comprehensive insight into the individual processes that lead to the overexpression of individual *E2F*'s and the potential for exploiting these mechanisms using chemotherapy.

The use of a stable E2F-1 overexpression system as a tool to investigate the effects of E2F-1 overexpression on chemosensitivity is prone to the same limitations mentioned above in the context of the inducible system. However, in addition, the permanent expression of high levels of E2F-1 potentially leads to alterations in E2F-regulated genes downstream within the retinoblastoma pathway. It could be argued that this would create an artificial environment not observed in human tumours or instead it would provide a more

132

realistic picture compared to the inducible system as overexpression of E2F-1 in human tumours may be assumed a permanent fixture.

Results showed an increase in E2F-1 expression level in two E2F-1 overexpressing clones after 240 hours of induction. In contrast, E2F-1 expression was reduced in the E2F-1 anti-sense clone (AS 44) in the absence of doxocycline. Equal E2F-1 expression levels were observed in non-induced and induced pTRE300 11 control cells. In an attempt to investigate the functionality of the overexpressed E2F-1 protein FACS analysis of serum starved non-induced and induced E2F-1 2 were carried out. In contrast to prior investigations an increase of 5% of the percentage of cells in S phase was observed in induced E2F-1 2 and E2F-1 13 cells following release from serum starvation. All four clones examined did not undergo complete cell cycle arrest in G1 phase as would be expected following serum starvation.

A repeat experiment using nocodazole to induce a G2 arrest showed a distinct G2 arrest in both non-induced and induced E2F-1 2 cells. A 2fold increase in percentage of cells in S phase following release from G2 arrest was observed in induced cells compared to non-induced cells at 4 hours post arrest.

The above data did demonstrate the potential for exogenously expressed E2F-1 to promote S phase entry in quiescent or cell cycle arrested cells. However, the observed percentage increase of cells in S phase was not as marked as had been published previously in Johnson *et al.* and Shan *et al.*. A suggested cause for the lack of a more significant inappropriate S phase entry in E2F-1 overexpressing HT1080 cells could be the HT1080 Tet-Off cell line itself. As a transformed cell line it is presumed to contain a higher basal level of E2F-1 expression than for example the Rat-2 or REF52 cells used in previous studies (Johnson *et al.*, 1993; Shan *et al.*, 1994). An already elevated level of E2F-1 expression would substantially obscure the effect of a further increase in E2F-1 expression as well as make it difficult for cells to be arrested in G0/G1 by serum starvation.

Finally, growth inhibition assays were performed to determine the effect of E2F-1 overexpression on chemosensitivity in HT1080 Neo cells. No statistically significant increase or decrease in chemosensitivity in response to BGIII21 or cisplatin treatment was observed. Therefore it was concluded that E2F-1 overexpression was not the underlying factor causing an increased resistance to BGIII21.

3.4.1 Aberrations of *Rb* pathway constituents and treatment prognosis

It has been proposed that aberration of a single constituent of the *Rb* pathway appears to be sufficient to alter cell cycle regulation. Furthermore, genetic alteration within any one gene within the *Rb* pathway potentially eliminates the selective pressure for additional aberrations. Thus *Rb* or $p16^{INK4a}$ inactivation and cyclin D1 overexpression have been suggested to occur as mutually exclusive events.

Studies have revealed various malignancies to exhibit correlations between genetic alterations of individual members of the *Rb* pathway. Investigating the frequency of *Rb* deletions and cyclin D1 alterations, *Rb* deletions were found to be inversely correlated to cyclin D1 alterations in multiple myeloma (Krämer *et al.*, 2002). However, no correlation was found between $p16^{INK4a}$ hypermethylation and *cyclin D1* or *Rb* aberrations (Krämer *et al.*, 2002). Further it was found that alterations within the *cyclin D1* gene as well as *Rb* deletions resulted in a worse prognosis compared to $p16^{INK4a}$ hypermethylation which had no impact on survival (Krämer *et al.*, 2002).

Further evidence of an existing inverse correlation between cyclin D1 overexpression and *Rb* inactivation was reported by Schauer *et al.* looking at the expression levels of the respective proteins and their potential role in the etiology of lung cancer (Schauer *et al.*, 1994). It has been suggested that different mechanisms account for the aberrations regarding cell cycle regulation within small and non-small cell lung cancer. Within non-small cell lung cancer cell lines cyclin D1 expression levels were found to be elevated compared to expression levels observed in small cell lung cancer and an immortalised human bronchoepithelial cell line. In contrast, non-small cell lung cancer cell lines expressed phosphorylation competent pRb at a constant level while expression of pRb in small cell lung cancer cell lines was non-detectable (Schauer *et al.*, 1994). Therefore it was concluded that an inverse correlation between cyclin D1 overexpression and *Rb* deletion exists within two different types of lung cancer (Schauer *et al.*, 1994).

The above examples of the relationship between cell cycle regulators such as *Rb* and *cyclin D1* contribute to the understanding of aberrations of cell cycle constituents indicative of specific tumours. This knowledge aids the interpretation of data concerned with determining the potential prognostic effect these cell cycle elements have for the management of different types of cancer.

3.4.2 History of cell line and species cross-contamination

At present an estimated 20% of cell lines are assumed wrongly labelled as a direct consequence of intra- and inter-species contamination. The first extensively published case of cell cross-contamination involved HeLa. In 1968 Stan Gartler published the results of an investigation into the identity of 18 supposedly unique human cell lines. Analysing the expression of glucose-6-phosphate dehydrogenase and phosphoglucomutase he found HeLa and the 17 other cell lines to express the A form of glucose-6-dehydrogenase, almost exclusively found in black individuals, and to exhibit an identical phenotype for the polymorphic enzyme, phosphoglucomutase. Gartler concluded that all 18 cell lines might be HeLa cells (Masters, 2002). During the 1970s Walter Nelson-Rees continued to uncover HeLa cross-contaminations, nevertheless with little lasting success as a list of cell lines shows which have been proven to be HeLa but are still widely used under their original name in laboratories across the world (**Table 3.3**) (Masters, 2002; Nelson-Rees *et al.*, 1981).

A second significant case of cross-contamination of cell lines involves the human urinary bladder cancer cell line T24. Using isozyme analysis and human leukocyte antigen (HLA)-A-B-C typing O'Toole *et al.* found EJ(MGH-U1) and some cultures of J82 to be in fact T24 cells (O'Toole *et al.*, 1983). Further, applying cytogenetics and DNA profiling, the TSU-Pr1 and JCA-1 prostate carcinoma cell lines were identified to be derivatives of the bladder carcinoma cell line T24. Thus, TSU-Pr1 and JCA-1 are not of prostatic origin (van Bokhoven *et al.*, 2001).

Name	Supposed origin	Actual name and origin
KB	Oral cancer	HeLa (cervical cancer)
HEp-2	Larynx cancer	HeLa (cervical cancer)
WISH, AV3 and FL	Normal human amnion cells	HeLa (cervical cancer)
L132	Normal human embryonic lung cells	HeLa (cervical cancer)
Intestine 407	Intestinal epithelium	HeLa (cervical cancer)
Chang liver	Normal liver cells	HeLa (cervical cancer)

Table 3.3: Cross-contamination by HeLa cells. Illustration of cases in which identified HeLa cells are used under original names and functions of cell lines which have been eliminated by faster growing HeLa cells after cross-contamination of original cultures (Masters, 2002).

The above examples highlight the persisting problem of cross-contamination which in most cases result from poor cell culture technique when two cell lines accidentally enter the same culture and the faster dividing cell type outgrows the slower growing cells, or a clerical error – mislabelling growing or frozen stocks.

It is difficult to determine which of the above mistakes led to the cross-contamination of cells received from collaborators for the above investigation into the effects of E2F-1 overexpression on chemosensitivity. However, after examining original stocks of the supplied cell lines frozen down upon arrival and original stocks freshly supplied from the source it was possible to establish that any cross-contamination occurred at the source and not after cells had been supplied for the above investigation. In general cross-contamination of cell lines is an avoidable problem, if stringent controls of tissue culture technique are performed and karyotyping, isozyme analysis, human leukocyte antigen (HLA) typing or DNA fingerprinting (Stacey et al., 1992) are carried out upon any immediate possibility of cross-contamination having occurred (Masters, 2000). The latest technique suggested to provide an international reference standard for human cell lines is short tandem repeat (STR) profiling based on the amplification of polymorphic STR loci using commercially available sets of primers. PCR products are analysed with size standards using automated fluorescent detection techniques resulting in a unique numerical

code based on the lengths of the PCR products amplified at each locus. STR profiling has been shown to be inexpensive and work under routine conditions (Masters *et al.*, 2001).

4. BGIII21 CHEMOSENSITIVITY AND DNA REPAIR

4.1 Introduction

In the previous chapter analysis of the effects of E2F-1 overexpression on chemosensitivity to chemotherapeutic agents as well as a novel minor groove binding alkylating agent (BGIII21) was attempted. BGIII21, a distamycin A derivative was first described by Wyatt *et al.*, 1995. It is a tri-pyrrole compound that specifically binds to the minor groove of DNA in a sequence specific manner. The preferred binding site of BGIII21 is TTTTGPu. BGIII21 is a monofunctional alkylating agent, alkylating the N3-guanine or N3-adenine of the binding sequence, represented by Pu (Wyatt *et al.*, 1995). Sulphorhodamine B (SRB) growth inhibition assays revealed a marked resistance to BGIII21 in two E2F-1 overexpressing transfectants. However research into the presence of BGIII21 specific DNA lesions following treatment with BGIII21 was not successful, and further experiments revealed the two E2F-1 overexpressing cell lines to be of Chinese hamster ovary (CHO) origin.

Research into the decreased sensitivity within CHO compared with human cells, raised a number of questions. First, are BGIII21 specific DNA lesions produced within CHO cells? Does enhanced repair of BGIII21 lesions take place in CHO cells? What DNA repair pathways are involved and finally, what are the exact mechanisms of DNA damage recognition and repair?

A short introduction to the three principal DNA repair pathways examined in this chapter is given. Base excision repair (BER) was excluded from the investigation as BER is primarily concerned with the repair of endogenous DNA damage as a result of cellular metabolism (Hoeijmakers, 2001).

4.1.1 Nucleotide excision repair

Nucleotide excision repair (NER) is a versatile and highly conserved repair system capable of removing a wide range of helix-distorting DNA lesions, that interfere with base pairing and obstruct transcription and DNA replication. The majority of NER lesions are of exogenous origin and include the short-wave ultraviolet (UV) light-induced cyclobutane pyrimidine dimers, 6-4 photoproducts and bulky adducts. NER consists of two subpathways with overlapping substrate specificity. The general pathway termed global

genome repair (GGR) removes lesions from the entire genome and the specialised pathway referred to as transcription-coupled repair (TCR) concentrates on damage blocking RNA polymerases. The study of syndromes associated with inborn defects in NER, namely Xeroderma pigmentosum (XP) and Cockayne syndrome (CS) revealed seven XP genetic complementation groups (XP-A to XP-G) representing different proteins in the NER pathway (**Table 4.1**). In addition, two CS genetic complementation groups (CS-A and CS-B) exclusively associated with TCR were discovered (Hoeijmakers, 2001; Volker *et al.*, 2001) (**Table 4.1**).

NER repair proteins	Function
XPA	Binds damaged DNA; cooperates with replication protein A (RPA);
XPB	3' to 5' helicase
XPC	Binds damaged DNA; cooperates with hHR23B; recruits other NER proteins
XPD	5' to 3' helicase
XPE	?
XPF	Part of endonuclease (5' incision)
XPG	Endonuclease (3' incision)
ERCC1	Part of endonuclease (5' incision)
CS-A	Transcription-coupled repair
CS-B	Transcription-coupled repair

Table 4.1: Nucleotide excision repair (NER) proteins and their associated functions during global genome repair (GGR) and transcription-coupled repair (TCR).
XPA to XPG (Xeroderma pigmentosum A-G); CS-A and B (Cockayne's syndrome A and B)

NER is a multi-step process involving recognition of damaged DNA, opening up the surrounding DNA helix with helicases, followed by a dual incision and subsequent excision of the oligonucleotide containing the DNA lesion. A simplified view of the individual stages in mammalian global genome nucleotide excision repair is outlined in **Figure 4.1**.

4.1.2 Homologous recombination repair

Homologous recombination repair and non-homologous end joining are the primary two mechanisms involved in the repair of double strand breaks (DSB) caused by ionising radiation or X-rays, free radicals, chemicals and during the replication of single strand breaks (SSB). Moreover DSBs arise naturally during meiosis and rearrangement of gene segments (VDJ joining) during immune cell development.

Homologous recombination repair predominantly occurs during S and G2 phase as this is a homology-driven mechanism requiring regions of identical DNA sequence. Non-homologous end joining having no requirement for regions of identical DNA sequence is active almost exclusively during G1 phase of the cell cycle. However, it has been suggested that a certain amount of overlap exist between the two mechanisms. A simplified view of the classic model of homologous recombination repair is depicted in **Figure 4.2** (Hoeijmakers, 2001).

4.1.3 Mismatch repair

Mismatch repair (MMR) removes nucleotides mispaired by DNA polymerases and insertion/deletion loops (>1-10 base pairs) that result from slippage during replication of repetitive sequences or during recombination.

The principal steps involved in MMR include mismatch recognition primarily carried out by the MSH2/MSH6 (detects base mismatches and single-base loops) and MSH2/MSH3 (recognises insertion/deletion loops) heterodimers and interaction of the hMLH1/hPMS2 and hMLH1/hPMS1 heterodimeric complexes with the MSH complexes and replication factors as strand discrimination may be dependent on contact with the nearby replication machinery. A number of proteins are implicated in the excision of the new strand past the mismatch and re-synthesis steps including polδ/ε, RPA, PCNA, reduced folate carrier (RFC), exonuclease 1, and endonuclease FEN1 (Hoeijmakers, 2001).
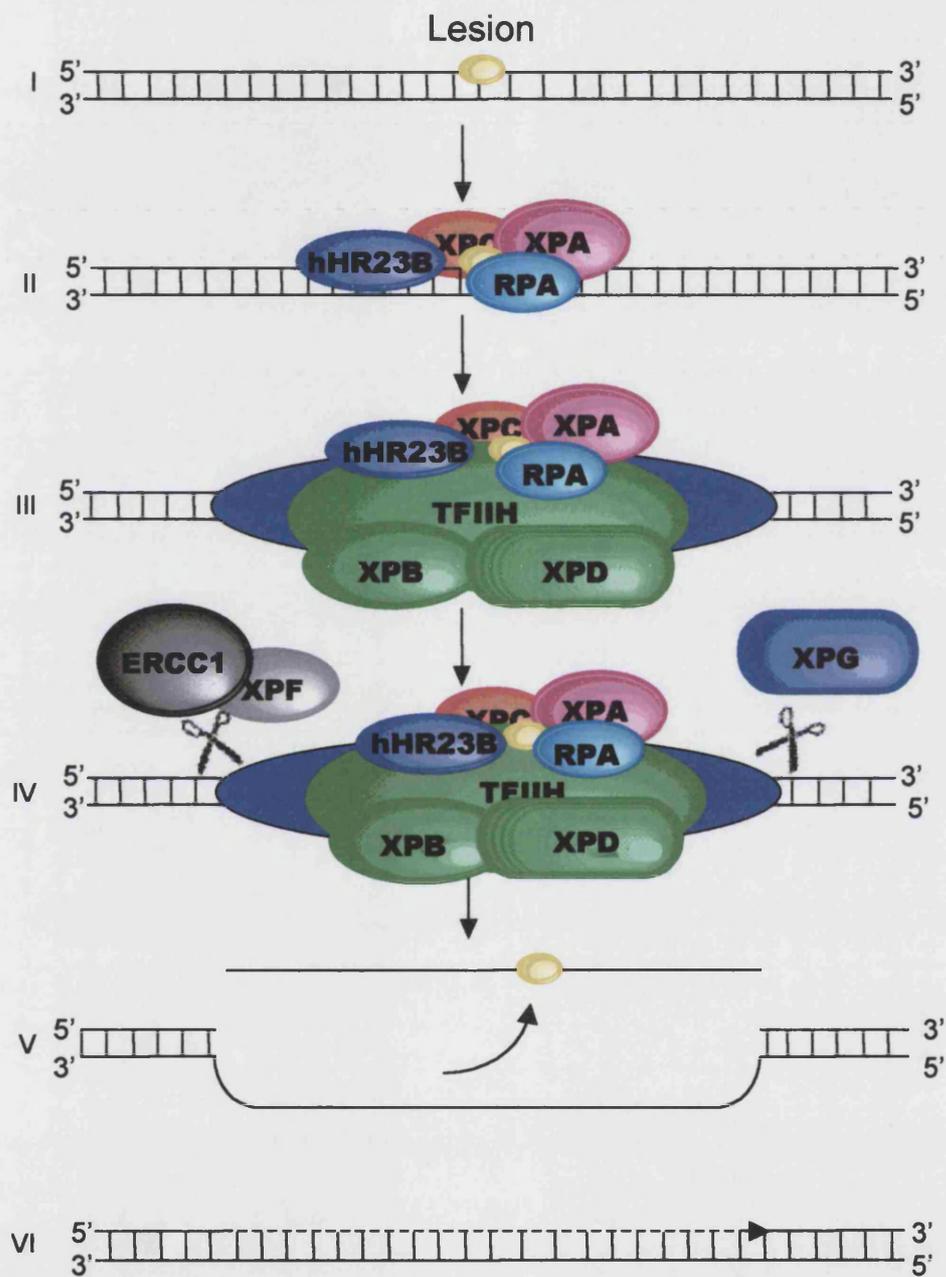
Fig. 4.1: Simplified diagram of mammalian nucleotide excision repair (McHugh *et al.*, 2001).

Fig 4.1: A simplified diagram of mammalian nucleotide excision repair (McHugh *et al.*, 2001). DNA damage recognition (II) is the first step, and the exact identity of the damage recognition factor has been a matter of debate. The proposed candidates involved, are the XPC-hHR23B and XPA-RPA complexes and evidence for their involvement in mammalian NER is contradictory. Assembly of the NER complex requires the recruitment of the basal transcription factor IIH (TFIIH) complex containing the helicases XPB and XPD necessary for unwinding ~30 base pairs of the DNA helix around the site of damage. The resulting open intermediate complex is stabilised by the single-stranded-binding protein RPA (III). The endonucleases ERCC1-XPF and XPG make an incision at the 5' and '3 end at either side of the DNA damage site (IV). Whereas ERCC1-XPF is dependent on XPA for its recruitment to the DNA damage and XPA has been implicated in assisting the anchoring of ERCC1-XPF in the incision complex, XPG recruitment is independent of XPA. However, incision by XPG appears to be dependent on activation by the XPA-RPA complex. Finally, the damage-containing oligonucleotide is released (V) and the DNA helix is restored by gap closure via DNA synthesis and ligation (VI) (Hoeijmakers, 2001; McHugh *et al.*, 2001; Volker *et al.*, 2001).
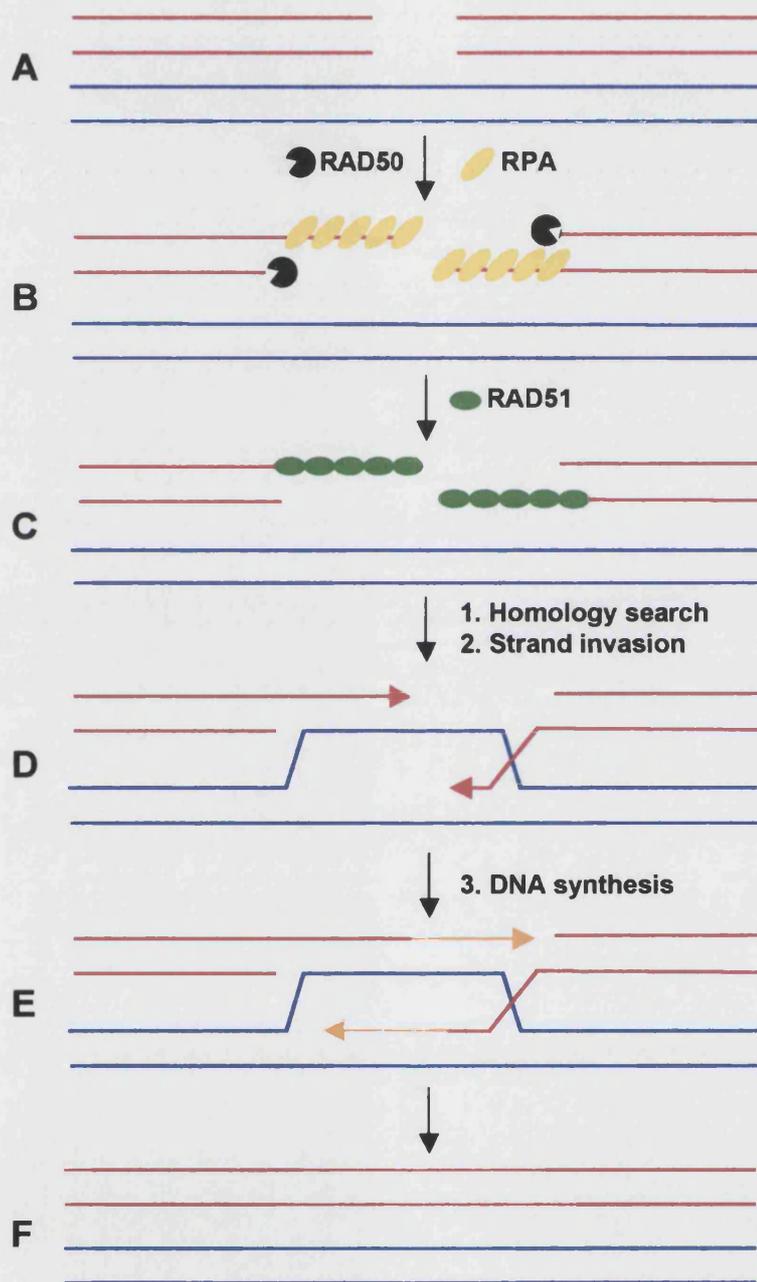
Fig. 4.2: A simplified diagram of mammalian homologous recombination repair (Hoeijmakers, 2001; McHugh *et al.*, 2001)

Fig. 4.2: A simplified diagram of mammalian homologous recombination repair (Hoeijmakers, 2001; McHugh *et al.*, 2001). An initial DSB instigates strand exchanges between sister chromatids or homologues (A). First, the 5'-3' exonuclease activity of the RAD50 complex exposes both 3' ends in order to promote strand invasion into the homologous sequences (B). Meanwhile, RPA facilitates the assembly of a RAD51 nucleoprotein filament that possibly includes RAD51-related proteins XRCC2, XRCC3, RAD51B, C and D (C). Next, the exchange of the single strand with the same sequence from a double-stranded DNA molecule occurs whereby correct positioning of the sister chromatids by cohesions facilitates the identification of the homologous sequence (D). Finally, the open ends are closed by DNA synthesis (E) and the existing Holliday junction is resolved by resolvases (F) (Hoeijmakers, 2001; McHugh *et al.*, 2001).

During the process of non-homologous end-joining, the ends of the existing DSB are simply joined together without any template, using the end-binding heterodimeric KU70/KU80 complex. Recruitment of DNA-PK stabilises the ends and facilitates ligation by the XRCC4/DNA ligase 4 complex. Non-homologous end-joining occurs primarily during G1 phase as cells are only provided with the homologous chromosome for recombination repair. However, this chromosome might be difficult to find in the complex genome and in addition there is a potential danger using it as a template for repair as it could lead to homozygosity of recessive mutations (Hoeijmakers, 2001; McHugh *et al.*, 2001).

144

4.1.4 Chapter aims

The aims of the following experiments were:

- to investigate BGIII21 specific DNA lesions in CHO cells

- to analyse differential repair of BGIII21 specific DNA lesions in CHO cells if present

- to determine the repair pathway involved in the removal of BGIII21 specific lesions in CHO cells

- to elucidate the mechanism of BGIII21 specific DNA damage recognition and repair in CHO cells

4.2 Materials and Methods

4.2.1 Experimental cell lines

4.2.1.1 Chinese hamster ovary (CHO)

The Chinese hamster ovary cell line (CHO-AA8) purchased from Clontech, Basingstoke, UK was maintained in F-12 HAM medium supplemented with 10% FCS and 2mM glutamine. Confluent cultures were seeded at $1\text{-}3\times10^4$ cells/cm^2 unless otherwise stated (ECACC).

4.2.1.2 NER deficient CHO cell lines

AA8 is the parental strain for all NER deficient cell lines. Both, parental and repair deficient cell lines were grown in F-12 HAM medium supplemented with 10% FCS and 2mM glutamine. The parental plus all NER deficient cell lines are listed in **Table 4.2**.

Name	Defective gene
AA8	None (wild-type)
UV23	XPB
UV47	XPF
UV61	CSB
UV96	ERCC1
UV135	XPG

Table 4.2: NER deficient CHO cell lines used

4.2.1.3 Homologous recombination repair deficient CHO cell lines

V79, AA8 and CHO-K1 are the parental strains for the homologous recombination deficient cell lines *irs1* (XRCC2 deficient), *irs1SF* (XRCC3 deficient) and *xrs5* (XRCC5 deficient) respectively. The parental and repair deficient cell lines were maintained in F12-HAM medium supplemented with 10% FCS and 2mM glutamine.

4.2.1.4 Mismatch repair deficient CHO cell lines

The mismatch repair deficient CHO clone B cell line was supplied by Gabriele Aquilina, Istituto Superiore di Sanita, Section of Chemical Carcinogenesis, Rome, Italy. The clone B cells were isolated from CHO cells in 1988 by selection for tolerance to methylating agents (Aquilina *et al.*, 1988). Clone B is defective in mismatch binding and exhibits a mutator phenotype and microsatellite instability (Aquilina *et al.*, 1994; Aquilina *et al.*, 2001). The mismatch defect is not characterised. The CHO clone B and parent cell line were maintained in F12-HAM supplemented with 10% FCS and 2mM glutamine.

4.2.1.5 Mismatch repair deficient human colon cancer cell lines

All colon cancer cell lines were maintained in F12-HAM supplemented with 10% FCS and 2mM glutamine. They were obtained from the departmental cell culture stock. Cell lines include LoVo (Drewinko *et al.*, 1976), HT29 (von Kleist *et al.*, 1975), LS174T (Rutzky *et al.*, 1979) and HCT15 (Tibbetts *et al.*, 1977).

4.2.1.6 Mismatch repair deficient human prostate cancer cell lines

All prostate cancer cell lines were kindly provided by John Masters, Dept. Urology, UCL, UK. Cells were maintained in DMEM supplemented with 10% FCS and 2mM glutamine. Cell lines include LNCaP (Gibas *et al.*, 1984), DU145 (Starring *et al.*, 1982) and PC3 (Kaighn *et al.*, 1979).

4.3 Results

4.3.1 Resistance to BGIII21 in CHO –AA8 cells

Following the results obtained in the previous chapter it was considered of importance to obtain a fully characterised CHO cell line to determine the basis of BGIII21 resistance in CHO cells as compared with human cells. Sulphorhodamine B (SRB) growth inhibition assays were performed to verify results previously obtained with respect to the novel minor groove binding alkylating agent BGIII21. As shown in **Figure 4.3**, the graph for CHO-AA8 confirmed the previously observed statistically significant decrease in sensitivity to BGIII21 (IC_{50} > 50µM) compared to HT1080 Neo (p < 0.0001). HT1080 Neo (IC_{50} = 0.68µM) and 'HT1080 E2F 1-1' (CHO) (IC_{50} > 50µM) were used as reference cell lines in these experiments. The IC_{50}s were determined from each graph representing 3 or more individual experiments.

4.3.2 BGIII21 DNA lesions produced in CHO-AA8 cells

DNA sequence alterations detected within the N-*ras* promoter region of CHO cells led to the selection of the sequenced hypoxanthine guanine phosphoribosyltransferase (*HPRT*) exon 9 region as a DNA region suitable to perform Sslig-PCRs on (Rossiter *et al.*, 1991). The 336bp long *HPRT* exon 9 DNA sequence obtained after restriction cutting with *Sca*I (NEB, Hitchin, UK) contains a single BGIII21 specific binding site (TTTTGA).

The experimental parameters were identical to the Sslig protocol used for the analysis of the N-*ras* promoter region. Cells were incubated with increasing concentrations of BGIII21 for 5 hours, harvested and processed as described in section (2.2.10).
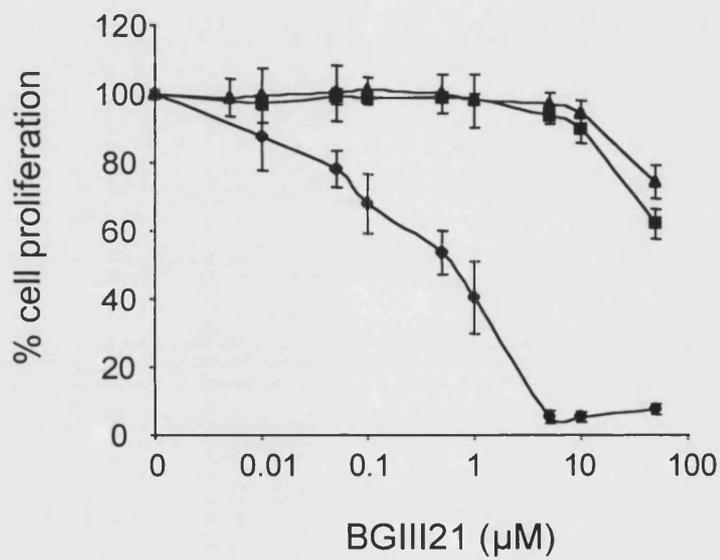
Fig. 4.3: Inhibition of proliferation by BGIII21 on CHO-AA8, HT1080 Neo and 'E2F 1-1' cells as measured by Sulphorhodamine B growth inhibition assay. Drug exposure was continuous (72 hrs) and graphs represent combined data of 3 or more experiments.
◆ HT1080 Neo; ■ HT1080 E2F 1-1; ▲ CHO-AA8

In the CHO-AA8 cells BGIII21 specific DNA lesions were produced in two sites within the chosen *HPRT* DNA sequence at 50μM BGIII21 (**Fig. 4.4**). The lower band marked the TTTTGA BGIII21 specific binding site present within the *HPRT* sequence. The upper BGIII21 specific DNA lesion represented a binding site within an A-T rich region of DNA previously not recognised as a BGIII21 specific binding site. Both bands representing BGIII21 lesions were reproduced throughout a number of experimental repeats.

For comparison, a representative Sslig experiment showing BGIII21 specific DNA lesions within HT1080 Neo cells was included in **Figure 4.4**. An increase in intensity of the BGIII21 specific lesions with increasing drug concentrations in HT1080 Neo cells was observed. In contrast, no BGIII21 specific lesions were produced at 10μM BGIII21 in CHO-AA8 cells. Bands representing BGIII21 lesions were present at 50μM BGIII21. BGIII21 uptake was suggested to be inhibited in CHO-AA8 cells up to a threshold concentration placed between 10 and 50μM BGIII21. Once the threshold concentration was reached BGIII21 entered the CHO-AA8 cells resulting in two bands representing the BGIII21 specific DNA lesions.

4.3.3 No repair of BGIII21 specific DNA lesions in HT1080 Neo or CHO-AA8

Previously two observations regarding the HT1080 Neo and CHO-AA8 cell lines were made. First, CHO-AA8 alone exhibited resistance to BGIII21 and second, BGIII21 specific DNA lesions were produced in both, the HT1080 Neo and CHO-AA8 cell lines. In order to determine the underlying causes for the differences in cell growth inhibition of BGIII21 in both cell lines, Sslig-PCRs were performed to examine the repair of BGIII21 induced DNA damage. HT1080 Neo and CHO-AA8 cells were incubated with 50μM BGIII21 for 5 hours and samples were taken immediately before and after drug exposure. Following drug removal, samples were collected at 24 hrs, 48 hrs and 72hrs post drug exposure. The post drug exposure time-points provided a scale on which to observe either the lack of DNA repair i.e. lesions persist at 72hrs, or to observe DNA repair i.e. lesions are expected to have decreased in intensity or disappeared within 72 hours. The drug concentration of 50μM BGIII21 was selected to provide a comparison between the two cell lines. 50μM BGIII21 were expected to generate a clearly detectable amount of DNA damage in HT1080 Neo and
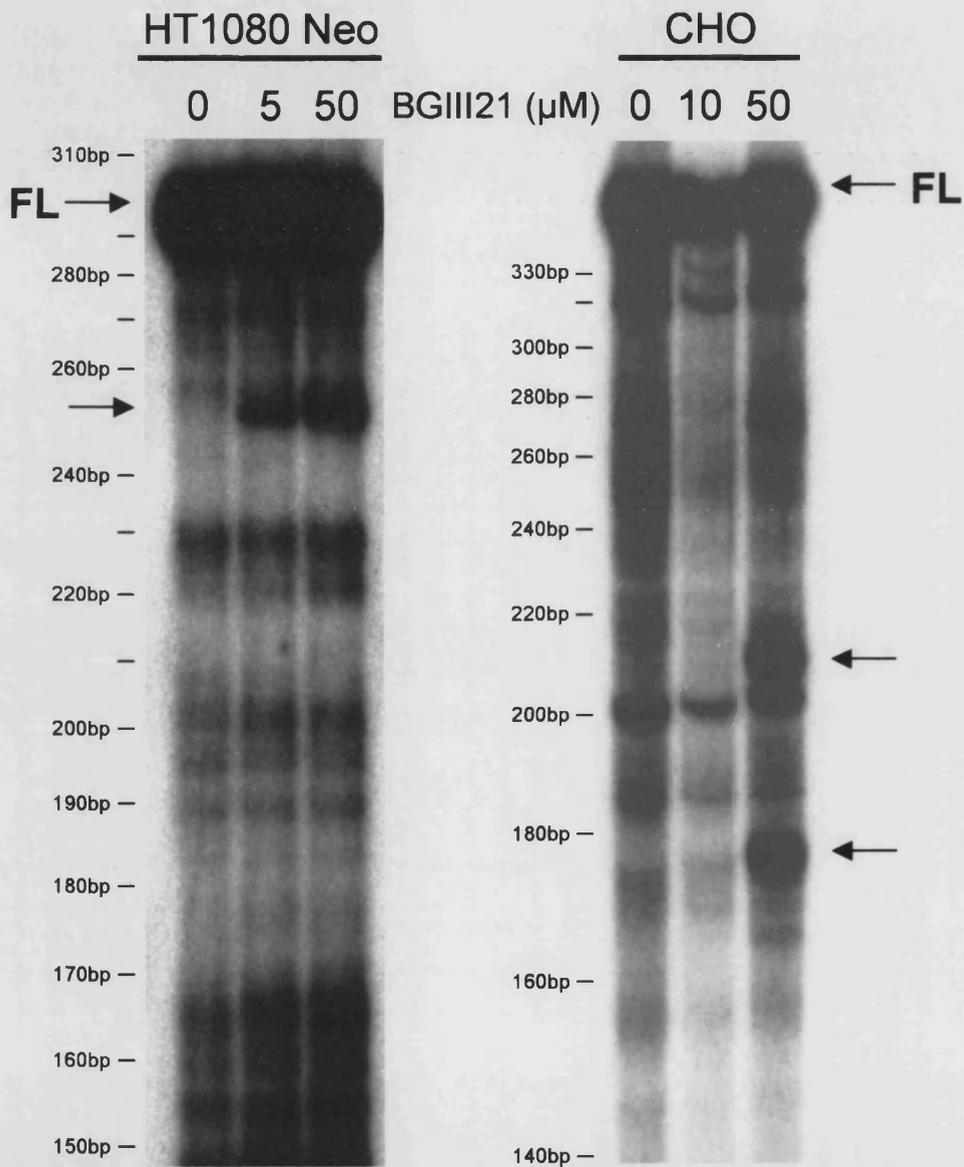
Fig. 4.4: BGIII21 specific DNA lesions (⟶) produced within HT1080 Neo and CHO-AA8 cells as measured by Sslig-PCR. Cells were incubated with BGIII21 for 5 hours. Correct size of BGIII21 lesions was verified with radio-labelled 10bp DNA ladder run alongside samples. FL (full length PCR product)

CHO-AA8 cells and the 72 hours duration for DNA repair was considered sufficient for any DNA repair to become visible as a reduction in band intensity.

As shown in **Figure 4.5** and **4.6**, no DNA repair of BGIII21 lesions was observed throughout the post exposure time-span in both HT1080 Neo and CHO-AA8 cells. The BGIII21 specific DNA lesions remained clearly visible at 72 hours post drug exposure. The intensity of the bands representing the BGIII21 specific DNA lesions did not alter throughout the post drug exposure time-course.

Although no DNA repair was observed in either of the two cell lines, a complete lack of DNA repair in CHO-AA8 cells seemed unlikely. As established previously CHO ('HT1080 E2F 1-1') cells continued to proliferate even after exposure to 50µM BGIII21 albeit with an altered cell cycle profile (section 3.3.8). Also, as proven by Sslig-PCR, 50µM BGIII21 caused BGIII21 specific DNA lesions in CHO-AA8 cells. It appears that CHO-AA8 cells continue proliferating after having sustained a significant amount of DNA damage. A more detailed analysis of DNA repair occurring was proposed, as DNA repair is considered essential to maintain genomic integrity for cell survival. The failure to detect any amount of DNA repair using the Sslig method might be attributed to the initial high concentration of BGIII21 required to giving rise to detectable DNA damage.

4.3.4 NER and repair of BGIII21 specific DNA damage

To analyse any repair of BGIII21 specific lesions in CHO-AA8 cells, it was necessary to investigate the involvement of a variety of specific DNA repair mechanisms in the repair of the BGIII21 specific lesions. To explore the involvement of nucleotide excision repair (NER) in the removal of BGIII21 specific DNA damage, a parental and 5 NER deficient CHO cell lines (section 4.2.1.2) were exposed to increasing concentrations of BGIII21 in a continuous SRB growth inhibition assay.

None of the NER deficient cell lines were significantly more sensitive to BGIII21 in comparison to each other and the parental cell line (p = 0.1510) (**Fig 4.7**). Although values for the percentage of cell proliferation for respective BGIII21 concentrations in five cell lines were similar up to 10µM BGIII21, the CSB deficient cell line appeared more resistant (IC_{75} = 10µM) than the parental AA8 cell line (IC_{75} = 5.9µM) suggesting loss of transcription coupled repair to increase resistance to BGIII21. However, any divergence of graphs was not reflected in the result of the subsequent statistical analyses (**Fig. 4.7**).
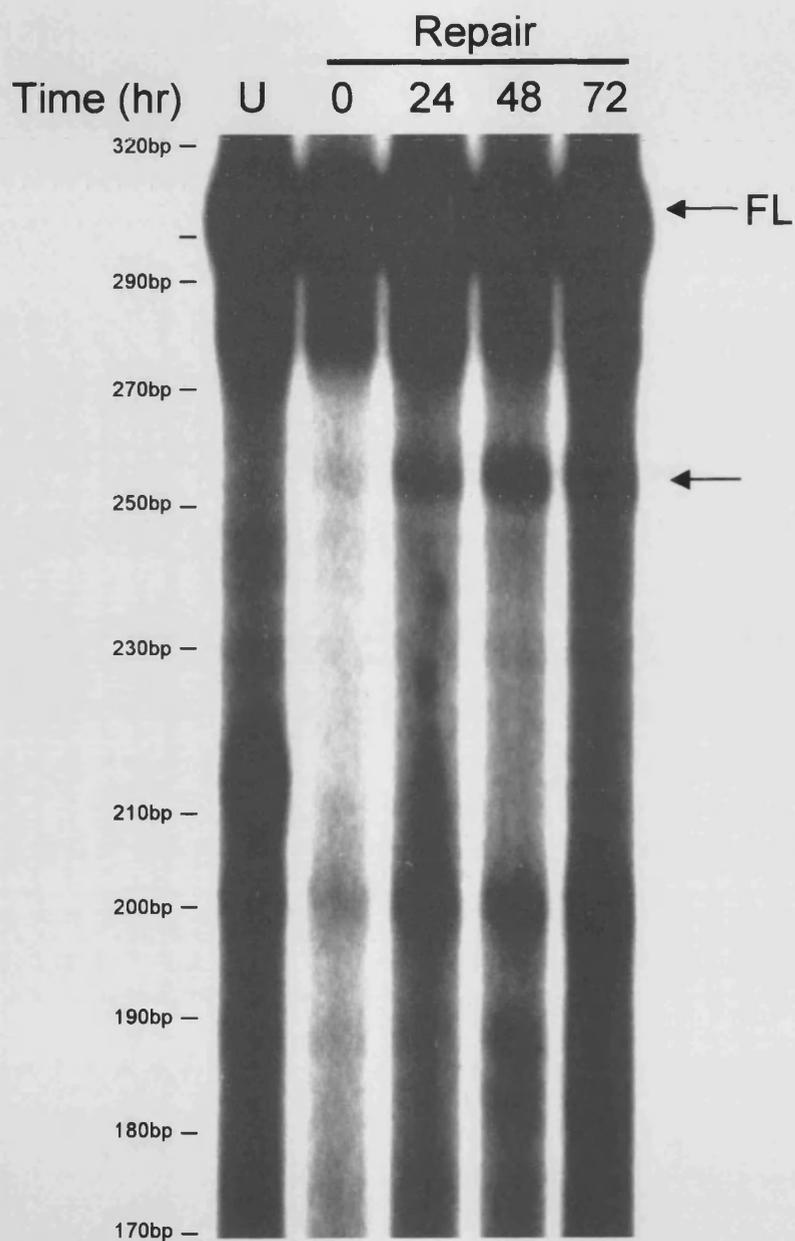
Fig. 4.5: No repair of BGIII21 specific DNA lesions (⟶) in HT 1080 Neo cells as measured by Sslig-PCR. Cells were treated with 50 μM BGIII21 for 5 hours prior to repair time-course. Correct size of DNA lesion was verified with radio-labelled 10bp size marker run alongside samples. FL (full length PCR product)
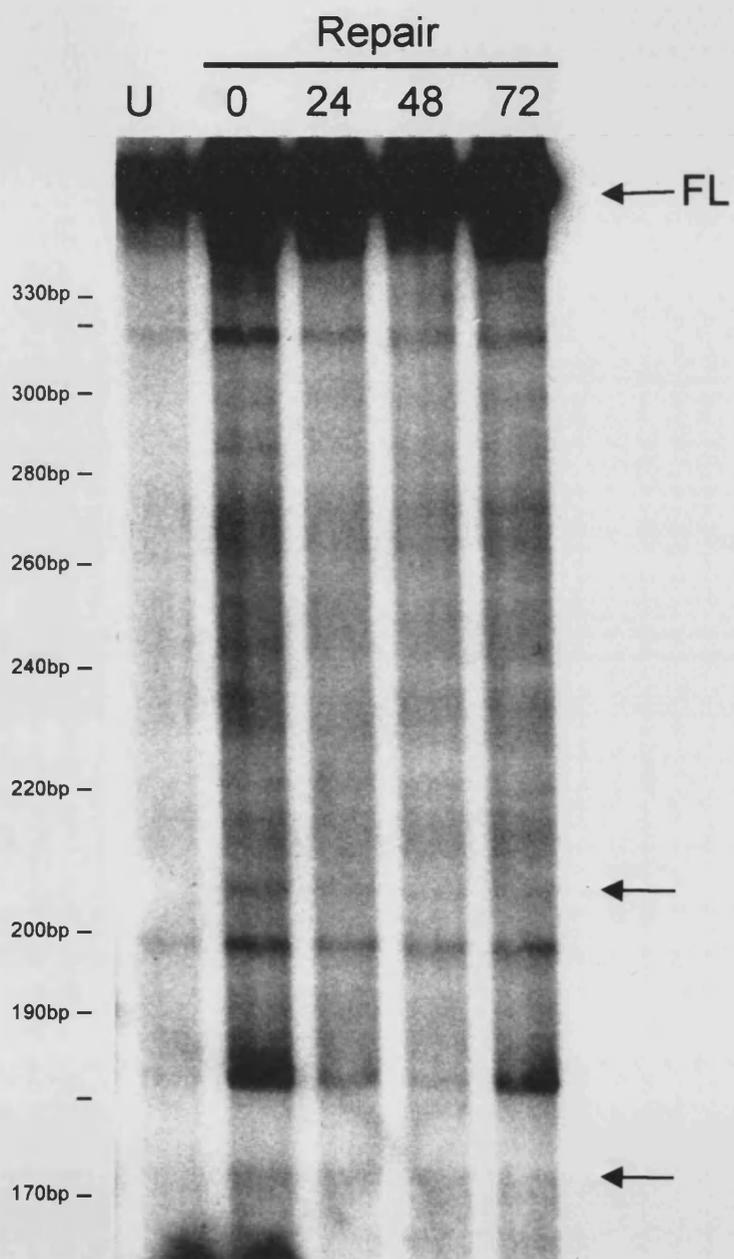
Fig. 4.6: No repair of BGIII21 specific DNA lesions (⟵) in CHO-AA8 cells as measured by Sslig-PCR. Cells were treated with 50μM BGIII21 for 5 hours prior to repair time-course. Correct size of BGIII21 lesion was verified with radio-labelled 10bp size marker. FL (full length PCR product)
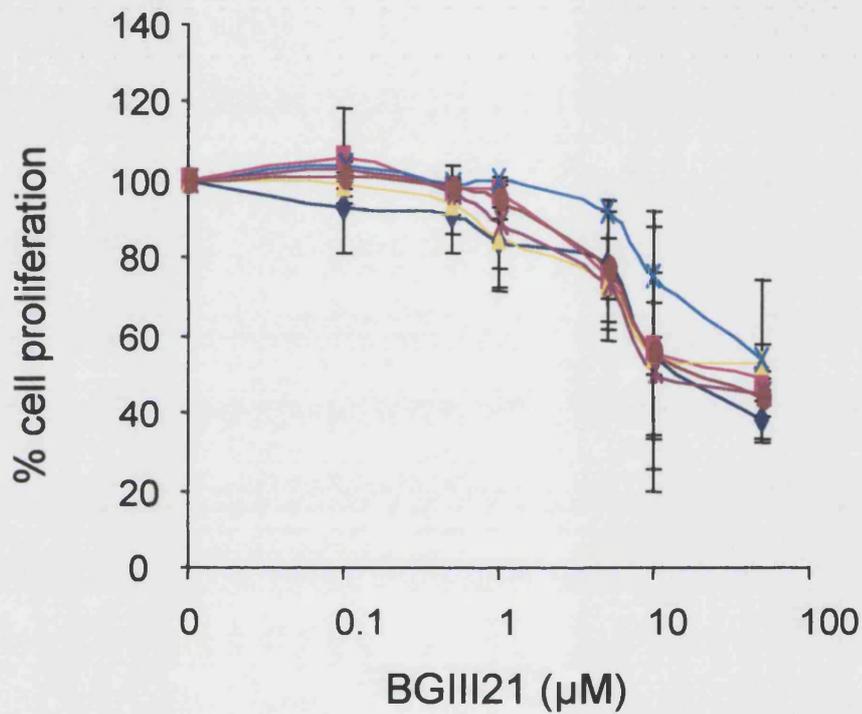
Fig. 4.7: Inhibition of proliferation by BGIII21 on NER deficient CHO cell lines after continuous exposure (72 hours) to BGIII21 as measured by SRB growth inhibition assay. Mean IC_{75} values were determined from the combined data of 3 or more separate experiments.

In conclusion, no significant difference in sensitivity was observed with respect to BGIII21 when comparing various NER deficient cell lines to the parental AA8 cell line using multiple regression analysis. Therefore BGIII21 specific DNA lesions do not appear to be repaired by NER.

4.3.5 Homologous recombination repair and BGIII21 specific DNA damage

The investigation was extended to include homologous recombination repair deficient CHO cell lines. Homologous recombination repair deficient cell lines were selected including *irs1* and *irs1*SF, deficient in the RAD51-like XRCC2 and XRCC3 protein respectively. In addition, *xrs5* deficient in XRCC5, a protein involved in non-homologous end-joining, was chosen. SRB growth inhibition assays were performed as before and the mean IC_{50} values determined from three or more separate experiments. Results for all three homologous recombination repair deficient cell lines in comparison to each respective parental cell line exhibited no significant difference in sensitivity in response to BGIII21 (**Fig. 4.8**). The *XRCC2* deficient cells were no more sensitive (IC50 = 13μM) than the V79 parental cell line (IC50= 13.8μM). Similarly, the IC_{50} for the *XRCC3* deficient cell line (IC50 = 65μM) was insignificantly lower than the IC_{50} (= 70μM) for the parental cell line AA8. Finally, the *XRCC5* deficient cell line (IC_{50} = 35μM) appeared to be marginally more sensitive to BGIII21 than the CHO-K1 parental cell line (IC_{50} = 49μM). The above results were further substantiated by statistical analysis using multiple regression analysis (section 2.2.3.3). No significant difference in chemosensitivity to BGIII21 was found between V79 vs. *irs1* (p = 0.1723), AA8 vs. *irs1*SF (p = 0.9180 and CHO-K1 vs. *xrs5* (p = 0.0052) respectively. In conclusion, neither NER nor homologous recombination repair was involved in the repair of BGIII21 specific lesions in CHO cells as illustrated by the above results.

Following the above results sets of human mismatch repair deficient colon and prostate cancer cells were selected to investigate the involvement of MMR in the removal of BGIII21 lesions. The selection of the colon and prostate cancer cell lines, in part, resulted from the temporary lack of availability of MMR-deficient CHO cell lines. Although differences in protein expression due to species- and tissue-specificity were taken into account, investigation into the involvement of MMR in the repair of BGIII21 lesions using these cell lines was considered a valuable indicator of the mechanisms underlying repair.

XRCC2 deficient

XRCC3 deficient

XRCC5 deficient
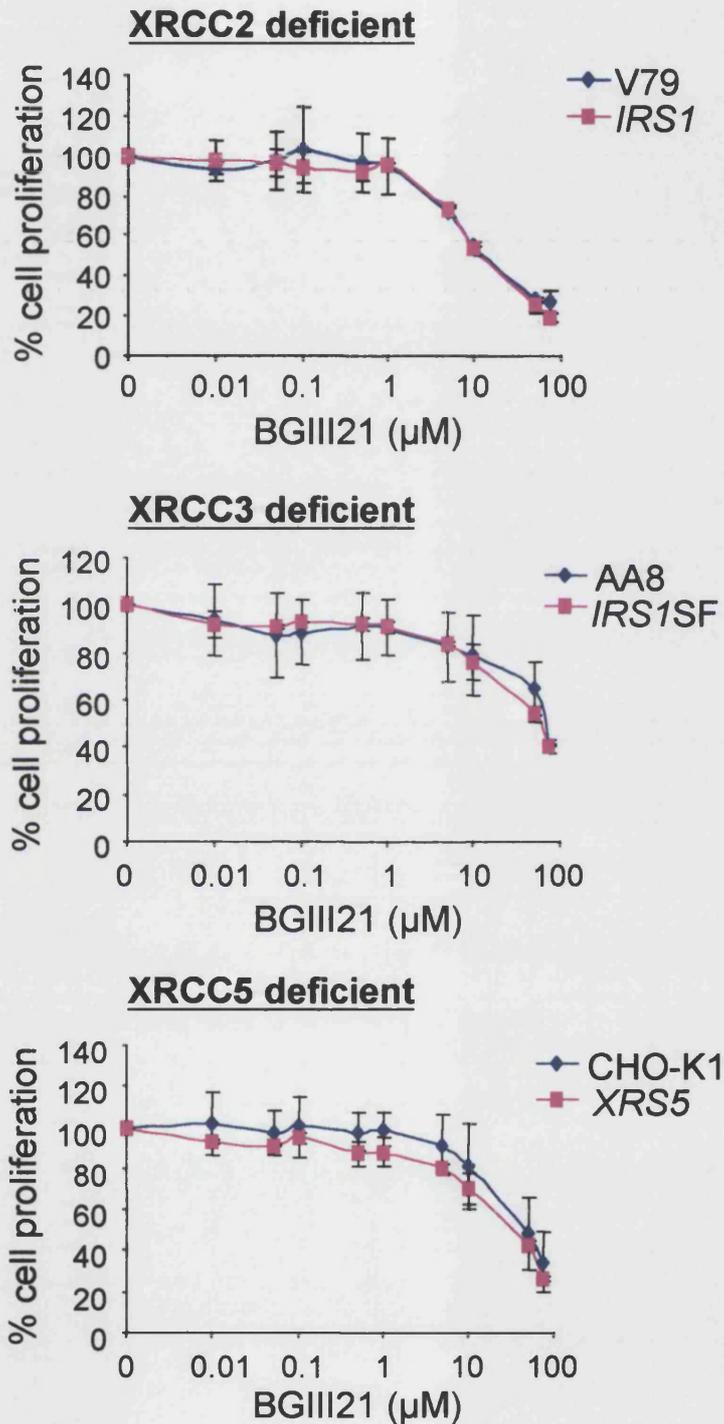
Fig. 4.8: Inhibition of proliferation by BGIII21 on homologous recombination deficient CHO cells following continuous exposure (72hours) to BGIII21 as measured by SRB growth inhibition assay. Mean IC_{50} values were determined from the combined data of 3 or more separate experiments.

156

4.3.6 Mismatch repair implicated in resistance to BGIII21 in human colon cancer

A number of genetic alterations have been described in colorectal cancers including allelic losses on specific chromosomal arms, mutations of oncogenes, tumour suppressor genes and mismatch repair genes, microsatellite instability in coding repeat sequences of target genes and methylation defects in gene promoters. Hence, a great genetic heterogeneity occurs within hereditary non-polyposis (HNPCC) and sporadic colorectal carcinomas that is reflected in a comprehensive study performed by Gayet *et al.*, characterising a series of human colorectal cancer cell lines for genetic alterations (Gayet *et al.*, 2001). On the basis of the above study, colon cancer cell lines were selected for further experiments in order to analyse the involvement of mismatch repair (MMR) as a mechanism responsible for the repair of BGIII21 specific damage. These included LoVo, LS174T, HCT15 and HT29 containing a range of differences in mismatch repair protein deficiency or complete mismatch repair proficiency. The mismatch repair deficiency characteristics of each cell line are illustrated in **Table 4.3**.

	hMSH2	hMSH3	hMSH6	hMLH1	hPMS1	hPMS2
LoVo	-	+	+	+	N/A	+
LS174T	+	-	-	-	+	+
HCT15	+	+	-	+	+	+
HT29	+	+	+	+	+	+

Table 4.3: Mismatch repair protein deficiencies in a variety of human colon cancer cell lines according to Gayet *et al.*, 2001. + (proficient); - (deficient); N/A (not analysed)

Continuous SRB growth inhibition assays including all four human colon cancer cell lines were performed as described previously (section 2.2.3.1). These provided a drug response profile showing LoVo (IC_{50} = 79μM) and HCT15 (IC_{50} = 42μM) cell lines to be more resistant to BGIII21 than the LS174T (IC_{50} = 7μM) and HT29 (IC_{50} = 8.2μM) cell lines (**Fig. 4.9**). As before, mean IC_{50} values were determined from 3 or more separate experiments. Statistical analysis including a global multivariate model revealed significant differences in chemosensitivity to BGIII21 between HCT15 and LoVo on one hand compared to LS174T and HT29 on the other hand. Differences in chemosensitivity between
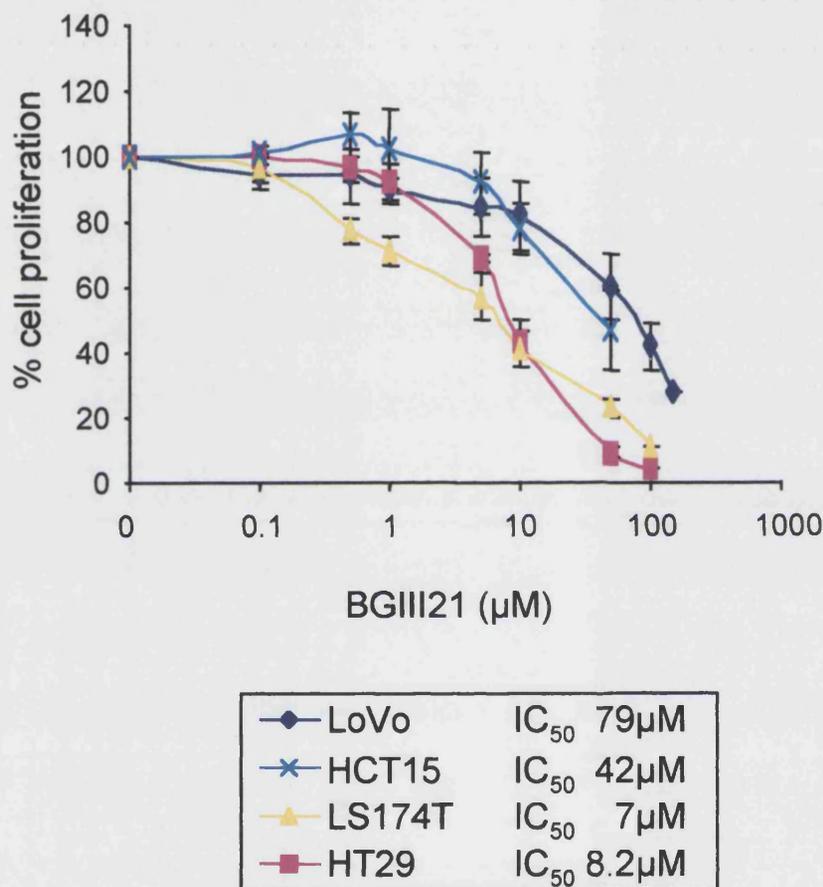
Fig. 4.9: Inhibition of proliferation by BGIII21 on MMR deficient human colon cancer cell lines as measured by SRB growth inhibition assay. Cell were incubated with increasing concentrations of BGIII21 for 72 hours. Mean IC_{50} values were determined from the combined data of 3 or more separate experiments.

HCT15 and LoVo as well as LS174T and HT29 were non-significant. The difference in sensitivity between the two sets of cell lines appeared to be independent of deficiency in any specific mismatch repair protein. However, O'Regan *et al.* stated in a study investigating the DNA mismatch recognition by human proteins that LoVo and DLD1/HCT15 cells are defective in G•T mismatch binding while LS174T cells are G•T mismatch binding proficient. All three human colon cancer cell lines appeared proficient in A•C mismatch binding (O'Regan *et al.*, 1996). Hence it might be possible to explain differences in BGIII21 chemosensitivity in human colon cancer cell lines with the loss of G•T mismatch binding proficiency.

4.3.7. Mismatch repair implicated in resistance to BGIII21 in human prostate cancer

In addition to the analysis of MMR deficient human colon cancer cell lines to establish a relationship between mismatch repair protein deficiency and resistance to the novel minor groove binding alkylating agent BGIII21, MMR deficient human prostate cancer cell lines were selected for further SRB growth inhibition assays. The range of prostate cancer cell lines chosen included LNCaP, PC3 and DU145. Cell line specific mismatch repair protein deficiencies are described in **Table 4.4** and are based on studies by Chen *et al.* and Leach *et al.* The prostate cancer cell lines were characterised in view of the presence or absence of specific MMR proteins as determined by Western blot analysis. All three characterised cell lines exhibited microsatellite instability as determined by the pCAR-IF/OF β-galactosidase assay (Chen *et al.*, 2001).

	hMSH2	*hMSH3*	*hMSH6*	*hMLH1*	*hPMS1*	*hPMS2*
LNCaP	-	+	+	+	+	+
PC3	+	-	+	+	+	+
DU145	+	+	+	-	-	-

Table 4.4: Presence (+) or absence (-) of mismatch repair proteins in human prostate cancer cell lines as determined by Western blot analysis (Chen *et al.*, 2001; Leach *et al.*, 2000).

In **Figure 4.10** continuous SRB growth inhibition assays performed as described (section 2.2.3.1) showed LNCaP (IC_{50} = 7.4μM) and PC3 (IC_{50} = 7.4μM) cells to exhibit a higher resistance to BGIII21 compared to observed sensitivity to BGIII21 in DU145 cells (IC_{50} = 1.3μM). The mean IC_{50} values were calculated from 3 or more separate experiments. The statement above was further validated by statistical analysis using a global multivariate model that showed significant differences between DU145 and LNCaP as well as DU145 and PC3 but no significant differences in chemosensitivity between LNCaP and PC3 (section 2.2.3.3).

Following the above completion of the experimental series shown above, an MMR-deficient CHO cell line became available and was subsequently included in the investigation. Analysis of the involvement of MMR in the removal of BGIII21 lesions within the CHO genetic background was suggested to provide a more accurate insight into the potential involvement repair mechanisms that result in the resistance effect observed in response to BGIII21 in CHO cells.

4.3.8 No increased resistance to BGIII21 in MMR deficient CHO Clone B cells

In addition to the investigations into the relationship between resistance to BGIII21 and MMR deficiency in colon and prostate cancer cell lines, experiments were performed using an MMR deficient CHO cell line. The MMR deficiency in the CHO Clone B cell line has not been characterised. Studies with BGIII21 were carried out as the resistance effect to BGIII21 had been previously observed in a CHO-AA8 cell line. SRB growth inhibition assays were performed and the mean IC_{50} calculated from 3 repeat experiments. In addition to BGIII21, cisplatin was included in the study as a second investigative drug as MMR deficient cells have been reported to display resistance to cisplatin (Fink *et al.*, 1998). An increase in sensitivity to BGIII21 was observed in the MMR deficient CHO Clone B cells (IC_{50} = 9μM) compared to the parental CHO cells (IC_{50} = 17μM). A minimal decrease in sensitivity to cisplatin was observed in the MMR CHO Clone B cells (IC_{50} = 2.3μM) compared to the CHO parent strain (IC_{50} = 1.9μM) (**Fig. 4.11**). However, statistical analysis revealed neither differences in chemosensitivity between Clone B and parental cells to be significant at $p < 0.0001$ (p = 0.3111 for BGIII21; p = 0.8480).
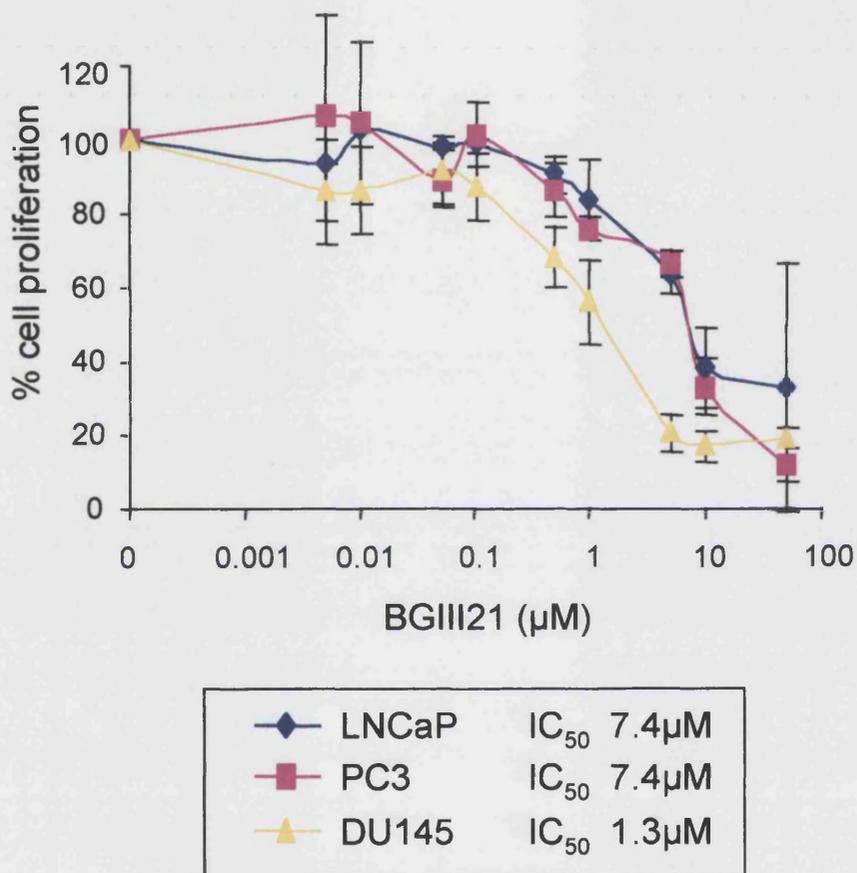
Fig. 4.10: Inhibition of proliferation by BGIII21 on MMR deficient human prostate cancer cell lines as measured by SRB growth inhibition assay. Cells were incubated with increasing concentrations of BGIII21 for 72 hours. Mean IC_{50} values were determined from the combined data of 3 or more separate experiments.
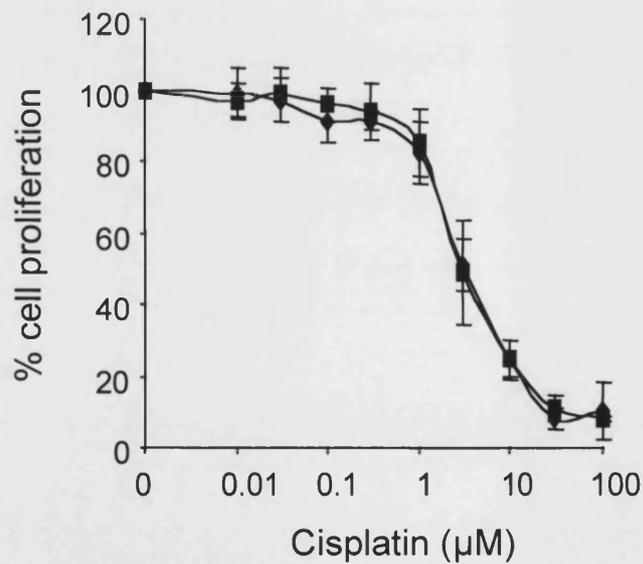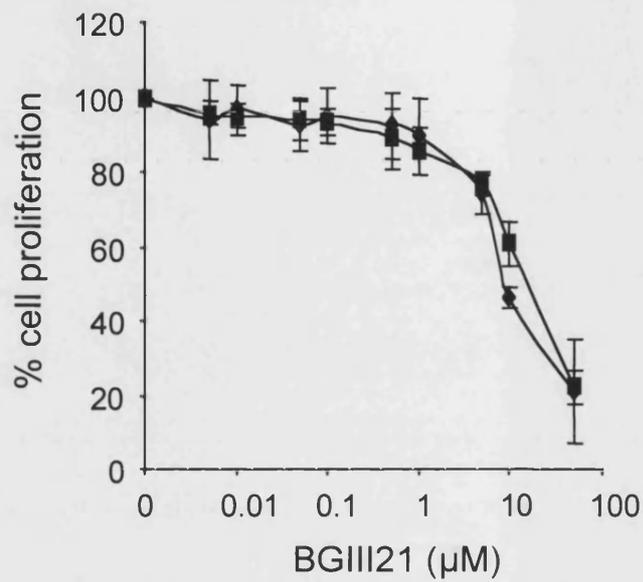
Fig. 4.11: Inhibition of proliferation in MMR deficient CHO clone B cells following continuous exposure (72hours) to BGIII21 and Cisplatin as measured by SRB growth inhibition assay. Mean IC_{50} values were determined from the combined data of 3 or more separate experiments.

◆ Clone B; ■ Parent strain

4.5 Discussion

4.5.1 Resistance to BGIII21 and drug uptake

In this chapter resistance to BGIII21 previously observed in CHO cells as compared with human cells was confirmed. In an SRB growth inhibition assay the newly obtained CHO-AA8 cell line proved to be more than 70fold more resistant to the novel minor groove binding alkylating agent BGIII21 than the HT1080 Neo cell line.

To investigate the underlying mechanism of BGIII21 resistance in CHO-AA8 cells a number of Sslig-PCR analyses were performed on the *HPRT* exon 9 region. Results showed two BGIII21 specific DNA binding sites at 50μM BGIII21. The DNA sequence of one binding site (TTTTGA) had been described previously by Wyatt *et al.* The second binding site was found in an A-T rich region within the 336bp DNA fragment obtained after restriction digest with *Sca*I. No BGIII21 specific lesions were produced at 10μM BGIII21. In contrast, in HT1080 Neo cells BGIII21 specific lesions of increasing intensity occurred at 5μM and 50μM BGIII21, respectively. The discrepancy in the production of DNA damage between both cell lines suggested an underlying difference in drug uptake. While BGIII21 readily entered HT1080 Neo cells within the concentration range, a drug concentration threshold appeared to prevent BGIII21 from entering CHO-AA8 cells at 10μM BGIII21. Therefore, the suggested concentration threshold lay between 10μM and 50μM as BGIII21 specific lesion formation showed BGIII21 drug uptake in CHO-AA8 unaffected at 50μM. To confirm the above observation of a differential drug uptake in HT1080 Neo and CHO-AA8 cells, experiments using radioactively labelled BGIII21 would need to be performed. Unfortunately at this point such as radioactively labelled substrate is not available.

4.5.2 NER and homologous recombination repair of BGIII21 specific DNA lesions

The investigation into the underlying mechanism involved in resistance to BGIII21 in CHO cells showed in a number of Sslig-PCRs, that BGIII21 lesions were not repaired in either HT1080 Neo or CHO-AA8 cells. This result challenged the hypothesis that CHO-AA8 cells were resistant to BGIII21 due to a more efficient repair of BGIII21 induced DNA damage compared to HT1080 Neo cells. BGIII21 induced DNA damage was not repaired in HT1080 Neo cells that subsequently underwent apoptosis as observed before (section

163

3.3.9). In contrast, persistence of BGIII21 induced DNA damage was tolerated in CHO-AA8 cells and cellular viability was maintained. This would lead to continual acquisition of irreparable DNA damage leading to mutagenesis and long-term loss of genomic integrity. Therefore, considering the high dose of BGIII21 required the production of DNA lesions it was suggested that low levels of DNA repair activity might not have been detectable.

Nucleotide excision and homologous recombination repair deficient CHO cell lines were selected to examine the potential involvement of these repair pathways in the removal of BGIII21 specific DNA damage. NER deficient cell lines plus the parental strain were exposed to increasing concentrations of BGIII21. Analysis of the cell growth inhibition profiles revealed none of the NER deficient cell lines to be more resistant to BGIII21 than the parental cell line. To conclude NER repair was not involved in the repair of BGIII21 specific DNA lesions.

Further, three homologous recombination repair deficient CHO cell lines and respective parental strains were treated with increasing concentrations of BGIII21. Neither *XRCC2*, *XRCC3* nor *XRCC5* deficient cell lines were more sensitive to BGIII21 when compared to the respective parental strain. Therefore it was concluded that homologous recombination repair did not participate in the removal BGIII21 specific DNA damage.

4.5.3 Mismatch repair of BGIII21 specific DNA lesions

Defective mismatch repair is associated with hereditary non-polyposis colon cancer (HNPCC) and many sporadic cancers including endometrial, small and non-small cell lung cancer, pancreatic, gastric, ovarian, cervix and breast cancer (Fink *et al.*, 1998). In addition, loss of mismatch repair has been observed in prostate cancer (Chen *et al.*, 2001). Loss of MMR results in drug resistance directly by impairing the ability of the cell to detect DNA damage and activate apoptosis and indirectly by increasing the mutation rate throughout the genome (Fink *et al.*, 1998).

Within eukaryotes post-replicative MMR in connection with DNA polymerase proof-reading maintains the fidelity of the genome. Any remaining errors following proof-reading and editing are also corrected by MMR (Aquilina *et al.*, 2001). MMR function is carried out by MutSα (hMSH2:hMSH6), MutSβ (hMSH2:hMSH3) and MutLα (hMLH1: hPMS2) complexes. The MutSα and MutSβ complexes partake in the recognition of replication errors, whereby MutSα preferentially recognises single mismatches and loops of

1 base and MutSβ binds insertion and deletion loops (IDL) of 2 to 8 bases. Some functional overlap between the complexes exists with respect to the recognition of 1 base IDLs (Aquilina *et al.*, 2001). Upon initial recognition of the mismatch or IDL by MutSα and MutSβ, MutLα associates with either recognition complex. This association is suggested to increase the efficiency of MutS binding to mismatched DNA (Aquilina *et al.*, 2001).

As MMR deficient CHO cell lines were not available to investigate the effects of MMR deficiency on growth inhibition in response to BGIII21 treatment initially, a variety of MMR deficient human colon and prostate cancer cell lines were selected for a preliminary investigative screening. Characterisation of MMR deficiency in each cell line, based on published data, is supplied in **Table 4.3** and **4.4**. Collectively, the chosen cell lines cover the range of MMR deficiencies characterised.

SRB growth inhibition assays revealed the two colon cancer cell lines LoVo and HCT15 to be more resistant to BGIII21 in comparison to LS174T and the MMR proficient HT29 colon cancer cell lines. A 10fold increase in resistance was observed in LoVo, and HCT15 cells were 5-6 times more resistant compared to LS174T and HT29. Analysis of three MMR deficient prostate cancer cell lines showed LNCaP and PC3 to be 7 times more resistant to BGIII21 than DU145. A comparison of BGIII21 resistance and MMR protein deficiency was carried out, taking account of tissue related drug sensitivity and a pattern with respect to BGIII21 resistance emerged (**Table 4.5**). Both *hMSH2* deficient as well as *hMSH6* or *hMSH3* deficient cell lines were more resistant to BGIII21 than either *hMLH1* deficient cell lines. Note was taken that LS174T cells were also deficient in hMSH6 and *hMSH3*. Finally, the MMR proficient HT29 colon cancer cell line was sensitive to BGIII21. In conclusion, MMR deficiency plays a critical role in the resistance to BGIII21 observed in human colon and prostate cancer cells. It appears that *hMSH2* and *hMSH6* or *hMSH3* deficiency predisposes to BGIII21 resistance while *hMLH1* deficiency promotes cellular sensitivity to BGIII21.

Name	MMR status	IC_{50} value	Resistant/Sensitive
LoVo (CC)	hMSH2	79μM	R
LNCaP (PC)	deficient	7.4μM	R
HCT15 (CC)	hMSH6 or hMSH3	42μM	R
PC3 (PC)	deficient	7.4μM	R
LS174T (CC)	hMLH1	7μM	S
DU145 (PC)	deficient	1.3μM	S
HT29 (CC)	proficient	8.2μM	S

Table 4.5: Comparison of MMR status with resistance (R) or sensitivity (S) observed in colon cancer (CC) and prostate cancer (PC) cell lines.

In previous studies MMR-deficient cells have been shown to be more resistant to the cytotoxic effect of alkylating agents such as the monofunctional methylating agents N-methyl-N'-nitro-N-nitrosoguanidine (MNNG) and N-methyl-N-nitrosourea (MNU), bulky chemicals such as cisplatin and ionising radiation (Jiricny, 1998; Karran, 2001). In, addition Colella *et al.* reported a 2-3fold increase in resistance of MMR deficient HCT-116 colon cancer cells to a number of minor groove binding alkylating agents including tallimustine, carzelesin and CC-1065 (Colella *et al.*, 1999).

In view of the results obtained for colon and prostate cancer cell lines in this study, it was suggested that lack of *hMSH2* and *hMSH6* or *hMSH3* deficiency cause cells not to recognise BGIII21 induced damage hence lead to alkylation tolerance. It appears that *hMSH2* alone is not able to convey an apoptotic signal to initiate programmed cell death but is dependent on the presence of *hMSH6* or *hMSH3*. However, this theory appears incorrect with respect to LS174T cells, as these are *hMSH6* and *hMSH3* deficient and would therefore be expected to exhibit alkylation tolerance. Nevertheless, the additional absence of *hMLH1* may reverse any potential for alkylation tolerance and instead sensitises LS174T cells to BGIII21 treatment. This reversal theory is supported by the BGIII21 sensitivity observed in *hMLH1* deficient DU145 prostate cancer cells. Further research into the relationships between individual mismatch repair complexes and their recognition and

apoptosis function to initiate programmed cell death following BGIII21 specific DNA damage in human colon and prostate cancer cell lines is required.

Following the preliminary screening of human colon and prostate cancer cell lines to investigate the effects of DNA repair deficiencies on altering the chemosensitive response, MMR-deficient CHO Clone B cells were obtained. Although experiments performed using the human colon and prostate cancer cell lines resulted in a number of observations that could be potentially useful in unravelling the mechanism underlying the decreased sensitivity seen in CHO cells following treatment with BGIII21, any further investigation required an MMR-deficient CHO cell line to eliminate species and tissue-related differential gene expression.

A series of growth inhibition experiments showed the Clone B cells to be twice as sensitive to BGIII21 than the parental CHO cell line. In addition, the parental CHO cell line exhibited a more than 2fold increase in sensitivity to BGIII21 compared to the CHO-AA8 cell line used in previous experiments. This result highlights the fact that even when using cell lines of the same identity, differences in response to drug treatment may occur. Possible explanation for any observed variations in sensitivity to treatment with the same drug, may be prior differences in growth media and supplements used as well as differences in passage number. Further, depending on the longevity of growth of the cell line, additional genotypic alterations may have occurred within resulting subclones of the same cell line that result in an altered chemosensitivity within those subclones in response to drug exposure. However, in contrast to results obtained for BGIII21, the parental and MMR deficient cell line in response to cisplatin showed a similar degree of sensitivity.

As mentioned previously the MMR protein deficiency in CHO Clone B cells has not been characterised. However, attempts by Aquilina et al. to complement hMSH2 deficient LoVo cell extracts with CHO Clone B extracts in order to restore MMR failed, indicating that these cell lines share a common defect – hMSH2 deficiency. Further, CHO Clone B cells were shown to be resistant to DNA methylation damage as a consequence of containing a defective G•T mismatch binding protein (Aquilina et al., 1994).

To conclude, indications exist for CHO Clone B cells to be hMSH2 deficient and CHO Clone B cells have been proven to be defective in G•T mismatch binding. Therefore CHO Clone B cells, in view of previous observations made in human colon and prostate

cancer cells would be expected to be more resistant to BGIII21 than the parental CHO cells. Instead, CHO Clone B cells display an increased sensitivity to BGIII21.

Studies by Mello *et al.* have shown that hMSH2 recognises and specifically binds DNA, containing cisplatin adducts *in vitro* (Mello *et al.*, 1996). Two mechanisms for the involvement of MMR in the modulation of chemosensitivity to cisplatin exist. First, recognition and binding of ciplatin-modified bases by *hMSH2*, followed by the recruitment of additional MMR proteins would result in misdirected repair attempts at the sites of cisplatin damage. Futile rounds of MMR lead to an accumulation of double strand breaks resulting in signal for apoptosis (Mello *et al.*, 1996).

Secondly it has been proposed that the elevated levels of *hMSH2* found particular in ovarian and testicular tissue aid to shield cisplatin adducts from nucleotide excision repair (Mello *et al.*, 1996). Therefore an *hMSH2* deficiency in CHO Clone B cell would either be expected to result in tolerance of cisplatin adducts due to lack of recognition and repair or an increased sensitivity to cisplatin following the loss of the protective mechanism.

To draw any comparisons between results seen within the human colon and prostate cancer cell lines and MMR-deficient CHO cells, MMR proficiency would need to be restored within the MMR-deficient human colon and prostate cells in order to investigate any alterations in chemosensitivity in response to BGIII21. In addition, the relative levels of MMR protein expression would need to be analysed to eliminate the possibility of differential protein expression having an effect on chemosensitivity in response to BGIII21. However, species- and tissue-related differences in gene expression continue to persist and need to be taken into account. Hence, results obtained from the preliminary screening of the human colon and prostate cancer cells should rather be taken as an suggestion into potential repair mechanisms involved and provide an indication for further research required to be carried out in CHO cell lines. Further investigations into the involvement of MMR in the removal of BGIII21 lesions require the full characterisation of MMR-deficiencies in the CHO Clone B cell line as well as establishing CHO cell lines covering a range of MMR protein deficiencies.

In conclusion, it was found that BGIII21 specific DNA damage was produced within HT1080 Neo and CHO-AA8 cell lines and was not repaired by NER or homologous recombination repair pathways. Results indicate that MMR, in particular the MutSα and

MutSβ complexes, is involved in the removal of BGIII21 specific DNA damage in human prostate and colon cancer cell lines. However, the above results could not be verified within the CHO cell line.

Finally, a proposed model for the mechanism involved in the repair of DNA damage produced by alkylating agents suggests the persisting DNA lesions to initiate futile rounds of mismatch repair where the DNA polymerase attempts to match the alkylation site with a complementary nucleotide resulting in an imperfect base pair. The MutSα complex of the mismatch repair machinery detects the mismatch followed by the DNA polymerase failing to complement the alkylation site once more. Repair is re-initiated resulting in futile rounds of replication and repair. It has been suggested that these rounds of 'futile repair' result in a signal to the apoptotic machinery to initiate programmed cell death in a p53-independent manner (Hickman et al., 1999; Jiricny, 1998).

In contrast, a second model proposes the alkylation site in the template strand to bring about chain termination and dissociation of the DNA polymerase followed by continuation of DNA synthesis behind the damage. The resulting single strand gap opposite the alkylation site causes a double strand break during the following cycle of DNA replication (Jiricny, 1998). In MMR deficient cells absence of DNA damage recognition and repair results in the persistence of alkylated base damage causing alkylation tolerance.

The mismatch repair complex involved in mismatch recognition and apoptotic signalling pathway, with respect to the methylating agent MNNG appear to be the MutSα (Hickman et al., 1999). However, cisplatin-induced growth inhibition in HCT-116 cells was found to be dependent on MutSα or MutSβ in combination with functional MutLα (Aebi *et al.*, 1997).

In addition, exogenous damage is usually removed more rapidly from the transcribed strands than from non-transcribed strands of active genes. MMR proteins in connection with NER proteins have been found to participate in the removal of DNA damage from the transcribed strand (Peltomaeki, 2001). This combination repair system might explain the suggested involvement of transcription-coupled repair in the removal of BGIII21 adducts from transcribed strands.

5. E2F-1 INHIBITION AND CHEMOSENSITIVITY

5.1 Introduction

5.1.1 Peptides as therapeutic agents

There has been sustained interest in the development and application of synthetic or organic peptides able to interfere with protein components of important biological pathways. These peptides have the potential to inhibit the biochemical activities of a target protein, are able to delineate the target protein interactions within a biological pathway and present a novel approach for the discovery of potential therapeutic targets. New therapeutic approaches include the application of peptides as a treatment for infectious diseases, immune system disorders, cardiovascular disease, neurological disorders and cancer (Lauta, 2000).

The majority of synthetic peptides are produced via solid phase synthesis (up to 50 residues) or recombinant DNA technology (more than 50 residues). In order to achieve optimum levels of peptide activity for therapeutic applications structural modifications are carried out including formulation, glycosylation and disulphide bond formation. The post-synthetic assessment of the chemical and physical properties of the peptide includes the structural analysis, solubility, dimensions, antigenicity and immunogenic properties to ensure effective biological activity. Size and structure of a peptide influences stability and degradation of the peptide. For example, small linear peptides with no structural modifications are rapidly degraded having a half-life of 2-5 minutes. In contrast, larger modified peptides are more stable with a half-life of 1-2 hours (Lauta, 2000).

Initial selection of peptides with specific inhibitory functions may be accomplished with the use of a counter-selectable yeast two-hybrid system called 'reverse two-hybrid system'. This system is based upon the interaction of two known binding partners whereby binding results in the activation of a negative selectable marker. Negative selection is avoided through the inhibitory action of a third component. This system provides information about the interaction between two known binding partners and helps to identify molecules able to disrupt a given protein-protein interaction (Hoppe-Seyler *et al.*, 2001).

In contrast, the peptide aptamer system allows selection of peptides on the basis of their ability to bind to a given target protein. The selected peptides are further evaluated for

their inhibitory effect on the activity and binding of the target protein to its interaction partner. For the selection of inhibitory aptamers neither the structure of the target protein nor the identity of the binding partner are required (Hoppe-Seyler *et al.*, 2001). The peptide aptamer system has been proven successful in the elucidation of novel components within regulatory pathways and functional studies of known regulatory proteins *in vitro* and *in vivo*.

As an example, Cohen *et al.* isolated a peptide that bound CDK2 and inhibited its associated kinase. Inhibition of CDK2 was competitive and prevented progression through G1 phase of the cell cycle by interrupting the activity of CDK2 on substrates required for G1-S phase progression (Cohen *et al.*, 1998).

Another study showed the expression of two peptides to cause substrate specific inhibition of essential cyclin-dependent kinases DmCDK1 and DmCDK2 in *Drosophila melanogaster*. Simultaneous inhibition of DmCDK1 and DmCDK2 during eye morphogenesis resulted in a 'rough' eye phenotype due to disruption of normal eye development as a result of cell cycle inhibition. Subsequent overexpression of both cyclin-dependent kinases alleviated the inhibitory function of the peptides as observed by the development of wild-type eyes (Kolonin *et al.*, 1998).

5.1.2 E2F inhibition by peptides

Peptides were generated to inhibit E2F, a transcription factor controlling the transition from G1 to S phase of the cell cycle. The inhibitory peptides were isolated using a yeast two-hybrid assay. Two selected peptides (Apt4 and Apt5) were shown to inhibit E2F/DP1 heterodimerisation *in vitro* and blocked cell cycle progression of synchronised primary human fibroblasts from G1 to S phase *in vivo*. A third modified peptide (Pept5) inhibited E2F/DP1 heterodimerisation with an increased efficiency. Further, Pept5 abolished the formation E2F-pocket protein complexes as detected by EMSA analysis, reduced transactivation of an E2F-responsive promoter and prevented human fibroblasts microinjected with Pept5 from re-entering S phase. Mutation analysis suggested that E2F inhibitory peptides compete with DP1 by binding to E2F within the region of the DP1 heterodimersation domain therefore preventing the formation of transcriptionally active E2F/DP heterodimers (Fabbrizio *et al.*, 1999).

In an earlier study, Bandara *et al.* isolated E2F-1 inhibitory peptides H and H2 which inhibited the DNA binding activity of E2F-1 in F9 embryonal carcinoma cell extracts. DNA binding analysis of an H2 peptide containing two mutated residues within the DEF box domain suggested the DEF domain to be necessary for effective heterodimerisation of E2F-1 and DP-1. Cells treated with penetratin tagged H2 exhibited a change in cellular morphology indicative of programmed cell death while treatment with tagged peptides mutated within the DEF domain or containing a scrambled sequence of residues resulted in a lack of apoptosis. Finally, to assess the transcriptional activity of the cyclin A promoter regulated through a repressing E2F site, U20S cells were treated with H2 resulting in a significant increase in promoter activity and cyclin A expression (Bandara *et al.*, 1997).

5.1.3 Chapter aims

A concise strategy for the development of E2F-1 antagonists as part of a potential therapy for the treatment of diseases such as cancer is shown in **Figure 5.1**. In a first step, novel E2F/DP1 antagonists are obtained in high throughput E2F/DP-1 activity assays, followed by analysis of peptide activity in mammalian cell-based activity assays. Peptides exhibiting potential anti-proliferative effects are selected and further evaluated using mouse-based progression assays. Peptides resulting in a significant reduction of tumour or interference with the tumour growth are further selected to partake in clinical evaluations.

Following the results obtained by Bandara *et al.*, this project was intended to evaluate the use of peptides for the treatment of uncontrolled cell proliferation as a result of deregulated expression of E2F-1. Experiments focused on the analysis of peptide activity in mammalian cell-based assays. As the results by Bandara *et al.* suggested the activity of the E2F-1 inhibiting peptide (H2) promoted apoptotic cell death as part of the cellular response to E2F-1 inhibition by the H2 peptide, the aim was

- to investigate the application of the E2F-1 inhibitory peptides in a variety of established cancer cell lines in order to examine the relationship between tissue specific E2F-1 expression and inhibitory activity of the peptide.
- to investigate the potential treatment advantages of combining the inhibitory peptide with a variety of cell cycle specific and non-specific anti-cancer agents. This

included an examination of the effect the inhibitory peptide has on the cell cycle distribution of various cancer cell lines.
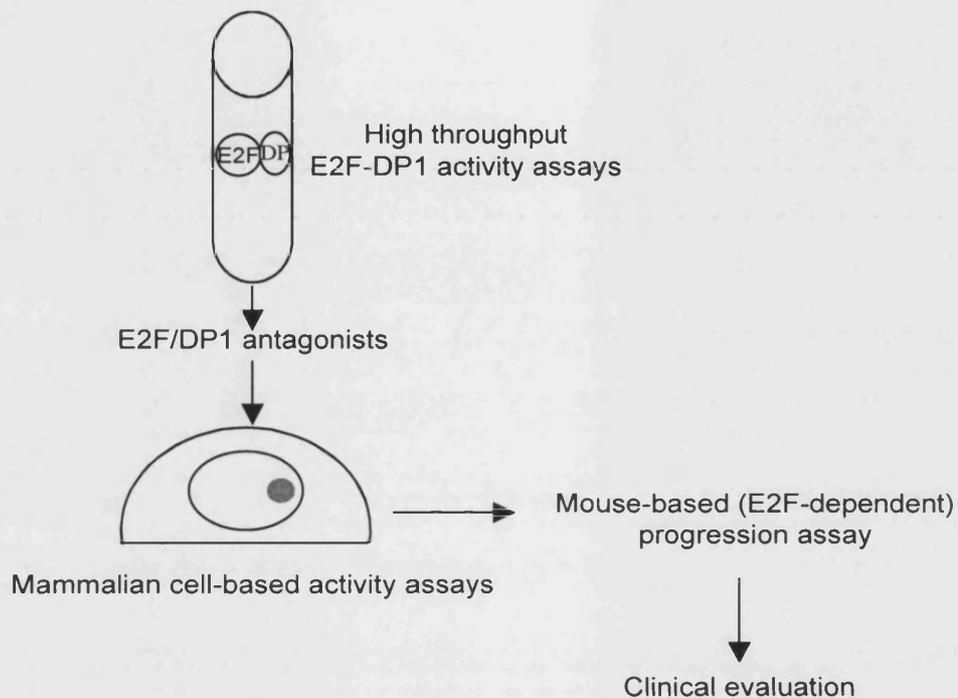
Fig. 5.1: Strategy for the development of novel small peptide therapeutics for the treatment of proliferative diseases. For details refer to text.

5.2 Materials and Methods

5.2.1 E2F inhibitory peptides AH2 and D611

E2F-1 inhibiting peptides were supplied by Prolifix, 91, Milton Park, Abingdon, Oxon, UK and G. Bloomberg, Dept. Biochemistry, Medical School, University of Bristol, UK (**table 5.1**).

173

Name (structure)	Amino acid sequence	Function
AH2 (linear)	RQIKIWFQNRRMKWKK-RRRVYDALNVLMAMNIISK	Prevents heterodimer formation between E2F and DP subunit
AHS2	RQIKIWFQNRRMKWKK-DRVKAVRNLMIASYRNMLI	Control to AH2
D611(branched)	not available	Prevents heterodimer formation between E2F and DP subunit
Mut	not available	Control to D611

Table 5.1: E2F inhibiting peptides

Underlined sequence represents the penetratin subunit of the peptide required for cell entry.

Peptides were dissolved in double distilled water (ddH_2O) to give a 1mM stock solution and were stored at $-80°C$ until further use. Subsequent serial dilutions were made in complete growth medium.

Lack of solubility of the peptides was encountered, particularly with respect to the peptides supplied by G. Bloomberg, Bristol. In order to increase the solubility of the peptides, DMSO (up to 10%) were added. Control experiments showed the percentage of DMSO to have no effect on cell viability when used.

5.2.2 Experimental cell lines

5.2.2.1 HT1080 and derivatives HT1080 Neo, 'E2F1-1' (CHO) and 'E2F 1-6' (CHO)

As experimental investigations for projects described in chapter 3 and 5 were performed simultaneously, the results concerning the CHO identity of 'HT1080 E2F1-1' and 'HT1080 E2F 1-6 ' cells influenced results within the following investigation. However, certain data obtained from preliminary experiments was included in the results section of this chapter. HT1080 Neo and 'HT1080 E2F1-1' cell lines were propagated as previously described in section 3.2.1.1.

5.2.2.2 MCF-7

Confluent cultures of the human breast cancer cell line (Soule *et al.*, 1973) were seeded 2-
4×10^4 cells/cm^2 according to ECACC

5.2.2.3 Human suspension cell lines

All suspension cell lines were maintained in RPMI 1640 medium supplemented with 10%
FCS and 2mM glutamine. Suspension cell lines included HL60 (Fontana *et al.*, 1980),
Jurkat (Weiss *et al.*, 1984), K562 (Andersson *et al.*, 1979) and U937 (Sundstrom *et al.*,
1976). HL60 and K562 cultures were maintained at a concentration between 1-5×10^5
cell/ml (ECACC). Jurkat and U937 were maintained at concentrations of 3-9×10^6 cells/ml
and 2-9x106 cells/ml, respectively (ECACC).

5.3 Results

5.3.1 Correlation between inhibitory peptide activity and endogenous level of E2F-1

In an investigation to establish a potential relationship between the level of endogenous
E2F-1 expression and the inhibitory effect of the inhibitory peptides, the HT1080 Neo and
identified CHO cell lines 'HT1080 E2F1-1' and 'HT1080 E2F1-6' were treated with
increasing doses of AH2 and D611 peptide. The data regarding both CHO cell lines is
included in this chapter as a higher E2F-1 expression level was observed in the CHO cells
compared to HT1080 Neo and these experiments were performed prior to full
characterisation of the E2F-1 overexpressing cell lines (section 3.3.2).

Figure 5.2 shows representative experiments for HT1080 Neo, 'E2F 1-1' (CHO)
and 'E2F 1-6' (CHO) cell lines treated with either inhibitory peptide AH2 or D611 for 72
hours. Each experiment included the respective control peptides. HT1080 Neo cells
exhibited an increased sensitivity to AH2 compared to either 'E2F1-1' (CHO) or 'E2F1-6'
(CHO). At 15µM AH2, cell proliferation was inhibited by 30% in HT1080 Neo while 90%
of 'E2F1-1' (CHO) and 'E2F1-6' (CHO) cells continued to proliferate in response to
treatment with AH2. A unreduced level of cell proliferation was observed with respect to
the AHS2 control peptide in all three cell lines.
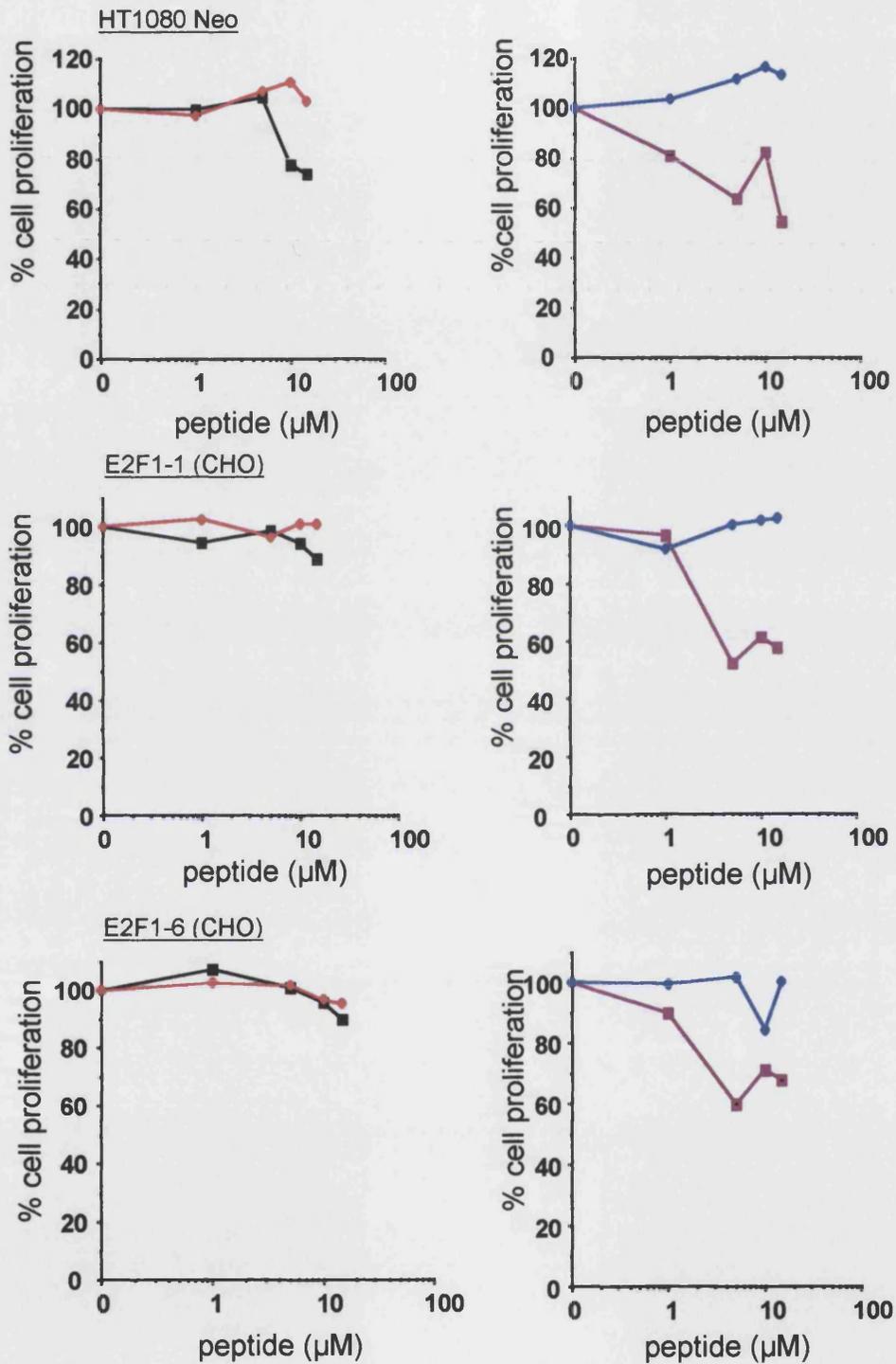
Fig. 5.2: Inhibition of proliferation by E2F-1 inhibitory peptides on HT1080 Neo, 'E2F1-1' (CHO) and 'E2F1-6' (CHO) cells as measured by representative SRB growth inhibition assays. Exposure to peptides was continuous (72 hours).━■━ AH2; ━●━ AHS2; ━■━ D611; ━◆━ Mut

Following 72 hours exposure to D611, a 45% inhibition of cell proliferation was observed for HT1080 Neo at 15μM D611 whilst inhibition of cell proliferation for 'E2F1-1' (CHO) and 'E2F1-6' (CHO) was highest at 5μM D611 with 48% and 40%, respectively. The values for inhibition of cell proliferation at 10 and 15μM D611 in 'E2F1-1' (CHO) and E2F1-6' (CHO) suggested the D611 activity to have reached its peak and no further increase in activity at higher peptide concentrations occurs.

The data indicated that an increased level of E2F-1 expression results in a decrease in inhibition of cell proliferation following AH2 treatment, as a consequence of E2F-1 being in excess compared to the AH2 inhibitory peptide. In contrast, treatment with D611 caused a reduction in cell proliferation across the spectrum of cell lines. HT1080 Neo cells showed a more progressive reduction in cell proliferation whilst a 100% cell proliferation of 'E2F1-1' (CHO) and 'E2F1-6' (CHO) cells was maintained up to 1μM D611 followed by a decrease in cell proliferation with increasing concentration of peptide to a level seen in HT1080 Neo cells. In conclusion, inhibitory activity of AH2 and D611 was suggested to be dependent on the endogenous level of E2F-1 expression within cells. D611 inhibitory activity in cells with an elevated level of endogenous E2F-1 appears most effective between 1 and 5μM concentration.

5.3.2 Effect on cell proliferation in response to combined peptide/drug treatment

To evaluate the potential use of the inhibitory peptides in combination with chemotherapeutic agents, HT1080 Neo and 'E2F1-1' (CHO) cells were treated with 1 or 10μM AH2 individually and in combination with 1 or 10μM BGIII21. BGIII21 is a novel minor groove binding alkylating agent that had been shown to produce sequence specific DNA damage in HT1080 as well as CHO cells (section 3.3.10 and 4.3.2). 'E2F1-1' (CHO) cells had previously exhibited a marked resistance to BGIII21 which was shown to occur independently of E2F-1 overexpression and was suggested to be a consequence of an underlying mismatch repair deficiency. For all drug/peptide combination experiments results were analysed according to the following criteria.

- Additive - an additive effect was defined as the observed combined decrease in cell proliferation of individual treatments following combination treatment.

- More than additive - a more than additive effect was considered a decrease in cell proliferation in excess of the expected additive effect.

As the majority of experiments presented in this chapter are representative data, a more than additive decrease in cell proliferation following combined treatment was defined as a ≥10% decrease in cell proliferation in addition to the additive effect to account for variation seen in repeat experiments. The variations seen within experiments and experimental series were considered to be results of differences in activity encountered and were suggested to be a consequence of using different peptide batches, differences in length of storage of peptides with the result of loss of inhibitory activity of peptide and marked variations with respect to the solubility of the peptides from separate suppliers.

Representative results of combination experiments showed in response to the combined treatment of HT1080 Neo cells with 10μM AH2 and 1μM BGIII21 a more than additive increase in growth inhibition (26.5%) compared to AH2 (85.5%) and BGIII21 (46.5%) alone (**Fig. 5.3 A**). No such decrease in cell proliferation was found with respect to any of the other peptide/ drug treatment combinations. A more than additive decrease in cell proliferation was observed in response to the combined treatment of HT1080 Neo cells with 10μM AHS2 and 1μM BGIII21 (33.7%) relative to AHS2 (108%) and BGIII21 (41.8%) alone (**Fig. 5.3 B**). Again none of the other peptide/drug combination treatments exhibited a pronounced decrease in cell proliferation in comparison to the inhibitory effect observed for individual peptide or drug treatments.

In contrast, 'E2F1-1' (CHO) cells exhibited a more than additive decrease in cell proliferation in response to all combination treatments with AH2 and BGIII21 (**Fig. 5.4 A**). The percentage of cell proliferation was found to be 96% and 100% for 10μM and 1μM AH2 respectively. Equally, values of 91.6% and 105.7% cell proliferation were determined for 10μM BGIII21 and 1μM respectively. A range of values between 66.7% to 82.9% was obtained for all four peptide/drug combination treatments.

Evaluation of the data obtained after combined treatment of 'E2F1-1' (CHO) cells with AHS2 and BGIII21, showed a more than additive decrease in cell proliferation across all combinations as observed with AH2 before (**Fig. 5.4 B**). Therefore, inhibitory or control
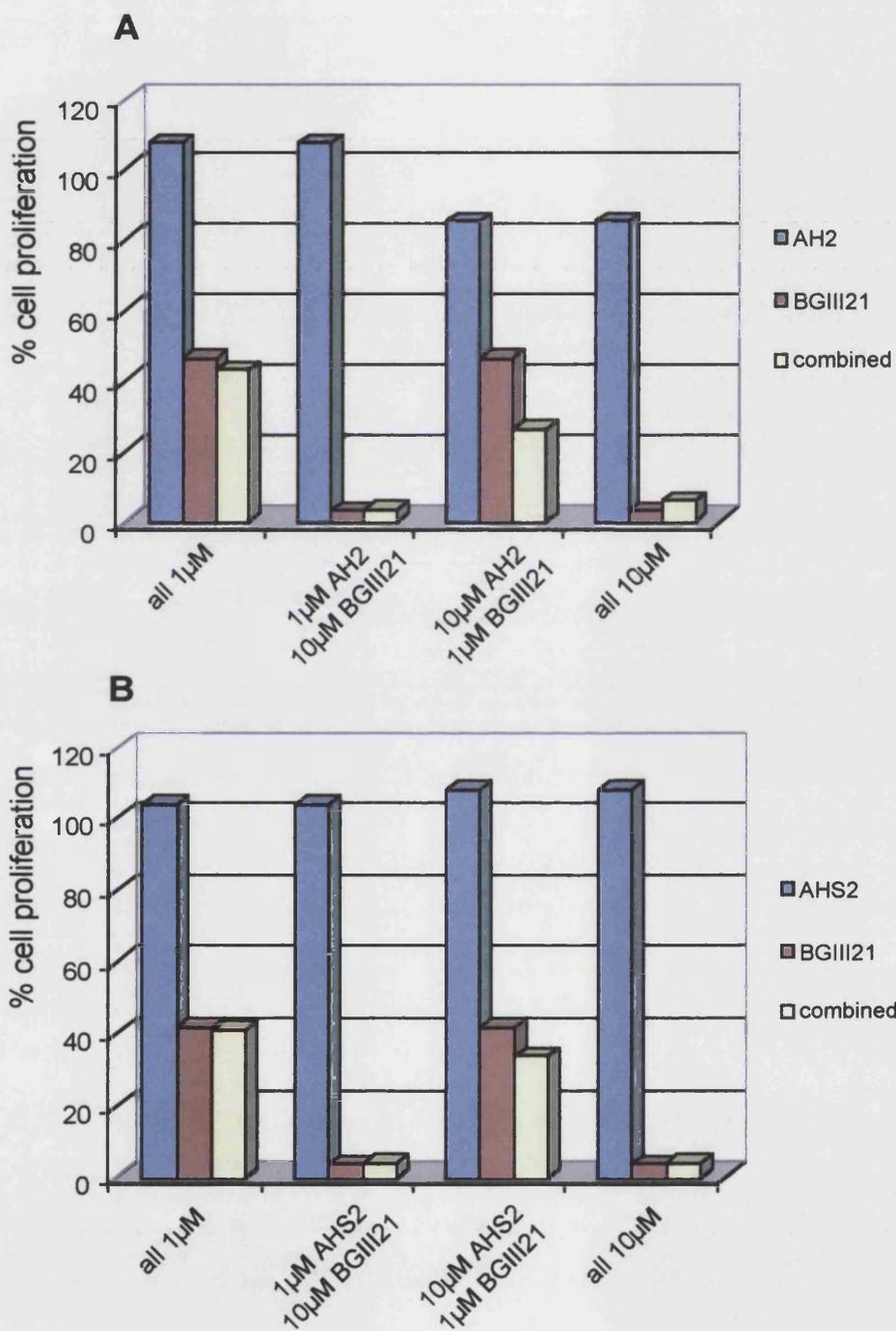
Fig. 5.3: Representative drug/ peptide combination assay to show individual and combined effects of BGIII21 and E2F-1 inhibiting peptide on HT1080 Neo cells. Cells were incubated with peptide and BGIII21 separately or in combination for 72 hrs.

179
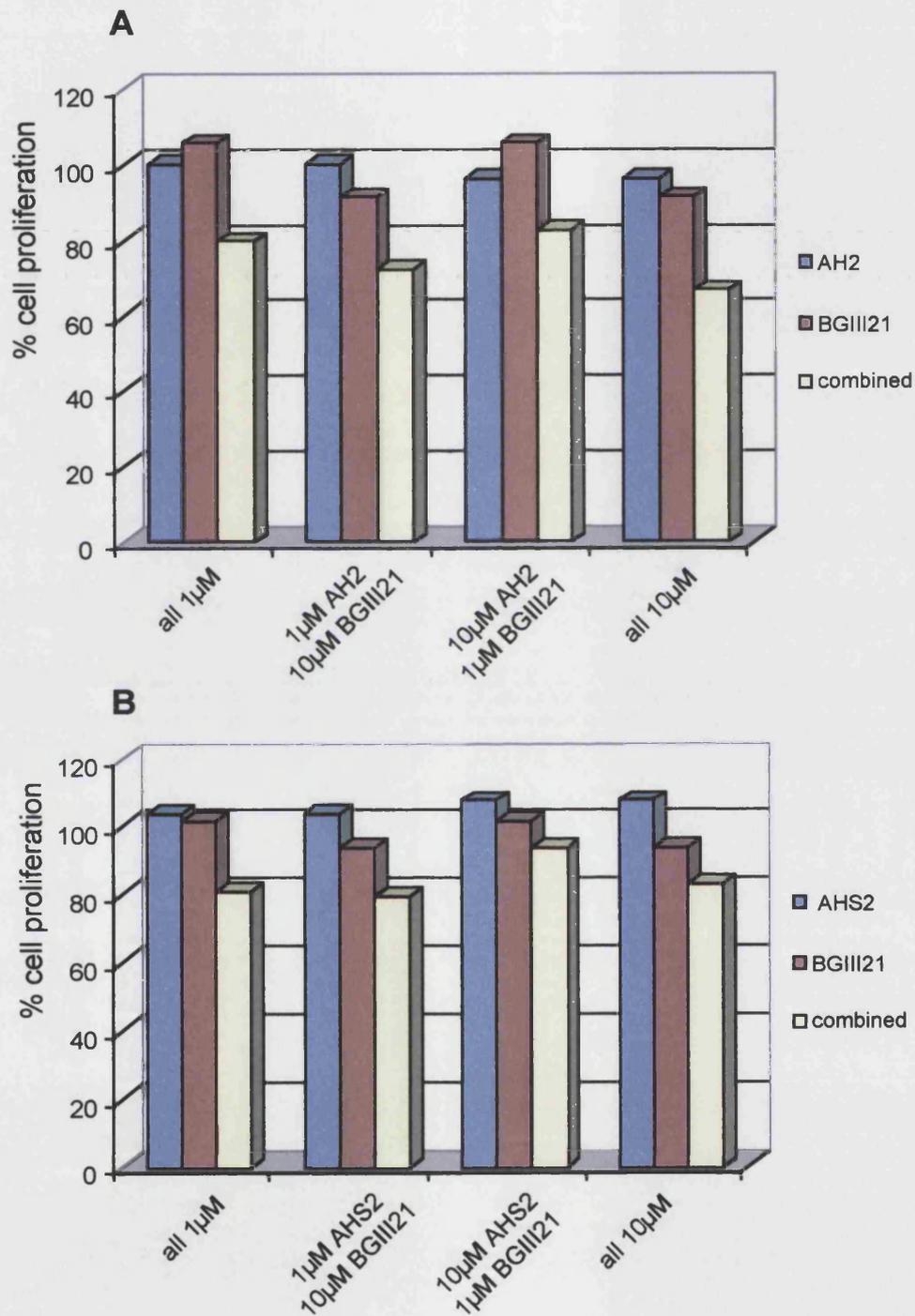
Fig. 5.4: Representative drug/ peptide combination assay to show individual and combined effects of BGIII21 and E2F-1 inhibiting peptide on 'E2F 1-1' (CHO) cells. Cells were incubated with peptide and BGIII21 separately or in combination for 72 hrs.

peptide plus drug in combination were suggested to work together to achieve a decrease in percentage of cell proliferation not seen with peptide or drug individually.

5.3.3 Increased sensitivity of MCF-7 cells to inhibitory peptides

An aim of this study was to evaluate the effect of the inhibitory peptides on a variety of cancer cell lines. To this end, MCF-7 cells were exposed to increasing doses of AH2 and D611 for 72 hours. **Figure 5.5** shows an observed increase in sensitivity in response to both peptides. At 15 μM AH2 a 38% decrease in the percentage of cell proliferation with regard to MCF-7 cells was detected. In contrast, a 20% decrease in the percentage of cell proliferation was observed in response to 15μM D611. To conclude, MCF-7 cells were found to be more sensitive to AH2 than D611 following continuous exposure. This stands in contrast to results previously obtained for HT1080 Neo and 'E2F1-1' (CHO) cells.

5.3.4 Effect on cell proliferation in response to combined peptide/drug treatment

Following the finding of increased sensitivity of MCF-7 cells to AH2, a number of peptide/drug treatment combinations were investigated. The drugs selected were the novel minor groove binding alkylating agent BGIII21 and melphalan, a representative alkylating agent.

An additive decrease in cell proliferation was observed with regard to all AH2/BGIII21 combination treatments compared to individual peptide or drug treatments (**Fig. 5.6 A**). Combining 1μM AH2 (97.6%) and1μM BGIII21 (96.8%) gave a more than additive decrease (83.3%) in cell proliferation. In contrast, the combination of 1μM AH2 (97.6%) and 10μM BGIII21 (34.3%) resulted in an additive decrease in the percentage of cell proliferation (29.2%). Finally, the combination of 10μM AH2 (91.1%) and 1μM BGIII21 (96.8%) as well as 10μM AH2 (91.1%) and 10μM BGIII21 (34.3%) had a more than additive effect (80.8% and 16.1% respectively) on the percentage of cell proliferation.

A more than additive decrease (17.2%) in the percentage of cell proliferation occurred in response to the combination of 10μM AH2 (54.9%) and 1μM melphalan (74%) (**Fig. 5.6 B**). However, the combination of 1μM AH2 (93.8%) and 10μM melphalan (35%) as well as 10μM AH2 (54.9%) and 10μM melphalan (35%) resulted in a protective effect upon combination (55.8% and 26.2% respectively). Finally, the remaining combination
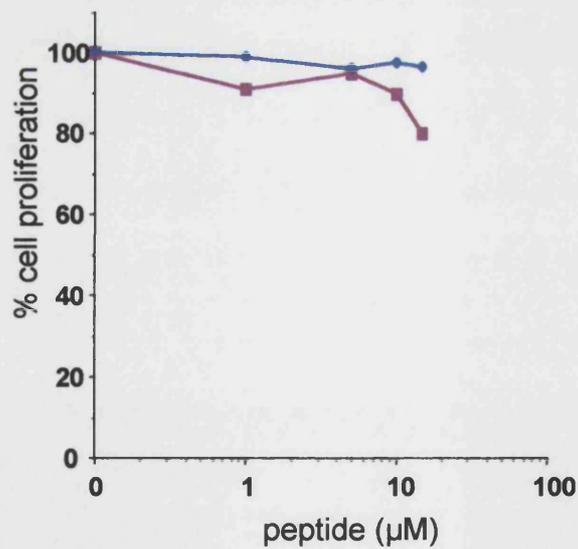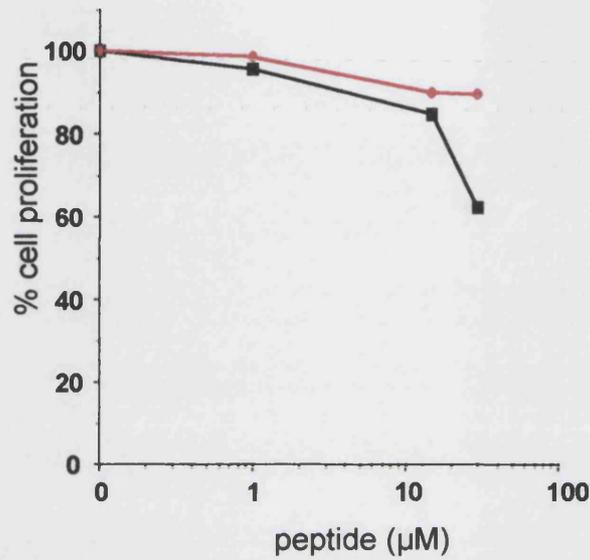
Fig. 5.5: Inhibition of proliferation by E2F-1 inhibiting peptides on MCF-7 cells as measured by representative continuous SRB growth inhibition assays. ■ AH2; ● AHS2; ■ D611; ● Mut
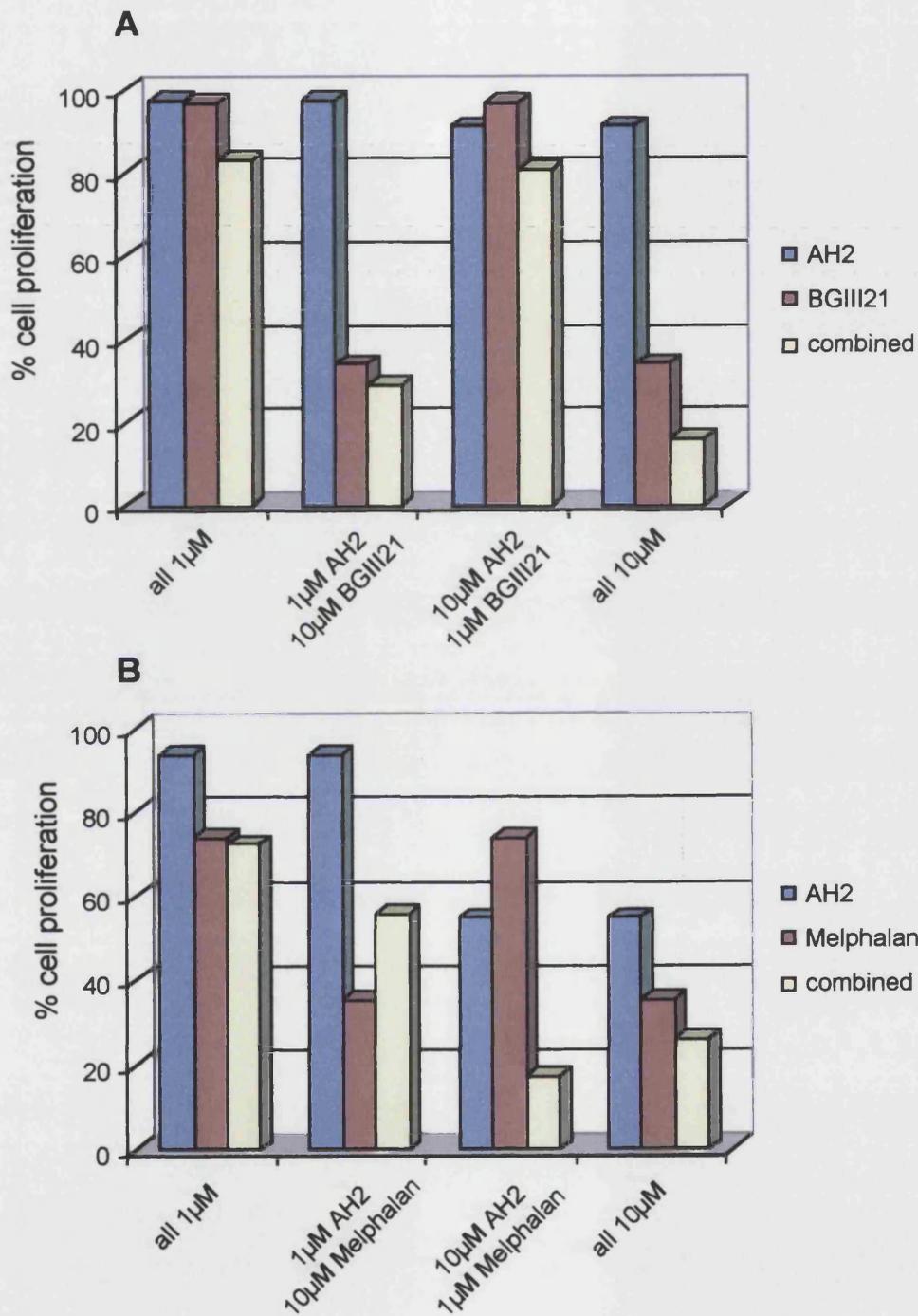
Fig. 5.6: Representative drug/ peptide combination assay to show individual and combined effects of BGIII21 or Melphalan and E2F-1 inhibiting peptide on MCF-7 cells. Cells were incubated with peptide and BGIII21 separately or in combination for 72 hrs.

treatment consisting of 1μM AH2 (93.8%) and 1μM melphalan (74%) produced no further decrease in cell proliferation (72.4%). To conclude, a more than additive reduction in the percentage of cell proliferation in MCF-7 cells resulted from the combination of 1μM AH2 and 1μM BGIII21 as well as 10μM AH2 and 1μM melphalan. However, no reproducible pattern emerged with respect to the effectiveness of each of the individual peptide/drug combinations.

5.3.5 Relative levels of endogenous E2F-1 expression in leukemic cell lines

Prior to investigating the effect of the inhibitory peptides on a number of leukemic cell lines, it was of importance to examine the relative level of endogenous E2F-1 expression in each of the cell lines. To this end, Western blot analysis (Method 2) was performed. **Figure 5.7** shows U937 to express the highest level of endogenous E2F-1. By comparison U937 was found to contain more E2F-1 than Jurkat. Both HL60 and K562 exhibited an almost 10fold lower level of endogenous E2F-1 expression.

To complement the above result, the doubling times for the leukemic cell lines were measured as described in section 2.1.3.3 **(table 5.2)**. The results show that none of the doubling times for HL60, K562 and U937 were differed markedly from each other. Therefore, there was no direct correlation between the amount of E2F-1 expressed and the time required for cells to traverse the cell cycle.

Cell line	Doubling time (hours)
HL60	36
Jurkat	N/A
K562	45
U937	41

Table 5.2: Doubling times for established leukemic cell lines

HL60 Jurkat K562 U937
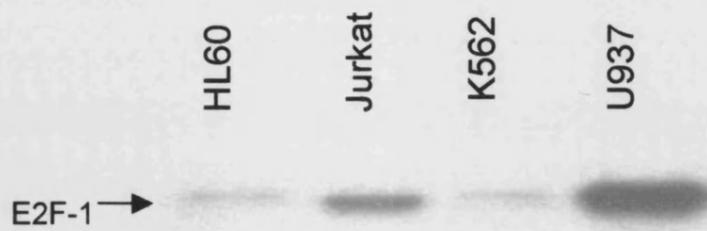
E2F-1 →

Fig. 5.7: Relative level of endogenous E2F-1 expression in leukemic cell lines as determined by Western blot analysis. Correct size of E2F-1 protein band was confirmed with Kaleidoscope pre-stained standard size marker. Equal loading was verified by staining blot with Coomassie blue. Levels of protein loading are not shown as staining of pre-selected reference bands was too weak.

5.3.6 Correlation between inhibitory peptide activity and endogenous E2F-1 expression in leukemic cell lines

Leukemic cancer cell lines were selected in order to examine the effect of the AH2 and D611 inhibitory peptides on cell proliferation and cell cycle distribution. The choice of a leukemic cell system was based on an anticipated clinical application of the peptide and reports suggesting a 100% bioavailability of peptide to target cells following intravenous injection (Lauta, 2000). The high percentage of bioavailability within the bloodstream could lead to a high degree of peptide activity at individual target sites throughout the body. In addition, the intravenous route offers a relatively easy way of introducing the peptides to the body.

Following continuous incubation, the HL60 cell line was found to be equally sensitive to both, the AH2 (IC_{50} = 3.9μM) and D611 (IC_{50} = 4.3μM) inhibitory peptide in a representative experiment (**Fig. 5.8**). However, an increased sensitivity in response to the control peptide AHS2 (IC_{50} = 16.5μM) was also noted. In contrast, a 10% decrease in cell proliferation was detected following exposure to 15μM Mut control peptide.

K562 cells were less sensitive to AH2 (IC_{50} = 16μM) compared to HL60 but were found to be equally as sensitive to AHS2 (IC_{50} = 19μM) as HL60 cells. Finally, Jurkat cells were more resistant to D611 (IC_{50} = >15μM) compared to HL60. All mean IC_{50}s were calculated from 3 or more experiments.

5.3.7 Apoptotic cell death in response to inhibitory peptides

Following the observation that an increased amount of endogenous E2F-1 in cells appears to lead to a more than additive decrease in cell viability in response to combined treatment an investigation into the effect of each individual treatment on the cell cycle profile was necessary. This would provide information to establish the most effective treatment routine with respect to timing of application and dose of peptide or drug.

In a representative experiment U937 and HL60 cells were treated continuously for 72 hours with 15μM of AH2 and D611 including the relevant control peptides. Samples were taken at 24, 48 and 72 hours and cell cycle analysis performed to determine the relative DNA content of the peptide treated cells. In **Figure 5.9** a continual increase in the percentage of apoptotic cells as depicted by the sub-G1 phase was observed following
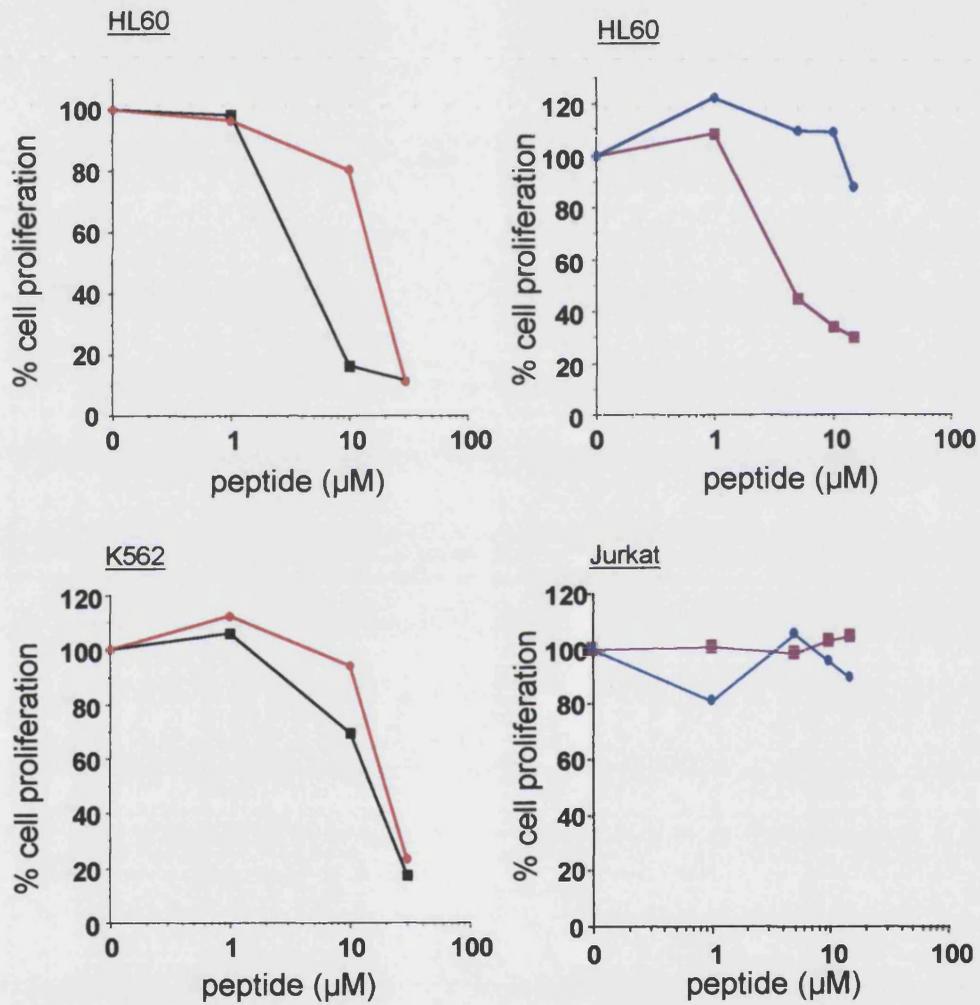
Fig. 5.8: Inhibition of proliferation by E2F-1 inhibiting peptides on a variety of leukemic cell lines as measured by representative continuous MTT cell survival assays.

■— AH2; ●— AHS2; ■— D611; ●— Mut

24 hours

48 hours
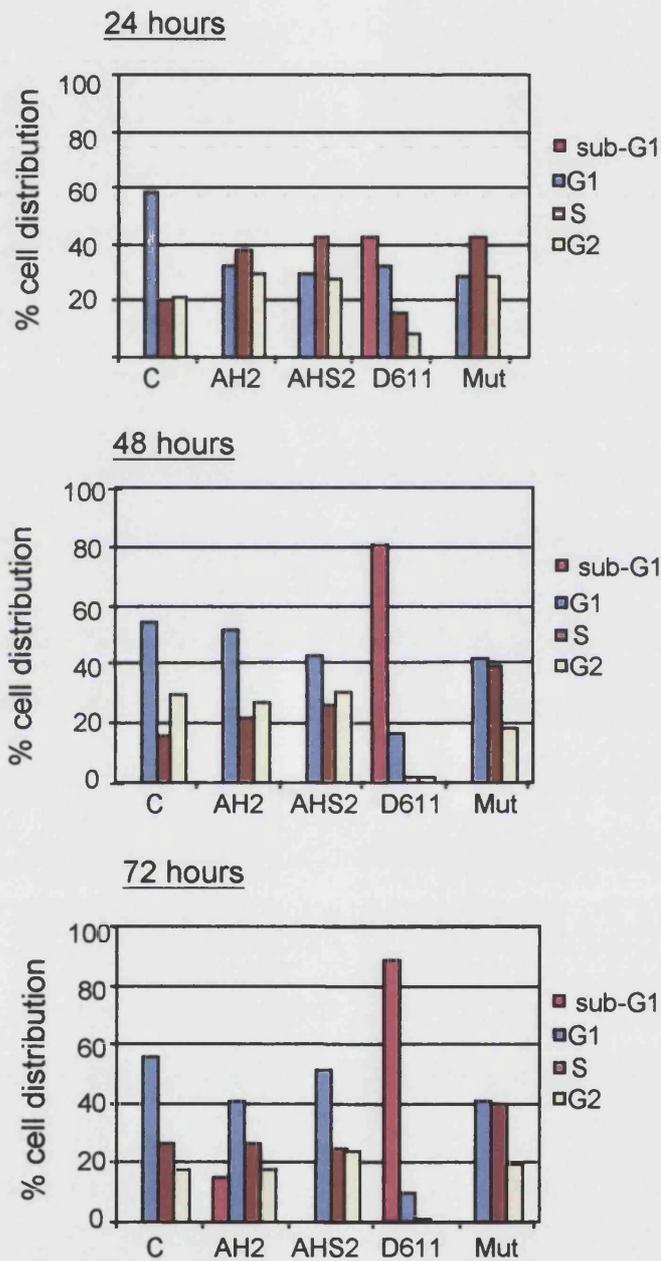
72 hours

Fig. 5.9: Cell cycle profiles of U937 cells following incubation with 15μM E2F-1inhibiting peptides for 24, 48 or 72 hours as determined by FACS analysis. Sub-G1 phase (sub-G1) is indicative of apoptosis. G1 (G1 phase/2n); S (S phase/ 2-4n); G2 (G2 phase/ 4n)

188

exposure of U937 cells to D611. After 72 hours around 90% of D611 treated U937 cells had undergone apoptosis. By contrast, only 16% of U937 cells underwent apoptosis after treatment with 15μM AH2 for 72 hours. Neither AHS2 nor Mut appeared to affect the cell cycle distribution of U937 cells.

HL60 cells exhibited a G1 arrest after treatment with 15μM D611 for 48 hours (**Fig. 5.10**). The G1 arrest persisted throughout the remaining time-course. No effect of AH2 was observed on HL60 cells for the duration of the experiment. Treatment with the Mut control peptide for 24 hours provoked a decline in G1 phase with a concomitant increase in the percentage of cells in S phase. A similar pattern had been observed with respect to AH2, AHS2 and Mut treated U937 cells after 24 hours.

5.3.8 Effect of inhibitory peptides on cell proliferation of HL60 and K562

A new supply of peptide was obtained from G. Bloomberg, Dept. Biochemistry, University of Bristol, UK. The new AH2 and AHS2 peptides ordered were synthesised having the sequence of residues as listed in section 5.1.1. It was not possible to obtain any D611 or Mut peptides as information on the amino acid sequence was not available. Cell proliferation assays were performed to determine the inhibitory effect of the new batch of peptides on a selection of leukemic cell lines used during previous experiments. **Figure 5.11** shows all cell lines were sensitive to AH2 and AHS2. HL60 cells were found to be the most sensitive to AH2 and AHS2 with IC_{50} values of 4.1μM and 9.9μM respectively. A similar range of IC_{50} values was determined for Jurkat cells in response to AH2 (IC_{50} = 7.1μM) and AHS2 (IC_{50} = 13μM). By comparison K562 cells turned out to be least sensitive to AH2 (IC_{50} = 18μM) and AHS2 (IC_{50} = 23μM). All IC_{50} values are based on 3 or more experiments. As previously observed in section 5.3.6,

HL60 were found to be the most sensitive to AH2 and AHS2. However, HL60 appeared more sensitive to AHS2 compared to earlier results. K562 cells retained the level of sensitivity in response to AH2 and AHS2. No comparison was possible for Jurkat cells as these had been exposed to D611 and Mut rather than AH2 and AHS2 in previous experiments.
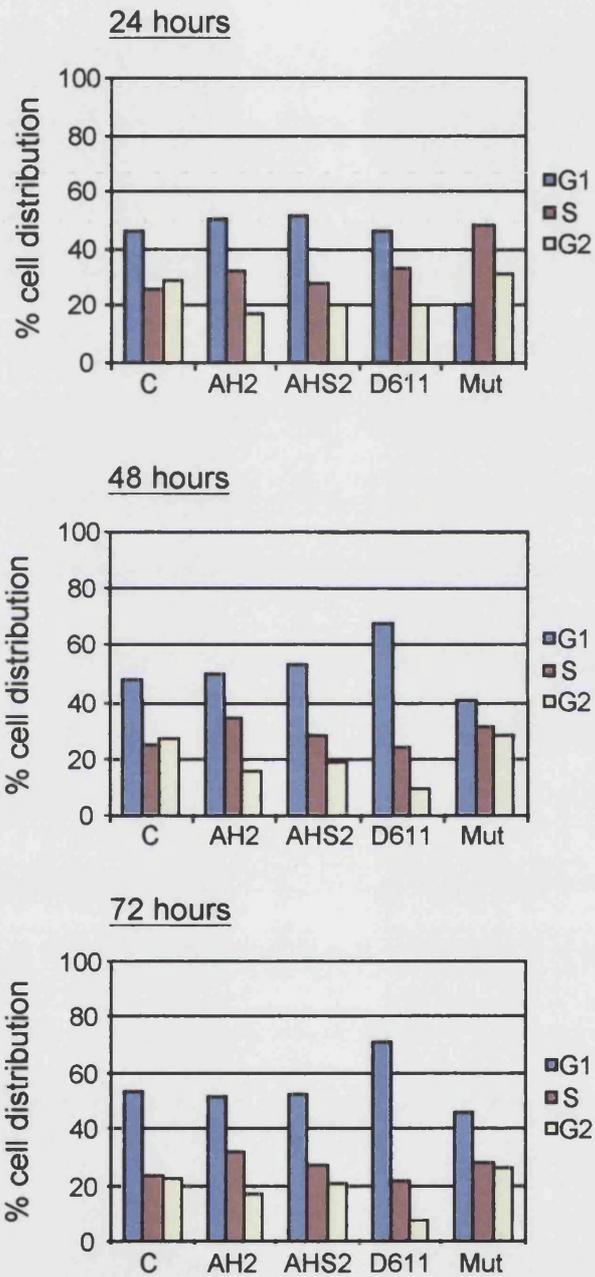
Fig. 5.10: Cell cycle profiles of HL60 cells following incubation with 15μM E2F-1inhibiting peptides for 24, 48 or 72 hours as determined by FACS analysis. Sub-G1 (sub-G1) phase is indicative of apoptosis. G1 (G1 phase/2n); S (S phase/ 2-4n); G2 (G2 phase/ 4n)
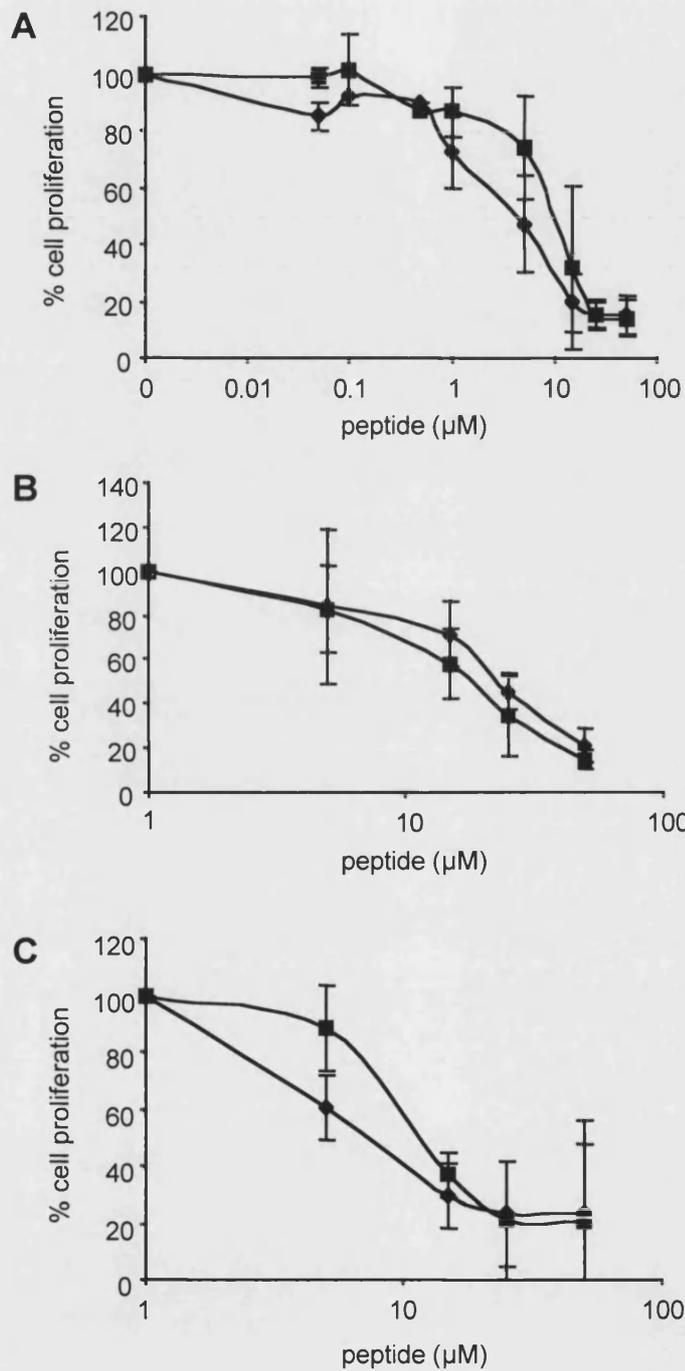
Fig. 5.11: Inhibition of proliferation by E2F-1 inhibiting peptide on A) HL60, B) K562 and C) Jurkat cell line as measured by representative continuous MTT survival assays. ⬥ AH2; ■ AHS2

5.3.9 G1 arrest in response to inhibitory peptide

To continue the ongoing investigation into the evaluation of the effects of peptide treatment on leukemic cell lines, HL60 and K562 were dosed with 10μM and 25μM AH2 or AHS2 for 24, 48 and 72 hours as described before (section 5.3.7). A G1 arrest was observed in HL60 cells after treatment with 25μM AH2 for 24 hours with a concomitant decrease in the percentage cells in G2 phase (**Fig 5.12 A**). The lack of G1 arrest after 24 hour long exposure to 10μM AH2 indicated the cell cycle alterations to be dose-dependent. The G1 arrest was maintained throughout the 48 and 72 hours samples suggesting that no peptide activity had been lost throughout the time-course or cells were unable to re-enter the cell cycle. No G1 arrest was detected in K562 cells following FACS analysis of the all time-course samples (**Fig. 5.12 B**).

5.4 Discussion

The development of peptides that interfere with specific proteins offers a number of novel opportunities to study specific protein functions *in vivo*, investigate interactions between protein components within biological pathways and aid the discovery of unknown binding partners of target proteins. In addition, novel peptides designed to inhibit the activity of proteins involved in cell proliferation such as CDK2 and E2F-1, provide a means to elucidate the molecular basis of diseases such as cancer as well as present a potential new type of therapy.

The aim of the above study was to evaluate the potential benefits associated with the treatment of cancer cells with E2F-1 inhibiting peptides. The active peptides chosen were AH2 and D611 for which only the amino acid sequence of the former is available. The AH2 peptide is linear in structure not containing any known post-synthetic modifications. AH2 is linked to a penetratin subunit derived from the third helix of the *Drosophila melanogaster* antennapedia homeodomain protein in order to ensure translocation across the cell membrane (Bandara *et al.*, 1997).

The respective control peptides for AH2 and D611 were AHS2 and Mut. Again, only the amino acid sequence of the former is available. AHS2 consists of the scrambled amino acid sequence of AH2 linked to a penetratin subunit.

A) HL60

B) K562
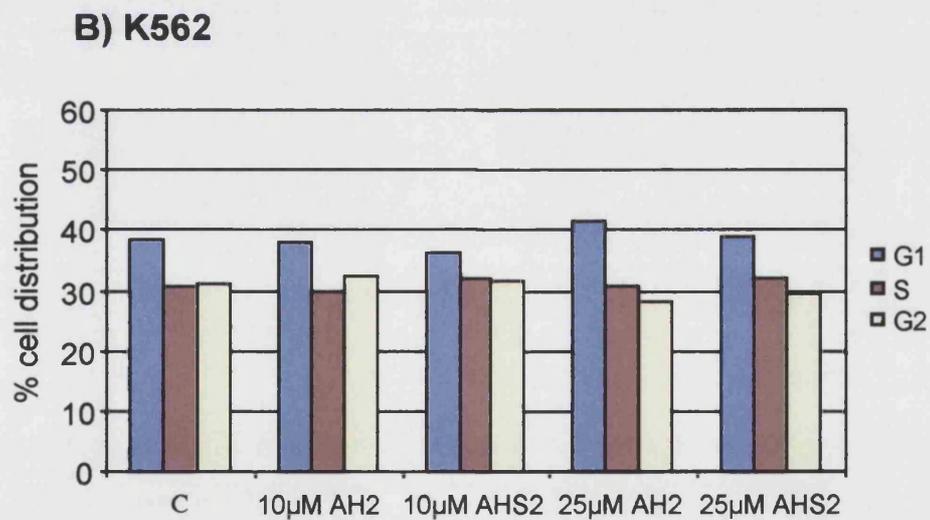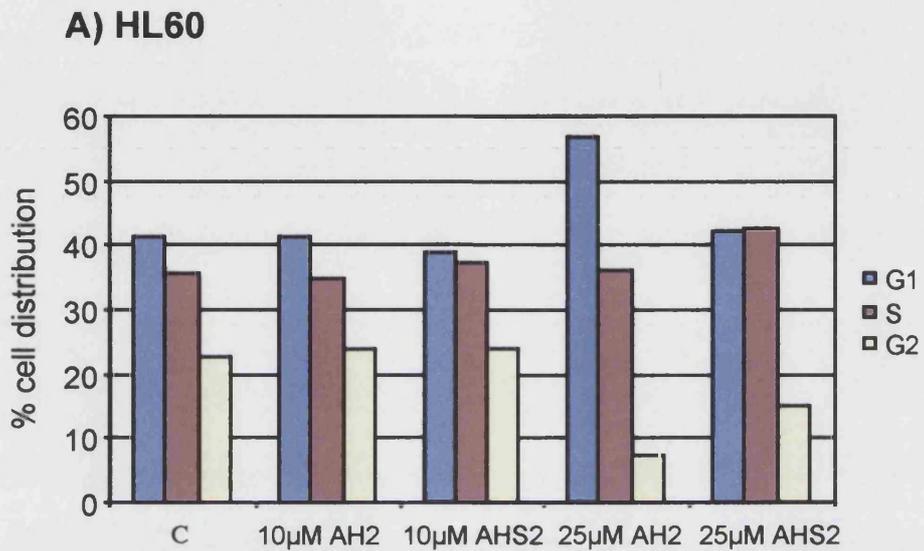
Fig. 5.12: Cell cycle analysis to show the effect of AH2 and AHS2 peptides on the cell cycle distribution of HL60 and K562 cells after 24 and 72 hours incubation, respectively.
G1 (G1 phase/ 2n); S (S phase/ 2-4n); G2 (G2 phase/ 4n)

193

5.4.1 Variations observed with respect to peptide activity

The majority of data presented in the results section were representative experiments of an experimental series as it proved difficult to obtain homogenous sets of data due to significant inter-experimental variation. However, despite inter-experimental variation, observed trends were preserved between individual experiments. As an example, in figure 5.8, HL60 dosed with AH2 and AHS2 showed an 80% decrease in cell proliferation at 10μM AH2 and a 17% decrease in response to AHS2. The experiment shown is representative as a result of marked variation in peptide activity observed (cell proliferation values ranged from 30% decrease to 100% decrease) when repeats were performed. Further experiments using a new peptide supply (G. Bloomberg, Bristol) showed persistent variations in peptide activity although to a lesser extent which allowed standard deviations to be included in the graphs (**Fig. 5.11A**). A possible explanation for the increased inter-experimental variation might be an inconsistent level of activity within peptide samples due to a number of factors such as:

5.4.1.1 Variation in peptide activity between batches

Peptides were supplied in 2-5 vials of 1mg or 2mg each by the manufacturer. In general, one or two vials were required for each experiment. Invariably a new peptide batch had to be ordered in order to complete an experimental series. As a result, variations observed within experimental series may be explained by differences in activity between different batches supplied by the manufacturer.

5.4.1.2 Progressive loss of activity following different length of storage periods

As experiments were not performed simultaneously but rather in sequence, variations in length of storage periods did occur and might have contributed to the differences in activity of peptide seen within experimental series. It may be speculated that peptide activity decreased with increasing length of storage in powder form and/or that peptide activity decreased with increasing length of storage once the peptide had been solubilised.

5.4.1.3 Variations in solubility of peptides

Further, marked differences in solubility were seen with respect to peptides supplied by the original manufacturer compared to peptides supplied by the second supplier (G. Bloomberg, Bristol). While peptide batches supplied by the manufacturer were on average soluble in distilled water with the occasional addition of DMSO, peptides supplied by G. Bloomberg always required additional DMSO in order to completely solubilise the peptides. The difference in solubility may have been a result of secondary structural modifications of the peptides by the manufacturer that were not indicated to the new supplier.

5.4.1.4 Structural modifications of peptides

Observed differences in activity and solubility of peptides supplied by the manufacturer and G. Bloomberg, Bristol were suggested to be a result of structural modifications of the peptides following initial amino acid chain synthesis. For example, the addition of disulphide bonds would increase the stability of the peptides and prolong their period of activity compared to unmodified peptides. As information on any potential modifications to the peptide structure was not available, any peptide supply from a secondary source contained unmodified peptides only.

5.4.1.5 Effect of growth state and cell cycle distribution of cells on peptide activity

Differences in passage number and growth states of individual cell lines could also provide an explanation for the differences in peptide activity seen within an experimental series. Possible improvements to the previous experimental set-ups might include the use of cells with the exact same passage number as well as FACS analysis to examine the cell cycle distribution of the cells used for the peptide experiment to ensure that the cell cycle distribution remains constant for each experimental repeat.

5.4.1.6 Interaction of peptides with components of cell culture medium

Although the peptides were dissolved in ddH_2O, preparation of further dilutions in serum containing medium and potential interaction of peptides with serum components could account for the variability in peptide activity observed.

5.4.2 Studies to investigate peptide activity

In addition to the studies into the activity of the E2F-1 inhibitory peptides carried out by Bandara *et al.*, further investigations should include experiments that observe any changes of mRNA and protein levels of selected E2F-1 target genes in response to peptide. Additional assays to investigate the levels of peptide activity are reporter assays that show the effect of peptide activity on gene expression (Bandara *et al.*, 1997).

Multi-protein complexes involved in regulatory processes and transcription including transcriptional activation and inactivation are associated with chromatin structure. Hence, protein-protein and DNA-protein interactions may be examined using the chromatin immunoprecipitation (CHIP) assay. Therefore the CHIP assay potentially provides a means of analysing the effect of inhibitory peptide action on E2F-1-protein (e.g. DP-1) interactions as well as E2F-1 DNA-binding. Finally, microarrays may be used to examine the gene expression levels of a wide range E2F-1 regulated genes in response to inhibitory peptide.

5.4.3 Discussion of representative experimental data and conclusion

The majority of experiments for the above investigation yielded representative data as a result of inter-experimental variations in peptide activity. Possible explanations for the differences in peptide activity seen are given in section 5.4.1.

The investigation to examine the relationship between inhibitory peptide activity and the level of endogenous E2F-1 expression, a direct correlation between E2F-1 protein expression and AH2 activity was observed. In contrast, the level of endogenous E2F-1 expression had no direct effect on the activity of D611. Instead, D611 inhibitory activity displayed the same trend with respect to all experimental cell lines. A levelling off in D611 activity was observed with increasing peptide concentrations in cells expressing high levels of E2F-1. The plateau in activity was suggested to be the result of D611 reaching its maximum level of protein-protein interaction and activity. Consequently, no further increase in E2F-1 inhibition is possible. No such plateau phase was detected in cells containing an overall lower level of E2F-1.

In HT1080 Neo cells, combination treatment with inhibitory peptide AH2 and BGIII21, resulted in an additive or more than additive inhibitory effect in three of the four peptide/drug combinations used. It was noted that 10μM AH2 appeared to protect a small fraction of HT1080 Neo cells from cell death after treatment with 10μM BGIII21 for 72 hours. Combining AHS2 and BGIII21 produced an additive decrease in cell proliferation for all four possible combinations.

By contrast, a consistent more than additive decrease in cell proliferation was observed for all four combination treatments in E2F1-1 (CHO) cells, presented as a further decrease in the percentage of cell proliferation in addition to the expected additive inhibitory effect. As **Figure 5.5** shows, neither AH2 nor BGIII21 alone caused a significant loss of cell proliferation. However, upon combination a marked loss in cell proliferation was observed. Simultaneous incubation of cells with peptide appeared to increase sensitivity of E2F-1 (CHO) cells towards BGIII21. Nevertheless no explanation for the underlying mechanism for this peptide " priming" of 'E2F1-1' (CHO) cells is given at this point in time.

A more than additive decrease in the percentage of cell proliferation of 'E2F 1-1' (CHO) was detected following two combinations of AHS2 and BGIII21. As AHS2 alone was shown to have no marked effect on cell proliferation in 'E2F1-1' (CHO) cells in the SRB growth inhibition studies (**Fig. 5.5 B**), the more than additive loss in cell proliferation was suggested to be a result of introducing exogenous peptide into cells. This hypothesis however does not hold true for the lack of combined effect observed in HT1080 Neo cells unless the differential response to the introduced peptide is based on tissue specificity.

A third cell system in the form of MCF-7 breast cancer cells was selected and initial SRB growth inhibition assays showed MCF-7 cells to be more sensitive to the same concentration of AH2 than D611. Continuous exposure to either control peptides did not result in a marked decrease in the percentage of cell proliferation. Following combination treatment with 1μM AH2 and BGIII21 an additional decrease in cell proliferation was observed to the expected additive inhibitory effect, indicating combined activity between AH2 and BGIII21. The remaining three peptide/drug combinations resulted in an additive or more than additive decrease in percentage cell proliferation. In comparison to 'E2F1-1' (CHO), MCF-7 cells were more sensitive to BGIII21 but not as sensitive as HT1080 Neo

cells. Levels of sensitivity towards both concentrations of AH2 were found to be within a close range of each other.

A suggested pattern emerged whereby sensitivity towards BGIII21 potentially led to loss of more than additive cell proliferation with respect to combination treatments. HT1080 Neo was most sensitive to BGIII21 but showed no more than additive sensitivity regarding peptide/drug combinations. In contrast, 'E2F1-1' (CHO) cells were least sensitive to BGIII21 but exhibited more than additive loss of cell proliferation with respect to each peptide/drug combination. MCF-7 cells showed an intermediate level of sensitivity with respect to BGIII21 and subsequent loss of cell proliferation was more than additive in the context of some but not all combination treatments. To conclude, a more than additive effect of peptide and drug treatment in combination appeared to be dependent on the level of sensitivity observed towards the drug alone within a particular cell system.

To investigate whether the above hypothesis was specific for BGIII21 alone or whether it applies to other drugs, MCF-7 cells were exposed to peptide/drug combinations including melphalan. MCF-7 cells were more sensitive to $1\mu M$ melphalan than $1\mu M$ BGIII21. Sensitivities to $10\mu M$ melphalan and $10\mu M$ BGIII21 were equal. A more than additive effect was observed as a result of combining $10\mu M$ AH2 and $1\mu M$ melphalan. However in contrast to previous data, exposure to $10\mu M$ AH2 resulted in a 50% decrease in cell proliferation therefore suggesting an enhancement of peptide inhibitory effect through additional drug rather than an increased sensitivity towards the drug through the presence of the peptide.

In addition, for the treatment combination of $1\mu M$ AH2 and $10\mu M$ melphalan, the combined result showed an increase in the percentage of cell proliferation compared to melphalan alone suggesting a protective effect. Overall, the above data for MCF-7 cells and combination treatment including melphalan remain inconclusive.

As part of the investigation to expose a range of different cancer cell lines to the inhibitory peptides alone or in combination with drugs, a number of leukemic cell lines were selected. Leukemic cell lines have the advantage of being suspension cell lines so that any promising discoveries within this study had the potential of being translated into the next phase of the therapeutic peptide development. Part of the development of any new anti-cancer agent is the consideration of how to best target the specific agent to the cancer

cells. In contrast to most localised solid tumours leukemic cells may be easily targeted via the intravenous route. In addition, 100% bioavailability of the peptide is accomplished as the peptide is just required to translocate across the cell membrane and does not need to cross any further endothelial or epithelial barriers to reach its target. The disadvantage of this system is that healthy as well as cancer cells will be targeted unless there is a way of discriminating the two and a substantially higher dose of peptide would be required as the peptide will be diluted upon application.

In a first step, the relative level of endogenous E2F-1 expression was examined and U937 cells were found to contain 3-5 fold more E2F-1 than Jurkat. Jurkat however expressed around 10 fold more E2F-1 than either HL60 or K562. Analysis of each individual cell lines doubling time revealed HL60 to be the fastest growing cell line (36 hours) and K562 the slowest (45 hours). The doubling time for Jurkat cells was not obtained. The doubling times of the leukemic cell lines did not correlate to the endogenous level of E2F-1 expression

Cell proliferation assays found HL60 cells to be equally as sensitive to AH2 and D611. However, whereby HL60 exhibited a low degree of sensitivity towards Mut, the precentage of cell proliferation was markedly decreased in response to AHS2. K562 cells were less sensitive to AH2 than HL60 but exhibited the same degree of loss of cell viability following treatment with AH2 or AHS2. No data for K562 cells treated with D611 was obtained. Further, no significant decrease in the precentage of cell proliferation was observed for Jurkat in response to D611. No data was obtained for Jurkat treated with AH2. In conclusion HL60 cells appeared to be most sensitive to either inhibitory peptide. It is possible to speculate that a faster cell doubling time might result in an increased sensitivity to the E2F-1 inhibiting peptides. However, a more comprehensive investigation is required to substantiate the above speculation.

Following the cell proliferation studies, an investigation into the effect of peptide treatment on the cell cycle profile of each cell line was carried out. U937 and HL60 cells were treated with 15µM of each peptide for 24, 48 and 72 hours. Cell cycle analysis showed that U937 cells underwent apoptotic cell death in response to exposure to D611. This result supported previous results by Bandara *et al.* who reported the occurrence of apoptosis as a result of treatment with E2F-1 inhibiting peptide in E2F-4/Ha-*ras*

transformed cells. It was proposed that the observed apoptotic cell death correlated directly with the E2F-regulating activity of the peptide as E2F-1 was implicated in the initiation of apoptosis via the p16^{Arf}-MDM2-p53 pathway (Bandara *et al.*, 1997). Hence, apoptosis observed in response to D611 was suggested to be a direct result of the more effective E2F-regulating activity of D611 compared to the less effective AH2 peptide. By contrast, a lack of apoptosis was observed with respect to AH2.

Further, the level of endogenous E2F-1 expressed was suggested to raise susceptibility to the apoptosis-inducing activity of the peptide (Bandara *et al.*, 1997). A lack of apoptosis observed in HL60 cells suggests a correlation between endogenous E2F-1 levels and initiation of apoptosis following E2F-1 inhibiting peptide treatment especially as U937 cells were shown to contain a higher level of E2F-1 than HL60 cells. G1 arrest induced by D611 in HL60 cells might be regarded as the precursor to programmed cell death.

The investigation was continued with new stocks of AH2 and AHS2. To ensure a similar level of activity of the new peptides compared to previous batches, cell proliferation assays were carried out using HL60, K562 and Jurkat cell lines. As previously observed, HL60 cells were most sensitive to AH2 compared to K562 or Jurkat. The level of sensitivity was equal to the previous level observed with the old stock of AH2 peptide. The Jurkat cell line was less sensitive to AH2 than HL60 but nevertheless more sensitive than K562 cells. It was noted that Jurkat cells appeared to be significantly more susceptible to AH2 than D611 activity. A similar result had been previously observed in MCF-7. In contrast, HT1080 Neo, 'E2F1-1' (CHO) and HL60 cells were substantially more sensitive to D611 than AH2. This suggests that a differential sensitivity to both peptides maybe based on cell line specificity.

HL60, K562 and Jurkat showed a decrease in the percentage of cell proliferation following exposure to AHS2. Whether this decrease in cell proliferation was due to an underlying E2F-1 inhibitory activity of the control peptide (AHS2) or whether it was a result of peptide introduction to the cells, remains to be elucidated. However, the former seemed unlikely, as the amino acid sequence of AHS2 was scrambled and retention of E2F-1 inhibiting activity seemed unlikely.

In a repeat of earlier experiments using the new stock of peptides, cell cycle analysis was performed to assess the effect of inhibitory peptide treatment on HL60 and K562 cells. The two cell lines were chosen as they represented the most and the least sensitive cell line to AH2 and AHS2, respectively. A pronounced G1 arrest was observed in HL60 cells in response to $25\mu M$ AH2 after 24 hours while an increase in the percentage of cells in G1 phase was detected in K562 for the same concentration after 72 hours. Based on the suggestion that inhibitory activity of the peptide is correlated to the level of endogenous E2F-1, a marked G1 arrest would have been expected in K562 cells at an earlier time-point as the level of E2F-1 expression is equal in both cell lines. It has been proposed for G1 arrest to act as the precursor to apoptosis in peptide treated cells (Bandara et al., 1997). However, increasing concentrations of AH2 maintained G1 arrest rather than initiate apoptosis in HL60. Hence it was suggested that D611 and AH2 activity manifests itself in different ways within cells, the former resulting in apoptotic cell death and the latter merely initiating G1 arrest.

In conclusion, E2F-1 inhibiting peptide activity appears to employ its inhibitory activity through a number of pathways within different cell lines resulting in a range of varied physiological responses of the one or possibly several independent origins. Therefore, until these response pathways are elucidated, peptide treatment does not constitute a potential therapy for the treatment of diseases as a result of disturbed cell cycle regulation.

6. DISCUSSION AND CONCLUSION

Perturbation of the balance between the mechanisms of cell proliferation, differentiation and apoptosis is a hallmark of cancer. The constitutive activation of oncogenes such as *ras* and functional inactivation of tumour suppressor genes such as *Rb* and *p53* leads to aberrant gene expression of genes that regulate the cell cycle, cellular differentiation and apoptosis leading to cellular transformation (Gottlieb *et al.*, 1996; Liu *et al.*, 1995). The family of *E2F* transcription factors plays an important role in cell cycle regulation, differentiation, apoptosis and oncogenic transformation. The *E2F* transcriptional activators have been found to be part of the G1 restriction point mechanism deciding on cell cycle progression or apoptosis (Johnson *et al.*, 1998; Slansky *et al.*, 1996). *E2F-1* as part of the *Rb*- tumour suppressor pathway has been found to be deregulated in a number of cancer as a result of cyclin D1 overexpression (Bartkova *et al.*, 1995) and mutation or deletion of *Rb* or the *p16INK4a* cyclin-dependent kinase inhibitor gene (Kaelin, 1999; Schauer *et al.*, 1994; Weinberg *et al.*, 1995). Understanding of the regulatory pathways of gene expression provides a starting point for the design of molecular tools that reverse or utilise deregulated transcription levels and inhibit tumour-cell growth and progression. The aim is to develop new measures that have a direct or indirect effect on components of the transcription regulatory pathway such as *E2F* resulting in the counteraction of deregulated transcription activity. The investigations within this PhD thesis were set out to elucidate the effects of deregulated E2F-1 expression on chemosensitivity to a variety of chemotherapeutic agents. Further, the use of a novel E2F-1 antagonising peptide was examined for its potential to inhibit E2F-1, in order to restrain or alter aberrant cell cycle progression within E2F-1 overexpressing cells and to provide a rational approach for the development of a peptide and drug combination treatment for receptive cancer types.

Aside from providing a number of valuable results the data presented also highlighted the pitfalls of scientific research in the form of inter-species cross-contamination. Measures for the prevention of inter- as well as intra-species cross-contamination are discussed within the relevant chapter (chapter 3) and hence have been exempt from the following discussion.

Results in the first chapter concerned with the deregulation of E2F-1 expression and chemosensitivity, indicated the basal level of E2F-1 expression to be significantly higher in CHO cells relative to the HT1080 cells. No alteration in chemosensitivity was found in response to etoposide in CHO cells. Hence, results did not confirm previous reports of an increased level of E2F-1 expression to result in an increase in chemosensitivity to etoposide in E2F-1 overexpressing HT1080 as well as 32D.3 myeloid progenitor cells (Banerjee *et al.*, 1998; Nip *et al.*, 1997). In conclusion, results suggest cell lineage to be an important factor in determining degrees of chemosensitivity to various agents.

An inducible *E2F-1* expression system using HT1080 cells was developed in order to examine the possibility of E2F-1 overexpression directly influencing the chemosensitivity of HT1080 to the novel minor groove binding alkylating agent BGIII21. The hypothesis was that an increase in E2F-1 expression leads to a decrease in chemosensitivity in response to treatment with BGIII21. However no decrease in chemosensitivity in E2F-1 overexpressing HT1080 cells was observed in response to BGIII21 treatment.

Furthermore, although induction through doxocycline removal resulted in a 10fold increase in E2F-1 expression, the percentage of cells entering premature S phase remained low. A possible explanation for the lack of a pronounced increase in the fraction of cells entering S phase could lie in the choice of cell line. As HT1080 cells are an immortalised cancer cell line, it has been suggested that mutations, deletions or amplifications of genes within the *Rb* pathway have occurred previously thereby resulting in an increased basal level of E2F-1 expression. Hence, it would be of importance to create a second inducible system using a primary cell line and repeat the above investigation to excluding the possibility of an increased basal level of E2F-1 expression.

The marked resistance of CHO cells to the novel minor groove binding agent BGIII21 was confirmed in experiments using a characterised CHO-AA8 cell line. Following exposure to drug, BGIII21 specific DNA lesions were observed and mapped to a previously reported target sequence as well as an A-T rich region of DNA within the selected *Hprt* exon 9 DNA fragment. A comparison of BGIII21 specific DNA damage produced in HT1080 and CHO-AA8 cells found a differential amount of DNA lesions to be produced. The difference in amount of DNA damage produced was suggested to depend on a differential drug uptake between HT1080 and CHO-AA8 cells. However, any

investigation into a potential difference in affecting BGIII21 uptake could not be carried out as neither fluorescent nor radioactively labelled drug was available. Repair analysis using single strand-ligation PCR found no repair to take place within HT1080 or CHO cells. Further investigations showed that neither NER nor homologous recombination repair pathways partake in the removal of BGIII21 specific DNA lesions. Analysis of BGIII21 resistance in MMR deficient human colon and prostate cancer cell lines suggested decreased chemosensitivity to BGIII21 to be a consequence of mismatch repair protein deficiencies affecting the MutSα and MutSβ mismatch recognition complexes.

In contrast, the mismatch repair deficient CHO Clone B cell line was found to be twice as sensitive to BGIII21 than the parental CHO line. This result contradicted the hypothesis that MMR deficient cells exhibited resistance to minor groove binding alkylating agents. Previous reports suggested the CHO Clone B cell line to lack the mismatch repair protein *hMSH2* that forms an essential part of the MutSα and MutSβ mismatch recognition complexes (Aquilina *et al.*, 1994). Following these reports, CHO Clone B cells would be expected to be more resistant to BGIII21 than the parental CHO cell line. No explanation for the above discrepancy can be provided at this point.

In contrast to the investigations described above which exclusively focused on exploiting an increased level of E2F-1 expression as a means to increase chemosensitivity to various chemotherapeutic agents, the third part of this thesis was designed to counteract E2F-1 overexpression by means of an antagonistic peptide therefore sensitising cells to a subsequent treatment with a variety of drugs.

Attempts were made to utilise the knowledge available about E2F transcription factors for a rational approach for the development of an E2F-1 inhibitory peptide. Two inhibitory peptides were obtained through collaborators both of which inhibited the formation of active E2F-DP heterodimers with the result of inhibiting transcriptional activation but not DNA binding. Success within this part of the PhD project was limited in that the data obtained revealed inconsistencies in the form of inter-experimental as well as tissue specific variation. However, a direct correlation between endogenous E2F-1 levels and peptide activity was observed with respect to the linear peptide AH2 but not the branched peptide D611. Results of the investigations into the benefits of combining peptide and drug treatments ranged from additive to more than additive effects suggesting the effect

to be dependent on the initial level of chemosensitivity of the cells analysed to the drug used. Data for CHO cells showed the linear peptide to "prime" cells causing an increased sensitivity to drug when peptide and drug combined.

However, an observed sensitivity to control peptide suggested that instead of the above hypothesis, any effects observed using peptide/drug combinations might be a result of peptide introduction into cells alone causing an unspecific sensitisation of cells to the drug. In addition, it is necessary to take into account the difference of origin and molecular background of the cell lines used in the investigation. The level of E2F-1 present in the HT1080, CHO and MCF-7 cell lines might not be increased compared to the level of E2F-1 expression in non-cancerous cells with the same origin.

Therefore it was suggested that the observed peptide activity might be due to the general presence of peptide rather than a result of the specific antagonistic action of the peptide. In addition, any effect observed following peptide and drug combinations was again suggested to be due to the introduction of exogenous peptide to the cells than due to the specific E2F-1 antagonising action of the peptide. Therefore this particular peptide approach was deemed unreliable unless significantly more research is carried out.

Investigations using an alternative cell system of leukemic cells revealed the E2F-1 expression level not to correlate with the doubling times of the cells. This data contradicts previous statements whereby an increased expression of E2F-1 results in a faster traversal of cells through G1 to S phase leading to an increased fraction of cells in S phase. Nevertheless an observed increase in sensitivity to the AH2 and D611 antagonistic peptides was suggested to be a result of a faster doubling time of HL60 cells compared to the other leukemic cell lines. Further a correlation between the endogenous level of E2F-1 and the occurrence of apoptotic cell death were suggested as apoptosis was observed in U937 cells expressing a high level of E2F-1 compared to HL60 and K562 cells both expressing a lower level of E2F-1. Instead, HL60 and K562 cells exhibited a persistent G1 arrest.

Regarding the relationship between E2F-1 deregulation and chemosensitivity several conclusions can be drawn:
- No increase in chemosensitivity was observed in E2F-1 overexpressing cell in response to any chemotherapeutic agents used.

- A decreased chemosensitivity to the minor groove binding alkylating agent BGIII21 was found to be the result of an underlying MMR deficiency in human colon and prostate cancer cell lines but not CHO Clone B cells.

- Investigations into the effects of E2F antagonising peptides alone or in combination with chemotherapeutic agents require more research regarding the origin and molecular background of cell lines and the pathways through which the inhibitory peptides initiate either apoptosis or cell cycle arrest

6.1 Alternative approaches and future directions

A promising success for an alternative approach to counteract E2F activity has been reported by two independent groups using an oligonucleotide decoy for the E2F transcription factor that successfully abolished the *in vitro* DNA binding activity of E2F. Cell growth following serum stimulation was inhibited in human and rat mesangial cells upon cationic liposome transfection with the E2F oligonucleotide decoy and severe reductions in CDK2 kinase and *PCNA* mRNA as well as protein levels were detected in E2F decoy transfected human and rat mesangial cells. (Maeshima *et al.*, 1998; Tomita *et al.*, 1998). These studies show that an efficient and specific inhibition of E2F activity is possible using an E2F oligonucleotide decoy rather than a peptide strategy. Several studies report that transcription factor-decoy technology has been successfully implemented to inhibit the expression of several genes using synthetic double-stranded oligonucleotide decoys containing the consensus binding sequence of a transcription factor (Bielinska *et al.*, 1990; Sullenger *et al.*, 1990). However, decoy therapy depends on the efficient delivery of the decoy oligonucleotide to its target cells.

A number of other direct or indirect approaches to controlling the aberrant cell cycle progression as a result of E2F deregulation have been put forward. These include analysis of tissue specific expression of E2Fs, more specific targeting of chemotherapeutic agents to DNA sequences such as the *E2F* recognition site within the promoter regions of E2F regulated genes as well as the use of chemotherapeutic agents that target other components of the G1 restriction point resulting in an indirect regulation of transcription activity. Further, the use of histone deacetylase inhibitors has been proposed as a new measure to control deregulated transcription activity.

Analysis of E2F-1 expression patterns within normal and cancerous cells within certain tissue types by Northern blot analysis and microarrays provide a useful decision-making tool for the selection of an appropriate treatment regimen for a specific cancer type. For example, any direct approach to counteract the transactivation activity of E2F-1 using an antagonistic peptide or decoy oligonucleotide is only of use in cancer cells whose E2F-1 expression level is significantly higher relative to normal cells. In addition, knowledge about the relative E2F-1 expression levels within cancer types provides a good indication about the potential success of chemotherapy with an E2F-regulated gene product as the drug target. It has been reported that lung metastasis originating from a colorectal cancer contain a higher level of TS than liver metastasis of the same origin and are therefore less responsive to treatment with 5-fluorouracil. Analysis of a number of tumour samples found the resistance to 5-fluorouracil a direct consequence of the lung metastasis having a significantly higher E2F-1 expression level compared to the hepatic metastasis leading to an equally high increase in TS, a target enzyme for 5-fluorouracil (Banerjee et al., 2000).

A classic example of specific targeting of chemotherapeutic agents to DNA sequences such as the E2F recognition site within the promoter regions of E2F regulated genes are the microgonotropen (MGT) DNA binding drugs based on the chemical structure of distamycin. MGTs have been found to be potent inhibitors of transcription factor binding to promoter sequences with the result of disrupting gene expression. The MGTs mimic the transcription factor by sharing a common DNA sequence recognition and groove preference with the transcription factor. Most DNA binding drugs were limited in the sequence preference to either A-T or G-C rich regions and were only able to bind to one DNA groove. However, Chiang et al. found MGTs that more specifically recognise the binding site of the E2F-1 transcription factor are substantially more effective as inhibitors than substances that compete only for a portion of the transcription factor binding site on the DHFR promoter (Chiang et al., 1997).

Chemotherapeutic agents to target other components of the G1 restriction point resulting in an indirect regulation of transcription activity fall into several categories. The class of cyclin-dependent kinase inhibitors include flavopiridol and UCN-01. Both are potent inhibitors of CDKs 1,2 and 4 while the former also inhibits CDK7 and the latter has been shown to be a specific inhibitor of protein kinase C (PKC). Flavopiridol and UCN-01 induce cell cycle arrest at G1/S transition as a direct result of a decrease in cyclin D

expression and dephosphorylation of pRb and CDK2s respectively. UCN-01 also induces p21and p27. Both drugs are currently undergoing Phase I clinical trials (Owa *et al.*, 2001). In a study, flavopiridol was shown to potentitate gemcitabine-induced apoptosis in human pancreatic, colorectal and gastric cancer cells treated with gemcitabine and flavopiridol in a sequence–dependent manner. The potentiation was dependent on the downregulation of RR-M2 expression and RR-M2 downregulation was a direct result of flavopiridol induced proteasome-mediated degradation of E2F-1 and hypophosphorylation of pRB (Jung *et al.*, 2001). This shows how treatment with flavopiridol, a cyclin-dependent kinase inhibitor indirectly the transactivation potential of E2F-1 leading to a reduction in E2F-regulated gene expression levels and subsequent cell death.

Finally, histone-deacetylase inhibitors induce hyperacetylation to reactivate gene expression of tumour suppressor genes as part of a multitude of cellular effects that inhibit the growth and survival of tumour cells. Histone-deacetylase inhibitors include sodium butylate, trichostatin A, FR901228 and MS-27-275 which all have been found to induce G1 cell cycle arrest, apoptosis and differentiation *in vitro* and exhibited potent anti-tumour activities *in vivo* suggesting potential therapeutic utility (Johnstone, 2002; Owa *et al.*, 2001). Specifically, HDAC inhibitors were found to activate transcription of the cyclin-dependent kinase inhibitor p21 therefore inhibiting cyclin E-CDK2 and cyclin A-CDK2, resulting in the hypophosphorylation of pRb followed by the inhibition of S phase progression as transcription of E2F regulated genes required for S phase entry is stalled. Therefore elucidation of the substrate and functional specificities of HDACs coupled with the production of specific HDAC inhibitors will lead to a more targeted and efficient approach to regulating the expression of specific genes or gene subsets using HDAC inhibitors (Johnstone, 2002).

REFERENCES

Aebi, S., Fink, D., Gordon, R., Kim, H., Zheng, H. *et al.* (1997) Resistance to cytotoxic drugs in DNA mismatch repair-deficient cells. *Clin Cancer Res*, **3**, 1763-1767.

Albert, F., Eckdahl, T., Fitzgerald, D., Anderson, J. (1999) Heterogeneity in the actions of drugs that bind in the DNA minor groove. *Biochemistry*, **38**, 10135-10146.

Allen, K., de la Luna, S., Kerkhoven, R., Bernards, R., LaThangue, N. (1997) Distinct mechanisms of nuclear accumulation regulate the functional consequence of E2F transcription factors. *J Cell Sci* **110**, 2819-2831.

Andersson, L., Nilsson, K., Gahmberg, C. (1979) K562 – a human erythroleukemic cell line. *Int J Cancer*, **23**(2), 143-147.

Aquilina, G., Frosina, G., Zijno, A., Di Muccio, A., Dogliotti, E. *et al.* (1988) Isolation of clones displayed enhanced resistance to methylating agents in O^6-methylguanine-DNA methyltransferase-proficient CHO cells. *Carcinogenesis*, **9**(7), 1217-1222.

Aquilina, G., Hess, P., Branch, P., MacGeoch, C., Cascanio, I. *et al.* (1994) A mismatch recognition defect in colon carcinoma confers DNA microsatellite instability and a mutator phenotype. *Proc Natl Acad Sci USA*, **91**, 8905-8909.

Aquilina, G., Bignami, M. (2001) Mismatch repair in correction of replication errors and processing of DNA damage. *J Cell Phys*, **187**, 145-154

Arcamone , F., Penco, S., Orezzi, P., Nicolella, V., Pirelli, A. (1964) Structure and synthesis of distamycin A. *Nature*, **203**, 1064-1065.

Bagchi, S., Weinmann, R., Raychaudhuri, P. (1991) The retinoblastoma protein copurifies with E2F-I, an E1A-regulated inhibitor of the transcription factor E2F. *Cell*, **65**, 1063-1072.

Bandara, L., LaThangue, N. (1991) Adenovirus E1A prevents the retinoblastoma gene product from complexing with a cellular transcription factor. *Nature*, **351**, 494-497.

Bandara, L., Buck, V., Zamanian, M., Johnston, L., LaThangue, N. (1993) Functional synergy between DP-1 and E2F-1 in the cell cycle-regulating transcription factor DRTF1/E2F. *EMBO J*, **12**(11), 4317-4324.

Bandara, L., Lam, E., Sørensen, T., Zamanian, M., Girling, R., LaThangue, N. (1994) DP-1: a cell cycle-regulated and phosphorylated component of transcription factor DRTF1/E2F which is functionally important for recognition by pRb and the adenovirus E4 orf 6/7 protein. *EMBO J*, **13**(13), 3104-3114.

Bandara, L., Girling, R., LaThangue, N. (1997) Apoptosis induced in mammalian cells by small peptides that functionally antagonize the Rb-regulated E2F transcription factor. *Nat Biotechnol*, **15**(9), 896-901.

Banerjee, D., Schnieders, B., Fu, J., Adhikari, D., Zhao, S., Bertino, J. (1998) Role of E2F-1 in chemosensitivity. *Cancer Res*, **58**, 4292-4296.

Banerjee, D., Gorlick, R., Liefshitz, A., Danenberg, K., Danenberg, P. et al. (2000) Levels of E2F-1 expression are higher in lung metastasis of colon cancer as compared with hepatic metastasis and correlate with levels of thymidilate synthase. *Cancer Res*, **60**, 2365-2367.

Bartek, J., Lukas, J., Bartkova, J. (1999) Perspective: defects in cell cycle control and cancer. *J Pathol*, **187**, 95-99.

Bartkova, J., Lukas, J., Müller, H.,Strauss, M., Gusterson, B. et al. (1995) Abnormal patterns of D-type cyclin expression and G1 regulation in human head and neck cancer. *Cancer Res*, **55**, 949-956.

Bates, S., Phillips, A., Clark, P., Stott, F., Peters, G., Ludwig, R., Vousden, K. (1998) p14ARF links the tumour suppressors RB and p53. *Nature*, **395**, 124-125.

Bielinska, A, Shivdasani, R., Zhang, L., Nabel, G. (1990) Regulation of gene expression with double-stranded phosphorothioate oligonucleotides. *Science*, **250**, 997-1000.

Blakley, R. (1984) Dihydrofolate reductase in folates and pterins. in: Blakley, R., Benkovic, S. (editors), Chemistry and biochemistry of folates: dihydrofolate reductase, *Wiley, New York*, **Vol.1**, 191-251.

Bowdon, B., Waud, W., Wheeler, G., Hain, R., Dansby, L. et al. (1987) Comparison of 1,2-dihydropyrido[3,4]pyrazines (1-deaza-7,8-dihydropteridines) with several other inhibitors of mitsosis. *Cancer Res*, **47**(6), 1621-1626.

Brooks, N., McHugh, P., Lee, M., Hartley, J. (2000) Alteration in the choice of DNA repair pathway with increasing sequence selective DNA alkylation in the minor groove. *Chem Biol*, **7**, 659-668.

Brown, J., Wouters, B. (1999) Apoptosis, p53, and tumor cell sensitivity to anticancer agents. *Cancer Res*, **59**, 1391-1399.

Buckley, M., Sweeney, K., Hamilton, J., Sini, R., Manning, D. et al. (1993) Expression and amplification of cyclin genes in human breast cancer. *Oncogene*, **8**(8), 2127-2133.

Campanero, M., Flemington, E. (1997) Regulation of E2F through ubiquitin-proteasome-dependent degradation: stabilization by the pRb tumor suppressor protein. *Proc Natl Acad Sci USA*, **94**(6), 2221-2226.

Campanero, M., Armstrong, M., Flemington, E. (2000) CpG methylation as a mechanism for the regulation of E2F activity. *Proc Natl Acad Sci USA*, **97**(12), 6481-6486.

Carlson, B., Lahusen, T., Singh, S., Loaizi-Perez, A.,Worland, P. *et al.* (1999) Down-regulation of cyclin D1 by transcriptional repression in MCF-7 human breast carcinoma cells induced by flavopiridol. *Cancer Res*, **59**, 4634-4641.

Carmichael, J., DeGraff, W., Gazdar, A., Minna, J., Mitchell, J. (1987) Evaluation of a tetrazolium-based semiautomated colorimetric assay : assessment of chemosensitivity testing. *Cancer Res*, **47** (4), 936-942.

Camero, A. (2002) Targeting the cell cycle for cancer therapy. *Brit J Cancer*, **87**, 129-133.
Cartwright, P., Müller, H., Wagener, C., Holm, K., Helin, K. (1998) E2F-6: a novel member of the E2F family is an inhibitor of E2F-dependent transcription. *Oncogene*, **17**, 611-623.

Cascinu, S., Aschele, C., Barni, S., Dbernadis, D., Baldo, C. et al. (1999) Thymidylate synthase protein expression in advanced colon cancer: correlation with the sites of metastasis and the clinical reponse to leucovorin-modulated bolus 5-fluorouracil. *Clin Cancer Res*, **5**, 1996-1999.

Chellappan, S., Hiebert, S., Mudryi, M., Horowitz, J., Nevins, J. (1991) The E2F transcription factor is a cellular target for the Rb protein. *Cell*, **65**, 1053-1061.

Chen, J., Chen, Y., Wang, Y., Tseng, R., Chen, C. et al. (2002) Alterations of the p16^{INK4a} gene in resected non-small cell lung tumors and exfoliated cells within sputum. *Int J Cancer*, **98**, 724-731.

Chen, Y., Wang, J.,Fraig, M., Metcalf, J.,Turner, W. *et al.* (2001) Defects of DNA mismatch repair in human prostate cancer. *Cancer Res*, **61**, 4112-4121.

Chiang, S., Bruice, T., Azizkhan, J., Gawron, L., Beerman, T. (1997) Targeting E2F-1-DNA complexes with microgonotropen DNA binding agents. *Proc Natl Acad Sci USA*, **94**, 2811-2816.

Clisson, M., Dyson, N. (2001) p107 and p130: versatile proteins with interesting pockets. *Exp Cell Res*, **264**, 135-147.

Cohen, B., Colas, P., Brent, R. (1998) An artificial cell-cycle inhibitor isolated from a combinatorial library. *Proc Natl Acad USA*, **95**, 14272-14277.

Colella, G., Marchini, S., D'Incalci, M., Brown, R., Brogginni, M. (1999) Mismatch repair deficiency is associated with resistance to DNA minor groove alkylating agents. *Brit J Cancer*, **80**, 338-343.

Connor, R., Schaley, J., Feeney, G., Hearing, P. (2001) The p107 tumor suppressor induces stable E2F DNA binding to repress target promoters. *Oncogene*, **20**, 1882-1891.

Cress, W., Nevins, J. (1996) Use of the E2F transcription factor by DNA tumor virus regulatory proteins. *Curr Top Microbiol Immunol*, **208**, 63-78.

Dahiya, A., Gavin, M., Luo, R., Dean, D. (2000) Role of the LXCXE binding site in Rb function. *Mol Cell Biol*, **20**(18), 6799-6805.

Debbas, M., White, E. (1993) Wild-type p53 mediates apoptosis by E1A, which is inhibited by E1B. *Genes Dev*, **7**, 546-554.

DeGregori, J., Kowalik, T., Nevins, J. (1995) Cellular targets for activation by the E2F-1 transcription factor include DNA synthesis- and G1/S-regulatory genes. *Mol Cell Biol*, **15**(8), 4215-4224.

DeGregori, J., Leone, G., Miron, A., Jakoi, L., Nevins, J. (1997) Distinct roles for E2F proteins in cell growth control and apoptosis. *Proc Natl Acad Sci USA*, **94**, 7245-7250.

DiCiommo, D., Gallie, B., Bremner, R. (2000) Retinoblastoma: the disease, gene and protein provide critical leads to understand cancer. *Sem Cancer Biol*, **10**, 255-269.

D'Incalci, M. (1997) Differences in docetaxel and paclitaxel activity in resistant tumor cells which express MRP: need of comparative clinical trials in resistant patients. *Ann Oncol*, **8**(12):1183-4.

Draper, N., Smith, H. (1981) Applied regression analysis, 2nd ed., New York, *John Wiley and Sons.*

Drewinko, B., Romsdahl, M., Yang, L., Ahearn, M., Trujillo, J. (1976) Establishment of a human carcinoembryonic antigen-producing colon adenocarcinoma cell line. *Cancer Res,* **36**(2 Pt1), 467-475.

Dynlacht, B., Flores, O., Lees, J., Harlow, E. (1994) Differential regulation of E2F transactivation by cyclin/cdk2 complexes. *Genes Dev,* **8**, 1772-1786.

Dynlacht, B., Moberg, K., Lees, J., Harlow, E., Zhu, L. (1997) Specific regulation of E2F family members by cyclin-dependent kinases. *Mol Cell Biol,* **17**(7), 3867-3875.

Dyson, N. (1998) The regulation of E2F by pRb-family proteins. *Genes Dev,* **12**, 2245-2262.

Fabbrizio, E., Le Cam, L., Polanowska, J., Kaczorek, M., Lamb, N. et al. (1999) Inhibition of mammalian cell proliferation by genetically selected peptide aptamers that functionally anatgonize E2F activity. *Oncogene,* **18**, 4357-4363.

Fardel, O., Lecureur, V., Guillouzo, A. (1996) The P-glycoprotein multidrug transporter. *Gen Pharmac,* **27**(8), 1283-1291.

Ferreira, R., Magnaghi-Jaulin, L., Robin, P., Harel-Bellan, A., Trouche, D. (1998) The three members of the pocket protein family share the ability to repress E2F activity through recruitment of a histone deacetylase. *Proc Natl Acad Sci USA,* **95**, 10493-10498.

Field, S., Tsai, F., Kuo, F., Zubiaga, A., Kaelin, W. *et al.* (1996) E2F-1 functions in mice to promote apoptosis and suppress proliferation. *Cell,* **85**, 549-561.

Fink, D., Aebi, S., Howell, S. (1998) The role of DNA mismatch repair in drug resistance. *Clin Cancer Res*, **4**, 1-6.

Fontana, J., Wright, D., Schiffman, E., Corcoran, B., Deisseroth, A. (1980) Development of chemotactic responsiveness in myeloid precursor cells: studies with a human leukemia cell line. *Proc Natl Acad Sci USA*, **77**(6), 3664-3668.

Fry, C., Slansky, J., Farnham, P. (1997a) Position-dependent transcriptional regulation of the murine dihydrofolate reductase promoter by the E2F transactivation domain. *Mol Cell Biol*, **17**(4), 1966-1976.

Fry, C., Pearson, A., Malinowski, E., Bartley, S., Greenblatt, J., Farnham, P. (1997b) Activation of the murine dihydrofolate reductase promoter by E2F-1. *J Biol Chem*, **274**(22), 15883-15891.

Furukawa, Y., Terui, Y., Sakoe, M., Ohta, M., Saito, M. (1994) The role of cellular transcription factor E2F in the regulation of cdc2 mRNA expression and cell cycle control of human hematopoietic cells. *J Biol Chem*, **269**(42), 26249-26258.

Gayet, J., Zhou, X., Duval, A., Rolland, S., Hoang, J. *et al.* (2001) Extensive characterization of genetic alterations in a series of human colorectal cancer cell lines. *Oncogene*, **20**, 5025-5032.

Gibas, Z., Becher, R., Kawinski, E., Horoszewicz, J., Sandberg, A. (1984) A high-resolution study of chromosome chnages ina human prostatic carcinoma cell line (LNCaP). *Cancer Gent Cytogenet*, **11**(4), 399-404.

Girling, R., Partridge, J., Bandara, L., Burden, N., Totty, N. *et al.* (1993) A new component of the transcription factor DRTF1/E2F. *Nature*, **362**, 83-87.

Gorlick, R., Metzger, R., Danenberg, K., Salonga, D., Miles, G. et al. (1998) Higher levels of thymidyalte synthase expression in colorectal cancer metastases predicts for clinical outcome to fluorouracil-based chemotherapy. *J Clin Oncol*, **17**, 1760-1767.

Gossen, M., Bujard, H. (1992) Tight control of gene expression in mammalian cells by tetracycline-responsive promoters. *Proc Natl Acad Sci USA*, **89**, 5547-5551.

Gottlieb, T., Oren, M. (1996) p53 in growth control and neoplasia. *Biochem Biophys Acta*, **1287**, 77-102.

Hamburger, A., Salmon, S., Kim, M., Trent, J., Soehnlen, B. *et al.* (1978) Direct cloning of human ovarian carcinoma cells in agar. *Cancer Res*, **38** (10), 3438-3444.

Hanahan, D. (1983) Studies on transformation of *Escherichia coli* with plasmids. *J Mol Biol*, **166**(4), 557-580

Hanahan D., Weinberg, R. (2000) The hallmarks of cancer. *Cell*, **100**(1), 57-70.

Harbour, J., Dean, D. (2000) Rb function in cell-cycle regulation and apoptosis. *Nat Cell Biol*, **2**, E65-E67.

Hatakeyama, M., Weinberg, R. (1995) The role of RB in cell cycle control. *Prog Cell Cycle Res*, **1**, 9-19.

Hateboer, G., Kerkhoven, R., Shvarts, A., Bernards, R., Beijersbergen, R. (1996) Degradation of E2F by the ubiquitin-proteasome pathway: regulation by retinoblastoma family proteins and adenovirus transforming proteins. *Genes Dev*, **10**(23), 2960-2970.

Helin, K., Lees, J., Vidal, M., Dyson, N., Harlow, E., Fattaey, A. (1992) A cDNA encoding a pRb-binding protein with properties of the transcription factor E2F. *Cell*, **70**, 337-350.

Helin, K. (1998) Regulation of cell proliferation by the E2F transcription factors. *Curr Opin Genet Dev*, **8**, 28-35.

Herwig, S., Strauss, M. (1997) The retinoblastoma protein: a master regulator of cell cycle, differentiation and apoptosis. *Eur J Biochem*, **246**, 581-601.

Herzig,M., Trevino, A., Arnett, B., Woynarowski, J. (1999) Tallimustine lesions in cellular DNA are AT sequence-specific but not region-specific. *Biochemistry*, **38**, 14045-14055.

Hickman, M., Samson, L. (1999) Role of DNA mismatch repair and p53 in signaling induction of apoptosis by alkylating agents. *Proc Natl Acad Sci USA*, **96**, 10764-10769.

Hiebert, S., Packham, G., Strom, D., Haffner, R., Oren, M., Zambetti, G., Cleveland, J. (1995) E2F-1:DP-1 induces p53 and overrides survival factors to trigger apoptosis. *Mol Cell Biol*, **15**(12), 6864-6874.

Hochhauser, D., Schnieders, B., Ercikan-Abali, E., Gorlick, R., Muise-Helmericks, R., Li, W.,Fan, J., Banerjee, D., Bertino, J. (1996) Effect of cyclin D1 overexpression on drug sensitivity in a human fibrosarcoma cell line. *J Nat Cancer Inst*, **88**(18), 1269-1275

Hochhauser, D. (1997) Modulation of chemosensitivity through altered expression of cell cycle regulatory genes in cancer. *Anti-Cancer Drugs*, **8**, 903-910.

Hoefferer, M., Wirbelbauer, C., Humar, B., Krek, W. (1999) Increased levels of E2F-1-dependent DNA binding activity after UV- or γ-irradiation. *Nucleic Acids Res*, **27**(2), 491-495.

Hoeijmakers, J. (2001) Genome maintenance mechanisms for preventing cancer. *Nature*, **411**, 366-374.

Hofland, K., Petersen, B., Falck, J., Helin, K., Jensen, P., Sehested, M. (2000) Differential cytotoxic pathways of topoisomerase I and II anticancer agents after overexpression of the E2F-1/DP-1 transcription factor complex. *Clin Cancer Res*, **6**, 1488-1497.

Hofmann, F., Martelli, F., Livingston, D., Wang, Z. (1996) The retinoblastoma gene product protects E2F-1 from degradation by the ubiquitin-proteasome pathway. *Genes Dev*, **10**(23), 2949-2959.

Hoppe-Seyler, F., Crnkovic-Mertens, I., Denk, C., Fitscher, B., Klevenz, B. et al. (2001) Peptide aptamers: new tools to study protein interactions. *J Steroid Biochem Mol Biol*, **78**, 105-111.

Huber, H., Edwards, G., Goodhart, P., Patrick, D., Huang, P., Ivey-Hoyle, M., Barnett, S., Oliff, A., Heimbrook, D. (1993) Transcription factor E2F binds DNA as a heterodimer. *Proc Natl Acad Sci USA*, **90**, 3525-3529.

Hurley, L., Reynolds, V., Swenson, D., Petzold, G., Scahill, T. (1984) Reaction of the anti-tumour antibiotic CC-1065 with DNA: structure of a DNA adduct with DNA sequence specificity. *Science*, **226**, 843-844.

Irwin, M., Marin, M., Phillips, A., Seelan, R., Smith, D., Liu, W., Flores, E., Tsai, K., Jacks, T., Vousden, K., Kaelin, W. (2000) Role for the p53 homologue p73 in E2F-1-induced apoptosis. *Nature*, **407**, 645-648.

Ivey-Hoyle, M., Conroy, R., Huber, H., Goodhart, P., Oliff, A., Heimbrook, D. (1993) Cloning and characterisation of E2F-2, a novel protein with the biochemical properties of transcription factor E2F. *Mol Cell Biol*, **13**(12), 7802-7812.

Jiricny, J. (1998) Eukaryotic mismatch repair: an update. *Mutat Res*, **409**, 107-121

Johnson, D., Schwarz, J., Cress, W., Nevins, J. (1993) Expression of transcription factor E2F1 induces quiescent cells to enter S phase. *Nature*, **365**, 349-352.

Johnson, D., Ohtani, K., Nevins, J. (1994) Autoregulatory control of E2F1 expression in response to positive and negative regulators of cell cycle progression. *Genes Dev*, **8**, 1514-1525.

Johnson, D., Schneider-Broussard, R. (1998) Role of E2F in cell cycle control and cancer. *Frontiers in Bioscience*, **3**, 447-458.

Johnstone R. (2002) Histone-deacetylase inhibitors: novel drugs for the treatment of cancer. *Nat Rev Drug Discovery*, **1**, 287-299.

Jung, C., Motwani, M., Schwartz, G. (2001) Flavopiridol increases sensitization to gemcitabine in human gastrointestinal cancer cell lines and correlateswith down-regulation of ribonucleotide reductase M2 subunit. *Clin Cancer Res*, **7**, 2527-2536.

Kaelin, W., Krek, W., Sellers, W., DeCaprio, J., Ajchenbaum, F., Fuchs, C., Chittenden, T., Li, Y., Farnham, P., Blanar, M., Livingston, D., Flemington, E. (1992) Expression cloning of a cDNA encoding a retinoblastoma-binding protein with E2F-like properties. *Cell*, **70**, 351-364.

Kaelin W. (1999) Functions of the retinoblastoma protein. *BioEssays*, **21**, 950-958.

Kaighn, M., Narayan, K., Ohnuki, Y., Lechner, J., Jones, L. (1979) Establishment and characterization of a human prostatic carcinoma cell line (PC-3). *Invest Urol*, **17**(1), 16-23.

Kalma, Y., Marash, L., Lamed, Y., Ginsberg, D. (2001) Expression analysis using DNA microarrays demonstrates that E2F-1 up-regulates expression of DNA replication genes including replication protein A2. *Oncogene*, **20**, 1379-1387.

Karran, P. (2001) Mechanisms of tolerance to DNA damaging therapeutic drugs. *Carcinogenesis*, **22**(12), 1931-1937.

Kohn, K. (1996) Regulatory genes and drug sensitivity. *J Natl Cancer Inst*, **88**(18), 1255-1256.

Kolonin, M., Finley, R. (1998) Targeting cyclin-dependent kinases in Drosophila with peptide aptamers. *Proc Natl Acad Sci USA*, **95**, 14266-14271.

Komura, J., Riggs, A. (1998) Terminal transferase-dependent PCR: a versatile and sensitive method for *in vivo* footprinting and detection of DNA adducts. *Nucleic Acids Res*, **26** (7), 1807-1811.

Kovesdi, I., Reichel, R., Nevins, J. (1986) Identification of a cellular transcription factor involved in E1A trans-activation. *Cell*, **45**, 219-228.

Kowalik, T., DeGregori, J., Leone, G., Jakoi, L., Nevins, J. (1998) E2F-1 specific induction of apoptosis and p53 accumulation, which is blocked by Mdm2. *Cell Growth Diff*, **9**, 113-118.

Kowalski, D. (1979) A procedure for the quantitation of relaxed closed circular DNA in the presence of superhelical DNA: an improved fluorometric assay for nicking-closing enzyme. *Anal Biochem*, **93**, 346-354.

Krämer, A., Schultheis, B., Bergmann, J., Willer, A., Hegenbart, U. *et al.* (2002) Alterations of the cyclin D1/pRb/p16[INK4a] pathway in multiple myeloma. *Leukemia*, **16**, 1844-1851.

Krek, W., Ewen, M., Shirodkar, S., Arany, Z., Kaelin, W. et al. (1994) Negative regulation of the growth-promoting transcription factor E2F-1 by a stably bound cyclin A-dependent protein kinase. *Cell*, **78**, 161-172.

Krek, W., Xu, G., Livingston, D. (1995) Cyclin A-kinase regulation of E2F-1 DNA binding function underlies suppression of an S phase checkpoint. *Cell*, **83**, 1149-1158.

Lauta, V. (2000) Pharmacological elements in clinical application of synthetic peptides. *Fundam Clin Pharmacol*, **14**, 425-442.

Lavia, P., Jansen-Duerr, P. (1999) E2F target genes and cell-cycle checkpoint control. *BioEssays*, **21**, 221-230.

Leach, F., Velasco, A., Hsieh, J., Sagalowsky, A., McConnell, J. (2000) The mismatch repair gene hMSH2 is mutated in the prostate cancer cell line LNCaP. *J Urol*, **164**, 1830-1833.

Lees, J., Saito, M., Vidal, M., Valentine, M., Look, T. *et al.* (1993) The retinoblastoma protein binds to a family of E2F transcription factors. *Mol Cell Biol*, **13**(12), 7813-7825.

Li, W., Fan, D., Hochhauser, D., Banerjee, D., Zielinski, Z. et al. (1995) Lack of functional retinoblastoma protein mediates increased resistance to antimetabolites in human sarcoma cell lines. *Proc Natl Acad Sci USA*, **92**, 10436-10440.

Lindeman, G., Gaubatz, S., Livingston, D., Ginsberg, D. (1997) The subcellular localization of E2F-4 is cell-cycle dependent. *Proc Natl Acad Sci USA*, **94**, 5095-5100.

Lissy, N., Davis, P., Irwin, M., Kaelin, W., Dowdy, S. (2000) A common E2F-1 and p73 pathway mediates cell death induced by TCR activation. *Nature*, **407**, 642-645.

Liu, J., Chao, J., Jiang, M., Ng, S., Yen, J. et al. (1995) Ras-transformation results in elevated level of cyclin D1 and acceleration of G1 progression in NIH3T3 cells. *Molec Cell Biol*, **15**, 3654-3663.

Lowe, S., Ruley, H. (1993) Stabilization of the p53 tumor suppressor is induced by adenovirus 5 E1A and accompanies apoptosis. *Genes Dev*, **7**, 535-545.

Lukas, J., Petersen, B., Holm, K., Bartek, J., Helin, K. (1996) Deregulated expression of E2F family members induces S-phase entry and overcomes p16^{INK4A}-mediated growth suppression. *Mol Cell Biol*, **16**(3), 1047-1057.

Maeshima, Y., Kashihara, N., Yasuda, T., Sugiyama, H., Sekikawa, T. et al. (1998) Inhibition of mesangial cell proliferation by E2F decoy oligodeoxynucleotide in vitro and in vivo. *J Clin Invest*, **101**(11), 2589-2597.

Martinez-Balbas, M., Bauer, U., Nielsen, S., Brehm, A., Kouzarides, T. (2000) Regulation of E2F-1 activity by acetylation. *EMBO J*, **19**(4), 662-671.

Marzio, G., Wagener, C., Gutierrez, M., Cartwright, P., Helin, K. et al. (2000) E2F family members are differentially regulated by reversible acetylation. *J Biol Chem*, **275**(15), 10887-10892.

Masters, J. (2000) Human cancer cell lines: fact and fantasy. *Nat Rev Mol Cell Biol*, **1**, 233-236.

Masters, J., Thomson, J., Daly-Burns, B., Reid, Y., Dirks, W., Packer, P. *et al.* (2001) Short tandem repeat profiling provides an international reference standard for human cell lines. *Proc Natl Acad Sci USA*, **98**, 8012-8017.

Masters, J. (2002) HeLa cells 50 years on: the good, the bad and the ugly. *Nat Rev Cancer*, **2**, 315-318.

Mayol, X., Grana, X. (1998) The p130 pocket protein: keeping order at cell cycle exit/re-entrance transitions. *Frontiers in Bioscience*, **3**, 11-24.

McGurk, C., McHugh, P., Tilby, M., Grimaldi, K., Hartley, J. (2001) Measurement of covalent drug-DNA interactions at the nucleotide level in cells at pharmacologically relevant doses. *Methods Enzymol*, **340**, 358-376.

McHugh, P., Spanswick, V., Hartley J. (2001) Repair of DNA interstrand crosslinks: molecular mechanisms and clinical relevance. *Lancet Oncol*, **2**, 483490.

Meijer, L., Leclerc, S., Leost, M. (1999) Properties and potential-applications of chemical inhibitors of cyclin-dependent kinases. *Pharmacol Ther*, **82**(2-3), 279-284.

Mello, J., Acharya, S., Fishel, R., Essigmann, J. (1996) The mismatch-repair protein hMSH2 binds selectively to DNA adducts of the anticancer drug cisplatin. *Chem Biol*, **3**, 579-589.

Moberg, K., Starz, M., Lees, J. (1996) E2F-4 switches from p130 to p107 and pRb in response to cell cycle reentry. *Mol Cell Biol*, **16**, 1436-1449.

Mueller, H., Moroni, M., Vigo, E., Petersen, B., Bartek, J., Helin, K. (1997) Induction of S-phase entry by E2F transcription factors depends on their nuclear localization, *Mol Cell Biol*, **17**(9), 5508-5520.

Murray, V. (2000) A survey of the sequence-specific interaction of damaging agents with DNA: emphasis on antitumor agents. *Prog Nucleic Acids Res and Mol Biol*, **63**, 367-415

Nelson-Rees, W., Daniels, D., Flandermeyer, R. (1981) Cross-contamination of cells in culture. *Science*, **212**, 446-452.

Nevins J. (1998) Toward an understanding of the functional complexity of the E2F and retinoblastoma families. *Cell Growth Diff*, **9**, 585-593.

Nevins, J. (2001) The Rb/E2F pathway and cancer. *Human Mol Gen*,**10** (7), 699-703.

Nip, J., Strom, D., Fee, B., Zambetti, G., Cleveland, J., Hiebert, S. (1997) E2F-1 cooperates with topoisomerase II inhibition and DNA damage to selectively augment p53-independent apoptosis. *Mol Cell Biol*, **17**(3), 1049-1056.

Ohtani, K., DeGregori, J., Nevins, J. (1995) Regulation of the cyclin E gene by transcription factor E2F-1. *Proc Natl Acad Sci USA*, **92**, 12146-12150.

O'Regan, N., Branch, P., Macpherson, P., Karran, P. (1996) hMSH2-independent DNA mismatch recognition by human proteins. *J Biol Chem*, **271**(3), 1789-1796.

Ormerod, M. G. (1994) Analysis of DNA: general methods in flow cytometry: A Practical Approach, 2nd ed. (Ormerod, M. G., ed.), *IRL Press, Oxford, UK*, 118-135

O'Toole, C., Povey, S., Hepburn, P., Franks, L. (1983) Identity of some human bladder cancer cell lines. *Nature*, **301**, 429-430.

Owa, T., Yoshino, H., Yoshimatsu, K., Nagasu, T. (2001) Cell cycle regulation in the G1 phase: a promising target for the development of new chemotherapeutic anticancer agents. *Curr Med Chem*, **8**, 1487-1503.

Pan, H., Yin, C., Dyson, N., Harlow, E., Yamasaki, L., Van Dyke, T. (1998) Key roles for E2F1 in signaling p53-dependent apoptosis and in cell division within developing tumors. *Mol Cell*, **2**, 283-292.

Pardee, A. (1989) G1 events and regulation of cell proliferation. *Science*, **246**, 603-608.

Pardee A. (1974) A restriction point for control of normal animal cell proliferation. *Proc Natl Acad Sci USA*, **71**, 1286-1290.

Peltomäki, P. (2001) DNA mismatch repair and cancer. *Mutat Res*, **488**, 77-85.

Phillips, A., Ernst, M., Bates, S., Rice, N., Vousden, K. (1999) E2F-1 potentiates cell death by blocking anti-apoptotic signalling pathways. *Mol Cell*, **4**(5), 771-781.

Plumb, J. (1999) Cytotoxic drug resistance: cell sensitivity assays. *Meth Mol Med edited by Brown&Boger-Brown, Humana Press, Totowa, NJ, USA*, **28**, 17-23.

Prolifix, UK: http://www.prolifix.co.uk

Qin, X., Livingston, D., Kaelin, W., Adams, P. (1994) Deregulated transcription factor E2F-1 expression leads to S-phase entry and p53-mediated apoptosis. *Proc Natl Acad Sci USA*, **91**, 10918-10922.

Rossiter, B., Fuscoe, J., Muzny, D., Fox, M., Caskey, C. (1991) The Chinese hamster HPRT gene: restriction map, sequence analysis, and multiplex PCR deletion screen. *Genomics*, **9**(2), 247-256.

Rutzky, L., Tomita, J., Calenoff, M., Kahan, B. (1979) Human colon adenocarcinoma cells.III. In vitro organoid expression and carcinoembryonic antigen kinetics in hollow fiber culture. *J Natl Cancer Inst*, **63**(4), 893-902.

Sala, A., Nicolaides, N., Engelhard, A., Bellon, T., Lawe, ?? *et al.* (1994) Correlation between E2F-1 requirement in the S phase and E2F-1 transactivation of cell cycle-related genes in human cells. *Cancer Res*, **54**, 1402-1406.

Sambrook J., Fritsch E. F., Maniatis T. (1989) Molecular Cloning: A laboratory manual. *Cold Spring Harbour Press, New York, 3ʳᵈ edition*, Vol. 1,2,3

Sardet, C., Vidal, M., Cobrinik, D., Geng, Y., Onufryk, C., Chen, A., Weinberg, R. (1995) E2F-4 and E2F-5, two members of the E2F family, are expressed in the early phases of the cell cycle. *Proc Natl Acad Sci USA*, **92**, 2403-2407.

Sausville E., Zaharevitz, D., Gussio, R., Meijer, L., Lourn-Leost, M. et al. (1999) Cyclin-dependent kinases: initial approaches to exploit a novel therpaeutic target. *Pharmacol Ther*, **82**(2-3), 285-292.

Schauer, I., Siriwardana, S., Langan, T., Sclafani, R. (1994) Cyclin D1 overexpression vs. retinoblastoma inactivation: Implications for growth control evasion in non-small cell and small cell lung cancer. *Proc Natl Acad Sci USA*, **91**, 7827-7831.

Schwartz G., Ilson, D., Saltz, L., O'Reilly, E., Tong, W. et al. (2001) Inhibition of lung cancer proliferation by antisense cyclin D. *Cancer Gene Ther*, **3**(2), 131-135.

Schweitzer, B., Dicker, A., Bertino, J. (1990) Dihydrofolate reductase as a therapeutic target. *FASEB J.*, **4**, 2441-2452.

Scully, C., Field, J., Tanzawa, H. (2000) Genetic aberrations in oral or head and neck squamous cell carcinoma 2: chromosomal aberrations. *Oral Onc*, **36**, 311-327.

Sears, R., Ohtani, K., Nevins, J. (1997) Identification of positively and negatively acting elements regulating expression of the E2F-2 gene in response to cell growth signals. *Mol Cell Biol*, **17**, 5227-5235.

Sears, R., Ohtani, K., Nevins, J. (1997) Identification of positively and negatively acting elements regulating expression of the E2F-2 gene in response to cell growth signals. *Mol Cell Biol*, **17**(9), 5227-5235.

Senderowicz, A., Headlee, D., Stinson, S., Lush, R.,Kalil, N. et al. (1998) Phase I trial of continuous infusion flavopiridol, a novel cyclin-dependent kinase inhibitor, in patients with refractory neoplasms. *J Clin Oncol*, **16**(9), 2986-2999.

Senderowicz, A. (2001) Development of cyclin-dependent kinase modulators as novel therapeutic approaches for hematological malignancies. *Leukemia*, **15**(1), 1-9.

Shah M., Schwartz, G. (2001) Cell cycle-mediated drug resistance: an emerging concept in cancer therapy. *Clin Cancer Res*, **7**, 2168-2181.

Shan, B., Lee, W. (1994) Deregulated expression of E2F-1 induces S-phase entry and leads to apoptosis. *Mol Cell Biol*, **14**(12), 8166-8173.

Shan, B., Farmer, A., Lee, W. (1996) The molecular basis of E2F-1/DP-1 induced S-phase entry and apoptosis. *Cell Growth Diff*, **7**, 689-697.

Sharpless, N., DePinho, R. (1999) The *INK4A/ARF* locus and its two gene products. *Curr Opin Genet Dev*, **9**, 22-30.

Shenton, B. (1996) A Manual of practical flow cytometry. Multicentre Course in Flow Cytometry, Royal Microscopical Society, UK.

Sherr, C. (1996) Cancer cell cycles. *Science*, **274**, 1672-1677.

Sherr, C., Roberts, J. (1999) CDK inhibitors: positive and negative regulators of G1- phase progression. *Genes Dev*, **13**(12), 1501-1512.

Sherr C. (2000) The Pezcoller Lecture: Cancer cell cycles revisited. *Cancer Res*, **60**, 3689-3695.

Sherr C. (2001) The *INK4a/ARF* network in tumour suppression. *Nat Rev Mol Cell Biol*, **2**, 731-737.

Singh, P., Wong, S., Hong, W. (1994) Overexpression of E2F-1 in rat embryo fibroblasts leads to neoplastic transformation. *EMBO J*, **13**(14), 3329-3338.

Skehan, P., Storeng, R., Scudiero, D., Monks, A., McMahon, J. *et al.* (1990) New colourimetric cytotoxicity assay for anticancer-drug screening. *J Natl Cancer Inst*, **82** (13), 1107-1112.

Slansky, J., Farnham, P. (1996) Introduction to the E2F family: protein structure and gene regulation. *Curr Top Microbiol Immunol*, **208**, 1-30.

Souhami, R., Tobias, J. (1998) Cancer and its management, 3rd edition. *Blackwell Science Ltd., Oxford, UK.*

Soule, H., Vazguez, J., Long, A., Albert, S.,Brennan, M. (1973) A human cell line from pleural effusion derived from a breast carcinoma. *J Natl Cancer Inst*, **51**(5), 1409-1416.

Stacey, G., Bolton, B., Doyle, A. (1992) DNA fingerprinting transforms the art of cell authentication. *Nature*, **357**, 261-262.

Stadler, W., Vogelzang, N., Amato, R., Sosman, J., Taber, D. et al. (2000) Flavopiridol, a novel cyclin-dependent kinase inhibitor, in metastatic renal caner: a University of Chicago Phase II Consortium study. *J Clin Oncol*, **18**(2), 371-375.

Starling J., Sieg, S., Beckett, M., Schellhammer, P., Ladaga, L. *et al.* (1982) Monoclonal antibodies to human prostate and bladder tumor-associated antigens. *Cancer Res*, **42**(8), 3084-3089.

Sullenger, B., Gallardo, G.,Ungers, G., Gilboa, E. (1990) Overexpression of TAR sequences renders cells resistant to human immunodeficiency virus replication. *Cell*, **63**, 601-608.

Sundstrom, C., Nilsson, K. (1976) Establishment and characterization of a human histiocytic lymphoma cell line (U-937). *Int J Cancer*, **17**(5), 565-577.

Swenson, D., Li, L., Hurley, L., Rokem, J., Petzold, G. *et al.* (1982) Mechanism of interaction of CC-1065 (NSC 298223) with DNA. *Cancer Res*, **42**(7), 2821-2828.

Thorn, J., Todd, A., Warrilow, D., Watt, F., Molloy, P., Iland, H. (1991) Characterization of the human N-*ras* promoter region, *Oncogene*, **6**, 1843-1850

Tibbetts, L., Chu, M., Hager, J., Dexter, D., Calabresi, P. (1977) Chemotherapy of cell-line derived human colon carcinomas in mice immunosuppressed with anti-thymocyte serum. *Cancer*, **40**, 2651-2659.

Tomita, N.,Horiuchi, M., Tomita, S., Gibbons, G., Kim, J. et al. (1998) An oligonucleotide decoy for transcription factor E2F inhibits mesangial cell proliferation in vitro. *Am J Physiol*, **275** (Renal Physiol 44), F278-284.

Trimarchi, J., Fairchild, B., Verona, R., Moberg, K., Andon, N., Lees, J. (1998) E2F-6, a member of the E2F family that can behave as a transcriptional repressor. *Proc Natl Acad Sci USA*, **95**, 2850-2855.

Tsai, K., Hu, Y., Macleod, K., Crowley, D., Yamasaki, L., Jacks, T. (1998) Mutation of E2f-1 suppresses apoptosis an inappropriate S phase entry and extends survival of Rb-deficient mouse embryos. *Mol Cell*, **2**, 293-304.

Twentyman, P., Luscombe, M. (1987) A study of some variables in a tetrazolium dye (MTT) based assay for cell growth and chemosensitvity. *Br J Cancer*, **56** (3), 279-285.

Van Bokhoven, A., Varella-Garcia, M., Korch, C., Miller, G. (2001) TSU-Pr1 and JCA-1 cells are derivatives of T24 bladder carcinoma cells and are not of prostatic origin. *Cancer Res*, **61**, 6340-6344.

Van den Heuvel, S., Harlow, E. (1993) Distinct roles for cyclin-dependent kinases in cell cycle control. *Science*, **262**, 2050-2054.

Van der Sman, J., Thomas, S., Lam, E. (1999) Modulation of E2F complexes during G0 to S phase transition in human primary b-lymphocytes. *J Biol Chem*, **274**(17), 12009-12016.

Van Dyke, M., Hertzberg, R., Dervan, P. (1982) Map of distamycin A, netropsin and actinomycin binding sites on heterogeneous DNA: DNA cleavage-inhibition patterns with methidiumpropyl-EDTA.Fe(II). *Proc Natl Acad Sci USA*, **79**, 5470-5474.

Verona, R., Moberg, K., Estes, S., Starz, M., Vernon, J., Lees, J. (1997) E2F activity is regulated by cell cycle-dependent changes in subcellular localisation. *Mol Cell Biol*, **17**(12), 7268-7282.

Volker, M., Moné, M., Karmakar, P., van Hoffen, A., Schul, W. *et al.* (2001) Sequential assembly of the nucleotide excision repair factors *in vivo*. *Mol Cell*, **8**, 213-224.

von Kleist, S., Chany, E., Burtin, P., King, M., Fogh, J. (1975) Immunohistology of the antigenic pattern of a continuous cell line froma human colon cancer. *J Natl Cancer Inst*, **55**(3), 555-560.

Weinberg, R. (1995) The retinoblastoma protein and cell cycle control. *Cell*, **81**, 323-330.

Weintraub, S., Chow, K., Luo, R., Zhang, S., He, S. et al. (1995) Mechanism of active transcriptional repression by the retinoblastoma protein. *Nature*, **375**, 812-815.

Weiss, A., Wiskocil, R., Stobo, J. (1984) The role of T3 surface molecules in the activation of human T cells: a two-stimulus requirement for IL2 production reflects events occurring at a pre-translational level. *J Immunol*, **133**(1), 123-128.

Wu, X., Levine, A. (1994) p53 and E2F-1 cooperate to mediate apoptosis. *Proc Natl Acad Sci USA*, **91**, 3602-3606.

Wyatt, M., Lee, M., Garbiras, B., Souhami, R., Hartley, J. (1995) Sequence specificity of alkylation for a series of nitrogen mustard-containing analogues of distamycin of increasing binding site size: Evidence for increased cytotoxicity with enhanced sequence specificity. *Biochemistry*, **34**(40), 13034-13041.

Yamaski, L., Jacks, T., Bronson, R., Goillot, E., Harlow, E., Dyson, N. (1996) Tumor induction and tissue atrophy in mice lacking E2F-1, *Cell*, **85**, 537-548.

Yamasaki, L., Bronson, R., Williams, B., Dyson, N., Harlow, E., Jacks, T. (1998) Loss of E2F-1 reduces tumorigenesis and extends the lifespan of Rb1(+/-) mice. *Nat Genet*, **18**, 360-364.

Yang, H., Dong, Y., Elliott, M., Wong, S., McMasters, K. (2001) Additive effect of adenovirus-mediated E2F-1 gene transfer and topoisomerase II inhibitors on apoptosis in human osteosarcoma cells. *Cancer Gene Ther*, **8**(4), 241-251.

Zheng, N., Fraenkel, E., Pabo, C., Pavletich, N. (1999) Structural basis of DNA recognition by the heterodimeric cell cycle transcription factor E2F-DP. *Genes Dev*, **13**, 666-674.

Zhu, L., Zhu, L., Xie, E., Chang, L. (1995) Differential roles of two tandem E2F sites in repression of the human p107 by retinoblastoma and p107 proteins. *Mol Cell Biol*, **15**, 3552-3562.

Zöchbauer-Müller, S., Fong, K., Virmani, A., Geradts, J., Gazdar, A. (2001) Aberrant promoter methylation of multiple genes in non-small cell lung cancers. *Cancer Res*, **61**, 249-255.